

**SYNTHESIS, CHARACTERIZATION, AND
BIOLOGICAL INVESTIGATIONS OF
HETEROLEPTIC COMPLEXES OF
TETRACYCLINES AND SALICYLALDEHYDE
MIXED LIGANDS**



A THESIS SUBMITTED TO THE
CENTRAL DEPARTMENT OF CHEMISTRY
INSTITUTE OF SCIENCE AND TECHNOLOGY
TRIBHUVAN UNIVERSITY
NEPAL

FOR THE AWARD OF
DOCTOR OF PHILOSOPHY
IN CHEMISTRY

BY
ROHIT KUMAR DEV
FEBRUARY 2024

**SYNTHESIS, CHARACTERIZATION, AND
BIOLOGICAL INVESTIGATIONS OF
HETEROLEPTIC COMPLEXES OF
TETRACYCLINES AND SALICYLALDEHYDE
MIXED LIGANDS**



**A THESIS SUBMITTED TO THE
CENTRAL DEPARTMENT OF CHEMISTRY
INSTITUTE OF SCIENCE AND TECHNOLOGY
TRIBHUVAN UNIVERSITY
NEPAL**

**FOR THE AWARD OF
DOCTOR OF PHILOSOPHY
IN CHEMISTRY**

**BY
ROHIT KUMAR DEV
FEBRUARY 2024**



TRIBHUVAN UNIVERSITY
Institute of Science and Technology

DEAN'S OFFICE

Kirtipur, Kathmandu, Nepal



EXTERNAL EXAMINERS

ence No.:

The Title of Ph.D. Thesis: "Synthesis, Characterization, and Biological Investigations of Heteroleptic Complexes of Tetracyclines and Salicylaldehyde Mixed Ligands"

Name of Candidate: Rohit Kumar Dev

External Examiners:

- (1) Prof. Dr. Hem Raj Pant
Institute of Engineering
Pulchowk Campus
Tribhuvan University, NEPAL
- (2) Prof. Dr. Pranab Ghosh
Department of Chemistry
University of North Bengal
Darjiiling, INDIA
- (3) Dr. Santosh Aryal
University of Texas at Tyler
USA


February 11, 2024

Dr. Surendra Kumar Gautam
Asst. Dean

DECLARATION

The thesis entitled “**SYNTHESIS, CHARACTERIZATION, AND BIOLOGICAL INVESTIGATIONS OF HETEROLEPTIC COMPLEXES OF TETRACYCLINES AND SALICYLALDEHYDE MIXED LIGANDS**” which is being submitted to the Central Department of Chemistry, Institute of Science and Technology (IOST), Tribhuvan University, Nepal for the award of the degree of Doctor of Philosophy (Ph.D.), is a research work carried out by me under the supervision of Prof. Dr. Ajaya Bhattarai, Department of Chemistry, Tribhuvan University and co-supervised by Dr. Narendra Kumar Chaudhary, Department of Chemistry, Tribhuvan University, Mahendra Morang Adarsha Multiple Campus, Biratnagar, Morang, Nepal.

This research is original and has not been submitted earlier in part or full in this or any other form to any University or Institute, here or elsewhere, for the award of any degree.



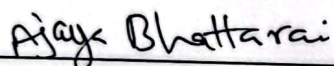
Rohit Kumar Dev

February 2024

RECOMMENDATION

This is to recommend that **Mr. Rohit Kumar Dev** has carried out research entitled **“SYNTHESIS, CHARACTERIZATION, AND BIOLOGICAL INVESTIGATIONS OF HETEROLEPTIC COMPLEXES OF TETRACYCLINES AND SALICYLALDEHYDE MIXED LIGANDS”** for the award of Doctor of Philosophy (Ph.D.) in **Chemistry** under our supervision. To our knowledge, this work has not been submitted for any other degree.

He has fulfilled all the requirements laid down by the Institute of Science and Technology (IoST), Tribhuvan University, Kirtipur for the submission of the thesis for the award of a Ph.D. degree.



Prof. Dr. Ajaya Bhattarai

Supervisor

(Professor)

Department of Chemistry, Mahendra Morang Adarsha Multiple
Campus, Tribhuvan University, Biratnagar, Morang, Nepal



Dr. Narendra Kumar Chaudhary

Co-supervisor

(Assist. Professor)

Department of Chemistry, Mahendra Morang Adarsha Multiple
Campus, Tribhuvan University, Biratnagar, Morang, Nepal



त्रिभुवन विश्वविद्यालय
TRIBHUVAN UNIVERSITY
विज्ञान तथा प्रविधि अध्ययन संस्थान
Institute of Science and Technology
रसायन शास्त्र केन्द्रीय विभाग
CENTRAL DEPARTMENT OF CHEMISTRY
कीर्तिपुर, काठमाडौं, नेपाल
Kirtipur, Kathmandu, NEPAL

संख्या:
f. No.:



Date: 2/13/2024

On the recommendation of Prof. Dr. Ajaya Bhattarai and Dr. Narendra Kumar Chaudhary, this Ph.D. thesis submitted by Mr. Rohit Kumar Dev, entitled "SYNTHESIS, CHARACTERIZATION, AND BIOLOGICAL INVESTIGATIONS OF HETEROLEPTIC COMPLEXES OF TETRACYCLINES AND SALICYLALDEHYDE MIXED LIGANDS" is forwarded by the Central Department Research Committee (CDRC) to the Dean, IOST, T.U.

Bhattarai

Prof. Dr. Jagadeesh Bhattarai

Professor

Head

Central Department of Chemistry

Tribhuvan University

Kirtipur, Kathmandu

Nepal

ACKNOWLEDGEMENTS

Today, the world is at the peak of its modernization. Every individual in the modern world is trying to establish his/her identity in this crew of brilliance. Without dwelling on this competition, we can't build a stable position but can play a trick on them. Thus, in my opinion, success is a great word. I extend my deepest praise and gratitude to the Almighty God, who has blessed me and given me all the strength to complete my Ph.D. work. I am grateful for the help of many people while completing my research work.

In this moment of accomplishment, I would like to express my sincere gratitude and appreciation to my supervisor, Professor Dr. Ajaya Bhattarai, and Co-supervisor, Dr. Narendra Kumar Chaudhary, who provided me with valuable guidance, provocative discussions, constant advice, encouragement, constructive criticism, and complete help from the beginning until the end of my Ph.D. journey. Hence, they are regarded as superheroes and role models in my life.

I would like to acknowledge, Professor Dr. Jagadeesh Bhattarai, H.O.D., Central Department of Chemistry, Kirtipur, Kathmandu, Professor Dr. Megh Raj Pokhrel, Professor Dr. Kedar Nath Ghimire, Professor Dr. Vinay Kumar Jha, Professor Dr. Paras Nath Yadav, Professor Dr. Amar Prasad Yadav, Assoc. Prof. Surya Kant Kalauni, Assoc. Prof. Achyut Adhikari of the Central Department of Chemistry for valuable comments and evaluation of the progress report during the Ph.D. session. I would like to thank all the teaching and non-teaching staff members of the Central Department of Chemistry who have supported and assisted me in various ways in the research work.

I would like to express my gratitude to Dr. Ramavatar Sharan (Campus Chief), Dr. Baburam Timilsina, and Prof. Dr. Mahendra Narayan Yadav (Ex-Campus Chief), Assist. Prof. Umesh Prasad Yadav (Assistant Campus Chief), Dr. Bishnu Dev Das, Dr. Pramod Kherwar (Ex-Assistant Campus Chief), Prof. Dr. Ajaya Bhattarai (H.O.D), Dr. Ghanshyam Srivastav, and Assoc. Prof. Sitaram Gupta (Ex-H.O.D.), Department of Chemistry, Mahendra Morang Adarsha Multiple Campus, Biratnagar, Morang, Nepal, for providing me with various laboratory facilities and spaces to pursue Ph.D. work.


I am indebted to my research colleagues, Mr. Yuv Raj Sahu, Mr. Janak Adhikari (Assist. Prof.), and Dr. Neelam Shahi for providing me with the necessary guidance and

suggestions. I am grateful to the staff and faculty members of the Department of Microbiology and Surface Chemistry Laboratory of Mahendra Morang Adarsha Multiple Campus, Biratnagar, Morang, Nepal, for their help and kind cooperation in all stages of the research work. I would also like to thank Mr. Balram Mandal and Mr. Ajit Kumar Mallik of Harinagra, Harinagar gaupalika for their motivation and encouragement.

I would like to express gratitude to the Nepal Academy of Science and Technology (NAST) Khumaltar, Lalitpur, Nepal, for providing a Ph.D. Fellowship. Furthermore, I thank the facilities of SAIF, IIT Bombay, CSIR-CDRI Lucknow, STIC Cochin, NRF Birjung, and NBU Siliguri for their continuous help during sample analysis and spectra recording of metal complexes of mixed ligands.

I express my deepest feelings of love and compassion to my beloved Mother Basanti Devi Dev and Father Dharendra Prasad Dev for their tireless efforts so that I can complete my Ph.D. research work today. I would also like to thank my dear brothers Roshan, Anil, Sunil Kumar Dev, and sister-in-law Lalita Poddar for their continuous courage and inspiration during the research work.

Lastly, I must thank my dear wife Mrs. Khusbu, my son Rishik Dev, daughter Kavya Dev, niece Anuska, Sonaxi, and nephew Aditya Dev, for their continuous support, love, and encouragement during the research work. So, I dedicate my Ph.D. work to my family.



Rohit Kumar Dev
(February 2024)

ABSTRACT

Today, the resistance of bacteria is due to their misuse and overdose of antibiotics. Therefore, researchers are working day and night to discover new antibiotics that can solve the challenges of multi-drug resistance. The present study describes the synthesis of the metal complexes with the help of the primary ligand, tetracycline/oxytetracycline (TC/OTC), secondary ligand, salicylaldehyde (Sal), and 4d-transition metal salts [M=Cd(II), Zr(II), Mo(III)/(V), and Pd(II)]. A calculated amount of equimolar mixture of primary ligand (TC) is dissolved in 70 % ethanol and stirred under magnetic stirrer. A stirred aqueous solution of metal salt is added dropwise to the TC solution. The stirred alcoholic solution of the secondary ligand (Sal) is also added to the above reaction mixture dropwise and refluxed in a reflux condenser. The pH is maintained by the adding ammonia solution resulting the formation of precipitate. The dried precipitate is recrystallized to obtain the amorphous form of metal complex. Furthermore, the complexes were analyzed using physical and spectral techniques. Here, the physical method includes elemental microanalysis, pH, specific conductivity, viscosity, surface tension, density, and melting point measurements. Similarly, the spectroscopic method includes FT-IR, (¹H and ¹³C)- NMR, UV/Visible, and ESI-MS spectrometry techniques. The results obtained from the conductivity data showed both electrolytic and non-electrolytic nature, which indicates that the metal complexes are correlatively bonded to the metal ions. Also, the findings from the UV/Vis. spectra confirmed the proposed structure as well as the geometry of the metal complex.

The thermal and kinetic stability of the complex was obtained from thermo gravimetric and differential thermal analysis (TGA/DTA) techniques. The thermodynamic parameters of various decomposition steps, ΔS^* , ΔH^* , ΔG^* , E^* , A , T , can be calculated from the well-known popular Coats- Redfern equation. The results obtained from the thermal data show that the complexes have high thermal stability and also non-spontaneous nature during different decomposition steps. The spectral studies of metal complexes showed better results with the molecular formula. The SEM (Scanning electron microscope) determines the surface morphology of the compound. The complexes were further supported by the information obtained from 3D molecular modeling viz: Chem 3D pro 12.0.2 software program, which provided the theoretical

predictions of the metal complexes and a better and more accurate evaluation of the proposed structure. Using the MM2 calculations, the energy optimization was repeated several times to note the minimum energy. The difference in M-N and M-O values indicates the coordination of metal ions with the ligand.

The metal complex was tested for *in vitro* antibacterial susceptibility by two strains of human clinical pathogenic bacteria: *Staphylococcus aureus* (gram-positive) and *Klebsiella pneumoniae*, *Escherichia coli*, *Proteus mirabilis*, and *Pseudomonas aeruginosa* (gram-negative). The tests were performed with the help of the well-known modified Kirby-Bauer paper disc diffusion method. Antimicrobial study results showed better results at higher concentrations and considerable activity at lower concentrations. The zone of inhibition was measured in diameter (mm) with the help of an antibiogram zone measuring scale. Here, all clinical pathogens were found to be more susceptible to the prepared derivatives of TCs. The antibacterial potency is based on the concept of Overton's and Tweedy's chelation principle which is related to the stability and easy permeation of the lipid layer of the organism by metal complexes.

सार

आज, ब्याक्टेरियाहरूको प्रतिरोध उनीहरूको दुरुपयोग र एन्टिबायोटिकको अधिक मात्राको कारण हो। तसर्थ, अनुसन्धानकर्ताहरू बहु-औषधि प्रतिरोधका चुनौतीहरू समाधान गर्न सक्ने नयाँ एन्टिबायोटिकहरू पत्ता लगाउन दिनरात काम गरिरहेका छन्। हालको अध्ययनले प्राइमरी लिगान्ड, Tetracycline/Oxytetracycline (TC वा OTC), सेकेन्डरी लिगान्ड, Salicylaldehyde (Sal), र 4d-ट्रान्जिसन धातु लवणहरू [M=Cd(II), Zr(II), Mo(III)/(V), र Pd(II)] को मद्दतबाट धातु कम्प्लेक्सहरूको निर्माण गर्ने बारे बर्णन गर्दछ। प्राइमरी लिगान्ड (TC)/(OTC) को समान मोलर (molar) मिश्रणको गणना गरिएको मात्रा, 70% इथेनोलमा घुलाए पछि चुम्बकीय स्टरर् द्वारा चलाईएको थियो। धातुको लवणको चलाईएको जलीय घोल TC को घोलमा थोपा-थोपा गरेर थपिएको थियो। सेकेन्डरी लिगान्ड (Sal) को चलाईएको अल्कोहलयुक्त घोल पनि माथिको प्रतिक्रिया मिश्रणमा थोपा-थोपा गरेर थपिएपछि रिफ्लक्स कन्डेनसरमा रिफ्लक्स गरिएको थियो। अमोनिया घोल थपेर पीएच (pH) मिलाएको परिणामस्वरूप धातु कम्प्लेक्सको गठन भएको थियो। धातु कम्प्लेक्सको घोललाई सुकाएर प्राप्त ठोसलाई शुद्ध बनाउन पुन क्रिस्टलिकरण गरिएको थियो। यसपछि, कम्प्लेक्सहरूलाई भौतिक र वर्णक्रमीय प्रविधिहरू प्रयोग गरेर विश्लेषण गरिएको थियो। जसमा, भौतिक विधिमा मौलिक सूक्ष्म विश्लेषण, pH, विशिष्ट चालकता (Specific conductivity), भिस्कोसिटी (viscosity), सतह तनाव (surface tension), घनत्व (density), र पिघलने बिन्दु मापन (Melting point measurement) लगायतका समावेश छन्। त्यस्तै, स्पेक्ट्रोस्कोपिक विधिमा FT-IR, (¹H र ¹³C)-NMR, UV/visible, र ESI-MS स्पेक्ट्रोमेट्री प्रविधिहरू समावेश छन्। चालकता डेटाबाट प्राप्त नतिजाहरूले धातु कम्प्लेक्सहरू इलेक्ट्रोलाइटिक र गैर-इलेक्ट्रोलाइटिक दुवै प्रकृतिका देखिएका थिए, जसले धातु कम्प्लेक्सहरू धातु आयनहरूसँग सहबद्ध रूपमा बाँधिएको संकेत गर्दछ। साथै, UV/Vis स्पेक्ट्राको निष्कर्षहरूले धातु कम्प्लेक्सहरूको प्रस्तावित संरचना र ज्यामितिलाई पुष्टि गर्दछ। कम्प्लेक्सको थर्मल र काइनेटिक स्थिरता थर्मो ग्रेभिमेट्रिक र विभेदक थर्मल विश्लेषण (TGA/DTA) प्रविधिहरूबाट प्राप्त गरिएको थियो। विभिन्न विघटन चरणहरूको थर्मोडायनामिक मापदण्डहरू, ΔS^* , ΔH^* , ΔG^* , E^* , A , T , प्रसिद्ध लोकप्रिय कोट्स- रेडफर्न समीकरणबाट गणना गरिएको थियो। थर्मल डाटाबाट प्राप्त नतिजाहरूले देखाउँछन् कि कम्प्लेक्सहरूमा उच्च थर्मल स्थिरता र विभिन्न विघटन चरणहरूमा गैर-स्वस्फूर्त प्रकृतिका थिए। धातु कम्प्लेक्सको वर्णक्रमीय अध्ययनले आणविक सूत्र अनुरूपको परिणाम

देखाएको थियो। SEM (स्क्यानइङ इलेक्ट्रोन माइक्रोस्कोप) अध्ययनद्वारा यौगिकको सतह आकारविज्ञान निर्धारण गरिएको थियो। कम्प्लेक्सहरूको संरचनाहरूलाई 3D आणविक मोडेलिङ जस्तै: Chem 3D प्रो 12.0.2 सफ्टवेयर प्रोग्रामबाट प्राप्त जानकारीद्वारा समर्थन गरिएको थियो, जसले धातु कम्प्लेक्सहरूको सैद्धान्तिक भविष्यवाणीहरू र प्रस्तावित संरचनाको राम्रो र सटीक मूल्याङ्कन गरेको थियो। MM2 गणनाहरू प्रयोग गरेर, न्यूनतम ऊर्जा प्राप्त गर्न ऊर्जा अनुकूलनलाई धेरै पटक दोहोर्याइएको थियो। M-N र M-O मानहरूमा भिन्नताले लिगान्डसँग धातु आयनहरूको समन्वयलाई संकेत गर्दछ।

धातु कम्प्लेक्सहरूलाई मानव रोगजनक ब्याक्टेरियाका दुई प्रकारहरूद्वारा इनभिट्रो एन्टिब्याक्टेरियल संवेदनशीलताको लागि परीक्षण गरिएको थियो; जसमा, स्टेफिलोकोकस ऑरियस (ग्राम- पोजिटिभ) र क्लेब्सिएला निमोनिया, एस्चेरिचिया कोलाई, प्रोटस मिराबिलिस, र स्पूडोमोनास एरुगिनोसा (ग्राम- नेगेटिभ) ब्याक्टेरियाहरू समावेश गरिएको थियो। प्रख्यात परिमार्जित किर्बी-बाउर पेपर डिस्क प्रसार विधिद्वारा परीक्षणहरू गरिएको थियो। एन्टिमाइक्रोबियल अध्ययन परिणामहरूले उच्च सांद्रतामा राम्रो नतिजा र कम सांद्रतामा उल्लेखनीय गतिविधि देखाएका थिए। एन्टिबायोग्राम जोन मापन स्केलको मद्दतले अवरोधको क्षेत्रको व्यास (मिमी) नापिएको थियो। यहाँ, सबै प्याथोजेनहरू TCs को तयार डेरिभेटिभहरूमा बढी संवेदनशील भएको पाइयो। जीवाणुरोधी क्षमता ओभरटन र ट्वीडीको चेलेसन सिद्धान्तको अवधारणामा आधारित छ जुन धातुको कम्प्लेक्सहरूद्वारा जीवको लिपिड तहको सहज पारगमनसँग सम्बन्धित छ।

LIST OF ACRONYMS AND ABBREVIATIONS

Amk	: Amikacin
<i>Abs</i>	: Absorbance
aq.	: Aqueous
Cm ³	: Cubic Centimeter
°C	: Degree Celsius
cm	: Centimeter
¹³ C-NMR	: Carbon-13 Isotope Nuclear Magnetic Resonance
cm ⁻¹	: Wavenumber Reciprocal Centimeter
DMSO	: Dimethyl Sulphoxide
DMF	: Dimethyl Formamide
DMSO-d ₆	: Deuterated Dimethyl Sulfoxide
DTA	: Differential Thermal Analysis
DTG	: Differential Thermogravimetric
<i>E. coli</i>	: <i>Escherichia coli</i>
ESI-MS	: Electrospray Ionization Mass Spectrometry
FT-IR	: Fourier Transform-Infrared
¹ H-NMR	: Proton Nuclear Magnetic Resonance
Hz	: Hertz
IR	: Infrared
<i>K. pneumoniae</i>	: <i>Klebsiella pneumoniae</i>
LMCT	: Ligand Metal Charge Transfer
MM2	: Molecular Mechanics 2
m.p.	: Melting Point
MS	: Mass Spectrum
mmol	: Millimol
m/z	: Mass-Charge-Ratio

MHz	: Mega Hertz
nm	: Nanometer
NMR	: Nuclear Magnetic Resonance
OTC	: Oxytetracycline
pH	: Logarithmic Scale of the Concentration of Hydronium Ion $\log [\text{H}_3\text{O}^+]$
ppm	: Parts Per Million
<i>P. aeruginosa</i>	: <i>Pseudomonas aeruginosa</i>
<i>P. mirabilis</i>	: <i>Proteus mirabilis</i>
<i>S. aureus</i>	: <i>Staphylococcus aureus</i>
SEM	: Scanning Electron Microscope
Sal	: Salicylaldehyde
TG	: Thermogravimetric
TGA	: Thermogravimetric Analysis
TMS	: Tetramethylsilane
TC	: Tetracycline
UV/Vis	: Ultraviolet/ Visible
Zr-TC/Sal	: Zirconium Complex of Tetracycline and Salicylaldehyde Mixed Ligand
Zr(II)Otc/Sal	: Zirconium Complex of Oxytetracycline and Salicylaldehyde Mixed Ligand

LIST OF SYMBOLS

A	: Absorbance
A°	: Angstrom
A	: Arrhenius Pre-Exponential Factor
β	: Linear Heating Rate
c	: Concentration of Solution in mole/L
E^*	: Activation Energy
ΔG^*	: Free Energy of Activation
ΔH^*	: Enthalpy of Activation
h	: Plank's Constant
I	: Intensity of Transmitted Light
I_o	: Intensity of Incident Light
k_B	: Boltzmann Constant
r	: Correlation Coefficient
R	: Gas Constant
ΔS^*	: Entropy of Activation
T	: Absolute Temperature
T	: Transmittance
% T	: Percentage Transmittance
λ	: Wavelength
ν	: Frequency of Absorption.
μ	: Micro
$\mu\text{g}/\mu\text{L}$: Microgram Per Microliter
μScm^{-1}	: Micro Siemens Per Centimeter

LIST OF TABLES

	Page No.
Table 1: Geometry, pH, specific conductivity, surface tension, viscosity, and density data of metal complexes.....	38
Table 2: Elemental microanalysis and physical measurement data of M-TC/Sal metal complexes [M=Cd(II), Zr(II), Mo(III), and Pd(II)]....	39
Table 3: Elemental microanalysis and physical measurement data of M-OTC/Sal metal complexes [M=Cd(II), Mo(V), Zr(II), and Pd(II)].....	39
Table 4: FT-IR spectral data of Cd-TC/Sal and Mo-TC/Sal metal complexes in cm^{-1}.....	41
Table 5: FT-IR spectral data of Zr-TC/Sal and Pd-TC/Sal metal complexes in cm^{-1}.....	41
Table 6: FT-IR spectral data of M-OTC/Sal [M=Cd(II), Mo(V)] metal complexes in cm^{-1}.....	42
Table 7: FT-IR spectral data of Zr(II)Otc/Sal and Pd(II)Otc/Sal metal complexes in cm^{-1}.....	42
Table 8: ^1H-NMR spectral data of Cd-TC/Sal, Mo-TC/Sal, Zr-TC/Sal, and Pd-TC/Sal metal complexes.....	44
Table 9: ^1H-NMR spectral data of Cd-OTC/Sal, Mo-OTC/Sal, Zr(II)Otc/Sal, and Pd(II)Otc/Sal metal complexes.....	45
Table 10: ^{13}C-NMR spectral data of Cd-TC/Sal, Mo-TC/Sal, Zr-TC/Sal, and Pd-TC/Sal metal complexes.....	47
Table 11: ^{13}C-NMR spectral data of the Cd-OTC/Sal, Zr(II)Otc/Sal, Mo-OTC/Sal, and Pd(II)Otc/Sal metal complexes.....	48
Table 12: Electronic spectral data of the M-TC/Sal and M-OTC/Sal metal complexes.....	58
Table 13: Kinetics and thermodynamic parameters of the M-TC/Sal metal complexes [M=Cd(II), Mo(III), Zr(II), and Pd(II)].....	61
Table 14: Thermal decomposition data of the M-TC/Sal metal complexes [M=Cd(II), Mo(III), Zr(II), and Pd(II)].....	62
Table 15: Kinetics and thermodynamic parameters of the Cd-OTC/Sal, Mo-OTC/Sal, Zr(II)Otc/Sal, and Pd(II)Otc/Sal metal complexes.....	68

Table 16: Thermal decomposition data of the Cd-OTC/Sal, Mo-OTC/Sal, Zr(II)Otc/Sal, and Pd(II)Otc/Sal metal complexes.....	69
Table 17: Selected bond lengths, bond angles, and bond energies of the M-TC/Sal metal complexes [M=Cd(II), Mo(III), Zr(II), and Pd(II)].....	78
Table 18: Selected bond lengths, bond angles, and bond energies of the M-OTC/Sal metal complexes [M=Cd(II), Mo(V), Zr(II), and Pd(II)].....	82
Table 19: Antibacterial growth data of the Cd-TC/Sal and Mo-TC/Sal metal complexes.....	85
Table 20: Antibacterial growth data of the Zr-TC/Sal and Pd-TC/Sal metal complexes.....	87
Table 21: Antibacterial growth data of the Cd-OTC/Sal and Mo-OTC/Sal metal complexes.....	91
Table 22: Antibacterial growth data of the Zr(II)Otc/Sal, and Pd(II)Otc/Sal metal complexes.....	93

LIST OF FIGURES

	Page No.
Figure 1: Structure of Tetracycline.....	6
Figure 2: Structure of Oxytetracycline and Salicylaldehyde.....	7
Figure 3: Synthetic route of metal complexes of mixed ligands.....	25
Figure 4: Pathogens, A (<i>S. aureus</i>), B (<i>E. coli</i>), C (<i>P. mirabilis</i>), D (<i>P. aeruginosa</i>), E (<i>K. pneumoniae</i>) [Note: scale bar, 1 μ m (A-D), scale bar, 5 μ m (E)].....	34
Figure 5: FT-IR spectrum of Pd-TC/Sal metal complex.....	40
Figure 6: FT-IR spectrum of Cd-OTC/Sal metal complex.....	42
Figure 7: Mass spectrum of Cd-TC/Sal metal complex.....	49
Figure 8: Mass spectrum of Mo-TC/Sal metal complex.....	50
Figure 9: Mass spectrum of Zr-TC/Sal metal complex.....	50
Figure 10: Mass spectrum of Pd-TC/Sal metal complex.....	51
Figure 11: Mass spectrum of Cd-OTC/Sal metal complex.....	52
Figure 12: Mass spectrum of Mo-OTC/Sal metal complex.....	52
Figure 13: Mass spectrum of Zr(II)Otc/Sal metal complex.....	53
Figure 14: Mass spectrum of Pd(II)Otc/Sal metal complex.....	53
Figure 15: Electronic absorption spectra of Cd-TC/Sal and Mo-TC/Sal metal complexes.....	55
Figure 16: Electronic absorption spectra of Zr-TC/Sal and Pd-TC/Sal metal complexes.....	55
Figure 17: Electronic absorption spectra of Cd-OTC/Sal and Mo-OTC/Sal metal complexes.....	57
Figure 18: Electronic absorption spectra of Zr(II)Otc/Sal and Pd(II)Otc/Sal metal complexes.....	57

Figure 19: Thermogram of Cd-TC/Sal metal complex.....	63
Figure 20: Thermogram of Mo-TC/Sal metal complex.....	63
Figure 21: Thermogram of Zr-TC/Sal metal complex.....	64
Figure 22: Thermogram of Pd-TC/Sal metal complex.....	64
Figure 23: Thermogram of Cd-OTC/Sal metal complex.....	66
Figure 24: Thermogram of Mo-OTC/Sal metal complex.....	67
Figure 25: Thermogram of Zr(II)Otc/Sal metal complex.....	67
Figure 26: Thermogram of Pd(II)Otc/Sal metal complex.....	68
Figure 27: SEM micrograph images of M-TC/Sal metal complexes	
[M=Cd(II), Mo(III), Zr(II) and Pd(II)].....	71
Figure 28: SEM micrograph images of M-OTC/Sal metal complexes	
[M=Cd(II), Mo(V), Zr(II), and Pd(II)].....	73
Figure 29: Optimized structure of Cd-TC/Sal metal complex.....	76
Figure 30: Optimized structure of Mo-TC/Sal metal complex.....	76
Figure 31: Optimized structure of Zr-TC/Sal metal complex.....	77
Figure 32: Optimized structure of Pd-TC/Sal metal complex.....	77
Figure 33: Optimized structure of Cd-OTC/Sal metal complex.....	80
Figure 34: Optimized structure of Mo-OTC/Sal metal complex.....	80
Figure 35: Optimized structure of Zr(II)Otc/Sal metal complex.....	81
Figure 36: Optimized structure of Pd(II)Otc/Sal metal complex.....	81
Figure 37: Bar graph of the antibacterial sensitivity of Cd-TC/Sal and	
Mo-TC/Sal metal complexes at 25 (µg/µL) concentration.....	85
Figure 38: Bar graph of the antibacterial sensitivity of Cd-TC/Sal and	
Mo-TC/Sal metal complexes at 12.5 (µg/µL) concentration.....	86
Figure 39: Bar graph of the antibacterial sensitivity of Cd-TC/Sal and	
Mo-TC/Sal metal complexes at 6.25 (µg/µL) concentration.....	86

Figure 40: Bar graph of the antibacterial sensitivity of Cd-TC/Sal and Mo-TC/Sal metal complexes at 3.125 ($\mu\text{g}/\mu\text{L}$) concentration.....	87
Figure 41: Bar graph of the antibacterial sensitivity of Zr-TC/Sal and Pd-TC/Sal metal complexes at 25 ($\mu\text{g}/\mu\text{L}$) concentration.....	88
Figure 42: Bar graph of the antibacterial sensitivity of Zr-TC/Sal and Pd-TC/Sal metal complexes at 12.5 ($\mu\text{g}/\mu\text{L}$) concentration.....	88
Figure 43: Bar graph of the antibacterial sensitivity of Zr-TC/Sal and Pd-TC/Sal metal complexes at 6.25 ($\mu\text{g}/\mu\text{L}$) concentration.....	89
Figure 44: Bar graph of the antibacterial sensitivity of Zr-TC/Sal and Pd-TC/Sal metal complexes at 3.125 ($\mu\text{g}/\mu\text{L}$) concentration.....	89
Figure 45: Bar graph of the antibacterial sensitivity of Cd-OTC/Sal and Mo-OTC/Sal metal complexes at 50 ($\mu\text{g}/\mu\text{L}$) concentration.....	91
Figure 46: Bar graph of the antibacterial sensitivity of Cd-OTC/Sal and Mo-OTC/Sal metal complexes at 25 ($\mu\text{g}/\mu\text{L}$) concentration.....	92
Figure 47: Bar graph of the antibacterial sensitivity of Cd-OTC/Sal and Mo-OTC/Sal metal complexes at 12.5 ($\mu\text{g}/\mu\text{L}$) concentration.....	92
Figure 48: Bar graph of the antibacterial sensitivity of Zr(II)Otc/Sal and Pd(II)Otc/Sal metal complexes at 50 ($\mu\text{g}/\mu\text{L}$) concentration.....	93
Figure 49: Bar graph of the antibacterial sensitivity of Zr(II)Otc/Sal and Pd(II)Otc/Sal metal complexes at 25 ($\mu\text{g}/\mu\text{L}$) concentration.....	94
Figure 50: Bar graph of the antibacterial sensitivity of Zr(II)Otc/Sal and Pd(II)Otc/Sal metal complexes at 12.5 ($\mu\text{g}/\mu\text{L}$) concentration.....	94

LIST OF SCHEMES

	Page No.
Scheme 1: The scheme for the synthesis of the M-TC/Sal [M= Cd(II), Zr(II), Mo(III), Pd(II)] metal complexes of mixed ligand.....	74
Scheme 2: The scheme for the synthesis of the M-OTC/Sal [M=Cd(II), Mo(V)] metal complexes of mixed ligand.....	74
Scheme 3: Proposed structure of the M-Otc/Sal [M= Zr(II), Pd (II)] metal complexes of mixed ligand.....	74

TABLE OF CONTENTS

	Page No.
Declaration.....	ii
Recommendation	iii
Letter of Approval.....	iv
Acknowledgements.....	v
Abstract	vii
शोधसार.....	ix
List of Acronyms and Abbreviations	xi
List of Symbols.....	xiii
List of Tables	xiv
List of Figures	xvi
List of Schemes	xix

CHAPTER 1

1. INTRODUCTION.....	1
1.1 General Perspective	1
1.2 Mixed Ligand and Their Chemistry	2
1.3 Biological Applications of Mixed Ligands and their Metal Complexes	3
1.4 Other Applications of Mixed Ligands and their Metal Complexes	3
1.5 Tetracycline Under Investigation	4
1.6 Oxytetracycline Under Investigation	6
1.7 Choice of Metallo-Elements Under Investigation.....	7
1.7.1 Cadmium.....	8
1.7.2 Zirconium.....	9
1.7.3 Molybdenum	9
1.7.4 Palladium.....	10
1.8 Rational of the Study.....	11
1.9 Objectives of the Present Study.....	11
1.9.1 General Objective	11
1.9.2 Specific Objective	11

1.10 Justification of the Study	12
---------------------------------------	----

CHAPTER 2

2. LITERATURE REVIEW	13
2.1 General Overview	13
2.2 Pharmaceutical and Biomedical Applications.....	14
2.3 Catalytic Applications	16
2.4 Applications in Modern Technologies	18
2.5 Surfactant and Corrosion Inhibition Applications.....	19
2.6 Research Gap.....	22

CHAPTER 3

3. MATERIALS AND METHODS.....	23
3.1 Materials/ Reagents	23
3.2 Synthesis of Metal Complexes	24
3.2.1 Synthesis of Cd-TC/Sal Metal Complex	24
3.2.2 Synthesis of Mo-TC/Sal Metal Complex	25
3.2.3 Synthesis of Zr-TC/Sal Metal Complex.....	25
3.2.4 Synthesis of Pd-TC/Sal Metal Complex	26
3.2.5 Synthesis of Cd-OTC/Sal Metal Complex	26
3.2.6 Synthesis of Mo-OTC/Sal Metal Complex	26
3.2.7 Synthesis of Zr(II)Otc/Sal Metal Complex	26
3.2.8 Synthesis of Pd(II)Otc/Sal Metal Complex.....	26
3.3 Characterization Techniques	27
3.3.1 Elemental Microanalysis	27
3.3.2 pH Measurement	27
3.3.3 Conductivity Measurement	28
3.3.4 Electronic Absorption Spectroscopy (EAS).....	28
3.3.5 FT-IR Spectral Study	28
3.3.6 ¹ H & ¹³ C-NMR Spectral Study	29
3.3.7 ESI-MS Spectral Study	29
3.3.8 TGA/DTA Study	29
3.3.9 Surface Morphology Analysis	30
3.4 Computational Study.....	30

3.5	Antibacterial Sensitivity Study.....	30
3.5.1	Sterilization of Equipment	31
3.5.2	Procedure for the Preparation of Media	31
3.5.3	Preparation of Culture Medium.....	31
3.5.4	Organism Information	32
3.5.5	Preparation of Paper Disc.....	35
3.5.6	Loading of Chemicals	35
3.5.7	Inoculation of Organisms and Measurement of Growth Inhibition Zone	35

CHAPTER 4

4.	RESULTS AND DISCUSSION.....	36
4.1	Physical Measurements	36
4.1.1	Colour	36
4.1.2	Solubility and Melting Points	36
4.1.3	Conductivity Measurement	37
4.1.4	pH Measurement	37
4.1.5	Surface Tension	37
4.1.6	Density.....	37
4.1.7	Viscosity	38
4.2	Micro analytical Results	38
4.3	Spectroscopic Results and Discussion	39
4.3.1	FT-IR Spectral Study	39
4.3.1.1	FT-IR Spectral Study of M-TC/Sal Metal Complexes	39
4.3.1.2	FT-IR Spectral Study of M-OTC/Sal Metal Complexes	41
4.3.2	¹ H & ¹³ C-NMR Spectral Study	42
4.3.2.1	¹ H-NMR spectral study of M-TC/Sal metal complexes.....	43
4.3.2.2	¹ H-NMR spectral study of the M-OTC/Sal metal complexes..	44
4.3.2.3	¹³ C-NMR Spectral Study of the M-TC/Sal Metal Complexes.	46
4.3.2.4	¹³ C-NMR Spectral Study of the M-OTC/Sal Metal Complexes	48
4.3.3.	Mass Spectral Study	49
4.3.3.1	Mass Spectral Study of M-TC/Sal Metal Complexes	49

4.3.3.2	Mass Spectral Study of M-OTC/Sal Metal Complexes	51
4.3.4	Electronic Absorption Spectroscopy (EAS).....	54
4.3.4.1	EAS of M-TC/Sal Metal Complexes.....	54
4.3.4.2	EAS of M-OTC/Sal Metal Complexes.....	56
4.4	Thermal Analysis	58
4.4.1	TGA/DTA Study of M-TC/Sal Metal Complexes	60
4.4.2	TGA/DTA Study of M-OTC/Sal Metal Complexes	65
4.5	Scanning Electron Microscope Study	69
4.5.1	SEM Study of M-TC/Sal Metal Complexes	69
4.5.2	SEM Study of M-OTC/Sal Metal Complexes.....	71
4.6	Proposed Molecular Structures and Geometry.....	73
4.7	Molecular Modeling Study.....	75
4.7.1	Molecular Modeling Study of M-TC/Sal Metal Complexes.....	75
4.7.2	Molecular Modeling Study of the M-OTC/Sal Metal Complexes....	79
4.8	Antibacterial Sensitivity Study.....	83
4.8.1	Antibacterial Sensitivity Study of M-TC/Sal Metal Complexes.....	84
4.8.2	Antibacterial Sensitivity Study of M-OTC/Sal Metal Complexes....	90

CHAPTER 5

5.	CONCLUSION AND RECOMMENDATIONS	95
5.1	Conclusion.....	95
5.2	Recommendations	97

CHAPTER 6

6.	SUMMARY	98
-----------	----------------------	-----------

REFERENCES	100
-------------------------	------------

APPENDIX.....	130
----------------------	------------

List of instruments and glassware apparatus

List of chemicals and reagents

Solubility data of metal complexes of mixed ligand

List of publications and scientific paper presentations

Antibacterial activity against pathogenic bacteria with
M-TC/Sal and M-OTC/Sal metal complexes

FT-IR spectral study of M-TC/Sal metal complexes

(¹H & ¹³C)-NMR spectral study of metal complexes

CHAPTER 1

INTRODUCTION

1.1 General Perspective

Today, the transition metal complex of coordination chemistry has attractive fields due to its wide applications in the fields of catalysis, photochemistry, bioinorganic, photophysics, and supramolecular chemistry (Al-Noaimi *et al.*, 2014). Coordination chemistry encourages researchers and chemists to prepare broad-spectrum antibiotics for biological, agricultural, analytical, clinical, medical, and therapeutic applications respectively (Damena *et al.*, 2022; Gupta *et al.*, 2021). Herbal-derived medicines are a traditional way of treating human diseases for ages (Tistaert *et al.*, 2011). Medicinal plants (Herbal) can be easily contaminated by absorbing heavy metals through the air, water, and soil. These heavy metals eventually enter the human body through consumption and can disrupt the normal function of kidneys, lungs, heart, and different types of cancer cells (Shaban, *et al.*, 2016). Therefore, medical inorganic chemistry is of great interest for researchers to develop new biologically active compounds. A variety of literature suggests that the bonding of drugs with metal ions increases their activity, with the complexes having a more curative nature than the parent drug (Mahmoud, *et al.*, 2013). The application of metal and metal complexes in medical science is increasing due to an increase in clinical and commercial purposes. Metal complexation is a method through which some metal ions can coordinate with organic functional ligands with an ionic bond, many interesting properties, and application for organometallic compounds with ion-dipole interactions (Mahmoud, *et al.*, 2015).

In the reported research, the complex formation between bioactive ligands (binding sites) and metal ions has gained great interest for researchers because they are used in various fields of coordination chemistry (Shobana, *et al.*, 2015). In coordination chemistry, metal ions, and ligands play an important role (Abebe & Hailemariam, 2016). In coordination chemistry, metals are concerned with coordination number,

geometry, thermodynamic and kinetic parameters of the ligand, and wide structural diversity (Rijt, *et. al.*, 2009).

Antibiotic resistance is a global problem that causes severe environmental and health, which can be reduced by awareness and strict regulation of antibiotic use (Siddappa, *et. al.*, 2014; Pulicharla *et al.*, 2017; Feio *et al.*, 2014; Gao *et al.*, 2021). These antibiotics are either natural or human-made compounds that are mostly used for bacterial infections and to improve the health of living plants and animals (Bouki *et al.*, 2013). So, the important objective of the current studies for researchers and chemists is the development and discovery of more powerful and better drugs that can solve the global problem, which is why most research work is being done in the field of metal-drug interactions (Adediji *et al.*, 2009).

1.2 Mixed Ligands and Their Chemistry

Metal complexes are widely used organic compounds, which are prepared by continuous stirring and refluxing the equimolar mixture of the primary ligand, secondary ligand, and their metal salts. Varieties of organic compounds applied in medicinal fields do not have organic action in the pure state but contain metal ions that may actively or indirectly help inactivation. Our human body contains 0.03 % metal ions and its complexes combine with their biomolecules. The ligand contains donor atoms (N, O, S, and P) that can easily coordinate with metal ions and behave as Lewis bases. The complex formation gives rise to Lewis acid-base reactions. Therefore, the organic nature of the ligand as well as the extent of metal degradation are significantly altered, resulting from the synergistic effect between ligand and metal ion (Refat *et al.*, 2014).

Organometallic compounds cannot have more than one metal bond of carbon, as in the case of Zeise's, the first platinum-based synthesized metal complex of an organic compound. Subsequently, most of the complexes were synthesized with the help of dissimilar transition metals like Zr, V, Ti, Ir, Cr, Mn, Fe, Co, Os, Pt, Pd, etc. These transition metal complexes have vast applications in the fields of catalysis, agricultural and biochemical, optics, and electroluminescent devices, and are mostly used in biological fields such as antimicrobial, anticancer, and antifungal activities

(Nandanwar & Kim, 2019). However, metal bonding with biologically active molecules can be used to overcome these activities. Quinolones can easily coordinate with metal ions; therefore, many studies have been done between quinolones and metallic ions (El-Halim *et al.*, 2011).

1.3 Biological Applications of Mixed Ligands and Their Metal Complexes

Metal complexes show good nucleolytic cleavage and help in the activation of enzymes. These complexes help in the storage and transport of active substances through the membranes. Schiff bases obtained through isatin show antipharmacological and neurophysiological effects such as antiviral, anticancer, antifungal, antimicrobial, antimycobacterial, herbicidal, antimalarial, antiprotozoal, cysticidal, and antihelminthic activity (Devi & Batra, 2015). The biological and toxic effects of platinum and palladium complexes in coordination chemistry are used in the pharmacological field. They also show biological importance because of their anticancer, antiamebic, antitumor, and catalytic behavior (Sharma and Sharma, 2011).

Drug interactions with biologically active compounds help to improve activity and overcome antibiotic resistance (El-Halim *et al.*, 2011). Metal complexes in many branches of analytical and biomedical fields like chemical science, magneto, and photochemistry, industrial and physical science, pollution control, antibacterial, antifungal, antithyroid, antipyretic, antitumor, antimycotic, antiviral, antimetabolites, anti-inflammatory, and surface anesthetic activities have wide applications (Ghanghas *et al.*, 2021; El-Sonbati *et al.*, 2020; Abu-Dief *et al.*, 2015; Shobana *et al.*, 2015).

1.4 Other Applications of Mixed Ligands and Their Metal Complexes

Metal complexes of organo trithiocarbonates are applied in the areas of analysis, agriculture, organic synthesis, medicine, and industry. Some of these applications are vulcanization, accelerators, pesticides, rust inhibitors, floatation agents, lubricating oil additives, etc., but some have anti-radiation drug activity (Alias *et al.*, 2014).

Most drugs have advanced toxic and medicinal properties as they occur in the form of metals. The metalloantibiotics used can reduce the dose and enter the body, increase bioavailability, and benefit the pharmacological effects of both metal ions and ligands (Ramotowska *et al.*, 2020). The stable complex formation is because of a lone pair electron of the azomethine (-N=CH-) group of the nitrogen atom of their structure. Thus, the obtained complexes have significant use in most biological fields such as biochemistry, molecular magnetism, and supramolecular chemistry (El-Sonbati *et al.*, 2019). In recent times, the potential of MOFs has been known. They are highly porous, heterogeneous solid-state compounds with pores of specific size and can uptake guests such as gases or soluble small molecules (Pullen & Clever, 2018).

The DNA-binding activity of transition-metal complexes is useful due to their potential use in drugs, tools for molecular biology, regulation of gene expression, and nano-technology. Cisplatin and platinum-based drugs used in the clinical field are used as anticancer agents that can covalently bind to DNA (Barve *et al.*, 2009; Medici *et al.*, 2015). Coumarins and their derivatives are well-known organic compounds found in various food sources such as herbs, fruits, and vegetables. They have wide applications in medical drugs such as spasmolytics, anticancer, antibacterial, anticoagulant, antifungal, and biological inhibitors, etc. (Kose *et al.*, 2014). Cd, In, and Pb oxides are components of advanced functional materials associated with solar cells and thin-film transistors. They can form coordination polymers and cluster complexes. The coordination complex helps to synthesize metal oxides and study sol-gel behavior (Khanderi *et al.*, 2016).

1.5 Tetracycline Under Investigation

Infection in our body is a complex mechanism caused by the entry of microbes such as viruses, fungi, bacteria, etc., and other factors such as trauma with physical and chemical agents. Today, most people die from infectious diseases caused by the bacteria, as their early diagnosis is lacking. Diagnosis helps to identify the root cause of infection. Scientists in the world received much attention in the field of antibiotic-drug interaction, and eventually, penicillin was discovered by Sir Alexander Fleming. Many antibiotics were discovered after this drug (Rolain *et al.*, 2016; Alanis, 2005; Zakeri and Lu, 2013).

Antibiotics are organic compounds mostly used to treat human infectious diseases, animal husbandry, and veterinary medicine. Due to its soluble nature, most antibiotics used by humans and animals are expelled or released into the environment in the form of urine or feces. As a result, the direct transfer of antibiotics takes place in humans (Chen *et al.*, 2019; Zhang *et al.*, 2015; Xiong *et al.*, 2018). TC antibiotics are widely used by human action. Once they are mixed into the water cycling system, they will pose a threat to human health and the environment (Cao *et. al.*, 2018). The discovery of tetracycline antibiotics in the 1940s by Dr. Benjamin Ming Dugar was widely used in the clinical field. The naturally occurring TCs are highly excessive type II polyketides, composed of a linear fusion of tetracyclic scaffolds, which are labeled as A, B, C, and D (**Fig. 1**). The 30S ribosome subunit inhibits the protein synthesis of bacteria by binding to 16S r-RNA and inhibits the accumulation of incoming aminocellic t-RNA of their acceptor site (A-site) (Markley & Wencewicz, 2018). TC also has many potential binding sites because it contains donor atoms: the oxygen atoms in the C10–C12 keto-phenol system, the nitrogen atom in C4, enolic oxygen in C3, and the carboxamide group of ring A. Currently, TCs is used to cure a variety of bacterial infections, such as eye infections, chlamydia, acne, urinary tract infections, pneumonia, periodontitis, rosacea, malaria, syphilis, and rheumatism etc. (Guerra *et al.*, 2016).

TC is the first antimicrobial agent with a wide range of bacteria. Before three decades, many developments have taken place in the field of bacterial resistance to TCs. Thus, these activities reduce the therapeutic use of antibiotics in human beings. Today, antibiotic resistance is a global health problem caused by the misuse and overdose of antibiotics, so awareness and strict regulation of antibiotics should be taken care (Pulicharla *et al.*, 2017). Due to its low cost and high antimicrobial activity, TC was used in the market of developing countries of the world. For example: in China, 1450 tons of TC were used in 2013. Also due to the soluble and incomplete metabolic nature of humans and animals, TCs are often detected in the aquatic system (Xie *et al.*, 2019).

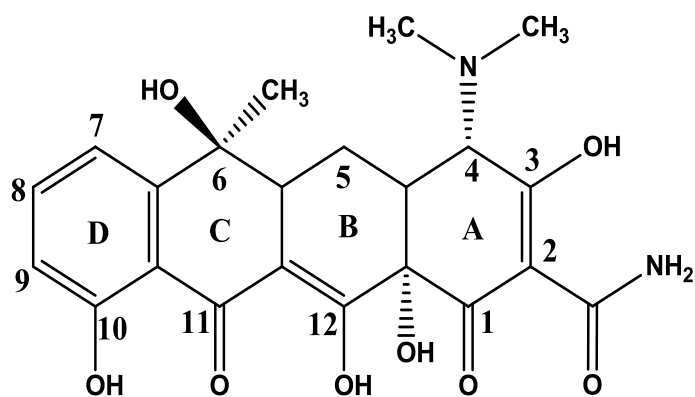


Figure 1: Structure of Tetracycline

1.6 Oxytetracycline Under Investigation

The role of metal complexes in the field of modern pharmacology is continuously increasing. Today, due to the increased antibiotic resistance, it is necessary for researchers and chemists to search for effective and powerful antibiotics to address the global issue (Ramotowska *et al.*, 2020). In recent years, many antibiotic residues have been detected in both soil and water environments, resulting in bacterial resistance among pathogenic microorganisms. Therefore, effective methods are applied for the unwanted pollution in seawater by using various technologies such as oxidation, adsorption, photochemical degradation, and enzymatic degradation (Hu *et al.*, 2017).

OTC is also a broad-spectrum antibiotic isolated from bacteria, called *Streptomyces rimosus*, which is found in soil. The main function of OTC is to inhibit protein synthesis inside bacteria (Leal *et al.*, 2018). OTC is also a broad-spectrum antibiotic. Structurally, OTC (**Fig. 2**) contains a naphthacene ring, as in the case of TC which contains multiple metal-binding sites. The only difference between TC is due to the substituent -OH group at C5 of the ring structure (Tongaree *et al.*, 1999). OTC is also related to TCs, which have many ionizable functional groups. The presence of amine and acid/base-active phenolic hydroxyl groups helps OTC undergo protonation and deprotonation reactions (Yuan *et al.*, 2019).

OTC is used to treat many diseases like acne, sinusitis, bronchitis, cholera, urinary tract infection, relapsing fever, leptospirosis, and many more. It is considered a growth promoter and is often used in animal breeding, such as in fish farms and swine feeding fields. The antibiotic entering the aquatic environment through industrial wastewater can be removed by conventional methods such as sedimentation, disinfection, digesters, and chemical coagulation techniques (da Silva *et al.*, 2015; Niazi *et al.*, 2008).

Currently, OTC is used in the survey analysis of soil adsorption behavior and the environment. Factors such as soil type, particle size, cation species, organic matter content, and aluminum and iron hydrous oxide (Cheng *et al.*, 2013). Similarly, the determination of a low concentration of OTC requires highly sensitive analytical techniques such as luminescence. It is characterized by HPLC (high-performance liquid chromatography), spectrophotometric, electrochemical, solid surface room-temperature phosphorescence, time-resolved luminescence, and second-derivative synchronous spectrophotometric techniques (Yegorova *et al.*, 2006).

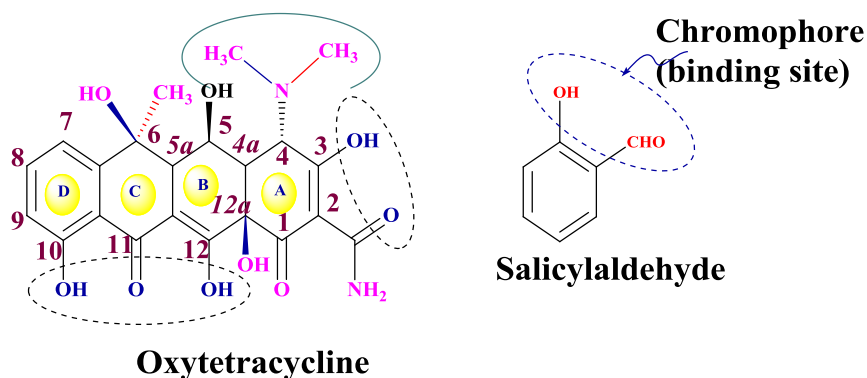


Figure 2: Structure of Oxytetracycline and Salicylaldehyde

1.7 Choice of Metallo-Elements Under Investigation

In coordination field studies, metal ions combined with different types of ligands enhanced the current development of medical and biomedical chemistry (Omar *et al.*, 2017). The coordination compound exhibits various properties on which the ligand-bound with metal ions forms a metal complex. The complexes were implemented in various areas of human interest. Also, they find large applications in the industry, as

well as food, pharmaceutical, and animal feed supplements (Abdel-Rahman *et al.*, 2017).

Metal complexes with heterocyclic ligands contain donor atoms such as nitrogen, oxygen, and sulfur. The study of such ligands is important for medicine because they have the potential properties of chelation to remove toxic metals from the body (Shoukry & Al-Mhayawi, 2013).

Today, environmental pollution is a major problem for the modern world because of contamination and pollution by heavy metals caused due to rapid urbanization and industrialization. Pollution is also caused by natural disasters such as volcanic eruptions, weathering of rocks containing metals, anthropogenic sources such as smelting, mining, industrial emissions, and agricultural activities like phosphate fertilizers and pesticides are also the cause of the pollution (Ali *et al.*, 2019). Vitamin C, also known as ascorbic acid, contains electron donor groups in biological systems. The acid acts as an antioxidant and protects against damage to living cells of the human body (Chandrathilaka *et al.*, 2013).

In the present study, 4d-transition metal salts viz. were selected for the preparation of the Cd(II), Zr(II), Pd(II), Mo(III)/(V) complexes. The above metal salts are partially or d-orbitals filled and exhibit an important role in the complexity of metal ion behavior. Therefore, the coordination of metal ions with organic ligands changes the biological profile of the molecules. Several research studies have enhanced the biological activities of ligands after complex formation. 4d-transition metals also possess complex formation properties with organic ligands and are found to possess superior biological functions.

1.7.1 Cadmium

In the field of coordination chemistry, cadmium (II) is of substantial interest due to its effect on the environment, toxic effect on marine organisms, and complexation by metallothioneins (Saghatforoush *et al.*, 2008; Al-Maythalyony *et al.*, 2008). During both acute and chronic exposure, cadmium is highly toxic to all living mammals. During the biological system, Cd²⁺ remains as a coordination complex with a

biological ligand and its toxicity is beyond doubt during the chelation process (Bernhoft, 2013; Bie *et al.*, 2020; Sun *et al.*, 2017). Because of the d^{10} configuration, cadmium forms complexes with a coordination number of four to eight and acts as a photoluminescence material, which shows the nature of fluorescence (Bie *et al.*, 2020). In living beings, cadmium is toxic and can be found as a part of complexes with the ligand. The biological function of the ligand is disrupted during coordination. Therefore, cadmium compounds can hamper the CNS (central nervous system), kidney, and cancer to the connective tissues, lungs, and liver (Singh *et al.*, 2017). Cadmium reduction occurs during inhalation and ingestion. Smoking plays an important role in tobacco due to the presence of heavy metal cadmium (Merian, 1990).

1.7.2 Zirconium

The chemistry of zirconium metal complexes has been widely studied due to its application in catalysts for polymerization. The use of oxygen donor atoms by these complexes during coordination is also concentrated (Singh *et al.*, 2013). Biologists and scientists can know the nature and interactions of metal-ligand in aqueous solutions with the help of the structure of zirconium-amino acid complexes (Pan *et al.*, 2008). Similarly, zirconium and hafnium can easily form a stable complex with phenol, catechol, oxo, and carbonic acids (Tomachynski *et al.*, 2001). Therefore, zirconium acts as a homogeneous catalyst in several organic pharmacological and biological changes (Sharma *et al.*, 2011). Recently, much attention has been paid to Zr-based metals organic frameworks (MOFs) because of their properties such as sensor materials, catalysts, and adsorbents (Oien *et al.*, 2014).

1.7.3 Molybdenum

In the field of coordination chemistry, molybdenum has interesting fields of research at present days, which is due to the presence of molybdenum in metalloenzymes as well as its importance in the catalytic and biochemical fields (Pasayat *et al.*, 2012). Molybdenum also focuses on researchers due to its oxidation state, ligating atoms, coordination numbers, reactivity, effects on structure, and the potential importance of its compound. Molybdenum is a biologically active trace metal that takes participation

in redox-active sites of molybdo-enzymes and is, therefore a micronutrient for animals, plants, and microorganisms (Maurya *et al.*, 2011; Nair *et al.*, 2011). Molybdenum is a versatile transition metal and has more stable and accessible oxidation states. Therefore, it plays an important role in biochemistry and catalytic chemistry (Ahmed *et al.*, 2012).

Nassar *et al.*, (2013) reported that molybdenum trioxide (MoO_3) is not only rich in chemistry with many valence states as well as high chemical and thermal stability. Molybdenum and tungsten are used to manufacture materials for various engines that can operate through halogen medium at high temperatures (Sliznev & Belova, 2016). The enzymatic role of molybdenum is in biochemical reactions, mainly in the oxidation of aldehydes, sulfides, and purines. They also play an important role in various chemicals such as oxygen transfer, hydro sulfurization, and olefin metathesis (Ahmed & Lal, 2013). Molybdenum complexes can also catalyze nitrogen fixation by microorganisms in plants (Taher *et al.*, 2010).

1.7.4 Palladium

Palladium is the most versatile transition metal with catalytic properties. Their complexes have a wide range of C-C coupling, hydrocarbon oxidation reactions, and C-H functionalization. For example, in 2010 A.D., the palladium-catalyzed reaction received the Nobel Prize in chemistry. Palladium has five oxidation states: 0, +1, +2, +3, +4, and +5. In the past, the Pd-catalyzed reactions have involved Pd (0) and Pd (II) oxidation states and have been investigated in detail (Nagalakshmi *et al.*, 2020; Mirica & Khusnutdinova, 2013). The Pd complex bears a good relationship between cytostatic and lipophilicity. The main importance of the Pd complex is that renal toxicity from cisplatin is less because of its metal-containing anticarcinogenic nature and is approximately 105-fold more reactive than Pt (II) complexes (Sharma *et al.*, 2016; Soliman *et al.*, 2016; Wang *et al.*, 2013).

Palladium dithiocarbamates are applied as catalysts, anticancer agents, and materials science. Currently, palladium is a chromogenic sensor for assessing mercury and the preparation of nanoscale materials (Prakasam *et al.*, 2016). Palladium is also an important metal for metallodrugs because it exhibits structural characteristics

compared to platinum and exhibits *in vitro* cytotoxicity. Therefore many scientific papers have been published about the antimicrobial, anticancer, antiviral, and antifungal activities of various palladium (II) metal complexes (Sharma *et al.*, 2016; Rubino *et al.*, 2017).

1.8 Rational of the Study

In recent years, increased antibacterial resistance due to misuse or overdose of antibiotics has become a global health problem. Most natural antibiotics have lost their action. Therefore, synthesizing or finding new potentially effective drugs in the field of coordination chemistry is a very big challenge for chemists and researchers.

1.9 Objectives of the Present Study

1.9.1 General Objective

The general objectives of the research work are synthesis, characterization, and evaluation of biological activities of heteroleptic complexes of Tetracyclines and salicylaldehyde mixed ligands.

1.9.2 Specific Objective

The present research work has the following specific objectives:

- Synthesis of metal complexes of mixed ligands using the primary ligand, Tetracycline/Oxytetracycline (TC/OTC), secondary ligand, salicylaldehyde (Sal), and 4d-transition metal salts [M= Cd(II), Zr(II), Mo(III)/(V), and Pd(II)].
- Measurement of the physical parameters and thermal analysis (TGA/DTA) of the synthesized metal complexes.
- Characterization of synthesized complexes using spectroscopic techniques (FT-IR, ¹H & ¹³C-NMR, UV/Visible, ESI-MS) and SEM studies.
- Investigation of the antimicrobial activities of metal complexes using the modified Kirby-Bauer Paper disc diffusion method

1.10 Justification of the Study

The metal complexes are useful for their trace and ultra-trace amounts and help with the normal body physiological function. The complexes have wide applications in various fields of chemistry. Today, there is a great challenging demand for researchers and chemists in Pharmaceuticals for the development of better active drugs to cure diseases. However, there is no research work related to metal complexes in the literature search. Because of the current global antibiotic resistance crisis, laboratory-based metal complexes were prepared using the TCs (primary ligand), Sal (secondary ligand), and 4d-transition metal salts [M= Cd(II), Zr(II), Mo(III)/(V), and Pd(II)]. Thus, the obtained synthesized compounds will be new hope for the development of better and more efficient antibiotic drugs in the field of therapeutics.

CHAPTER 2

LITERATURE REVIEW

2.1 General Overview

In the field of coordination chemistry, many research studies have been done in the present day due to their vast applications in various areas. Therefore, chemists and researchers are interested in working day and night to find fruitful results. Their applications will also be accompanied by numerous research works based on their synthesis, spectroscopic characterization, and antibacterial activities.

On the occasion of the 100th anniversary in 2013, the award was the first Nobel Prize for inorganic chemistry. Their work was based on coordination chemistry, which eventually gave rise to broad areas in modern chemistry such as catalysis, supramolecular, nanotechnology, and bioinorganic, metal-based chemistry (Constable & Gale, 2013). Alfred Werner's work on the structure of metal complexes has helped chemists and research investors to learn about metal-based drugs that support the drug action mechanisms, oxidation states, types, and geometry along with the number of coordinate ligands. In the 1990s, Kopf and Kopf-Maier were performed in a wide range of tests on metallocene complexes, which gave rise to titanocene dichloride in clinical trial action (Barry & Sadler, 2014; Zhang & Sadler, 2017).

For many years, Nickel has been considered a biological element participating in life development without any biological role. In 1975 A.D, this attitude changed when Nickel was found to be an active center of the enzyme urease. Because of its biological activity, nickel has many applications in fields such as antibiotics, antitumors, antiepileptics, and anticonvulsants. Additionally, Ni (II) complexes have been investigated for their antimicrobial, antioxidant, antiproliferative, and antileishmanial activity (Totta *et al.*, 2017). In 1983, Henry Taube was awarded the

Nobel Prize in coordination chemistry. His creative work was based mostly on experimental methods (Creutz *et al.*, 2006).

In 2005 A.D., the first metal complex acesulfame, namely bis (acesulfame- t_2N_3, O_4) bis (2-amino pyrimidine- tN_1) copper (II) was the first mixed ligand complex in the literature. Their structure was analyzed using the X-ray technique (Yurdakul & Kose, 2014).

In the 1980s two scientists, Marshall and Warren proved that *Helicobacter pylori* (*H. pylori*) is an important cause of peptic ulcers caused by consumption of spicy food, stress, and excess acid. In 2005, he received the Nobel Prize in Physiology and Medicine because of his great work and outstanding findings. The three scientists (W.S. Knowles, R. Noyori, and K.B. Sharpless) worked on the synthesis of catalytic asymmetric compounds and received the Nobel Prize. Similarly, Y. Chauvin, R. H. Grubbs, and R. R. Schrock worked on organic synthesis using the metathesis technique and received the Nobel Prize in 2005. In 2010, three scientists, namely E. Negishi, R. F. Heck, and A. Suzuki received the scientific and prestigious award for palladium-catalyzed cross-coupling development. With the help of the above discoveries, the door has been opened for the chemical and pharmaceutical industries to prepare products such as plastics, medicines, and many other useful products (Turel, 2015).

2.2 Pharmaceutical and Biomedical Applications

The fields of coordination chemistry are of current interest to researchers and scientists because of their vast application in various fields like antimicrobial, nonlinear optical, and electrical conductivity (Al-Noaimi *et al.*, 2014). Owing to the rapid progress of nanostructured materials, which have helped to create vast applications in biomedical fields such as drug delivery specific sites, novel tissue-engineering scaffolds, biosensing, and screening, therapeutics, and medical bio-analytical diagnostics. Examples include nanocomposites that stabilize and regenerate bone matrices, a biosensor for nanowires, and nanotubes (Xu *et al.*, 2007). Bridging ligands and metal connectors are selected in various fields such as ion exchange, separation and adsorption processes, drug delivery, sensor technologies, biomimetic catalysis, proton conductivity, and heterogeneous activity (Okasha *et al.*, 2019).

Porphyrin compounds are important for developing biomedical applications such as phototherapy, boron neutron-capture agents, and X-ray radiation enhancement. These surveys helped the ligands of saturated macrocyclic to design and tune their properties through chelation modifications (Mewis & Archibald, 2010). An interesting application of click reactions in the field of polymer science is considered an immediate achievement in biomedical science. Their applications in pharmacology are drug delivery, nanomedicine, linker chemistry, and so on (Hein *et al.*, 2008; Deming, 2007).

Aspartic acid is a naturally occurring amino acid that acts as an active center of some enzymes. It has three possible donor sites (one with an amine group and two carboxyls) and the coordination behavior may be investigated by comparing the complexes with a central metal with similar valency at certain pH values. Histidine, arginine, glutamic, and aspartic acid are the coordination compounds of amino acids. These compounds exhibit good antimicrobial properties (Aiyelabola *et al.*, 2016).

The most common amino acid is glutamic acid (Glu) (2-Aminoglutamic), which acts as a building block for protein synthesis. The acid is applied in biochemistry and brain memory, and acts as an anticancer drug by reducing toxicity against normal cells. Glutamic acid and the three possible coordination sites of a flexible skeleton help the complex behavior of the bi- or trident ligands. Similarly, arginine is an important amino acid that is physically active in the L-form. Antimicrobial activity behavior is enhanced against fungi and bacteria by L-arginine (Abdel-Mottaleb & Ismail, 2019).

Heterometallic transition-metal complexes have wide applications such as catalytic activity, magnetic devices, and liquid crystalline materials such as sensor design and finally therapeutic drugs (Majumder *et al.*, 2018). Similarly, 1,10-phenanthroline can synthesize metal complexes with the help of metal ions, because of its rigid central ring structure. In biological science, 1, 10-Phenanthroline and its derivatives are used in anti-mycoplasma, antifungal, and antibacterial studies (El-Halim *et al.*, 2017).

Beyond gold and silver, various bismuth, antimony, and mercury are used to prevent parasitic and bacterial infections. Likewise, *H. pylori* against leishmaniasis, bismuth, and antimony complexes are used to eradicate *H. pylori* infection. Also, arsenic

trioxide (As_2O_3) is the reference drug for the treatment of acute promyelocytic leukemia. Many inorganic complexes are used as gadolinium-based agents in clinical medicine (Bonaccorso *et al.*, 2020).

2.3 Catalytic Applications

Transition metal complexes, in the field of coordination chemistry, show very powerful catalytic properties in many organic reactions. Some of the important industrial water-gas shift reactions are converted by bacterial enzymes i.e. conversion of H_2O and CO into H_2 and CO_2 . A simple and inexpensive catalyst can mimic many other enzyme actions known as biomimetic or bioinspired catalysis. Cadmium is a toxic element that affects an organism through interference with a zinc-mediated cellular method. Under rare zinc conditions, marine diatoms can synthesize cadmium carbonic anhydrase (CDCA) enzymes that can exchange catalysis for either Zn or Cd (Pladzyk *et al.*, 2011).

Researchers and chemists are attracting great interest in multinuclear metal complexes because of their interesting functions and structures. Some metal complexes are used as catalysts in organic synthesis and enzyme model reactions. Covalently bonded macrocyclic polydent ligands are used by metal groups in space. In the chemistry of host-guest relations, a host molecule multiplies the recognition for guest molecules and plays an important role in catalysis, also used for molecular sensing, ionic/proton sensory conductivity, and biochemical and drug delivery mimics the active site for known metalloenzyme (Nath *et al.*, 2020).

Complexes of iron, pyridine-2, and 6-dicarboxylic acid were applied in water-soluble drugs, heterogeneous catalysts, enzyme inhibitors, and electron carriers. For the preparation of nanoparticles, inorganic complexes act as starting materials with the help of the thermal decomposition of small particles and high surface area. The thermal decomposition of nanoparticles can be controlled by the size, purity, and distribution of inorganic compounds (Razmara *et al.*, 2019).

One of the important trace elements is molybdenum, which can be part of the enzyme structure and catalyze redox reactions because it can combine with inorganic

compounds important for the formation of metal complexes. As simple molybdates, molybdenum can also absorb, transport, and emit its products. Plant growth and development can be achieved by molybdenum during nitrogen fixation and nitrate reduction. A variety of reactions such as metathesis, olefin epoxidation, and isomerization of allyl alcohol can catalyze the coordination compounds of molybdenum (Maurya *et al.*, 2011).

Earth's most abundant metal, i.e. vanadium, is of great interest for the design and oxidation of catalysts. The catalyst for the oxidation reaction is oxovanadium complexes that can catalyze aerobic oxidation with higher selectivity and better yields than secondary alcohols. Also, the use of polyoxidovanadates acts as effective oxidation to the benzylic alcohol of carbonyl compounds along with p-toluene sulfonic acid (Sutradhar *et al.*, 2015).

The elevation of more important non-precious metals can act as catalysts that are effective in oxidizing saturated hydrocarbons of both industrial and synthetic organic chemicals under mild conditions. During redox reactions, the C-H bonds of selective hydroxylation are catalyzed by the active site of iron or copper with enzymes methane monooxygenase and cytochrome proteins. Therefore, first-line transition metal complexes are important for homogeneous alkane oxidation catalysts (Tordin *et al.*, 2013).

The Complexes of ruthenium (II) coordination chemistry have been studied over the years because of widespread use in various branches viz. catalysis, photophysics, bioinorganic and supramolecular chemistry, and photochemistry. The chemotherapeutic agents of ruthenium (II) complexes contain DMSO-, chloro-, and pyridine-type ligands. Similarly, Ru (II) complexes contain chelating diphosphine and diamine ligands that are used in homogeneous catalysis. Chelating Ru (II) reduces the polarity and antimicrobial activity of metal ions and enhances the lipophilic character of central metal atoms (Al-Noaimi *et al.*, 2014).

2.4 Applications in Modern Technologies

Currently, great interest is being created in the coordination polymer of metal complexes. Scientists have attracted different topologies and complex structures for these solid metal complexes because of their attractive catalytic, magnetic, optical, and electrical properties. Among these, Cd(II) is an interesting supramolecular metal-based complex, which is a new functional material due to its photoluminescent nature and structure. Therefore, large energy is expended to design Cd (II) containing polymer that can form bonds with different donor atoms, respectively (Bai *et al.*, 2009).

In recent years, Hydrazones, along with their metal complexes, have been widely used by researchers and chemists because of their vast applications in various fields. Hydrazones also show tautomerism and exhibit coordination behavior during complexation. The parameters of reactions such as dentistry, nature, pH, the concentration of metal ions, and hydrazones result in diverse geometries and atoms. The heavy metal cadmium of the d^{10} configuration forms a heap of complexes with large coordination numbers ranging from four to eight (Kuriakose *et al.*, 2017).

Nowadays, the versatile monoanionic 1, 1-dithiol ligand dithiocarbamates attract researchers because of their unique chemistry and wide application for large-volume production. Currently, consumption is up to 25,000–35,000 metric tons worldwide. Dithiocarbamate (DTC) small organic molecules not only show chelating potential but are also widely applied in agricultural industries as fungicides and pesticides. Today, they are used as vulcanization accelerators in the rubber industry, antituberculosis, antibacterial, antifungal, and antioxidant, exhibit anticancer, anti-alkylation, and apoptosis-inducing activity (Balakrishnan *et al.*, 2019).

A variety of antibiotics and pharmaceutical products are practiced in the medical field, due to the increasing interest of researchers and scientists in the field of coordination complex. Many complexes have modified pharmacological and toxicological behaviors. When metalloantibiotics are introduced into the body, they decrease the dose and benefit the pharmaceutical effects of ligands and metal ions (Ramotowska *et al.*, 2020).

Soliman *et al.*, (2012) explained that sustainable chemistry with chemical research and engineering helps design products with minimal use and the generation of hazardous substances and energy at surrounding temperatures and pressures is called green chemistry.

Every year, more than 1.3 million lives die because of fungal infections. Therefore, the current demand is to discover and develop new and more efficient antifungal agents or strategies that can combine the current situations with fungal infections that are challenged by increasing multi-drug resistance. Sulfonamide drugs of metal complexes such as penicillin and fluoroquinolones have already been synthesized to enhance the drug efficacy during metallation. The Pd (II) metal complexes of tetracyclines have antibacterial potential against *E.coli* with a sixteen-fold potency of the parent compound (Dar *et al.*, 2019).

Currently, in the field of porous metal-organic frameworks (MOFs), there is explosive interest for researchers and scientists because of their large surface area, diverse topology, tailor-made pore structure, and well-modified surface properties. Until now, these materials have been used in various fields such as separation, gas storage, catalysis, drug delivery, luminescence, and adsorption of organic molecules. MOF-based adsorbents in the aqueous phase are concentrated in benzene micromolecules, phenols, organic dyes, and so on (Hu *et al.*, 2017).

For the characterization process of polyoxometalates (POMs), various methods like UV/Visible, IR, Raman, NMR, and electrochemical methods are used. Souchay was the first to apply polarography in their research of POMs solutions, due to their variable composition, synthesis, material features, magnetic, and catalytic activities. Phosphomolybdate Keggin was the first structurally characterized POM due to its catalytic behavior such as oxidation of aldehydes, CO, and oxidative dehydrogenase (Koyun *et al.*, 2017).

2.5 Surfactant and Corrosion Inhibition Applications

In a recent discovery of streamlined corrosion inhibitors, hydrochloric acid protects metallic substances. Many molecules of organic inhibitors include heteroatoms (NA,

AOA, and ASA) with various bonds to facilitate adsorption on the steel surface. In the same way, Benzylideneamine derivatives are represented by base formula C_6H_5ACH , NAC_6H_5 which is a good corrosion inhibitor because it contains the AC, NA group as well as p-electrons in the aromatic ring. The efficiency of inhibitory molecules depends on the characteristics of the environment, the nature of the metal, and the experimental factors (Belghiti *et al.*, 2020).

Organic molecules with polar atoms such as N, O, S, P, and an aromatic planar cycle, with unsaturated bonds, the ability to accept or donate electrons that are absorbed on the surface of the metal are called corrosion inhibitors. The adsorption occurs without electrostatic interactions or interactions between the corrosion inhibitor, which are electron pairs as well as p-electrons, and the metal surface (Fragoza-Mar *et al.*, 2012). The corrosion inhibitor triethanolamine (TEA) was used in curing agents for metal-cutting fluids, adhesives, epoxy and rubber polymers, antistatic and pharmaceutical intermediates, and an ointment emulsifier. TEA gives rise to coordination compounds known as silatranes when they form complexes with silicon. The drug has wide applications to heal wounds or stimulate hair growth, and to stimulate anticancer, antitumor, antibacterial, fungicidal, and anti-inflammatory activities such as stimulant drugs on animal and seed germination properties. Copper complexes here can control the freshwater algae of ponds and lakes and also serve as agricultural herbicides in the form of neutralizer dispersing agents (Ashurov *et al.*, 2015).

In recent years, carbon dioxide corrosion in carbon steel pipelines and increasing behavior in the oil and gas industry, CO_2 gas equipment, and injection have led to decrease in viscosity and an increase in oil formation. Carbon-to- carbon steel has a low CO_2 environment resistance and is therefore applied in the petroleum industry for economic purposes. An alternative method is used as an inhibitor to reduce corrosion in steel. The corrosion behavior of metals alters resistive adsorption and establishes a relationship between adsorption and corrosion inhibition (El-Lateef *et al.*, 2015).

Carbon steel is a very sensitive area of research because it can communicate in various media such as acidic environments. The medium has vast applications in industrial cleaning, descaling, oil well acidification, and petroleum processes. Therefore, various methods have been applied to prevent these corrosion processes.

Here, corrosion inhibitors are the best methods because of their high efficiency and environmental friendliness. Organic inhibitors of a specific class are surfactants with unique amphiphiles in their molecular structures that can be designed for low cost, high efficiency, and effective behavior to prevent corrosion (Feng *et al.*, 2018).

Copper as well as its alloys are used for seawater in many countries of the world owing to their effective corrosion resistance, low cost, ease of fabrication during installation and healthy water contributed to good health. Copper is environmentally friendly, as it can be recycled up to 100%. Because of toxicity, many corrosion inhibitors such as chromate and nitrite change with the help of organic molecules that are environmentally friendly. Pyrazolic molecules are the most widely applied inhibitors that attract most researchers (Hammouti *et al.*, 2012).

Approximately \$ 250 billion is used every year in the US industry for metal corrosion, which is a serious problem. It can be controlled by different methods such as anticorrosion organic coatings, corrosion inhibitors, cathodic or anodic protection, etc. Among them, surface chemical conversion coatings are used in the aerospace and automobile industries. In the method of surface chemical conversion method, the substrate on the first metal surface is first molded with chemicals to form a surface coating. The coating improves the anticorrosion property of metals and enhances the layers of paint through adhesion. The traditional conversion coating of phosphate and chromate is mostly applied in agriculture, equipment, and automotive industries. Zirconium-based is the most interesting technique and is achieved by a successful sol-gel process (Liu *et al.*, 2019).

Corrosion inhibitors are a technique that processes metal corrosion against acid attacks. The corrosion inhibitor can adsorb to the metal surface and inhibit the active site. Several applications of common inhibitors such as amino thiazoles, thiosemicarbazides, thiadiazole, thioimidazole, mercapto-5-triazole, and benzotriazoles have been used as potential inhibitors for acid solutions (Yadav *et al.*, 2013).

2.6 Research Gap

The ancient method of synthesis of metal complexes is an addition of an equimolar mixture of ligands with metal a salt. However, the modern technique of synthesis of the heteroleptic metal complex is the addition of an equimolar mixture of two different ligands with metal salts. Comparisons are also made between ligand and metal complexes in various physical, spectral, and antibacterial studies. The synthesized metal complexes are extensively used in coordination chemistry because of their simple method of preparation, thermal stability, and medicinal utility. The metal complexes of cadmium, zirconium, molybdenum, and palladium have wide applications in various fields such as antibacterial, antifungal, antioxidant, antitumor, antiviral, antipyretic, antimetabolites, antithyroid, antimycotic, and herbicidal. The synthesized metal complexes may be better and more efficient metal-based antibiotics in future therapeutics to solve the global antibiotic resistance problem. Very little work has been done in the literature on metal complexes of Niobium, Technetium, Ruthenium, Rhodium, and silver. So, the current research helps to explore the research work in a comprehensive manner which fulfills the research gap.

CHAPTER 3

MATERIALS AND METHODS

This chapter covers chemicals and reagents used during the synthesis of metal complexes. Various physicochemical and spectroscopic techniques have been applied in characterization techniques and the study of antimicrobial activity will also be explained here.

3.1 Materials/ Reagents

The solvents and chemicals applied during the present research study are of high purity with analytical reagent grade quality. Solvents, as well as chemicals were obtained from various pharmaceutical and international standard companies with the help of local and international dealers. During the synthesis process, double-distilled ethanol and triple-distilled water were used as solvents. These were dried and purified using standard techniques. Similarly, glassware is of high-grade borosils, which were selected for the highly accurate research work.

The complexes were synthesized by stirring and refluxing equimolar mixtures of the primary ligand (tetracycline, oxytetracycline), secondary ligand (salicylaldehyde), and metal salts. Four metal chloride salts [M= Cd (II), Zr (II), Mo (III)/(V), Pd (II)] were chosen for the synthesis of metal complexes. Due to the low solubility of tetracycline in alcohol, therefore 70% ethanol was used for the synthesis process. Antimicrobial activity was tested against human clinical pathogenic bacteria using a modified Kirby-Bauer paper disc diffusion method. The pathogenic bacteria were collected from the Microbiology Laboratory of Nobel Medical College Teaching Hospital, and Suraksha Hospital, Biratnagar, Morang, Nepal. The list of instruments and glassware apparatus, chemicals and reagents used during the synthesis process is presented in **Tables A1 and A2**. Similarly, the solubility data of metal complexes of mixed ligands are reported in **Table A3**.

3.2 Synthesis of Metal Complexes

Among the many synthetic methods of complex formation, solvent-free synthesis by microwave irradiation is a well-known benign method because of its short reaction time, clean reaction profile, and simple experimental/ product separation procedure (Soliman *et al.*, 2012; Guerra *et al.*, 2005; El-Tabl *et al.*, 2013). However, the reflux method for the preparation of metal complexes is a traditional technique that was widespread in research. In the present research study, the primary ligand was added dropwise with the calculated amounts of metal salts and stirred under a magnetic stirrer. The calculated amounts of the secondary ligand were also added to the above mixture. The whole mixture was refluxed under a reflux condenser above the magnetic stirrer (**Fig. 3**). The pH was maintained at 7-8 by using an ammonia solution. The amorphous, colored, solid metal complexes were recrystallized and placed inside a desiccator under anhydrous CaCl_2 . Finally, the dried complexes were filled into an airtight vial for future use.

3.2.1 Synthesis of Cd-TC/Sal Metal Complex

The metal complex was synthesized by continuous stirring and heating an equimolar mixture of the primary ligand, tetracycline (0.8890g, 2mmol), dissolved in 20ml of 70% ethanol. An aqueous solution of metal salts, $\text{CdCl}_2 \cdot \text{H}_2\text{O}$ (0.4029g, 2mmol), was separately placed in an R.B. flask and stirred in a magnetic stirrer for up to 4 h. The stirred salt solution was mixed dropwise in a tetracycline solution. The entire mixture solution was stirred for a few hours and then the secondary ligand, 10 ml alcoholic salicylaldehyde (0.2 ml, 2mmol), was added in a dropwise manner to the above mixture. Again, the entire solution was refluxed at 20 °C for 8 h. The pH was maintained at 7-8 by adding a drop of ammonia solution to obtain a precipitate. The precipitate obtained was thus, washed with an alcoholic solution. The dried precipitate was recrystallized again, and finally, a pale orange amorphous solid was placed inside an airtight vial and preserved in a desiccator containing anhydrous CaCl_2 . Finally, the percentage yield was 60-70%.

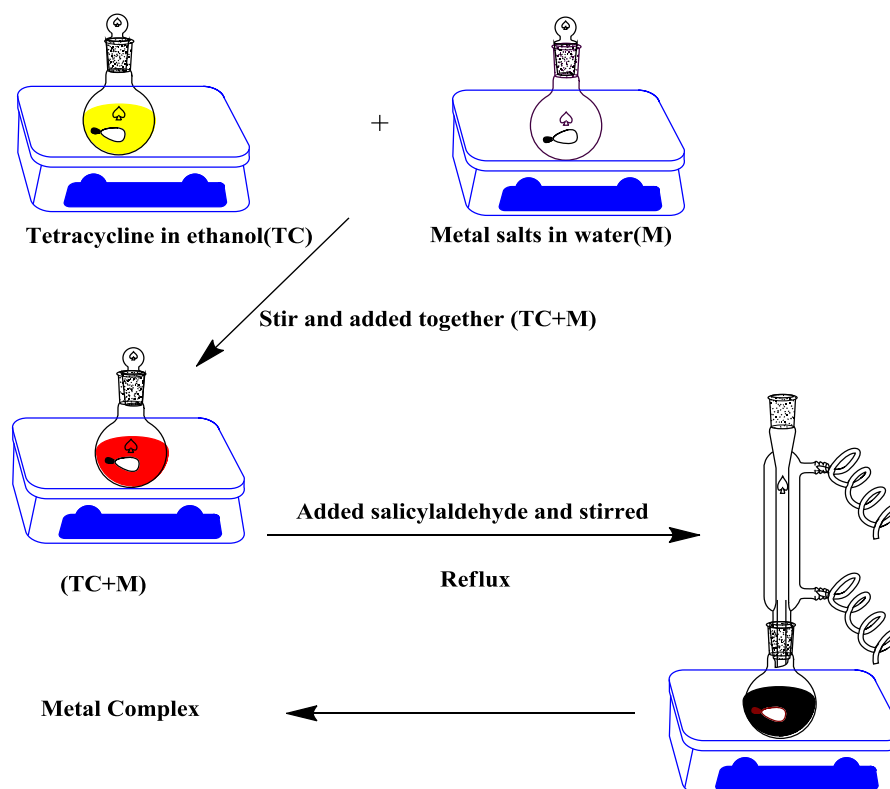


Figure 3: Synthetic route of metal complexes of mixed ligands.

3.2.2 Synthesis of Mo-TC/Sal Metal Complex

The synthesis of the metal complex by a normal process is shown in subunit 3.2.1. For the synthesis of the metal complex (Mo-TC/Sal), a 10ml (0.4050 g, 2mmol) alcoholic salt solution was used. A pale yellow amorphous solid was obtained and stored in an airtight vial for future use.

3.2.3 Synthesis of Zr-TC/Sal Metal Complex

The synthesis of the metal complex by a normal process is shown in subunit 3.2.1. For the synthesis of the metal complex (Zr-TC/Sal), a 10ml (0.6446g, 2mmol) aqueous salt solution was used. The black crystals were obtained and stored in an airtight vial for future use.

3.2.4 Synthesis of Pd-TC/Sal Metal Complex

The synthesis of the metal complex by a normal process is shown in subunit 3.2.1. For the synthesis of the metal complex (Pd-TC/Sal), a 10ml (0.7096 g, 2mmol) alcoholic salt solution was used. The black crystalline solid was obtained and stored in an airtight vial for future use.

3.2.5 Synthesis of Cd-OTC/Sal Metal Complex

The synthesis of the metal complex by a normal process is shown in subunit 3.2.1. For the synthesis of the metal complex (Cd-OTC/Sal), a calculated amount of the primary ligand, oxytetracycline hydrochloride (0.9941g, 2mmol), in 20 ml of 70% ethanol and 10 ml of an aqueous solution of CdCl₂.H₂O (0.4029 g, 2mmol) were used. A gray amorphous solid was obtained and stored in an airtight vial for future use.

3.2.6 Synthesis of Mo-OTC/Sal Metal Complex

The synthesis of the metal complex by a normal process is shown in subunit 3.2.5. For the synthesis of the metal complex (Mo-OTC/Sal), a 10ml (0.5469 g, 2mmol) alcoholic salt solution was used. A pale-brown amorphous solid was obtained and stored in an airtight vial for future use.

3.2.7 Synthesis of Zr(II)Otc/Sal Metal Complex

The synthesis of the metal complex by a normal process is shown in subunit 3.2.5. For the synthesis of the metal complex [Zr(II)Otc/Sal], a 10ml (0.6445 g, 2mmol) aqueous salt solution was used. A black crystalline solid was obtained and stored in an airtight vial for future use.

3.2.8 Synthesis of Pd(II)Otc/Sal Metal Complex

The synthesis of the metal complex by a normal process is shown in subunit 3.2.5. For the synthesis of the metal complex [Pd(II)Otc/Sal], a 10ml (0.3548 g, 2mmol)

alcoholic salt solution was used. A brown amorphous solid was obtained and stored in an airtight vial for future use.

3.3 Characterization Techniques

Physicochemical and spectroscopic characterization of the formulated metal complexes provides very important information to confirm the structure and its stereochemistry. Physicochemical techniques viz: CHN, surface tension, melting point, pH, viscosity, density, and conductivity measurement. In the same way, spectroscopic characterization methods like FT-IR, $^1\text{H-NMR}$ and $^{13}\text{C-NMR}$, UV/visible, SEM, ESI-MS spectrometry, and TGA/DTA analysis. Molecular modelings as well as antibacterial activity studies are the highlight of the current research work. All these will be discussed in the following subchapters.

3.3.1 Elemental Microanalysis

The micro-elemental analysis shows better results for the structural elucidation by giving the percentage composition of the element and also finalizing the molecular formula of the compound. The composition and purity of the prepared complex can also be ascertained from this analysis.

3.3.2 pH Measurement

The metallation behavior of the ligand for the formation of a metal complex is normally achieved by deprotonation, and the change in pH value during chemical reactions is determined as important evidence in synthetic chemistry. The ligands have a greater value than the metal complex, which symbolizes the formation of the metal complex during complexation. In the current research study, pH measurements were calculated by dissolving the metal complexes in 30% DMSO solvent, and readings were taken from Eutech Instruments pH 2700 pH/Mv/ $^{\circ}\text{C}/^{\circ}\text{F}$ meter.

3.3.3 Conductivity Measurement

Conductivity measurement is an instrumental physical technique that gives information about the electrolytic or non-electrolytic nature of a metal complex. In the field of coordination chemistry, it gives useful information regarding the formation of complexes. At room temperature (± 25 °C), the conductance value was measured by dissolving the metal complex in 30 % DMSO solvent at a concentration of M/1000. Complexity behavior is indicated by metal complexes with high values of conductivity.

3.3.4 Electronic Absorption Spectroscopy (EAS)

Electron absorption spectroscopy, also known as UV/visible spectroscopy, is an instrumental analytical technique for the determination, identification, and characterization of geometry as well as the binding modes of a compound. It also helps the chemist gain important knowledge regarding the transition of the metal complex. Electronic absorption was performed at room temperature, using DMSO solvent and the same solvent as the blank. The measurements were performed using an automated UV/Visible spectrometer (Varian Cary 5000).

3.3.5 FT-IR Spectral Study

FT-IR (Fourier transform infra-red) is also another useful tool to determine the functional groups associated with metal ions and the coordination sites formed during complex formation. The IR radiation of the electromagnetic spectrum is used by the instrument, which provides the vibration of a bond from which a lot of information can be obtained. The metal-ligand coordination band is located at the lower region ($400-500\text{ cm}^{-1}$) of the spectrum. Between the lower region ($400-500\text{ cm}^{-1}$), are bands of metal-ligand coordination. The FT-IR spectrum was recorded by an instrument called Perkin Elmer spectrum II at the wavenumber between $4000-400\text{ cm}^{-1}$ by using KBr pellets.

3.3.6 ^1H & ^{13}C -NMR Spectral Study

^1H and ^{13}C -NMR spectral analysis give valuable information for the structural elucidation of the compound. NMR spectroscopy is also an instrumental technique that gives characteristic peaks of different proton environments and coordination sites with the metal complex. In the present study, ^1H -NMR and ^{13}C -NMR spectra were recorded in DMSO-d_6 solvent on an instrument named Bruker Avance II-400 MHz spectrometer.

3.3.7 ESI-MS Spectral Study

ESI-MS (electrospray ionization mass spectrometry) is also a useful analytical instrumental technique that gives molecular masses of synthesized compounds or complexes. Spectrometry also determines the mass-charge-ratio of the charged particles of the compound and the information about the compound's molecular formula. The ESI technique has recently been used in MS because it is a soft ionization method where fragmentation takes place. ESI concerns MS-MS because it provides a very sensitive method for the analysis of the compound. In the present study, ESI-MS spectra were recorded in the mass range of 0-1000 m/z using a mass spectrometer, called water UPLC-TQD in positive mode.

3.3.8 TGA/DTA Study

Thermogravimetric analysis is an instrumental analysis technique that gives knowledge about the kinetic and thermal stability of an organic compound. TGA/DTA is also related to weight loss with an increase in temperature. With the help of the popular Coats-Redfern equation, various parameters can be calculated like A , E^* , ΔH^* , ΔS^* , and ΔG^* respectively. In the present investigation, TGA/DTA was recorded under a nitrogen atmosphere at 860 °C (room temperature) with a linear heating rate of 10 °C/min.

3.3.9 Surface Morphology Analysis

A scanning electron microscope (SEM) is an instrumental analytical tool to determine the surface morphology of a compound. A high electron beam of energy produces various signals on a solid surface, resulting in the picture, size, shape, strength, arrangement, and ductility of objects. SEM is also applied in forensic laboratories, metallurgy, medical science, and gemology (Pal *et al.*, 2018). In this study, SEM micrographs were performed using the JEOL model JSM-6390 LV.

3.4 Computational Study

Molecular modeling is a computer-based method for obtaining, representing, and manipulating the structure and reaction of molecules. The method is applied in the areas of computational chemistry, pharmaceutical design, material science, and computational biology. In our research investigation, the synthesized metal complexes were structurally analyzed with the help of 3D modeling software called Chem. 3D Pro 12.0.2, which shows a more precise and better measurement of the proposed structure of molecules. With the help of MM2 calculations, the optimized structure was calculated, and the optimization minimum energy of the molecular geometry was repeated several times to obtain the minimum energy. With the help of 3D modeling, selected bond angles, bond lengths, and atomic coordinates were also obtained during the study (Mahapatra *et al.*, 2015; Mahmoud *et al.*, 2017).

3.5 Antibacterial Sensitivity Study

Antibiotics are drugs that help to treat various bacterial infections. Today, due to antibiotic resistance caused by misuse or overdose of antibiotics in human medicine, veterinary and agriculture have become a serious health and environmental problems in the modern world (Shaikh *et al.*, 2015). So the present day, scientists and chemists are working day and night to synthesize or discover a powerful and better medicine that can solve the global problem. Therefore, many studies are being done on the metal-drug relationship. In the present investigation, the complexes were tested for antibacterial activity studies using the modified Kirby-Bauer paper disc diffusion method on different strains of human pathogenic bacteria with different

concentrations of metal complexes. Finally, the inhibition zone was measured in diameter (mm).

3.5.1 Sterilization of Equipment

Sterilization is the destruction or removal of all microorganisms such as spore-forming or non-spore-forming viruses, fungi, bacteria, and protozoa that can infect medicine or other living materials, causing health problems. Various techniques are applied for the sterilization processes like heating in an autoclave (steam sterilization), dry-heat sterilization, filtration, exposure to ionizing radiation, gas sterilization, etc. In the present work, all the glassware (Petri plates) and necessary equipment were first washed with liquid detergents followed by distilled water and then sterilized for half an hour in an autoclave. Finally, they were placed in a UV laminar flow for further use.

3.5.2 Procedure for the Preparation of Media

For antimicrobial susceptibility tests, the nutrient agar medium was applied for better growth of pathogens, as it contains sufficient nutrients that are necessary for the growth of microorganisms. The agar was prepared following the guidelines given by the manufacturer company. All the glassware and necessary equipment were washed properly and then autoclaved at 120 °C for half an hour. After cooling in the UV laminar flow, the media were properly transferred to each plate and the media was left to freeze without contamination.

3.5.3 Preparation of Culture Medium

Antibacterial tests were investigated *in vitro* for certain strains of human clinical pathogenic bacteria using the modified Kirby-Bauer paper disc diffusion method. The bacterial strains such as *S.aureus* (gram-positive), *P. mirabilis*, *E. coli*, *K. pneumoniae*, and *P. aeruginosa* (gram-negative) were selected for the test. Fresh cultures of clinical pathogens were received from the microbiology laboratory of Suraksha Hospital and Nobel Medical College and Teaching Hospital, Biratnagar, Morang, Nepal.

3.5.4 Organism Information

Staphylococcus aureus

S. aureus is a gram-positive microorganism of the spheroid in shape. The microorganism resembles a bunch of grapes under a light electron microscope after the gram is stained. The microscope also reveals nearly spherical-shaped cells with a smooth surface. *S. aureus* is a common skin microorganism and other major contaminated food and food products. They are found in the nose and also inhabit the skin and vagina. They can spread by contact with pus and user objects such as sheets, clothes, and a towel from infected patients. It is considered to be the most notorious microorganism resulting in infection with surgical death. Therefore, *S. aureus* is considered one of the bacteria-killers. About 20% of human populations in the world are long-term carriers of these bacteria (Abdelhamid & Wu, 2018).

Escherichia coli

E. coli is a gram-negative anaerobic with a rod-like shape, mostly seen in the warm-blooded organism in the lower intestine. *E. coli* is considered one of the fastest host microorganisms in genomic and genetic engineering due to its rapid growth and easy culture (Pontrelli *et al.*, 2018). It is an opportunistic pathogen that can cause urinary tract infections, meningitis, diarrhea, and sepsis. *E. coli* strains are important for etiological agents of diarrhea, while strains that develop from acquisition through gene transfer are persistent in the host (Gomes *et al.*, 2016).

Proteus mirabilis

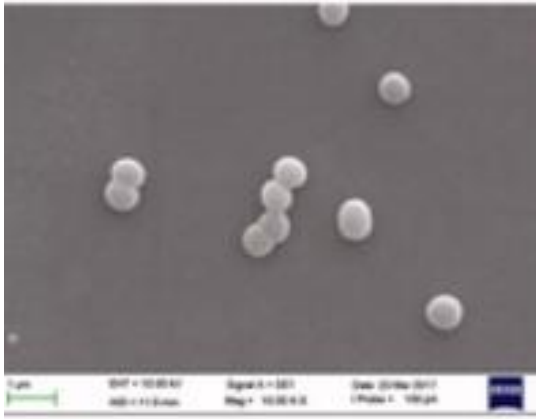
Jacobsen & Shirliff, (2011) reported that *Proteus mirabilis* is a gram-negative bacillus seen in the intestinal tracts of mammals, soil, and water, and can float in a coordinated manner on a solid surface. *P. mirabilis* is a causative agent of nasal infections, skin, wounds, eyes, ears, nose, throat, respiratory system, etc. Microorganisms can be severe because they can damage the kidney, and form stones in the bladder, and humans can suffer from acute, chronic pyelonephritis, and bacterial infection (Cestari *et al.*, 2013).

Pseudomonas aeruginosa

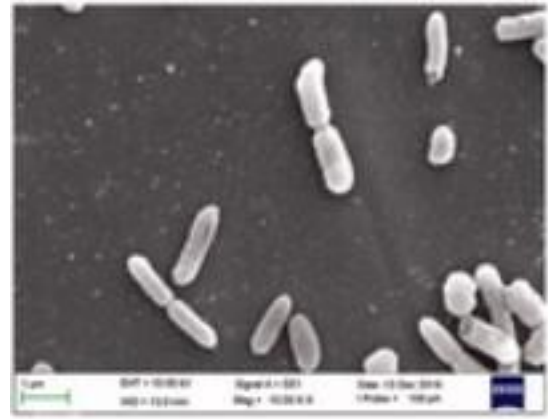
Pseudomonas aeruginosa, a gram-negative microorganism, is commonly encapsulated with rod-shaped structures and causes diseases in animals, plants, and humans. *Pseudomonas aeruginosa* is available in the soil, water, flora skin, and man-made environment of the world. *Pseudomonas aeruginosa* is the most important microorganism that can cause ventilator-associated pneumonia and infection in hospitalized patients (Pang *et al.*, 2019). Currently, it is recognized as a microorganism with malignancy for neutropenic hosts and causes nosocomial infection with invasive devices, and surgery in immune-compromised and immune-competent hosts (Giamarellou & kanellakopoulou, 2008).

Klebsiella pneumonia

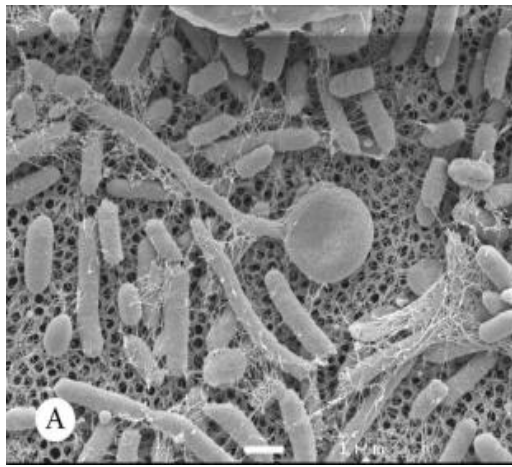
K. pneumoniae is a rod-shaped, encapsulated, gram-negative, non-motile, anaerobic, lactose-fermenting bacterium. The organism is mostly found in the surface water, soil, sewage, and mucosal surfaces of mammals. Due to broad-spectrum virulence factors, it plays an important role in causing pneumonia, urinary, pyogenic abscesses, and hemorrhagic infections in mammals (Cheng *et al.*, 2018). *K. pneumoniae* is also an opportunistic pathogen that can cause a multidrug-resistant increase in people infecting community-based and nosocomial infections (Azevedo *et al.*, 2019; Vuotto *et al.*, 2014). Patients who are suffering from diabetes mellitus, a debilitating condition, and extraintestinal will get *K. pneumonia* into their bodies. There is also a risk of pneumonia and also a chance for such germs to enter patients undergoing head injury or neurosurgery with or without CSF leakage (Fang *et al.*, 2000).



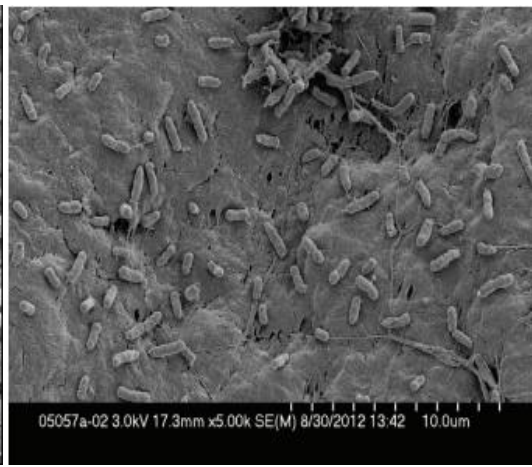
A



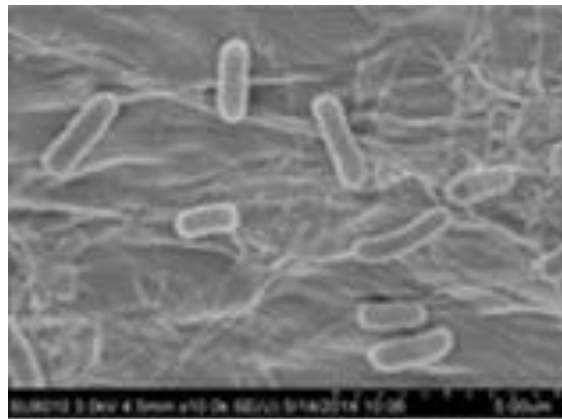
B



C



D



E

Figure 4: Pathogens, A (*S. aureus*), B (*E. coli*), C (*P. mirabilis*), D (*P. aeruginosa*), E (*K. pneumoniae*)
 [Note: scale bar, 1 μm (A-D), scale bar, 5 μm (E)]

Sources:

A: <https://www.tandfonline.com/doi/full/10.1080/14756366.2017.1396456>

B: <https://www.tandfonline.com/doi/full/10.1080/14756366.2017.1396456>

C: <https://sci-hub.hkvisa.net/10.1128/JB.00975-08>

D: <https://sci-hub.hkvisa.net/10.1155/2014/795281>

E: <https://sci-hub.hkvisa.net/10.1038/srep06216>

3.5.5 Preparation of Paper Disc

For the preparation of the paper disc, Whatman filter paper No. 1 was used for the testing. Using a simple punching machine, holes of about 5 or 6 mm diameter were perforated and precautions were followed to avoid overlap of holes. The paper disc curls after punching, so care is taken to keep a flat surface and apply pressure to it. Finally, the discs were autoclaved for 30 minutes under a pressure of 15 lbs.

3.5.6 Loading of Chemicals

For antibacterial susceptibility testing, the metal complexes were dissolved in a DMSO solvent of varying concentrations, and the blank paper discs were loaded with chemicals with the help of a micropipette. The loaded paper discs were finally dried and placed on a media plate with a swabbed bacterial culture.

3.5.7 Inoculation of Organisms and Measurement of Growth Inhibition Zone

The loaded paper discs were placed on sterile MHA (Muller Hinton Agar) media containing regenerated and fresh pathogens, and the discs were loaded with different concentrations of the prepared metal complex. Molecular size and solubility reflect chemical infiltration around the disc region. The pathogen will not grow in that area and the areas without pathogen are called clear zones or inhibition zones, measured with a Hi-Antibiotic Zone measuring Scale-C in diameter (mm) after 36 h of antibacterial testing (El-Sonbati *et al.*, 2019; Santos *et al.*, 2014).

CHAPTER 4

RESULTS AND DISCUSSION

4.1 Physical Measurements

The behavior of physicochemical techniques of complexes such as conductivity, pH, density, viscosity, melting point, color, solubility, and surface tension measurement can be better understood. All these necessary parameters help to give supportive information for complex formation during a chemical reaction. Likewise, due to the unique properties of various chemicals, it helps to design the mechanism and identify the nature of compound formation.

4.1.1 Colour

In transition metals, atoms, or ions, d-orbitals are degenerate (same energy). However, upon complexity, the d-orbitals of metal coordinates degenerate. When the d-orbital is not filled, the electron absorbs photons of suitable energy to propel the electron from the ground state to a higher excited energy state. If complexes absorb electromagnetic radiation in the visible region, it emits an energy complement to the absorbed radiation and forms color in the complexes. The color change is caused by various electronic d-d transitions, either by π bonding or non-bonding or by a free electron. Chromophores in the presence of auxochromes show electronic absorption in the UV region and give color to the complexes.

4.1.2 Solubility and Melting Points

The specific characteristics of compounds can be determined with the help of physical properties such as melting point and solubility measurements. Ligands were soluble in ethanol, DMF, and DMSO, whereas the complexes were soluble in organic solvents (DMSO and DMF). The melting point was measured using an instrument called VEEGO ASD-10013.

4.1.3 Conductivity Measurements

The electrolytic or non-electrolytic nature of a metal complex can be measured with the help of conductivity measurement. In the present study, the complexes are dissolved in DMSO solvent with a concentration of 0.001 M, and the calculated data are presented in **Table 1**. The complexes show higher conductivity than the ligand, which signifies the complexation between the ligand and metal ions. Data obtained from conductivity showed both electrolytic and non-electrolytic nature.

4.1.4 pH Measurement

The main reason for the difference in the metallation in coordination chemistry is the deprotonation of the ligands. Ligands have a higher pH value than metal complexes, which symbolizes the formation of metal complexes. The metal complex synthesis method does not affect the reaction between the molar ratio and pH, therefore indicating that the metal complexes are much more stable. Environment, temperature, and pH are essential factors for affecting the growth of bacteria. Most of the bacteria grow at pH 7.4 (slightly alkaline) and incubate at 34 °C.

4.1.5 Surface Tension

The surface tension determines the wettability of a solution that can spread or stick to the surface of a solid. The principle of surface tension determines the segregation dynamics of surface-active materials. The surface tension increases by decreasing the concentration. This is due to the interaction of liquid molecules larger than the molecules in the air or a non-polar solvent (Thakur *et. al.*, 2017). The surface tension was carried out with the help of an instrument called the KRUSS Easy Dyne Tensiometer.

4.1.6 Density

At room temperature (± 25 °C), the density of the metal complexes was measured by dissolving the complexes in the DMSO solvent at a concentration of M/1000. The calculation was done using an instrument called KRUSS Easy Dyne Tensiometer.

4.1.7 Viscosity

Viscosity is also an important factor in measuring the resistance to the flow of liquid and was measured using an Ostwald viscometer instrument. Complexes were measured at room temperature (± 25 °C) by dissolving the complexes in a DMSO solvent at a concentration of M/1000.

Table 1: Geometry, pH, specific conductivity, surface tension, viscosity, and density data of metal complexes

S.No.	Compounds	Geometry	pH	Conductivity ($\mu\text{S/cm}$)	Surface tension (mN/m)	Viscosity (cp)	Density (gm/ml)
1	TC	-	6.48	54.10	25.80	19.59	0.882
2	OTC	-	3.55	103.9	50.5	15.54	1.041
3	Cd-TC/Sal	Trig planar	6.16	14.10	59.80	15.43	1.085
4	Zr-TC/Sal	Tetrahedral	6.43	14.70	56.30	16.99	1.048
5	Mo-TC/Sal	Octahedral	4.82	14.90	57.00	19.94	1.042
6	Pd-TC/Sal	Square planar	5.78	17.80	57.5	22.50	1.076
7	Cd-OTC/Sal	Tetrahedral	5.42	23.33	61.80	20.74	0.954
8	Zr(II)Otc/Sal	Tetrahedral	5.46	15.92	60.6	18.94	0.999
9	Mo-OTC/Sal	Octahedral	4.84	243.40	60.5	21.03	0.976
10	Pd(II)Otc/Sal	Square planar	3.43	248.20	59.8	17.04	0.944

4.2 Microanalytical Results

Micro elemental analysis is an analytical method for identifying C, H, N, O, and other materials in organic compounds either qualitatively or quantitatively. It is also a cost-effective method that gives ideas and facts about the purity and composition of organic materials. In the present work, elemental microanalysis of metal complexes is given in **Tables 2 and 3**. It also gives a good idea about the proposed stereochemistry of the premises. Here, metal complexes show better results with the calculated values for the elemental microanalysis.

Table 2: Elemental microanalysis and physical measurement data of M-TC/Sal metal complexes [M=Cd(II), Zr(II), Mo(III), and Pd(II)]

Complexes	Empirical Formula	Mol. Wt.	Colour	m.p(°C)	Calculated (found)%			
					C	H	N	O
Cd-TC/Sal	C ₂₉ H ₂₈ CdN ₂ O ₁₀	676.95	Pale Orange	239.5	51.450 (51.102)	4.170 (5.706)	4.140 (4.256)	23.630 (14.251)
Zr-TC/Sal	C ₂₉ H ₂₈ ZrN ₂ O ₁₀	655.76	Black	175.9	53.12 (53.06)	4.30 (4.26)	4.27 (4.26)	24.40 (24.39)
Mo-TC/Sal	C ₂₉ H ₂₈ MoN ₂ O ₁₀	660.50	Pale Yellow	228.5	52.730 (42.789)	4.270 (4.635)	4.240 (4.686)	24.220 (17.003)
Pd-TC/Sal	C ₂₉ H ₂₈ PdN ₂ O ₁₀	670.96	Black	265.5	51.91 (51.87)	4.21 (4.17)	4.18 (4.17)	23.85 (23.84)

Table 3: Elemental microanalysis and physical measurement data of M-OTC/Sal metal complexes [M=Cd(II), Mo(V), Zr(II), and Pd(II)]

Complexes	Empirical Formula	Mol. Wt.	Colour	m.p. (°C)	Calculated (found)%					
					C	H	N	O	M	Cl
Cd-OTC/Sal	C ₂₉ H ₂₈ CdN ₂ O ₁₁	692.95	Gray	>260	50.26 (50.20)	4.07 (4.26)	4.04 (4.36)	25.40 (25.33)	16.22 (16.22)	-
Mo-OTC/Sal	C ₂₉ H ₂₈ MoN ₂ O ₁₁	747.41	Brown	>260	46.60 (46.59)	3.78 (3.77)	3.75 (3.74)	23.55 (23.54)	12.84 (12.83)	9.49 (9.48)
Zr(II)Otc /Sal	C ₂₉ H ₂₈ ZrN ₂ O ₁₁	671.76	Black	>260	51.85 (51.80)	4.20 (4.26)	4.17 (4.15)	26.20 (26.24)	13.58 (13.55)	-
Pd(II)Otc/Sal	C ₂₉ H ₂₈ PdN ₂ O ₁₁	686.96	Black	>260	50.70 (50.67)	4.11 (4.08)	4.08 (4.17)	25.62 (25.84)	15.49 (15.24)	-

4.3 Spectroscopic Results and Discussion

4.3.1 FT-IR Spectral Study

4.3.1.1 FT-IR Spectral Study of M-TC/Sal Metal Complexes

The FT-IR spectra give important information about the functional groups associated with the metal ions during complexation behavior. In the present study, the complex reflects different FT-IR spectral absorption bands, with different functional groups

present. The absorption bands of Cd-TC/Sal, Mo-TC/Sal, Zr-TC/Sal, and Pd-TC/Sal in the FT-IR spectrum, which lies at 3431 cm^{-1} , 3396 cm^{-1} , 3183 cm^{-1} , and 3407 cm^{-1} is attributed to the coalescence of stretching band $\nu(\text{O-H/N-H})$ (Shaker *et al.*, 2016; El-Shwiniy & Zordok, 2018; Maurya *et al.*, 2011; Guerra *et al.*, 2005). In addition, other absorption bands were observed at 1770 cm^{-1} , (Cd-TC/Sal), 1618 cm^{-1} , (Mo-TC/Sal), 1770 cm^{-1} , (Zr-TC/Sal), and 1773 cm^{-1} , (Pd-TC/Sal) was assigned to the $\nu(\text{C=O})$ group (Shakdofa *et al.*, 2017; Singh *et al.*, 2013; Ahmed & Lal, 2013; Soliman *et al.*, 2016). The lower frequency absorption bands lie in the region between $596\text{--}604\text{ cm}^{-1}$, assigned to absorption $\nu(\text{M-O})$ and $\nu(\text{M-N})$ both supporting the mode of complexation of the metal ions, and the lowest frequency lie in the region of $440\text{--}499\text{ cm}^{-1}$ (Omar *et al.*, 2017; Bajju *et al.*, 2013; Kumar *et al.*, 2011; Tyagi & Chandra, 2014). The FT-IR spectrum and the spectral study show the metallation of a metal ion with the amide functional group of the nitrogen atom. In this way, the overall data showed the interaction of the metal with the ligands. The FT-IR data are presented in **Tables 4 and 5** and are displayed in **(Fig. 5)**.

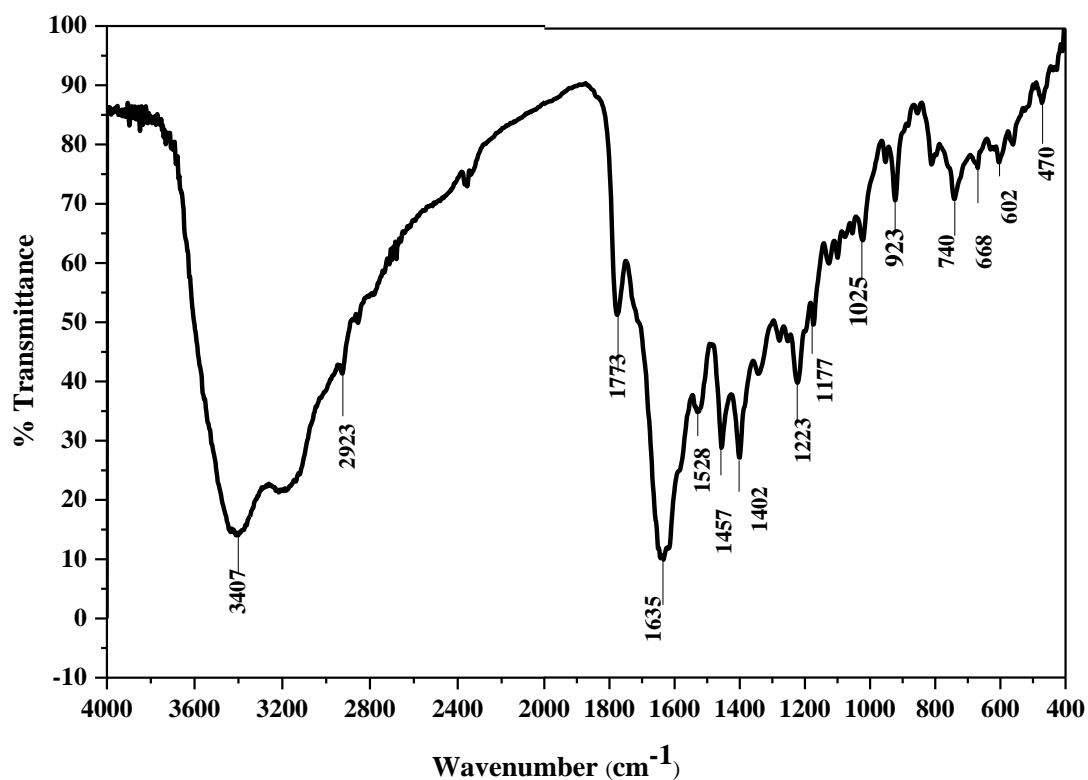


Figure 5: FT-IR Spectrum of Pd-TC/Sal metal complex

Table 4: FT-IR spectral data of Cd-TC/Sal and Mo-TC/Sal metal complexes in cm^{-1} .

Complexes	$\nu(\text{O-H/NH})$	$\nu(\text{CH})$	$\nu(\text{C=O})$	$\nu(\text{C=C})$	$\nu(\text{C-N})$	$\nu(\text{C-O})$	$\nu(\text{M-O})$	$\nu(\text{M-N})$
		Methyl		Aromatic	Amide			
Cd-TC/Sal	3431	2935	1770	1518	1457	1128	596	499
Mo-TC/Sal	3396	2925	1618	1576	1457	1133	602	440

Table 5: FT-IR spectral data of Zr-TC/Sal and Pd-TC/Sal metal complexes in cm^{-1} .

Complexes	$\nu(\text{O-H})$ or	$\nu(\text{C=O})$	$\nu(\text{C=N})$	ν_{asym}	ν_{sym}	$\nu(\text{C-O})$	$\nu(\text{M-O})$	$\nu(\text{M-N})$
	$\nu(\text{N-H})$			(COO^-)	(COO^-)			
TC Ligand	3384	1653	1615	1580	1399	1179	-	-
Zr-TC/Sal	3183	1770	1619	1570	1399	1152	604	476
Pd-TC/Sal	3407	1773	1635	1528	1402	1177	602	470

4.3.1.2 FT-IR Spectral Study of M-OTC/Sal metal Complexes

The characteristic FT-IR spectral absorption bands for M-OTC/Sal metal complexes of oxytetracycline are presented in **(Fig. 6)** and their characteristics absorption data are reported in **Tables 6 and 7**. Intensive absorption bands of Cd-OTC/Sal, Mo-OTC/Sal, Zr(II)Otc/Sal, and Pd(II)Otc/Sal in the FT-IR spectrum, which lies at 3432 cm^{-1} , 3437 cm^{-1} , 3426 cm^{-1} , and 3428 cm^{-1} are attributed to the coalescence of the $\nu(\text{O-H/N-H})$ stretching bands (Al-Farhan *et al.*, 2021; Kumar *et al.*, 2013; Khalil & Al-Seif, 2010; El-Saied *et al.*, 2017). In addition, the IR spectra of metal complexes [Cd-OTC/Sal, Mo-OTC/Sal, Zr(II)Otc/Sal, and Pd(II)Otc/Sal] detect absorption bands at the region of 1599 cm^{-1} , 1628 cm^{-1} , 1614 cm^{-1} , and 1622 cm^{-1} , correspond to the $\nu(\text{C=O})$ group. Similarly, the absorption bands at 1501 cm^{-1} (Cd-OTC/Sal), 1546 cm^{-1} (Mo-TC/Sal), 1502 cm^{-1} [Zr(II)Otc/Sal], and 1455 cm^{-1} [Pd(II)Otc/Sal] was assigned to the aromatic $\nu(\text{C=C})$ group (Alias *et al.*, 2013; Rao *et al.*, 2019; Nair *et al.*, 2011). Characteristic frequencies at 1178 cm^{-1} , 1164 cm^{-1} , 1240 cm^{-1} , and 1230 cm^{-1} , recommended the existence of a $\nu(\text{C-O})$ group. The absorption bands lying in the lower region of ($595, 517, 552, 603 \text{ cm}^{-1}$) and ($503, 463, 482 \text{ cm}^{-1}$) were assigned to $\nu(\text{M-O})$ and $\nu(\text{M-N})$ of the [Cd-OTC/Sal, Mo-OTC/Sal, Zr(II)Otc/Sal, Pd(II)Otc/Sal] metal complexes. These overall data value supports the coordination mode of the metal ions with the nitrogen atom of the ligand during complexation (Ahmed *et al.*, 2013; Singh & Nakate, 2014; Zhou *et al.*, 2013; Chandra *et al.*, 2011).

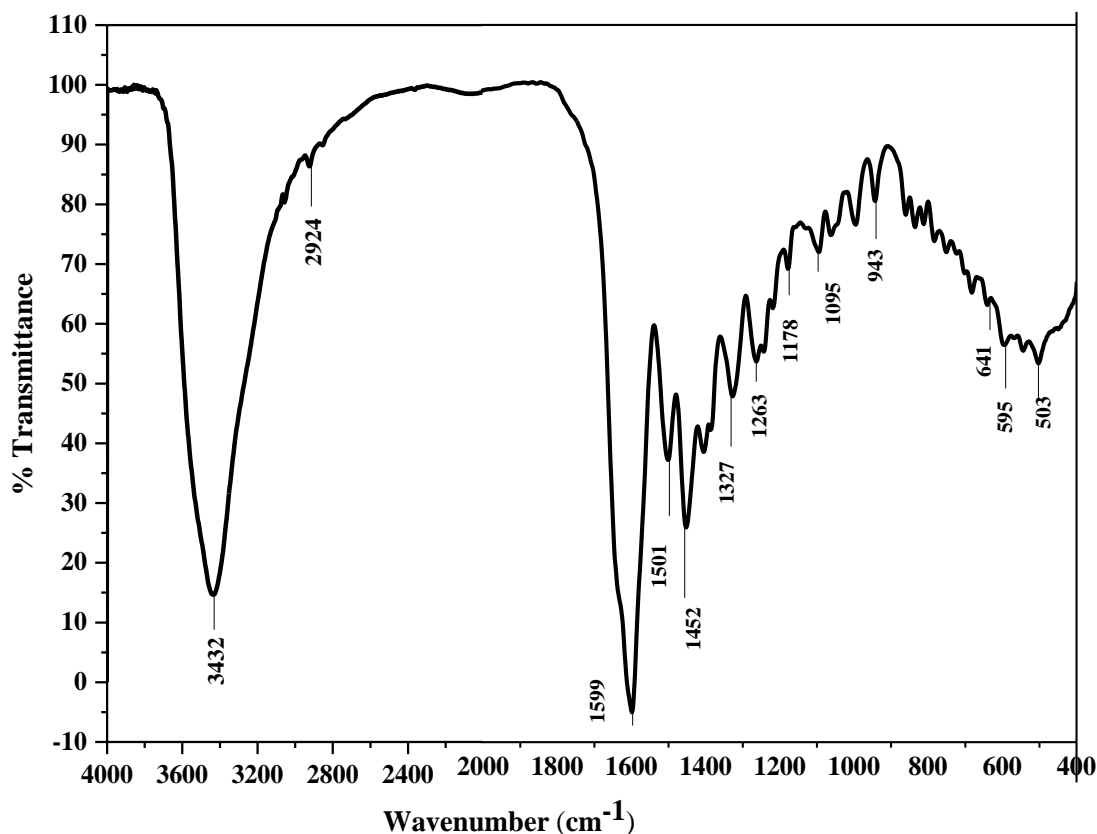


Figure 6: FT-IR Spectrum of Cd-OTC/Sal metal complex

Table 6: FT-IR spectral data of M-OTC/Sal [M=Cd(II), Mo(V)] metal complexes in cm^{-1} .

Complexes	$\nu(\text{OH/NH})$	$\nu(\text{CH})$	$\nu(\text{C=O})$	$\nu(\text{C=C})$	$\nu(\text{C-N})$	$\nu(\text{C-O})$	$\nu(\text{M-O})$	$\nu(\text{M-N})$
		Methyl		Aromatic				
Cd-OTCSal	3432	2924	1599	1501	1452	1178	595	503
Mo-OTCSal	3437	2928	1628	1546	1456	1164	517	463

Table 7: FT-IR spectral data of Zr(II)Otc/Sal and Pd(II)Otc/Sal metal complexes in cm^{-1} .

Complexes	$\nu(\text{OH/NH})$	$\nu(\text{CH})$	$\nu(\text{C=O})$	$\nu(\text{C=C})$	$\nu(\text{C-N})$	$\nu(\text{C-O})$	$\nu(\text{M-O})$
		Methyl		Aromatic			
Zr(II)Otc/Sal	3426	3055	1614	1502	1456	1240	552
Pd(II)Otc/Sal	3428	2941	1622	1455	1387	1230	603

4.3.2 ^1H & ^{13}C -NMR Spectral Study

NMR (Nuclear magnetic resonance) spectroscopy, which provides the number of magnetically distinct atoms, where one can determine the number of hydrogen nuclei of each type, and also the nature of the immediate environment. The deshielded

proton exhibits a signal at a high chemical shift value (δ ppm) and a shielded proton in a low chemical shift value region (Pavia, *et. al.*, 2013).

4.3.2.1 $^1\text{H-NMR}$ spectral study of M-TC/Sal metal complexes

The metal complex composition was also determined by $^1\text{H-NMR}$ spectroscopy, which is the most powerful tool for characterizing compounds in a solution. The spectral comparison provides information about the binding nature as well as the complexation behavior with the metal ions. NMR spectra were measured at room temperature and recorded with the help of a DMSO- d_6 solvent. In NMR spectroscopy, tetramethylsilane (TMS) serves as an internal reference standard, reflecting well-resolved signals for protons present in metal complexes. The spectrum of the Cd-TC/Sal metal complex showed a well-resolved and exhibited a signal at 1.495-1.896 ppm, attributed to the methyl proton, and 2.682-2.963 ppm attributed to the $-\text{NCH}_3$ group. Multiple signals at 6.904-7.539 ppm are due to protons of the aromatic ring and the sharp peak observed at 7.645-7.660 ppm is due to $-\text{CONH}_2$, while at 9.157 ppm the signal is due to the $-\text{CHO}$ group. In the same way, the Mo-TC/Sal metal complex exhibited a signal at 1.041-1.151 ppm responsible for the methyl proton, a signal at 2.742-3.007 ppm due to the $-\text{NCH}_3$ group. Multiple signals at 6.893-7.479 ppm are due to the protons in the aromatic ring and the sharp peak observed at 7.583-7.636 ppm is due to $-\text{CONH}_2$, while at 9.255-9.593 ppm, the signal was due to the $-\text{CHO}$ group (Kumar *et al.*, 2013; Mahapatra *et al.*, 2013; Maurya *et al.*, 2011; Moradi-Shoeili *et al.*, 2013). Similarly, the spectrum of the Zr-TC/Sal metal complex exhibits a signal at 2.491-2.523 ppm, attributed to the methyl proton, and 2.5-3.5 ppm is responsible for the $-\text{NCH}_3$ group. Multiple signals at 6.950-6.991 ppm are assigned to the protons of the aromatic ring and the sharp peak observed at 7.504-7.669 ppm is due to $-\text{CONH}_2$, while at 10.214 ppm, the signal is due to the $-\text{CHO}$ group. However, in the Pd-TC/Sal metal complex, the peak signal represents the CH_3 group at 1.059-1.226 ppm, the signals as $-\text{CH}_2\text{NH}$ group at 1.527- 1.544 ppm, and the signals at 3.51 ppm as the $-\text{OH}$ group. Peak values of the metal complexes from experimental data showed better results than the proposed structure and the recorded spectrum of M-TC/Sal metal complexes is given in **Table 8** (Singh *et al.*, 2013; El-ajaily *et al.*, 2015; Khan *et al.*, 2013; Smith & Slawin, 2000).

Table 8: ¹H-NMR spectral data of Cd-TC/Sal, Mo-TC/Sal, Zr-TC/Sal, and Pd-TC/Sal metal complexes

Compounds	Chemical shift (δ ppm)	Assignment
Cd-TC/Sal Complex	1.495-1.896	CH ₃
	2.682-2.963	-N-CH ₃
	4.955-5.013	-OH
	6.904-7.539	Aromatic Proton
	7.645-7.660	-CONH ₂
	9.157	-CHO
	11.356-11.960	-COOH
Mo-TC/Sal Complex	1.041-1.151	CH ₃
	1.235	R-CH ₂ -R
	1.810-1.916	CH ₃
	2.346-2.399	Ar-CH
	2.509-2.517	DMSO
	2.742-3.007	-N-CH ₃
	3.069-3.459	-CH-OH
	4.939-4.947	-OH
	6.893-7.479	Aromatic proton
	7.583-7.636	-CONH ₂
	9.255-9.593	-CHO
11.352	-COOH	
Zr-TC/Sal Complex	2.491-2.523	CH ₃
	2.5-3.5	-N-CH ₃
	3.327-3.513	-CH (Methine)
	2.491-2.523	DMSO
	6.950-6.991	Aromatic Proton
	7.504-7.669	-CH (Benzene)
	10.214	-CONH ₂
Pd-TC/Sal Complex	1.059-1.226	CH ₃
	1.527-1.544, 1.905-1.915	-CH ₂

4.3.2.2 ¹H-NMR spectral study of the M-OTC/Sal metal complexes

In M-OTC/Sal complexes, ¹H-NMR spectra were done in DMSO-d₆ solvent using TMS (tetramethylsilane) as an internal reference standard. The spectra of the Cd-OTC/Sal metal complex showed a well-resolved and exhibited a singlet at δ=1.670 ppm, attributed to methyl proton. The signals at δ=2.370-2.553 and 4.284-4.397 ppm, are attributed to -CH₂ and -NH proton. Multiple signals at δ=6.889-7.355 ppm are

due to the protons of the aromatic ring. Similarly, the spectra of the Mo-OTC/Sal metal complex showed a well-resolved and exhibited a singlet at $\delta=1.047-1.082$ ppm, attributed to methyl proton. The signals at $\delta=2.551$ ppm is attributed to $-\text{CH}_2$ proton. Multiple signals at $\delta=7.186-7.205$ ppm are due to the protons of the aromatic ring (El-Sonbati *et al.*, 2019; Hussein *et al.*, 2015; Kumar *et al.*, 2013; Al-Afyouni *et al.*, 2016). However, the spectra of the Zr(II)Otc/Sal metal complex showed a well-resolved and exhibited a singlet at $\delta=1.047-1.082$ ppm, attributed to methyl proton. The signals at $\delta=2.543, 4.418$ ppm, are attributed to $-\text{CH}_2$ and $-\text{NH}_2$ proton. Multiple signals at $\delta=7.023-7.279$ ppm are due to the protons of the aromatic ring. Similarly, the spectra of the Pd(II)Otc/Sal metal complex showed a well-resolved and exhibited a singlet at $\delta=1.040-1.075$ ppm, which are attributed to methyl proton. The signals at $\delta=2.088-2.180$ and $3.412-3.465$ ppm, are attributed to $-\text{CH}_2$ and $-\text{NH}_2$ proton. Multiple signals at $\delta=6.632-7.516$ ppm are due to the protons of the aromatic ring (Nakata *et al.*, 2019; Huynh *et al.*, 2004; Mandal *et al.*, 2017). The experimental data showed better results with the proposed structure in the metal complexes and the recorded spectrum of M-OTC/Sal metal complexes is given in **Table 9**.

Table 9: $^1\text{H-NMR}$ spectral data of Cd-OTC/Sal, Mo-OTC/Sal, Zr(II)Otc/Sal, and Pd(II)Otc/Sal metal complexes

Compounds	Chemical shift (δ ppm)	Assignment
Cd-OTC/Sal Complex	1.670	CH_3
	2.370-2.553	$-\text{CH}_2$
	4.284-4.397	$-\text{NH}$
	6.889-7.355	Ar Proton
Mo-OTC/Sal Complex	1.047-1.082	CH_3
	2.551	$-\text{CH}_2$
	2.503-2.541	DMSO
	3.303-3.339	$-\text{CH-OH}$
	4.402	$-\text{OH}$
	7.186-7.205	Ar proton
Zr(II)Otc/Sal Complex	1.047-1.082	CH_3
	2.543	DMSO
	3.399-3.406	$-\text{NCH}_3$
	4.418	$-\text{CH}_2$
	7.023-7.279	Ar proton
Pd(II)Otc/Sal Complex	1.040-1.075	CH_3

2.088-2.180	-CH ₂
2.500	DMSO
3.412-3.465	-NCH ₃
6.632-7.516	Ar proton

4.3.2.3 ¹³C-NMR Spectral Study of the M-TC/Sal Metal Complexes

The ¹³C-NMR spectrum of tetracycline with its respective metal complexes gives some useful information about the relationship of metal ions with the complex and their geometry. The spectrum also gives an idea of the electronic environment of different types of carbon atoms and their molecules. The ¹³C-NMR spectra of the Cd-TC/Sal metal complex were done in DMSO-d₆ solvent. The spectrum delivers a signal for -CH=N- at 147.175 ppm. The signal for -CH=CH₂ at 137.645 ppm. The signals for C=C, Aromatic ring, N(CH₃)₂, and DMSO-d₆ at (122.622-117.671, 131.161-117.67, 40.799-40.244, and 39.966-39.131) ppm (Mousavi *et al.*, 2020). Similarly, signals for Mo-TC/Sal metal complex at (199.513, 172.484-157.742, 111-131, and 40) ppm are assigned to the phenyl ketone, carbonyl group, aromatic carbon, and DMSO-d₆ solvent in the range of ppm (Pasayat *et al.*, 2012; de la Mata *et al.*, 1999; Nag & Sharma, 2019). Similarly, the signals of the Zr-TC/Sal metal complex at (39.166-40.832, 45.5, 113.635-126.652, 182.917) ppm are attributed to the DMSO-d₆ solvent, -N(CH₃)₂, aromatic ring carbon and carbonyl group -CO- (Hu *et al.*, 2013; Steinhuebel *et al.*, 1998) while the Pd-TC/Sal complex at (40, 134.539-137.972) ppm contain signals in the range of ppm are attributed to the DMSO-d₆ solvent and aromatic ring carbon (Huynh *et al.*, 2009; Smrecki *et al.*, 2016). The recorded spectrum of M-TC/Sal metal complexes is given in **Table 10**.

Table 10: ^{13}C -NMR spectral data of Cd-TC/Sal, Mo-TC/Sal, Zr-TC/Sal, and Pd-TC/Sal metal complexes

Compounds	Assignment	Chemical shift (δ ppm)
Cd-TC/Sal Complex	CH=N	147.175
	CH=CH ₂	137.645
	C=C	122.622, 122.561, 121.250, 117.671
	Aromatic ring carbon	131.161, 131.0, 122, 125.778, 122.622, 121.561, 121.250, 117.67
	N (CH ₃) ₂	40.799, 40.521, 40.244
	DMSO	39.966, 39.688, 39.410, 39.131
Mo-TC/Sal Complex	C ₆ H ₅ -C=O	199.513
	-CHO	188.369
	C=O	172.484, 172.295, 162.521, 157.824, 157.742
	-CH=CH ₂	138.979, 138.789, 132.878
	Ar-C	130.850, 130.498, 121.817, 121.690, 115.057, 112.097, 112.068, 111.057
	-CH=CN	108.650, 97.582
	R ₂ CO	76.781, 76.369
	-CH ₂ OH	66.302
	DMSO	40
	COCH ₃	26.049
	R-CH ₃	14.069
Zr-TC/Sal Complex	CH ₃	21.564
	CH	34.075-34.958
	DMSO	39.166-40.832
	C-C	74.243
	CH=CH	101.780
	Ar-C	113.635, 116.184, 121.874-122.637, 125.761, 126.652
	N (CH ₃) ₂	45.5
	C-O	162.426
	C=O	182.917
Pd-TC/Sal Complex	CH ₃	16.841, 18.579
	CH ₂	22.007, 23.022
	DMSO	40
	C-C	71.116-71.543
	C-N	78.579
	C=C	87.015-87.197
	Ar-C	134.539-137.972
	C-O	160.932-162.100

4.3.2.4 ^{13}C -NMR Spectral Study of the M-OTC/Sal Metal Complexes

In the Cd-OTC/Sal complex, ^{13}C -NMR spectra were performed in a DMSO- d_6 solvent. The signals observed in the range of 18.394, 40, 55.892 ppm were assigned to a methyl group, DMSO solvent, -CH group. The aromatic carbon signal is located in the region of 95.513-135.057 ppm. The Zr(II)Otc/Sal metal complex contains signals in the range 18.366, 40, 55.821-55.942 ppm have been attributed to the methyl group, DMSO solvent, and -CH group (Steinhuebel *et al.*, 1998). The ^{13}C -NMR spectra of the Mo-OTC/Sal metal complex showed a peak at 15.023 ppm for the methyl group and 65.357 ppm for the C-N group, respectively. The signal at 45 ppm was assigned to DMSO. The carbon of the aromatic ring appeared at 128.924 ppm (Huma *et al.*, 2022; Dupe *et al.*, 2015; Kargar *et al.*, 2021). Similarly, The Pd(II)Otc/Sal metal complex observed signals in the region of 34.257, 40, 71.543, 84.502, and 137.147 ppm were assigned to the methylene group, DMSO, -CH, -C=C-, and Ar-C (Smrecki *et al.*, 2016). The recorded spectrums of M-OTC/Sal metal complexes are reported in **Table 11**.

Table 11: ^{13}C -NMR spectral data of the Cd-OTC/Sal, Zr(II)Otc/Sal, Mo-OTC/Sal, and Pd(II)Otc/Sal metal complexes

Compounds	Assignment	Chemical Shift (δ ppm)
Cd-OTC/Sal Complex	CH_3	18.394
	DMSO	40
	-CH	55.892
	Ar-C	95.513, 103.870, 135.057
Zr(II)Otc/Sal Complex	CH_3	18.366
	DMSO	40
	CH	55.821-55.942
Mo-OTC/Sal Complex	CH_3	15.023
	DMSO	45
	C-N	65.357
	Ar-C	128.924
Pd(II)Otc/Sal Complex	CH_2	34.257
	DMSO	40
	CH	71.543
	C=C	84.502
	Ar-C	137.147

4.3.3 Mass Spectral Study

4.3.3.1 Mass Spectral Study of M-TC/Sal Metal Complexes

MS (Mass spectrometry) is an instrumental analytical method for measuring the mass-to-charge ratio (m/z) of a compound in solution. Their proposed formula was confirmed to the complexes with the help of a molecular ion peak $[M+H]^+$. In the mass spectrum, the pattern indicates the continuous degradation of target compounds containing different fragmented ion peaks. The Cd-TC/Sal and Mo-TC/Sal complexes showed ESI-MS spectra at m/z 677 and 661 amu indicating a molecular ion peak $[M+H]^+$, also denotes the molecular formula weight of the metal complex. The base peaks for these complexes appeared at m/z 327 and 427 amu. The remaining peaks in the spectrum are called fragment ion peaks with significant intensity (Warad *et al.*, 2014; Tabrizi *et al.*, 2016; Singh *et al.*, 2013). Similarly, the molecular ion peaks for the Zr-TC/Sal and Pd-TC/Sal complexes appear at 656 m/z and 671 m/z while the base peaks appear at 445 m/z and 171 m/z , respectively (Ramadan *et al.*, 2013; Hernandez *et al.*, 2013). Their proposed formula shows the molecular weight of the complex as represented in (Figs. 7-10).

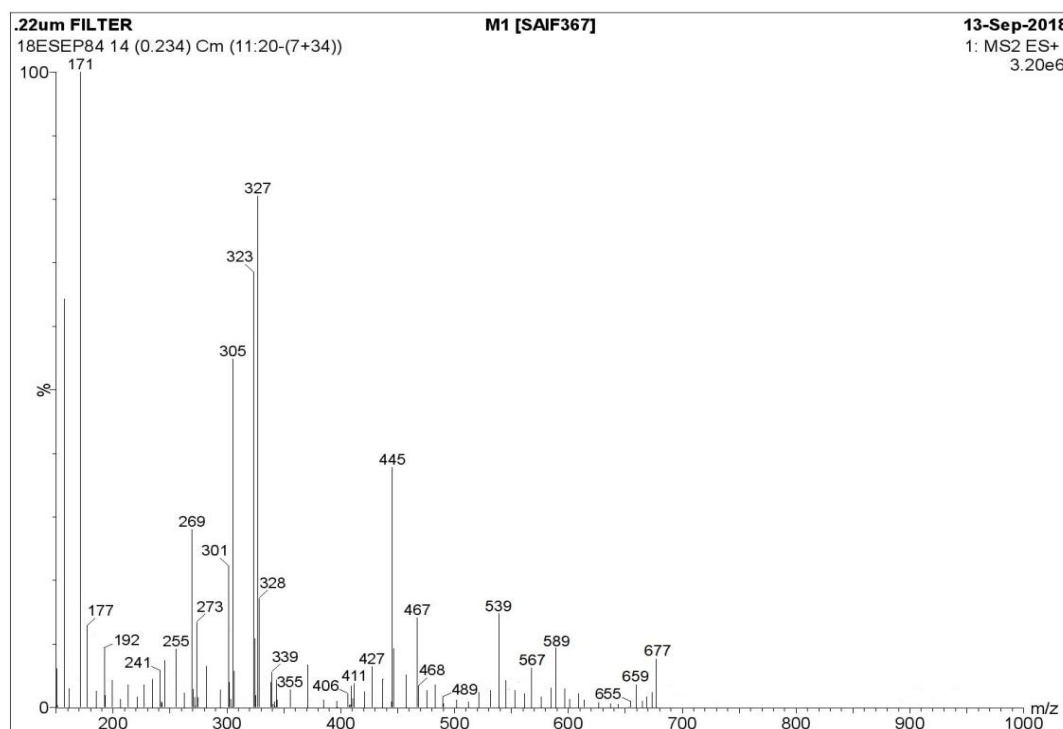


Figure 7: Mass Spectrum of Cd-TC/Sal metal complex

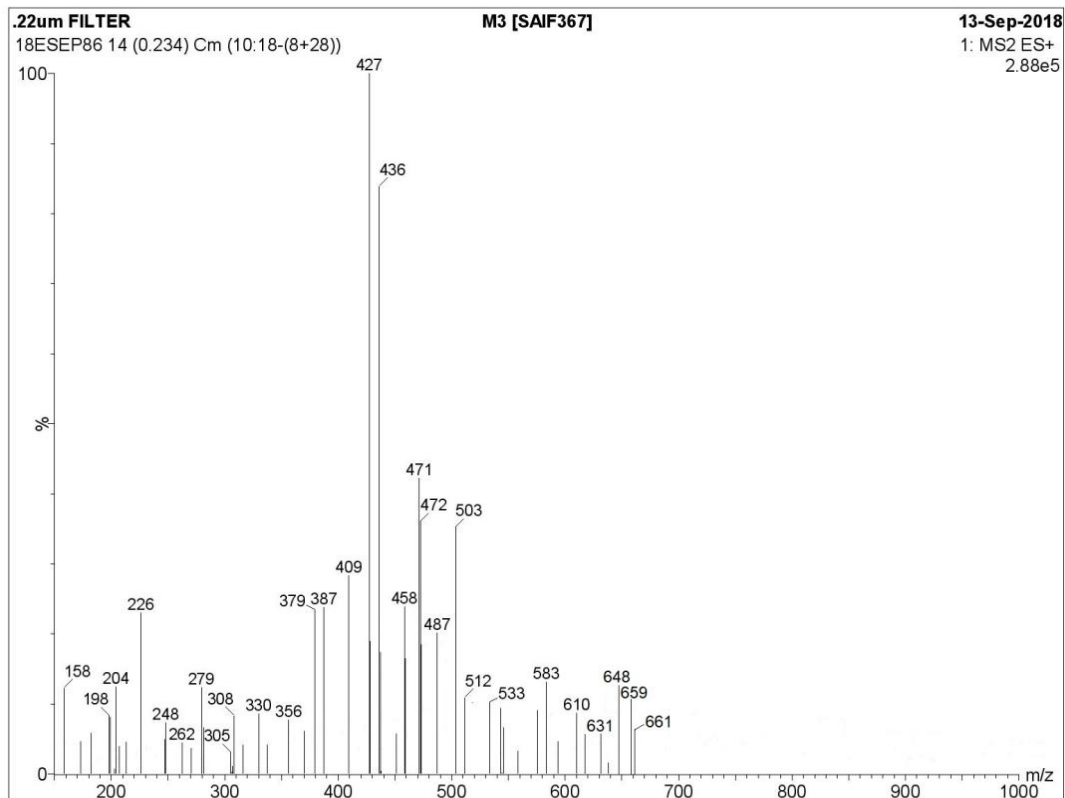


Figure 8: Mass Spectrum of Mo-TC/Sal metal complex

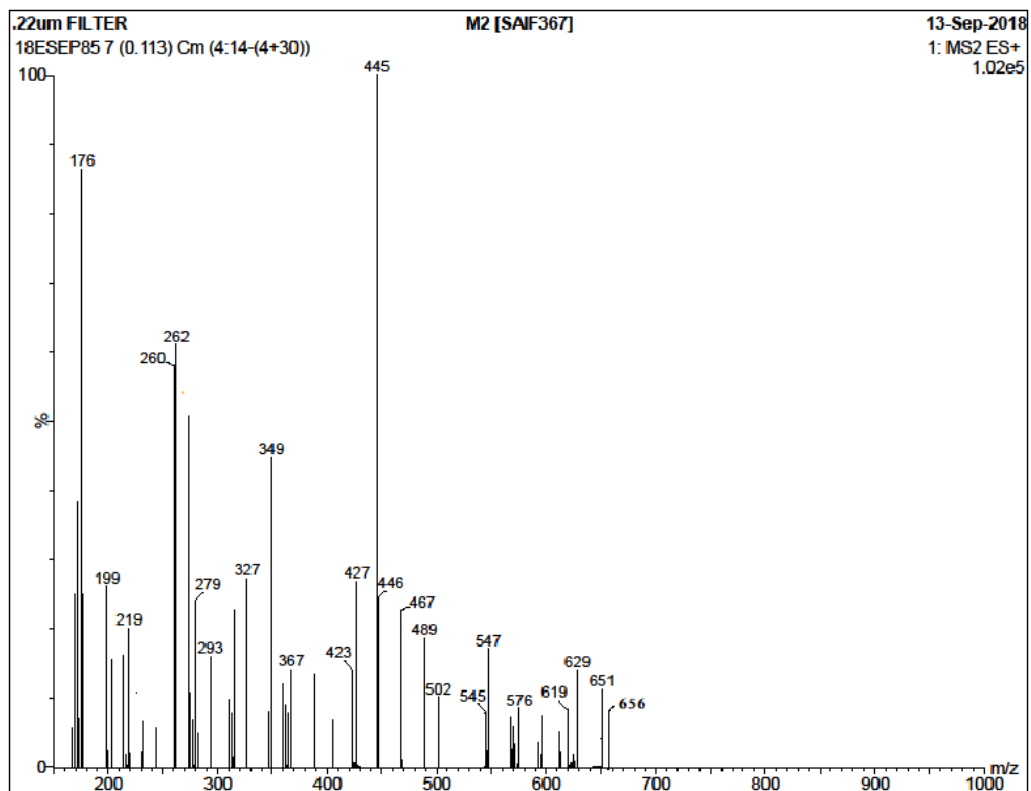


Figure 9: Mass Spectrum of Zr-TC/Sal metal complex

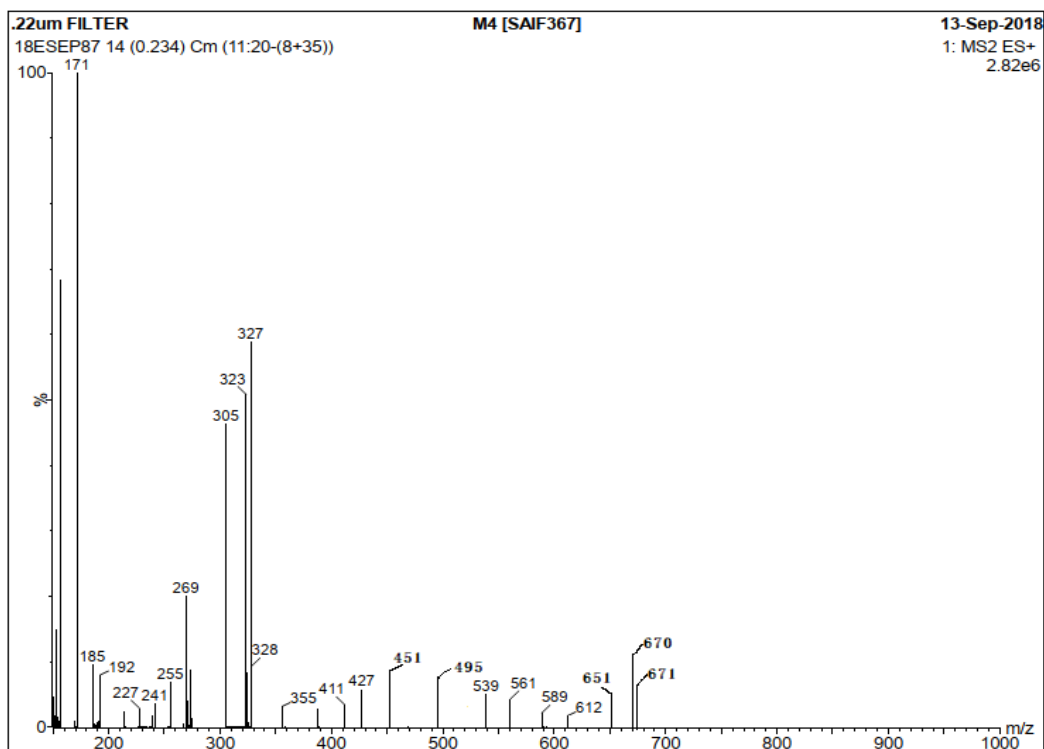


Figure 10: Mass Spectrum of Pd-TC/Sal metal complex

4.3.3.2 Mass Spectral Study of M-OTC/Sal Metal Complexes

The mass spectra of the four synthesized metal complexes (M-OTC/Sal) are presented in (Figs. 11-14). The Cd-OTC/Sal and Mo-OTC/Sal metal complexes showed positive ESI mode at m/z 693 and 747 amu, indicating a molecular ion peak $[M+H]^+$, the molecular formula weight of the metal complexes, and the base peak at m/z 461 and 616 amu. The complexes also have an additional peak known as the fragment ion peak obtained during the fragmentation of the molecular ion. Fragment ion peaks of Cd-OTC/Sal and Mo-OTC/Sal complexes of oxytetracycline lie at m/z (690, 620, 543, 483, 385, and 300) and (743, 728, 723, 709, 674, 640, 537, 473, and 450), respectively. Similarly, the Zr(II)Otc/Sal and Pd(II)Otc/Sal complexes displayed positive ESI mode at m/z 671 and 687 amu, indicating a molecular ion peak $[M+H]^+$, which signifies the molecular formula weight of the complexes and the base peak at m/z 433 and 365 amu. The complexes also have an additional peak known as the fragment ion peak obtained during the fragmentation of the molecular ion. The fragment ion peaks of Zr(II)Otc/Sal and Pd(II)Otc/Sal complexes are located at m/z (665, 536, 502, 453, 425, and 350) and (659, 620, 600, 563, 465, and 443),

respectively. All these data values of the molecular ion peak as well as the fragment ion peak are consistent with the proposed molecular formula weight of the metal complex.

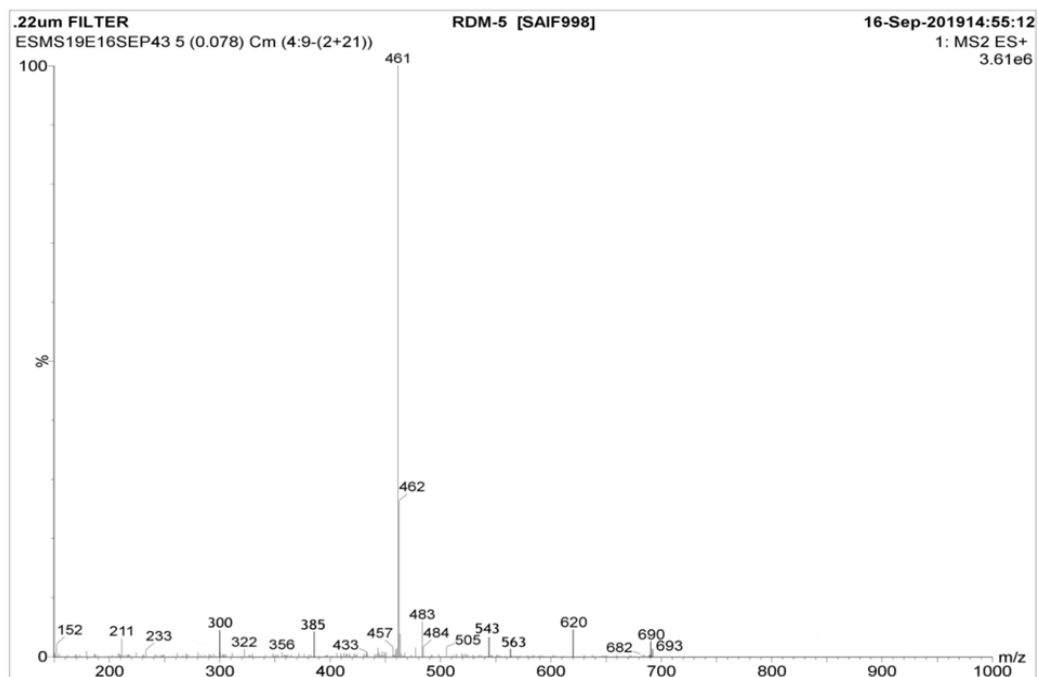


Figure 11: Mass Spectrum of Cd-OTC/Sal metal complex

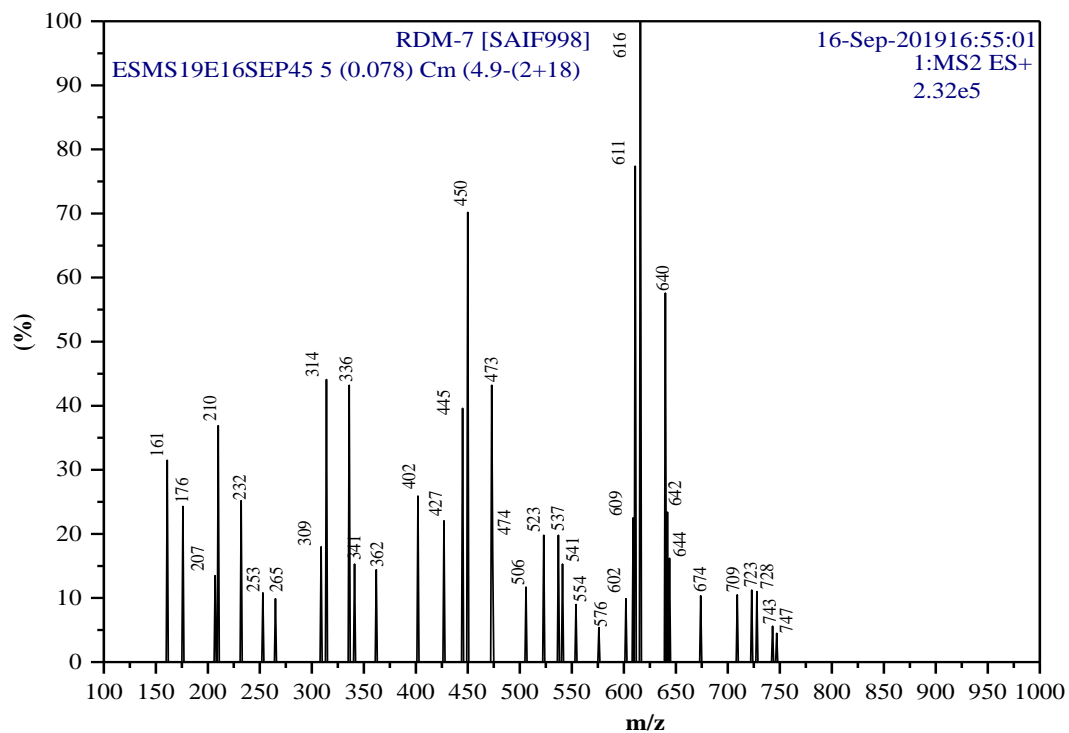


Figure 12: Mass Spectrum of Mo-OTC/Sal metal complex

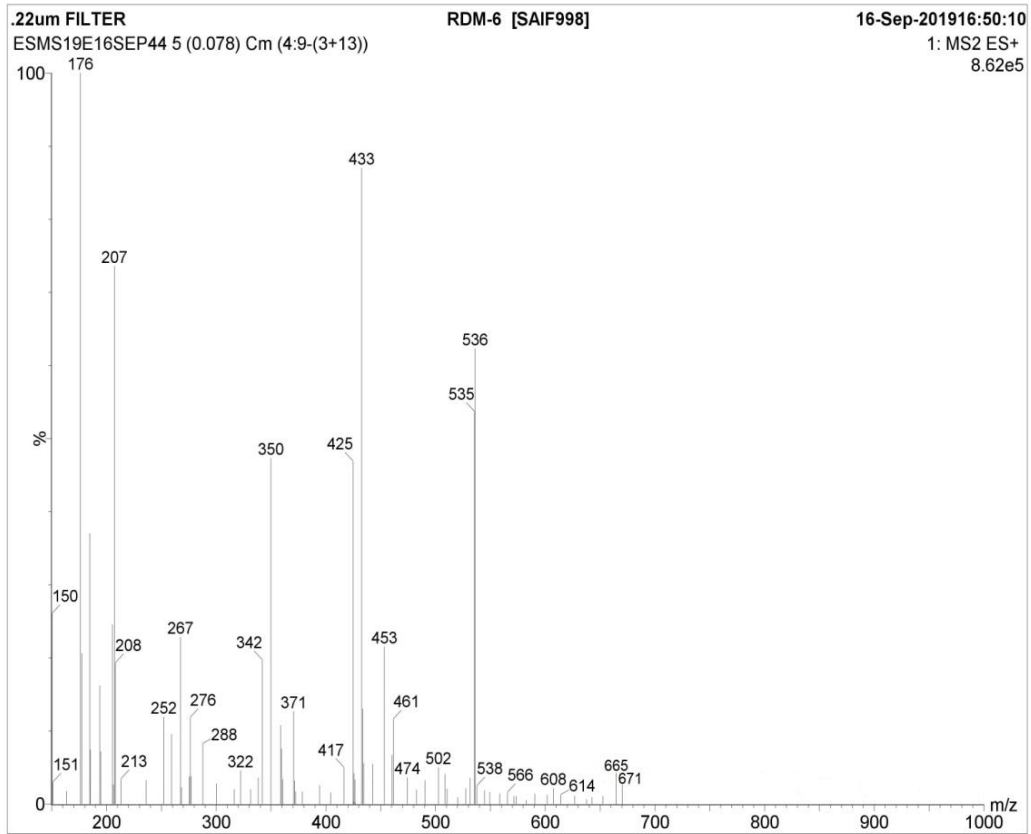


Figure 13: Mass Spectrum of Zr(II)Otc/Sal metal complex

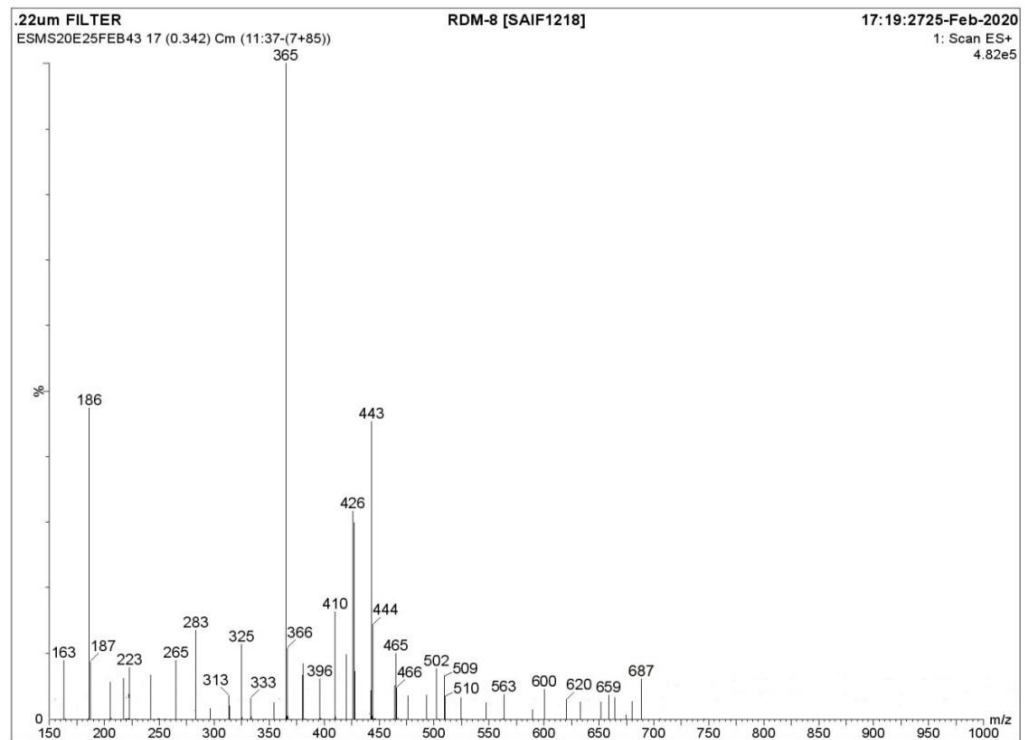


Figure 14: Mass Spectrum of Pd(II)Otc/Sal metal complex

4.3.4 Electronic Absorption Spectroscopy (EAS)

4.3.4.1 EAS of M-TC/Sal Metal Complexes

Electronic absorption spectroscopy is an instrumental analytical tool that helps to differentiate the characterization of a metal complex by examining its binding mode of action with the ligand (Tabrizi *et al.*, 2015). The paramagnetic or diamagnetic nature and geometry of the complexes can be calculated from the magnetic moment. Significant electronic spectra were taken using a DMSO solvent within the wavelength range of 250-800 nm, at room temperature. The same solvent was used as a blank using a 1 cm path length cuvette. The electronic spectrum of Cd-TC/Sal showed extremely high sharp peaks at 280, 369, and 768 nm, which was responsible for the transitions of $\pi \rightarrow \pi^*$ and $n \rightarrow \pi^*$, respectively. The diamagnetic Cd-TC/Sal complex shows no d-d transition band because its (d^{10}) electronic orbital is full, but can exhibit metal-ligand-charge transfer (MLCT) denoting the d^{10} system (Pal *et al.*, 2018; Dilip *et al.*, 2013). The metal complex (Mo-TC/Sal) showed three absorption bands at 297, 371, and 447 nm due to the transition of the $\pi \rightarrow \pi^*$ and $n \rightarrow \pi^*$. The band at 447 nm has been attributed to the MLCT (metal-to-ligand charge transfer) transition (Khalili & Al-Seif, 2008). Similarly, in the Zr-TC/Sal metal complex, two bands at a wavelength of 268 and 342 nm, are assigned to the ($\pi \rightarrow \pi^*$) transition inside the aromatic ring and remain unchanged. The next band is observed at 446 nm, which is due to the $n \rightarrow \pi^*$ transition within the $-C=N-$ group chromophore, indicating a bathochromic shift. Similarly, in the Pd-TC/Sal metal complex, the bands at 263, 307, and 343 nm are due to the $^1A_{2g} \rightarrow ^1A_{1g}$ transition to the square planar geometry around metal ions (Singh *et al.*, 2013; Aslan *et al.*, 2011). The electronic absorption spectra of M-TC/Sal metal complexes are presented in **(Figs. 15-16)**.

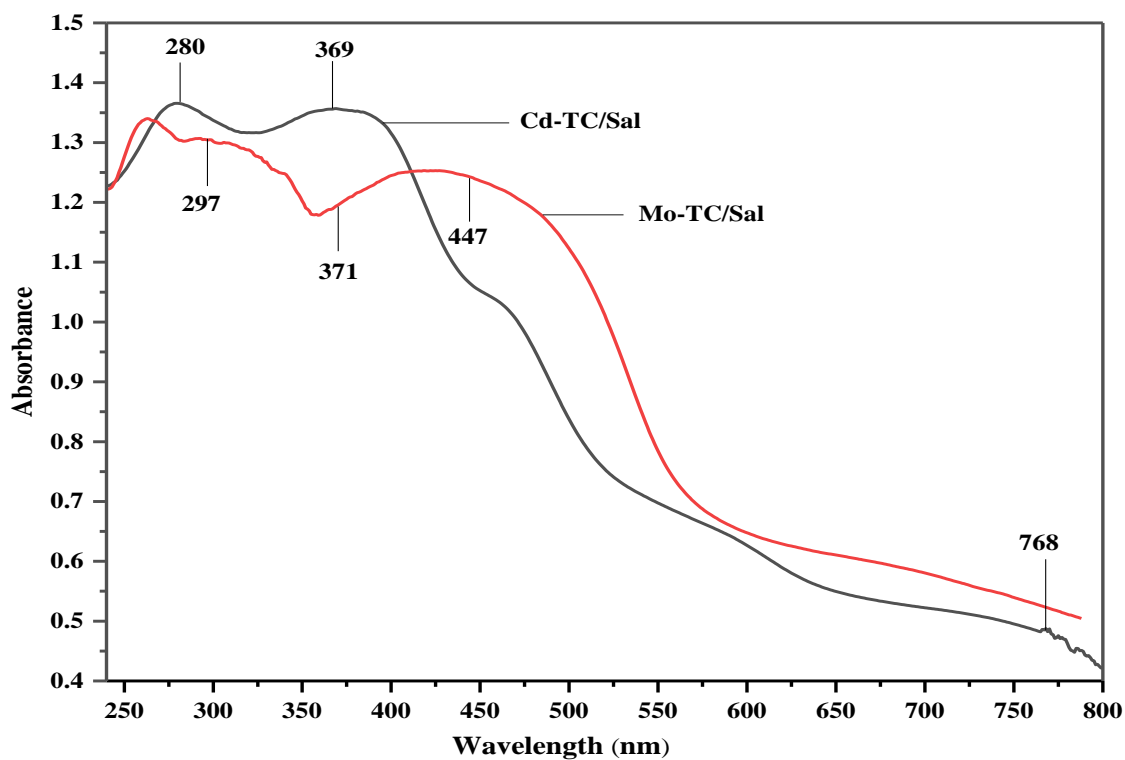


Figure 15: Electronic absorption spectra of Cd-TC/Sal and Mo-TC/Sal metal complexes.

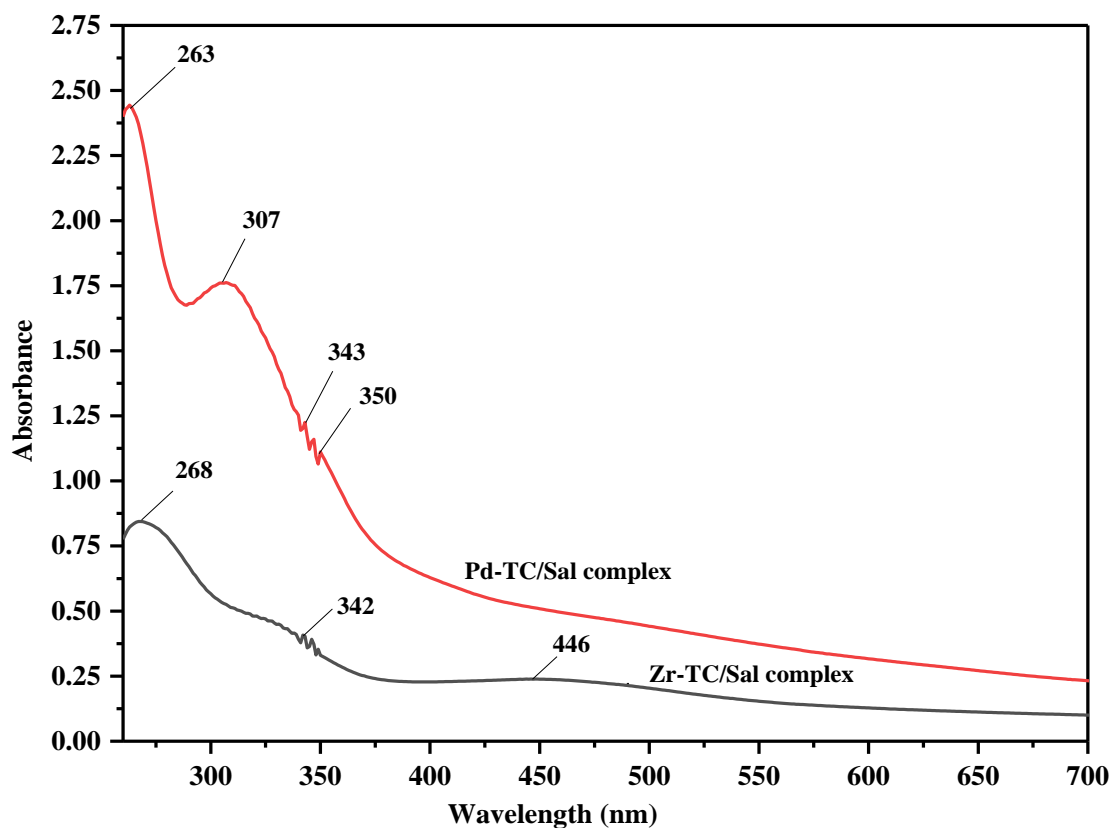


Figure 16: Electronic absorption spectra of Zr-TC/Sal and Pd-TC/Sal metal complexes.

4.3.4.2 EAS of M-OTC/Sal Metal Complexes

The electronic spectrum of Cd-OTC/Sal showed an extremely high intense peak at 267, 322, and 375 nm, assigning to ($\pi \rightarrow \pi^*$ and $n \rightarrow \pi^*$) transition. Furthermore, the diamagnetic Cd(II) complex does not appear to have any d-d transition band because its (d^{10}) electronic orbital is full but can exhibit ligand-metal-charge transfer (LMCT) reflecting the d^{10} system and is capable of giving tetrahedral geometry. The Mo-OTC/Sal metal complex showed two bands at 264 and 318 nm, attributed to the $\pi \rightarrow \pi^*$, $n \rightarrow \pi^*$ transition, and some charge transferred because of the nitrogen atom as an electron donor and the carbonyl group as the receptor. As the complex has an octahedral geometry and diamagnetic nature, it is attributed to LMCT (ligand-metal charge transfer) from HOMO (highest occupied molecular orbital) phenolic group of oxygen to LUMO (lowest unoccupied molecular orbital) of the molybdenum (Omar *et al.*, 2017; Maurya *et al.*, 2011). In the Zr(II)Otc/Sal metal complex, three bands are seen at wavelengths of 339, 343, and 347 nm, which are determined to be ($\pi \rightarrow \pi^*$) transitions inside the aromatic ring and remain unchanged. The fourth band is observed at 379 nm and is assigned to the $n \rightarrow \pi^*$ transition within the $-C=N$ -group chromophore, indicating a bathochromic shift. Likewise, in the Pd(II)Otc/Sal metal complex, two weak bands were observed at (265, 271, 386, 457) nm, are assigned to be ($\pi \rightarrow \pi^*$ and $n \rightarrow \pi^*$) transitions in the visible region which are assigned to $^1B_{1g} \leftarrow ^1A_{1g}$ and $^1A_{2g} \leftarrow ^1A_{1g}$ d-d transition, respectively. Therefore, these transitions denote the complex is diamagnetic and square planar geometry around the metal ions, as presented in **Table 12** (El-Shwiniy *et al.*, 2018; Sharma *et al.*, 2016; Abdul-ghani *et al.*, 2009; Aslan *et al.*, 2011; Naglah *et al.*, 2021). The EAS of M-OTC/Sal metal complexes are presented in (**Figs. 17-18**).

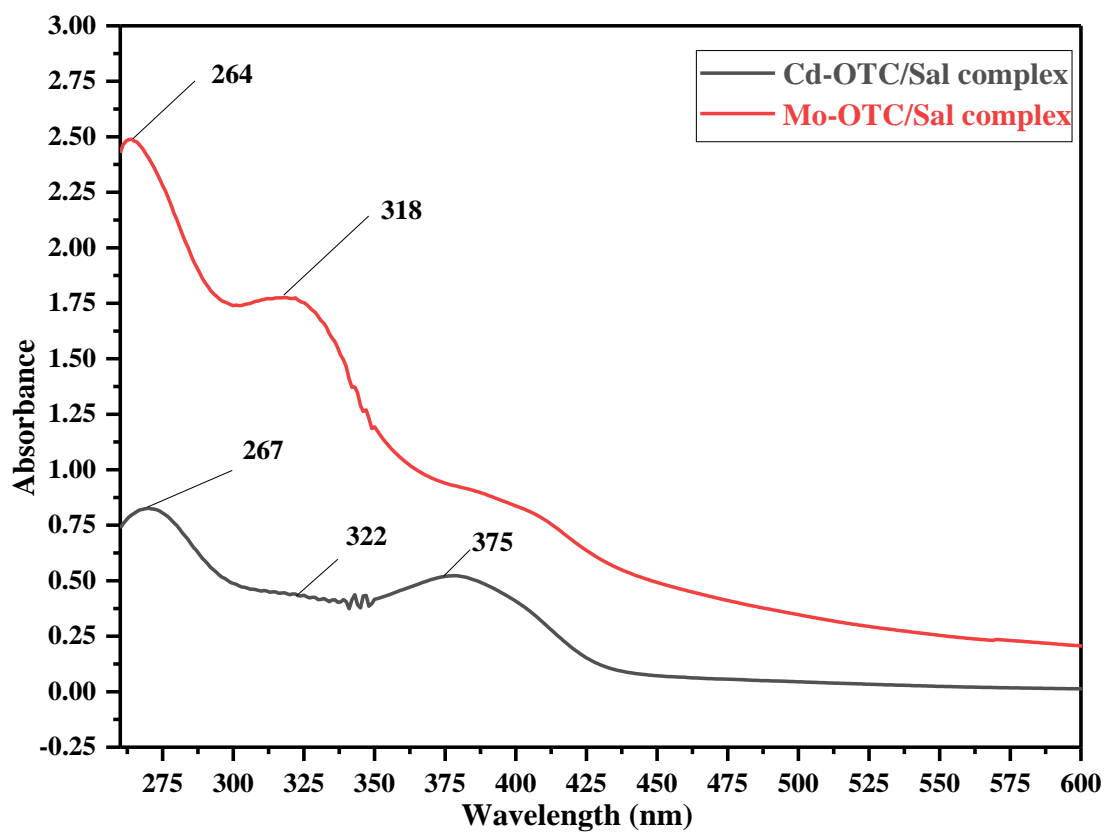


Figure 17: Electronic absorption spectra of Cd-OTC/Sal and Mo-OTC/Sal metal complexes

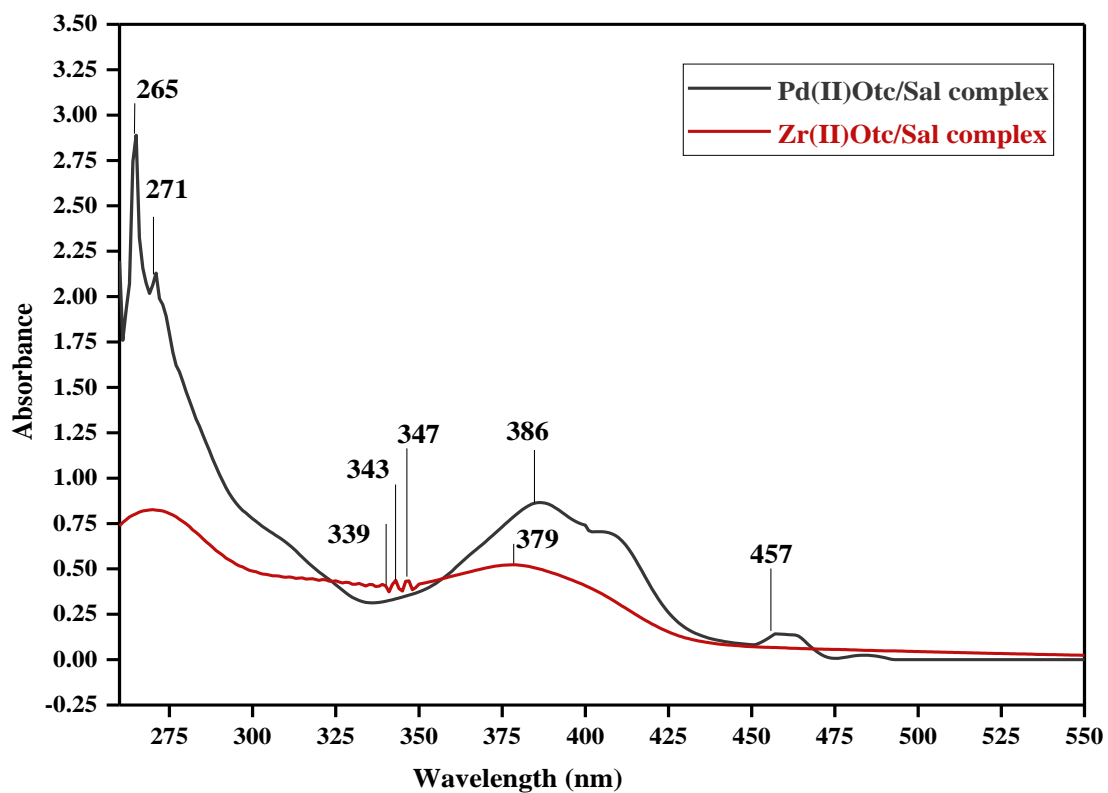


Figure 18: Electronic absorption spectra of Zr(II)Otc/Sal and Pd(II)Otc/Sal metal complexes.

Table 12: Electronic spectral data of M-TC/Sal and M-OTC/Sal metal complexes

Complexes	Peak positions (nm)	Assignments
Cd-TC/Sal	280, 369, 768	$\pi \rightarrow \pi^*$, $n \rightarrow \pi^*$, LMCT
Mo-TC/Sal	297, 371, 447	$\pi \rightarrow \pi^*$, $n \rightarrow \pi^*$, LMCT
Zr-TC/Sal	268, 342, 446	$\pi \rightarrow \pi^*$, $n \rightarrow \pi^*$
Pd-TC/Sal	263, 307, 343	$\pi \rightarrow \pi^*$, $n \rightarrow \pi^*$
Cd-OTC/Sal	267, 322, 375	$\pi \rightarrow \pi^*$, $n \rightarrow \pi^*$, LMCT
Mo-OTC/Sal	264, 318	$\pi \rightarrow \pi^*$, $n \rightarrow \pi^*$
Zr(II)Otc/Sal	339, 343, 347, 379	$\pi \rightarrow \pi^*$, $n \rightarrow \pi^*$
Pd(II)Otc/Sal	265, 271, 386, 457	$\pi \rightarrow \pi^*$, $n \rightarrow \pi^*$

4.4 Thermal Analysis

Thermal analysis or thermoanalytical is a useful method that has wide applications in various fields in recent times. This method helps to characterize a system at elevated temperatures as a function of increasing temperature by determining changes in the physicochemical process. The two methods are (a) DTA (differential thermal analysis), where the "heat content" is determined as a function of increasing temperature, and (b) TGA (thermal gravimetric analysis), where the weight loss is determined with increasing temperature (Coats & Redfern, 1963). Thermal gravimetric analysis is also a powerful tool for the verification of both the compositions and for predicting the stability of metal complexes (Pal *et al.*, 2019). This method is used for compounds that exhibit weight loss or gain because of different processes such as absorption, decomposition, oxidation and reduction, adsorption, and desorption of volatile components. Through thermal behavior, there is a great potential for metal ion coordination and comparison as well as free antibiotics (ligands), so it can be used in metallodrugs (Ramotowska *et al.*, 2020). A thermal analyzer is a device for measuring the thermal incidence of chemicals. The sample under analysis is heated under controlled conditions in a given atmosphere of gases such as nitrogen, argon, helium, carbon dioxide, etc., and a change in weight for a substance with increasing temperature or time is recorded. Here, the temperature can be raised at a constant rate to find out the initial weight of a substance, and various time intervals or changes in weight as a function of temperatures are re-recorded. Thus, a plot of the weight change that occurs against temperature is called a thermogravimetric curve or thermogram and the results from a thermogravimetric run

can be analyzed (a) the weight vs. temperature curve called a thermogravimetric curve, and (b) the rate of weight loss vs. temperature, called the DTG curve. The thermodynamic analysis is an important technique for thermodynamically calculating the activation parameters of a complex with various decomposition processes such as enthalpy of activation (ΔH^*), Gibb's free energy of activation (ΔG^*), and activation energy (E^*), which can be calculated graphically using the help of Coats-Redfern relation as follows:

$$\log \left[\frac{-\ln(1/(1-\alpha))}{T^2} \right] = \log \left[\frac{AR}{\beta E^*} \left(1 - \frac{2RT}{E^*} \right) \right] - \frac{E^*}{2.303RT}$$

Here, α represents the fraction of sample decomposes with temperature T , [$\alpha = \frac{W_i - W_t}{W_i - W_f}$], where W_i is the initial weight of the sample, W_f is the final weight of the sample, W_t is the weight of the sample at T K, E^* is the activation energy at kJmol^{-1} , A is the frequency factor, and β is the linear heating rate, $\left(\frac{dT}{dt}\right)$, and the term $\left(1 - \frac{2RT}{E^*}\right) \cong 1$. The plot of $\log \left[\frac{-\ln(1/(1-\alpha))}{T^2} \right]$ vs $1/T$ represents a straight line. E^* and A are calculated via a straight line having intercept and slope, respectively. In the current research work, several kinetic parameters were calculated and other parameter processes such as E^* (activation of energy), ΔS^* (entropy of activation), ΔH^* (enthalpy of activation), ΔG^* (Gibb's free energy of activation) and specific rate constants were calculated from the given relations:

$$\Delta S^* = 2.303 R \log \left[\frac{Ah}{K_B T_S} \right] = R \ln \left[\frac{Ah}{K_B T} \right]$$

$$\Delta H^* = E^* - RT$$

$$\Delta G^* = \Delta H^* - T \Delta S^*$$

$$\log K = \log A - \frac{E^*}{2.303RT_S}$$

Here, h denotes Plank's constant, K_B is the Boltzmann constant, and T_S is the peak temperatures of the DTA curve, respectively (Dilip *et al.*, 2013; Aziz *et al.*, 2012; Chaudhary *et al.*, 2019).

4.4.1 TGA/DTA Study of M-TC/Sal Metal Complexes

TGA/DTA analysis of metal complexes (M-TC/Sal) was performed at 860 °C with a linear heating rate of 10 °C/min under a nitrogen atmosphere at room temperature. The important objective of TGA is the association of water molecules within the metal complex with the help of micro-elemental analysis. Therefore, data analysis of thermal decomposition indicates good agreement with the analyzed micro elemental data. During research work, the following results were derived.

The thermogram of the metal complex, Cd-TC/Sal is presented in **(Fig. 19)** which shows that the decomposition takes place in three steps at temperatures from 246.89 °C - 634.32 °C. The decomposition of the first step results in a mass loss of 14.96% (-3.1143 mg) from 246.89 - 286.67 °C due to water molecule loss in the lattice of the outer sphere. The second and third decomposition steps range from 341.54 - 398.11 °C and 580.03 - 634.32 °C with a % mass loss of 11.7239 % (-11.7239 mg) and 1.9447 % (-1.9447 mg). Metal oxide (CdO) in the form of residue leads to the complete loss of the ligand from the metal complex in the final step of decomposition. Similarly, a thermogram of the Mo-TC/Sal metal complex **(Fig. 20)** shows that decomposition occurs in three steps within a temperature range of 197.38 - 805.15 °C. The first decomposition step results in a mass loss of 16.899% (-1.6899 mg) from 197.38-260.48 °C due to the loss of water molecules in the lattice of the outer sphere. The second and third decomposition steps occur from 721.21 - 742.98 °C and 789.75 - 805.15 °C with a % mass loss of 1.6459 % (-16.459mg) and 1.4743% (-1.4743 mg). The metal oxide (Mo₂O₃) as the residue is the complete loss of the ligand from the complex in the final step of decomposition.

The thermogram of the metal complex (Zr-TC/Sal) is reported in **(Fig. 21)** which shows that decomposition occurs in a temperature range of 50.7 - 755.48 °C in three steps. The first decomposition occurs at 50.7 - 108.05 °C with a % mass loss of 27.93 % (-5.9503 mg) due to water molecule loss in the lattice of the outer sphere. At 249.28 - 302.03 °C and 633.79 - 755.48 °C, the second and third decompositions occurred with a % mass loss of 40.60% (-1.197 mg) and 83.89% (-2.3386 mg). Metal oxide (ZrO) as a residue leads to the complete loss of the ligand from the complex in the final steps of decomposition. Similarly, the thermogram of the metal complex, Pd-

TC/Sal is presented in (Fig. 22) which shows that decomposition occurs in two steps at temperatures between 164.01 - 769.19 °C. The first decomposition step occurred in the range of 164.01 - 247.37 °C with a % mass loss of 20.60 % (-3.3048 mg) due to water molecule loss in the lattice of the outer sphere. A second decomposition step occurred in the range 709.75 - 769.19 °C with a % mass loss of 65.59 % (-1.4339 mg). Metal oxide (PdO) as a residue occurred due to the complete loss of ligands from the complex in the final stage of decomposition.

Kinetic Parameter

Thermodynamics with kinetic activation parameters as well as various thermal decomposition steps such as ΔH^* (enthalpy of activation), E^* (activation energy), ΔS^* (entropy of activation), and ΔG^* (Gibb's free energy of activation) calculated with the help of the Coats-Redfern equation (Dilip *et al.*, 2013; Gaber *et al.*, 2015). The results are shown in Tables 13 and 14 and the following are the comments:

1. Activation energies with increasing and higher values indicate higher thermal stabilities, caused by the covalent bonding nature.
2. The value change in ΔS^* (negative or positive both) reflects a more ordered activated complex than the slow nature of reaction from a normal.
3. The positive value of ΔH^* represents the endothermic decomposition process.
4. The positive value of ΔG^* explains the non-spontaneous nature of the metal complex.

Table 13: Kinetics and thermodynamic parameters of the M-TC/Sal metal complexes [M=Cd(II), Mo(III), Zr(II), and Pd(II)]

Complexes	R	A(s ⁻¹)	Tmax(K)	E*(kJ/mol)	ΔS^* (J/kmol)	ΔH^* (kJ/mol)	ΔG^* (kJ/mol)
Cd-TC/Sal	-0.9955	2.05x10 ¹⁷	531.18	184.920	120.970	18.505	116.248
	-0.9986	4.01x10 ²¹	644.85	263.260	162.240	257.901	153.281
	-0.9988	1.72x10 ²⁴	892.81	421.170	209.930	413.751	226.324
Mo-TC/Sal	-0.9979	7.55x10 ⁹	496.22	102.526	-60.040	98.401	128.196
	-0.9992	7.164x10 ⁶¹	1007.15	1196.867	929.110	1188.494	252.745
	-0.9963	1.59x10 ¹⁰⁴	1070.54	2100.898	216.17	2091.997	186.058
Zr-TC/Sal	-0.9993	1.68x10 ⁸	355.66	60.311	-88.91	57.354	88.976

	-0.9981	2.64×10^{14}	545.88	158.856	26.14	154.318	140.049
	-0.9993	7.14×10^{10}	979.71	222.049	-47.02	213.903	259.970
Pd-TC/Sal	-0.9942	7.3×10^6	470.13	70.608	-117.32	66.699	121.854
	-0.9990	2.71×10^{23}	1014.12	4498.82	193.5	4490.378	4294.096

Table 14: Thermal decomposition data of the M-TC/Sal metal complexes [M= Cd(II), Mo(III), Zr(II), and Pd(II)]

Complexes	TG range ($^{\circ}C$)		DTA				
	$\Delta m\%$ (cal.)	Ti	Tf	T_{DTG}	Mass loss	T_{dta}	Peak
Cd-TC/Sal	14.96	246.89	286.67	258.18	-3.1143	246.89	Exo
	11.7239	341.54	398.11	371.70	-11.7239	-	Exo
	1.9447	580.03	634.32	619.81	-1.9447	634.11	
Mo-TC/Sal	16.899	197.38	260.48	223.22	-1.6899	197.38	-
	1.6459	721.21	742.98	734.15	-16.459	-	-
	1.4743	789.75	805.15	797.54	-1.4743	805.15	-
Zr-TC/Sal	27.93	50.7	108.05	82.66	-5.9503	-	-
	40.60	249.28	302.03	272.88	-1.197		
	83.89	633.79	755.48	706.71	-2.3386	-	-
Pd-TC/Sal	20.60	164.01	247.37	197.13	-3.3048	-	-
	65.59	709.75	769.19	741.12	-1.4339		

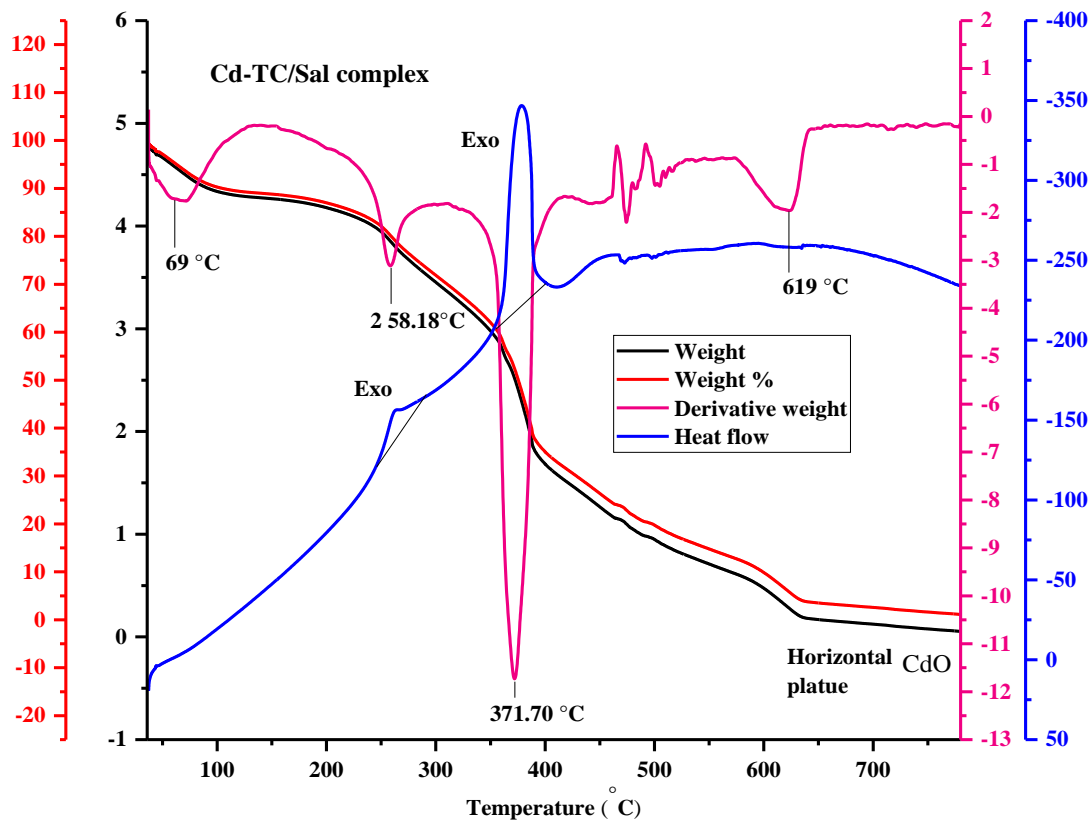


Figure 19: Thermogram of Cd-TC/Sal metal complex

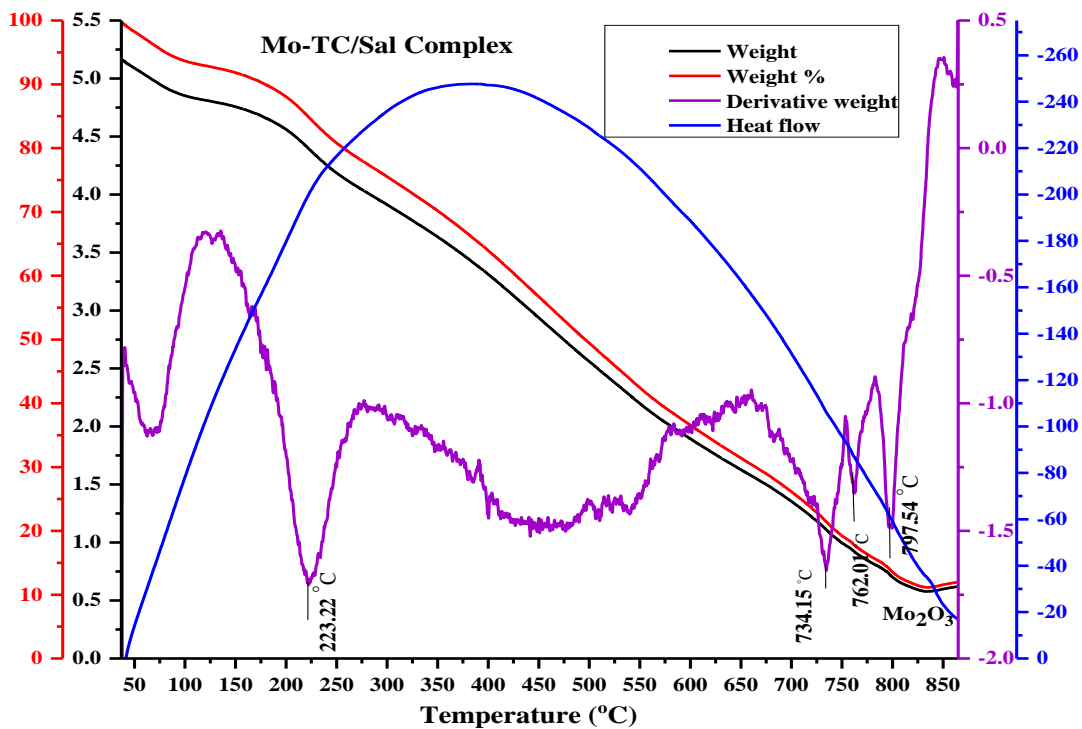


Figure 20: Thermogram of Mo-TC/Sal metal complex

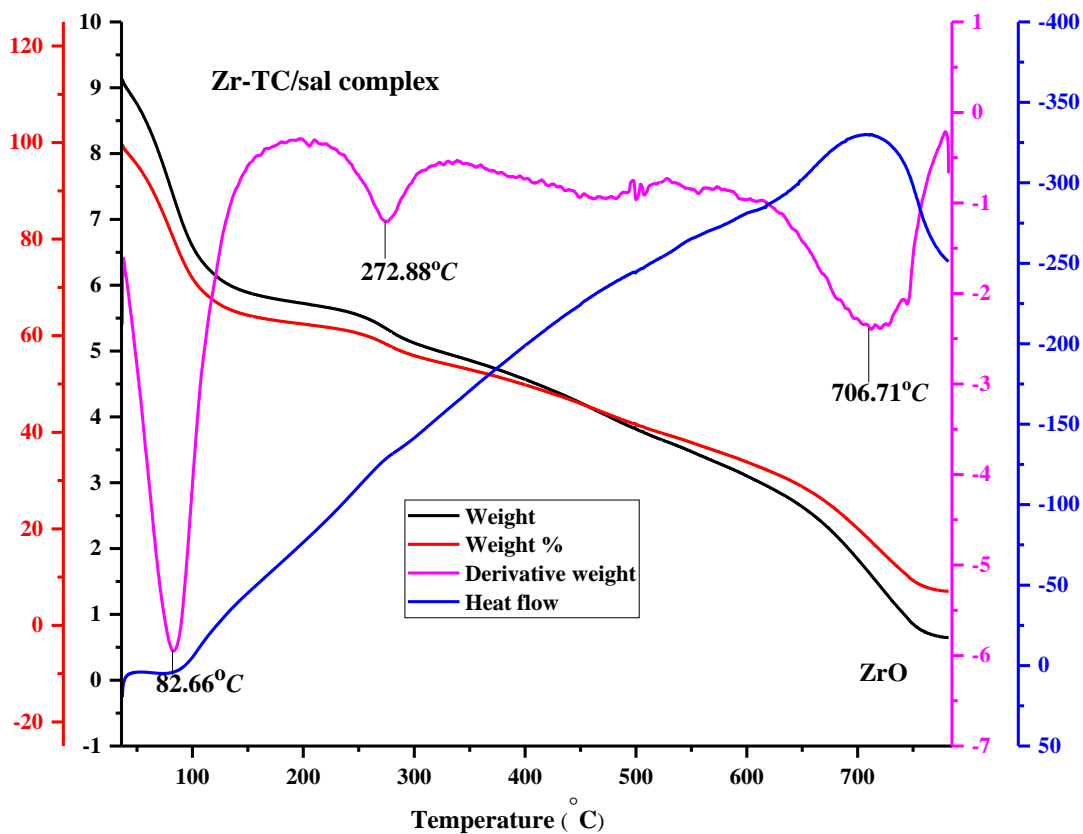


Figure 21: Thermogram of Zr-TC/Sal metal complex

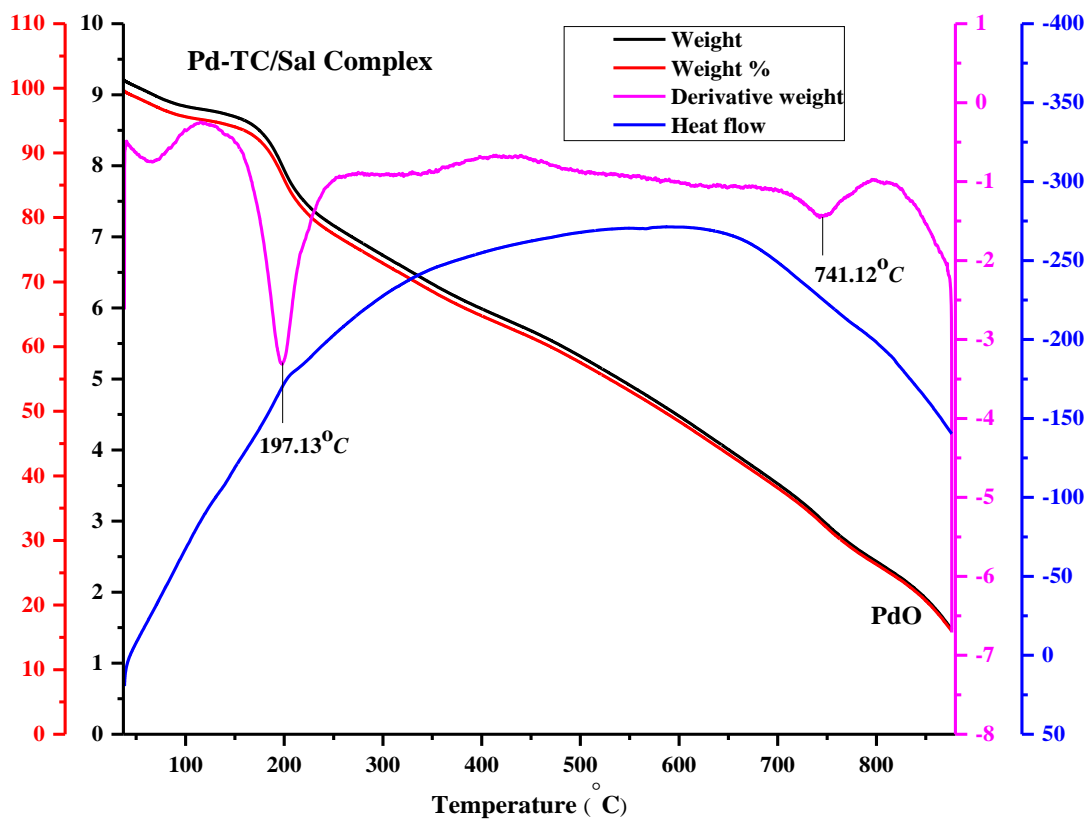


Figure 22: Thermogram of Pd-TC/Sal metal complex

4.4.2 TGA/DTA Study of M-OTC/Sal Metal Complexes

In the Cd-OTC/Sal metal complex, the thermogram (**Fig. 23**) shows that decomposition occurs in two steps at temperatures between 362.05 - 680.76 °C. The first decomposition step occurred from 362.05 - 448.12 °C with a % mass loss of 28.01 % (-0.837 mg), due to water molecule loss in the lattice of the outer sphere. The second step of decomposition occurred at 611.13 - 680.76 °C with a % mass loss of 9.58 % (-0.232 mg). Metal oxide (CdO) in the form of residue leads to a complete loss of ligands from the complex in the final step of decomposition. Similarly, in the Mo-OTC/Sal metal complex, the thermogram (**Fig. 24**) showed that decomposition occurred at three steps of temperature between 374.30 - 508.22 °C. The first step of decomposition occurred at 374.30 - 397.33 °C with a % mass loss of 13.022 % (-0.742 mg), due to water molecule loss in the lattice of the outer sphere. At temperatures (407.21 - 417.17 °C and 464.40 - 508.22 °C), decomposition of the second and third steps occurred with a % mass loss of 17.39 % (-0.548 mg) and 6.08 % (-0.657 mg). Complete loss of the ligand from the complex leaving the metal oxide (Mo₂O₅) as the residue in the final step of decomposition.

The thermogram of the Zr(II)Otc/Sal metal complex (**Fig. 25**) shows that decomposition occurs in three steps within a temperature range of 62.42 - 750.58 °C. The first step of the decomposition step occurred at 62.42 - 132.18 °C with a % mass loss of 1.19 % (-0.433 mg), due to water molecule loss in the outer region lattice. The second and third decomposition steps occurred in the range of 187.96 - 291.00 °C and 490.46 - 750.58 °C, with a % mass loss of 1.51 % (-0.350 mg) and 7.56 % (-0.929 mg). Metal oxide (ZrO) as a residue leads to the complete loss of ligands from the complex in the final steps of decomposition. Similarly, the thermogram of the Pd(II)Otc/Sal metal complex (**Fig. 26**) shows that decomposition occurred in two steps within a temperature between 45.34 - 252.87 °C. The first decomposition step occurred between 45.34 - 69.61 °C with a % mass loss of 4.31% (-2.535 mg), due to water molecule loss in the outer region lattice. The second step of decomposition occurred at 218.62 - 252.87 °C with a % mass loss of 8.69 % (-2.751 mg). Metal oxide (PdO) as the residue is caused by the complete loss of ligands from the complex in the final step of decomposition.

Kinetic Parameter

Kinetic activation parameters as well as thermodynamics using various thermal decomposition steps such as E^* (activation energy), ΔH^* (enthalpy of activation), ΔS^* (entropy of activation), and ΔG^* (Gibb's free energy of activation) was calculated with the help of the Coats-Redfern equation (Montazerzohori *et al.*, 2014; Al-Resayes, 2010; Ebrahimi-Kahrizangi & Abbasi, 2008). The results are shown in **Tables 15 and 16**. The results obtained from the following are the comments:

1. The activation energies with increasing and higher values indicate higher thermal stabilities, caused by the covalent bonding nature.
2. The value change in ΔS^* (negative) reflects a more ordered active complex than the slow nature of reaction compared to a reactant or a normal one.
3. With the negative value of ΔH^* , the decomposition process is exothermic.
4. The positive ΔG^* explains the non-spontaneous nature of the metal complex.

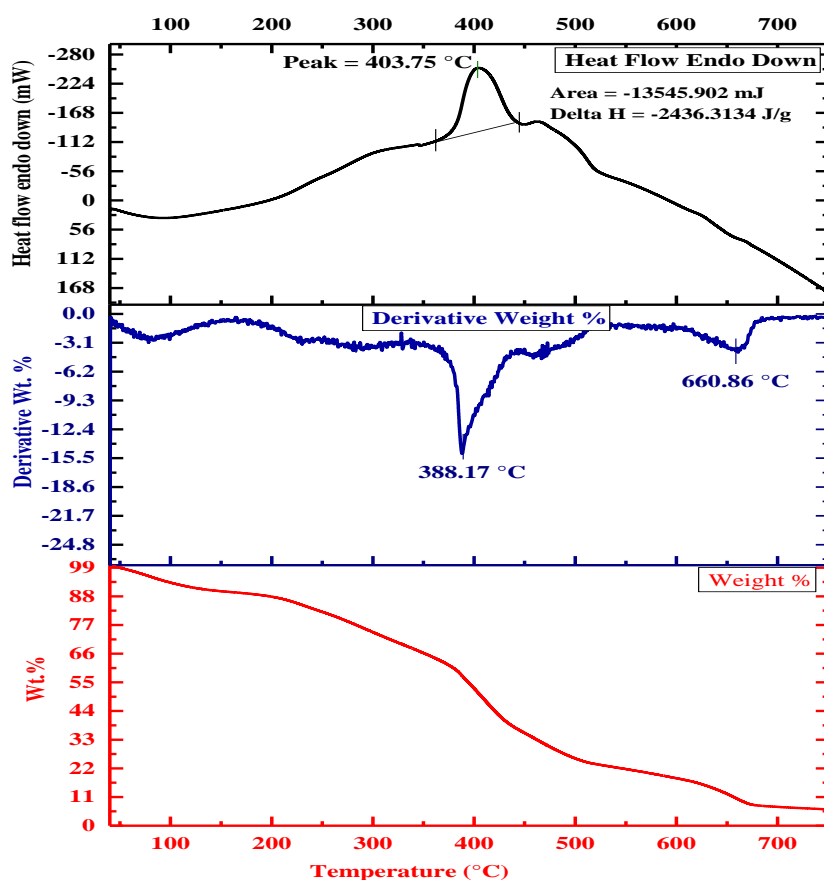


Figure 23: Thermogram of Cd-OTC/Sal metal complex

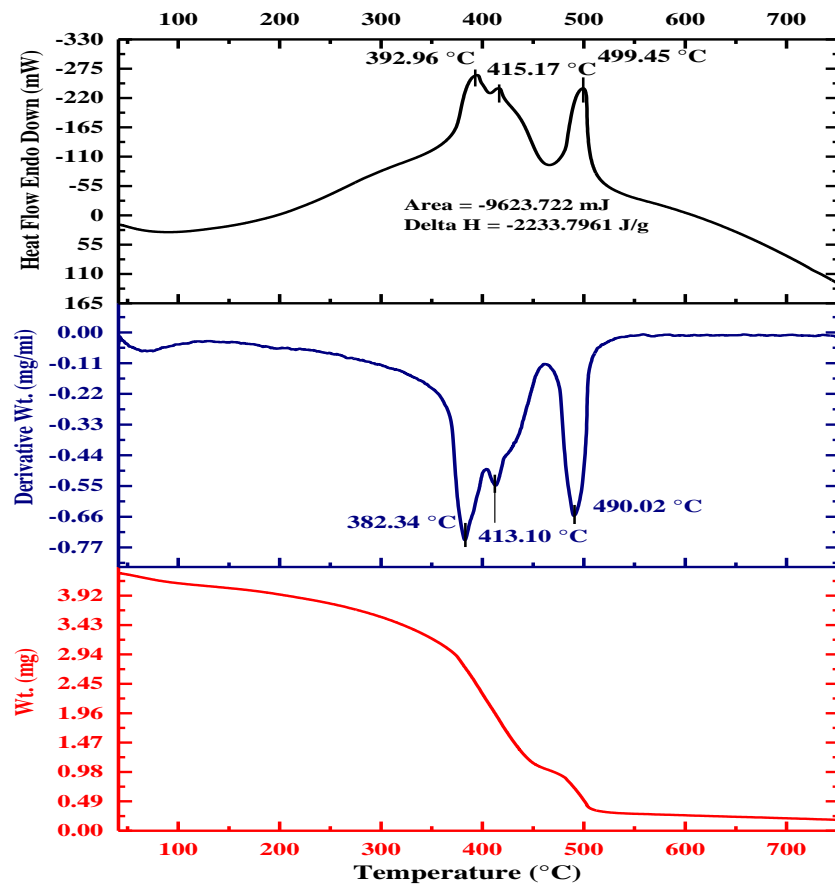


Figure 24: Thermogram of Mo-OTC/Sal metal complex

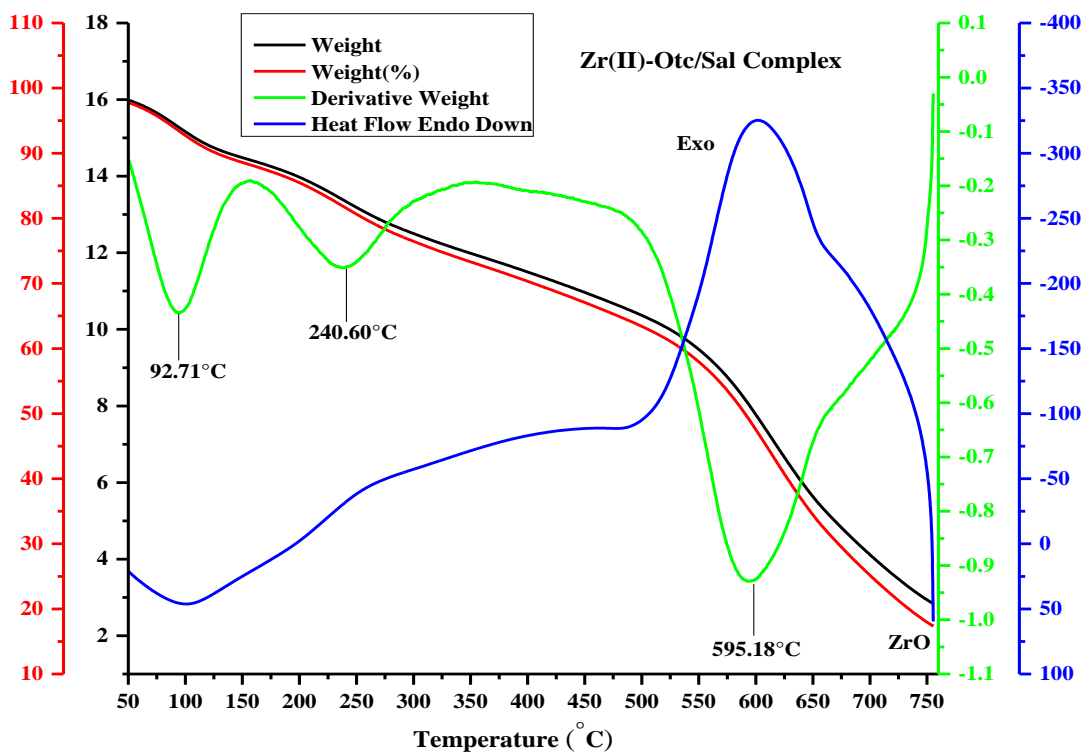


Figure 25: Thermogram of Zr(II)Otc/Sal metal complex

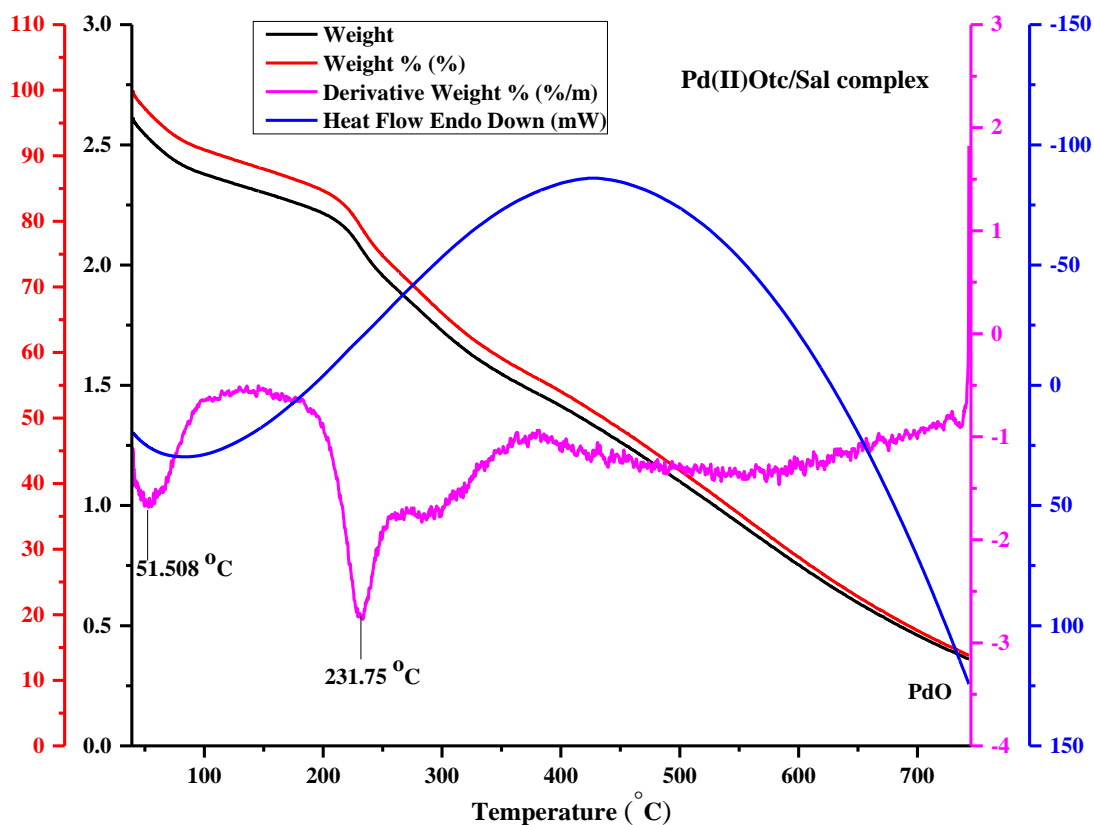


Figure 26: Thermogram of Pd(II)Otc/Sal metal complex

Table 15: Kinetics and thermodynamic parameters of the Cd-OTC/Sal, Mo-OTC/Sal, Zr(II)Otc/Sal, and Pd(II)Otc/Sal metal complexes

Complexes	R	A(s ⁻¹)	Tmax(K)	E* (kJ/mol)	ΔS* (J/kmol)	ΔH* (kJ/mol)	ΔG* (kJ/mol)
Cd-OTC/Sal	-0.99562	1468.354	661.32	341.955	-190.906	-5156.260	121095.353
	-0.99797	220.740	934.01	168.525	-209.533	-7596.834	188109.305
Mo-OTC/Sal	-0.98404	272.996	655.49	124.544	-204.823	-5325.200	128934.036
	-0.99555	124.558	686.25	53.708	-25.466	-5651.774	11824.561
	-0.99473	230.334	763.17	131.444	-207.500	-6213.551	152144.217
Zr(II)Otc/Sal	-0.99501	1727.835	365.86	1273.871	-184.630	-1766.642	65754.543
	-0.99424	890.887	513.75	968.248	-192.964	-3303.069	95831.954
	-0.98972	386.589	868.33	641.508	-204.268	-6577.787	170794.268
Pd(II)Otc/Sal	-0.99622	2.99740	324.51	0.63236	-236.490	-2697.330	-74045.570
	-0.99043	0.77258	504.75	0.30596	-251.430	-4196.190	122714.240

Table 16: Thermal decomposition data of the Cd-OTC/Sal, Mo-OTC/Sal, Zr(II)Otc/Sal, and Pd(II)Otc/Sal metal complexes

Complexes	TG range (°C)					DTA	
	$\Delta m\%$ (cal.)	Ti	Tf	T _{DTG}	Mass loss	T _{dta}	Peak
Cd-OTC/Sal	28.01	362.05	448.12	388.17	-0.837	403.75	Exo
	9.58	611.13	680.76	660.86	-0.232	-	
Mo-OTC/Sal	13.022	374.30	397.33	382.34	-0.742	392.96	Exo
	17.39	407.21	417.17	413.10	-0.548	415.17	Exo
	6.08	464.40	508.22	490.02	-0.657	499.45	Exo
Zr(II)Otc/Sal	1.19	62.42	132.18	92.71	-0.433	-	-
	1.51	187.96	291.00	240.60	-0.350		
	7.56	490.46	750.58	595.18	-0.929	-	Exo
Pd(II)Otc/Sal	4.31	45.34	69.61	51.508	-2.535	-	-
	8.69	218.62	252.87	231.75	-2.751		

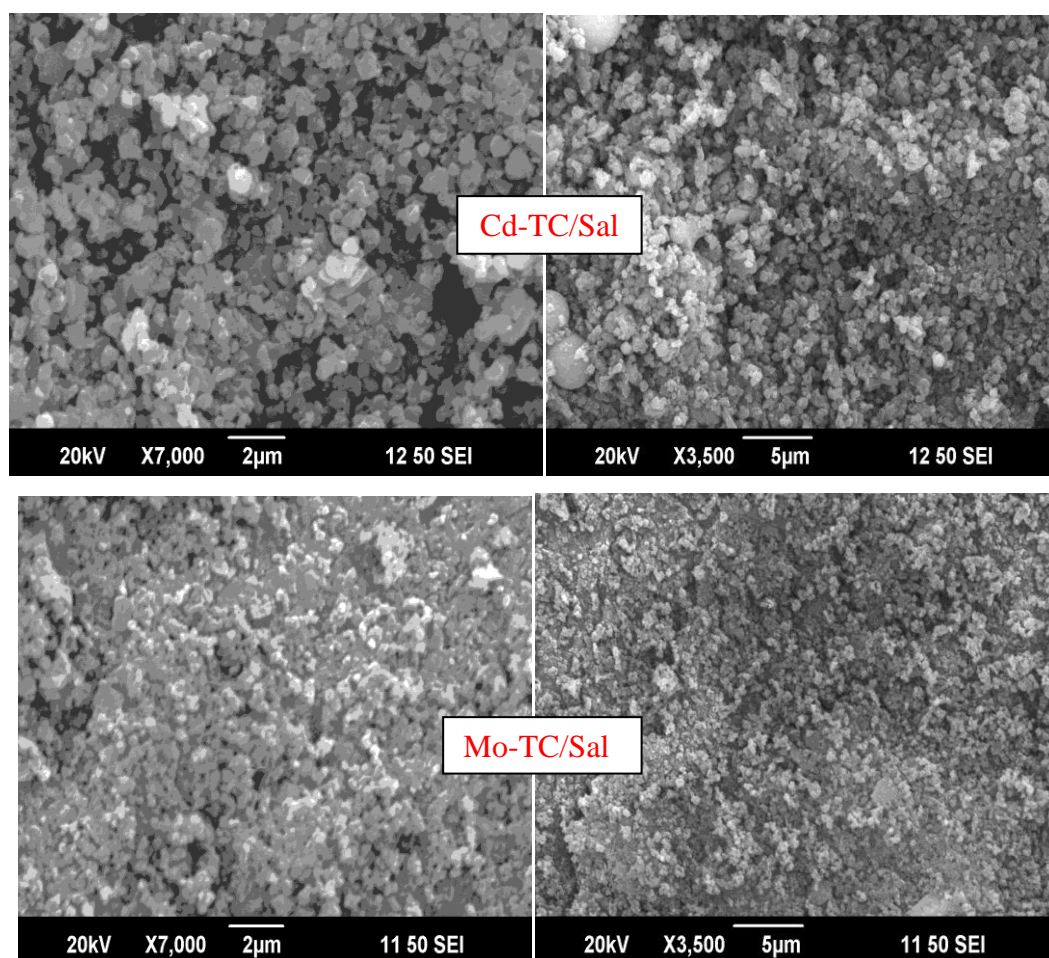
4.5 Scanning Electron Microscope Study

4.5.1 SEM Study of M-TC/Sal Metal Complexes

The prepared metal complex surface morphology was altered by metal coordination with the ligand and evaluated with the help of the SEM studies. The SEM is an analytical instrumental technique in which a beam of high-energy forms various signals on the surface of a solid material. The obtained signals provide information about the shape, size, and arrangement of atoms, ductility, and strength of materials in an object. Therefore, this technique is mostly used in metallurgical, geological, forensic, and medical science etc. (Pal *et al.*, 2018). The coordination between the donor site of the ligand and the metal ions is the difference in the SEM micrograph of the ligand and metal complex. Therefore, by changing the metal ions of the metal complex, SEM changes the surface morphology in the micrograph (Shakir *et al.*, 2015).

SEM micrographs of the M-TC/Sal metal complex are presented in (**Fig. 27**). From the micrograph, the Cd-TC/Sal metal complex, the particles show irregular morphology with different-sized particles and elucidate that the particles are

agglomerated in a structure caused by self-induced crystal growth (Desai *et al.*, 2017). Similarly, the Mo-TC/Sal metal complex reflects the size of micro-crystalline and nanograins (Divsalar *et al.*, 2016). SEM micrograph of the Zr-TC/Sal metal complex, particles showed that the metal complex is micro-crystalline in structure. The examination of the single-crystal was shown to be carefully sized nanoscale. In addition, a grain-like appearance was seen at low magnification (Selvam *et al.*, 2013; Kumari *et al.*, 2009). Similarly, the Pd-TC/Sal metal complex exhibits agglomeration of hybrid nanomaterials (Diaz-Sanchez *et al.*, 2019).



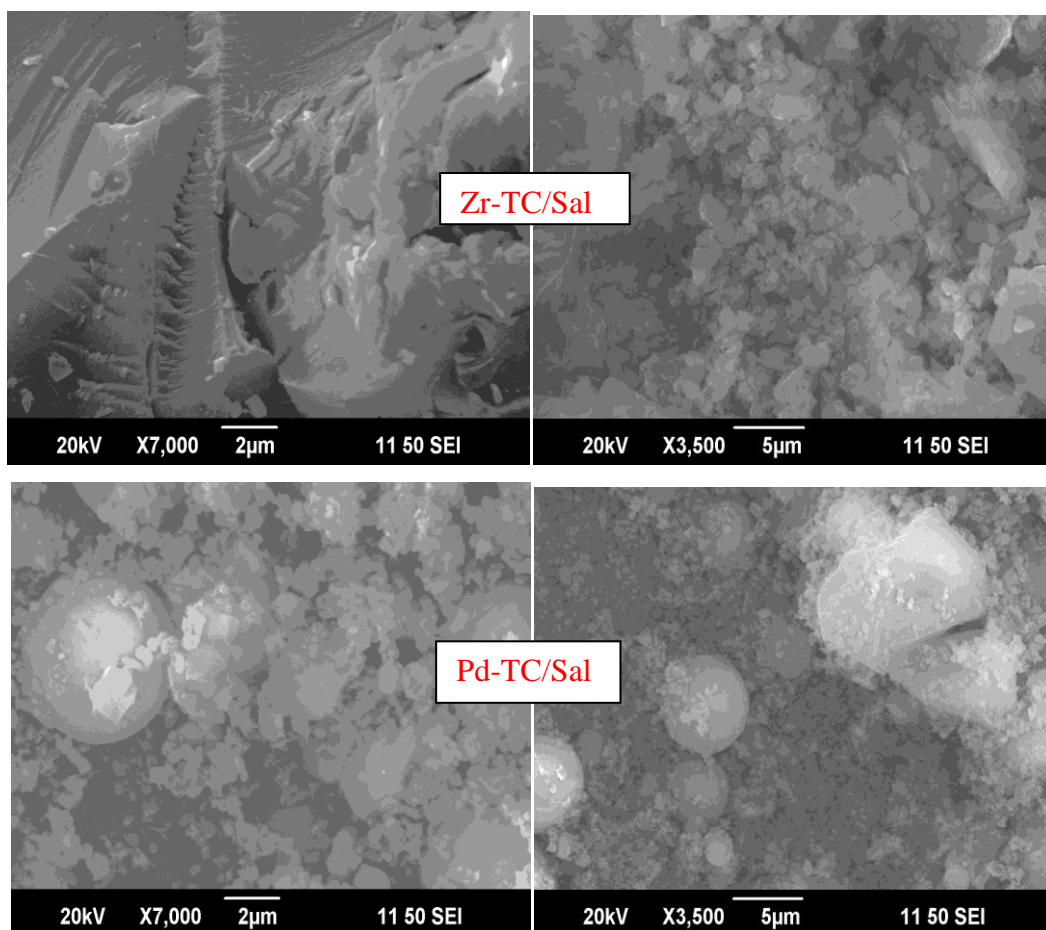
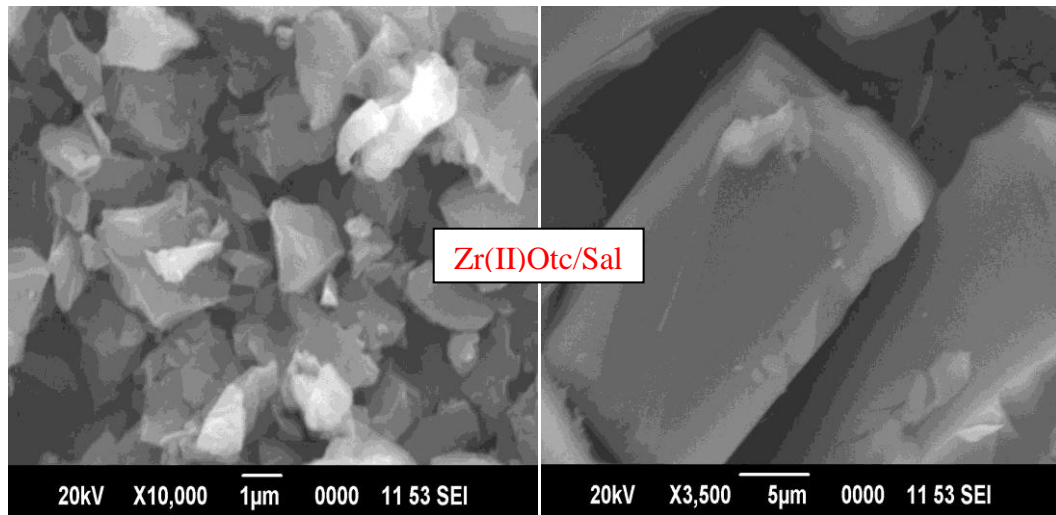
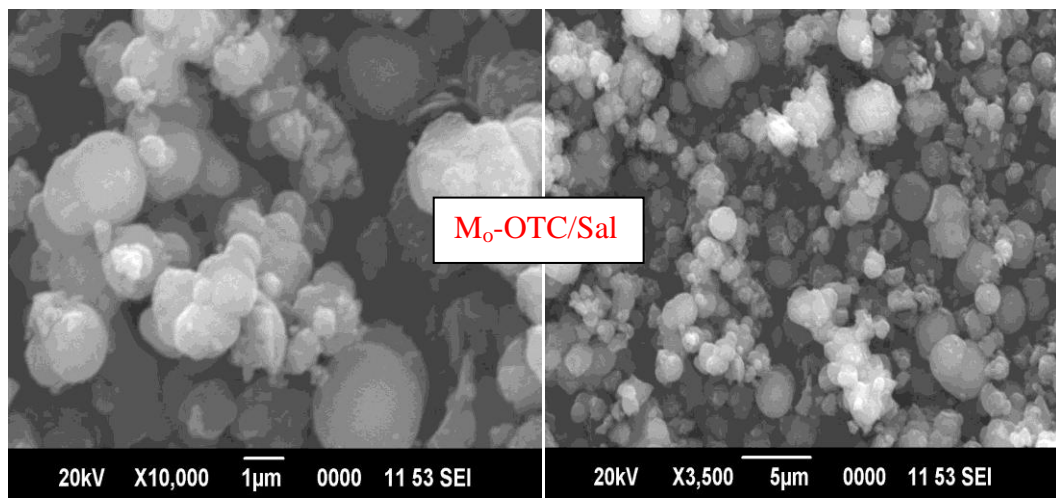
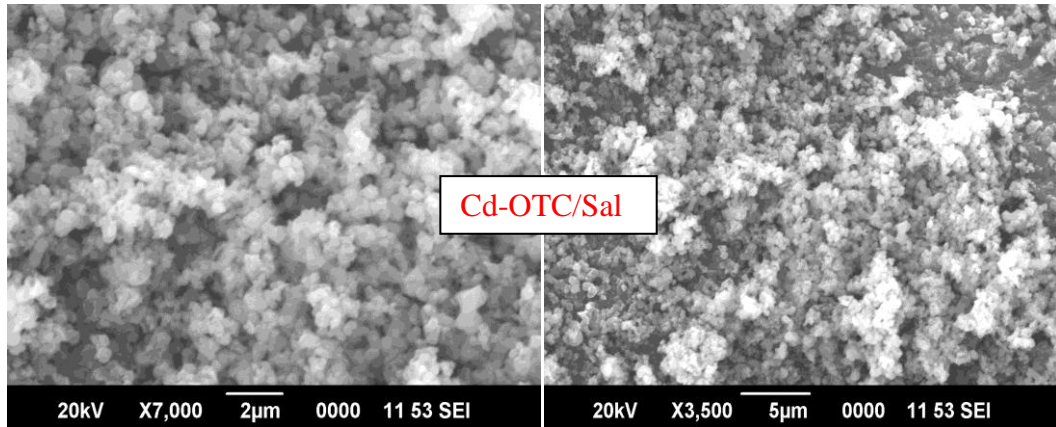


Figure 27: SEM micrograph images of M-TC/Sal metal complexes [M=Cd(II), Mo(III), Zr(II) and Pd(II)]

4.5.2 SEM Study of M-OTC/Sal Metal Complexes

The micrograph (SEM) of the metal complex, M-OTC/Sal is presented in (Fig. 28). In the Cd-OTC/Sal metal complex, the SEM micrograph demonstrates a microspherelike structure, aggregated with small nanoparticles, thus forming a large sphere (Gaur & Jeevanandam, 2015). The micrograph of the Mo-OTC/Sal metal complex reflects the morphology of spherical nanomaterials, the aggregation that increases in size to form a large sphere (Mohammadikish *et al.*, 2014). SEM image of Zr(II)Otc/Sal metal complex surface particles is smooth, clear, and not aggregated, but upon treatment of metal ions, surface particles are rough and completely covered (Prabhu *et al.*, 2015). The micrograph of the Pd(II)Otc/Sal metal complex exhibits uniform and spherical morphology on its surface (Sobhani & Zarifi, 2015).



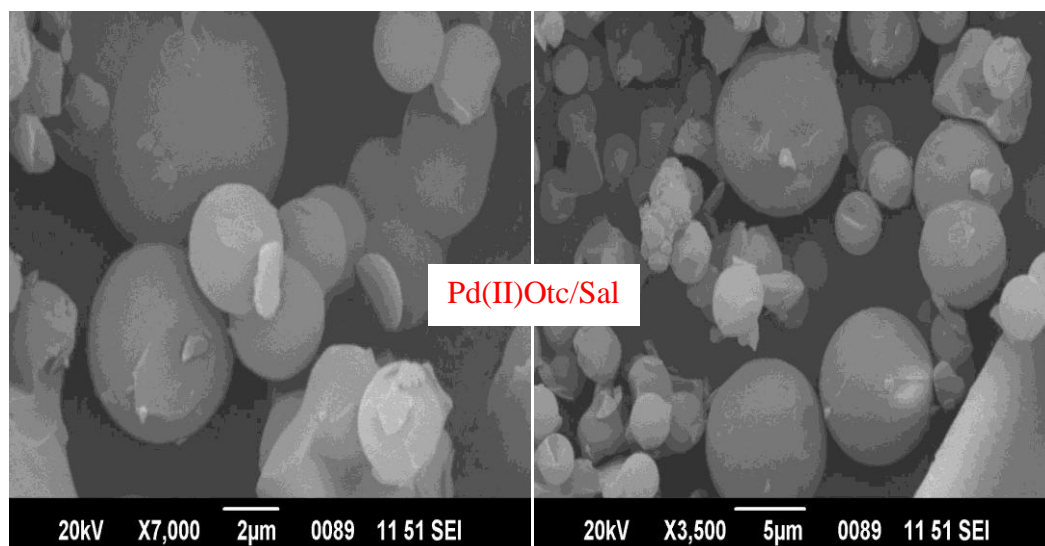
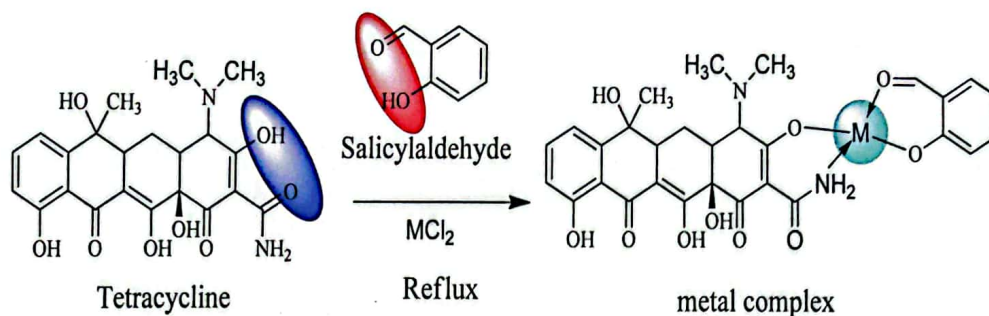


Figure 28: SEM micrograph images of M-OTC/Sal metal complexes [M=Cd(II), Mo(V), Zr(II), and Pd(II)]

4.6 Proposed Molecular Structures and Geometry

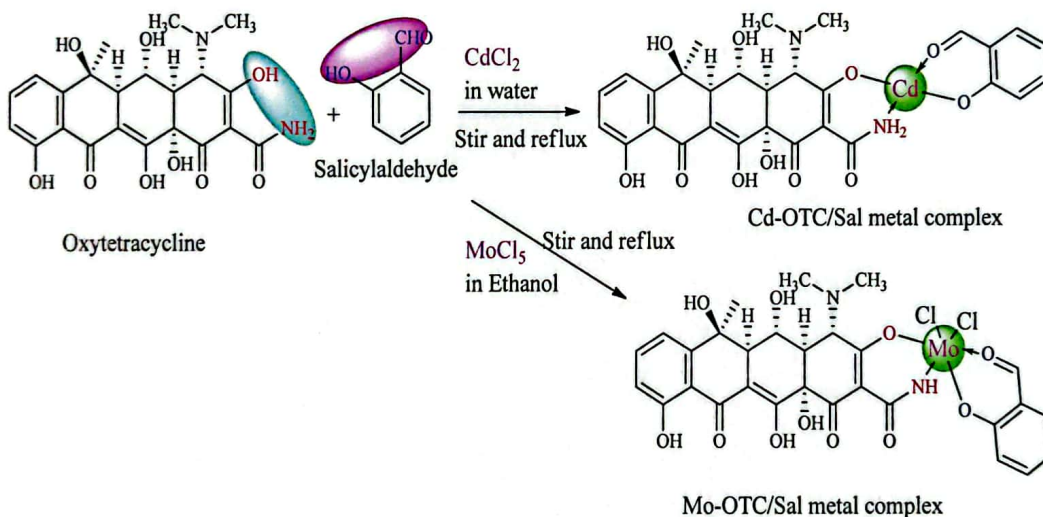
Metal complexes play a very important role in proposing molecular geometries, and physicochemical, analytical, and spectroscopic techniques. Computer software such as CsChem Draw Ultra-12.0.2 and Chem 3D Pro.12.0.2 helps to design the molecular structure of the complex. Bond angles, bond lengths, and bond energies of various bond parameters can be calculated from the 3D programming software, Chem 3D Pro.12.0.2. The current research investigation has shown that the proposed structures of the complex were done with the help of the above method. The possible proposed structures of the metal complexes under investigation are presented in (Schemes 1-3), respectively.

structures of the metal complexes under investigation are presented in (Scheme 1-3), respectively.

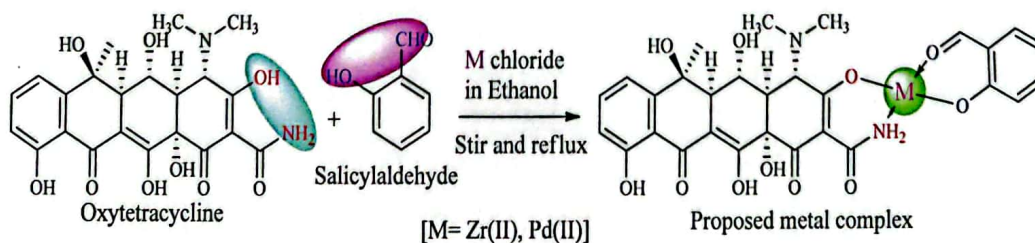


$\text{M}=\text{Cd(II), Zr(II), Mo(III), Pd(II)}$

Scheme 1: The scheme for the synthesis of the M-TC/Sal [M=Cd(II), Zr(II), Mo(III), Pd(II)] metal complexes of mixed ligand



Scheme 2: The scheme for the synthesis of the M-OTC/Sal [M= Cd(II), Mo(V)] metal complexes of mixed ligand



Scheme 3: Proposed structure of the M-Otc/Sal [M= Zr(II), Pd (II)] metal complexes of mixed ligand

4.7 Molecular Modeling Study

To better characterize the molecular structure of the metal complex, geometrical optimization, and 3D molecular modeling of the proposed structure of the metal complex were performed using Chem 3D Pro. 12.0.2 Version software. The potential energy of the complex was the sum of the following relation: $E = E_{\text{str}} + E_{\text{ang}} + E_{\text{tor}} + E_{\text{vdw}} + E_{\text{oop}} + E_{\text{ele}}$, where, E = energy value of different types of interaction (Kcal/mol). The subscripts str, ang, tor, vdw, oop, and ele denote bond stretching, angle bending, torsional deformation, Van der Waal interaction, out-of-plane bending, and electronic interactions respectively (Mahapatra *et al.*, 2015; Rao *et al.*, 2019; Khedr *et al.*, 2012; Siddappa *et al.*, 2014).

By performing the MM2 calculations, the optimized geometry and structure of the metal complex with minimum energy were calculated. The details of bond angles, bond lengths, and bond energies of various atoms in the compound are numbered in Arabic numerals. The maximum stability of the metal complex is indicated by the minimum energy optimization value. Therefore, the actual bond angles and bond length are close to the optimum value which confirms the proposed structure of the metal complex (Singh, 2013; El-Boraey *et al.*, 2018; Khedr *et al.*, 2011; Singh, 2011)

4.7.1 Molecular Modeling Study of M-TC/Sal Metal Complexes

The proposed molecular geometry of the metal complexes was assured by running MM2 functions in Chem 3D Pro.12.0.2 molecular modeling software. Various parameters such as bond angles, bond lengths, and bond energies were obtained, which are presented in (Figs. 29-32) and Table 17. Cd-TC/Sal and Mo-TC/Sal metal complexes were shown to have tetrahedral and octahedral geometries with optimized minimum energies of 916.7135 and 928.8980 kcal/mol, respectively. Similarly, the tetrahedral and square planar geometries are shown by the Zr-TC/Sal and Pd-TC/Sal metal complexes with optimized minimum energy of 1719.6070 and 1729.6133 kcal/mol, respectively. The obtained geometry of the complexes was also supported by various spectral methods. The minimization energy value of complexes signifies their maximum stability. Also, the difference in bond length values between metal-

nitrogen and metal-oxygen in comparison with ligand further denotes their coordination.

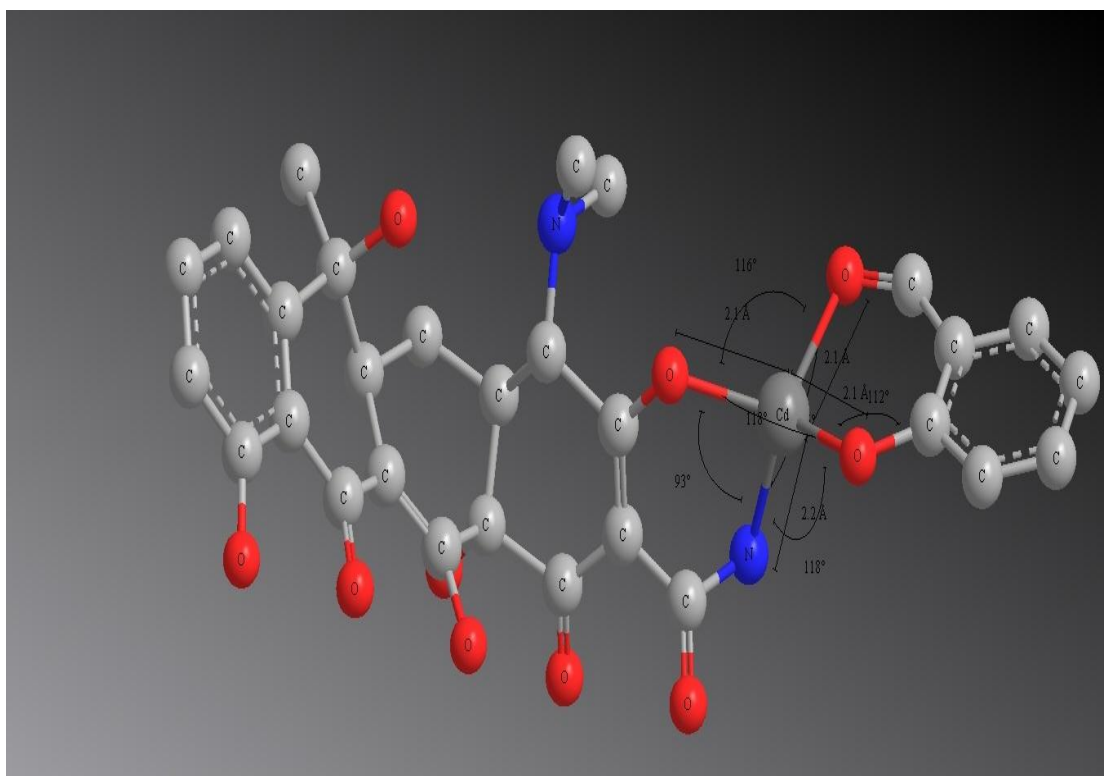


Figure 29: Optimized structure of Cd-TC/Sal metal complex

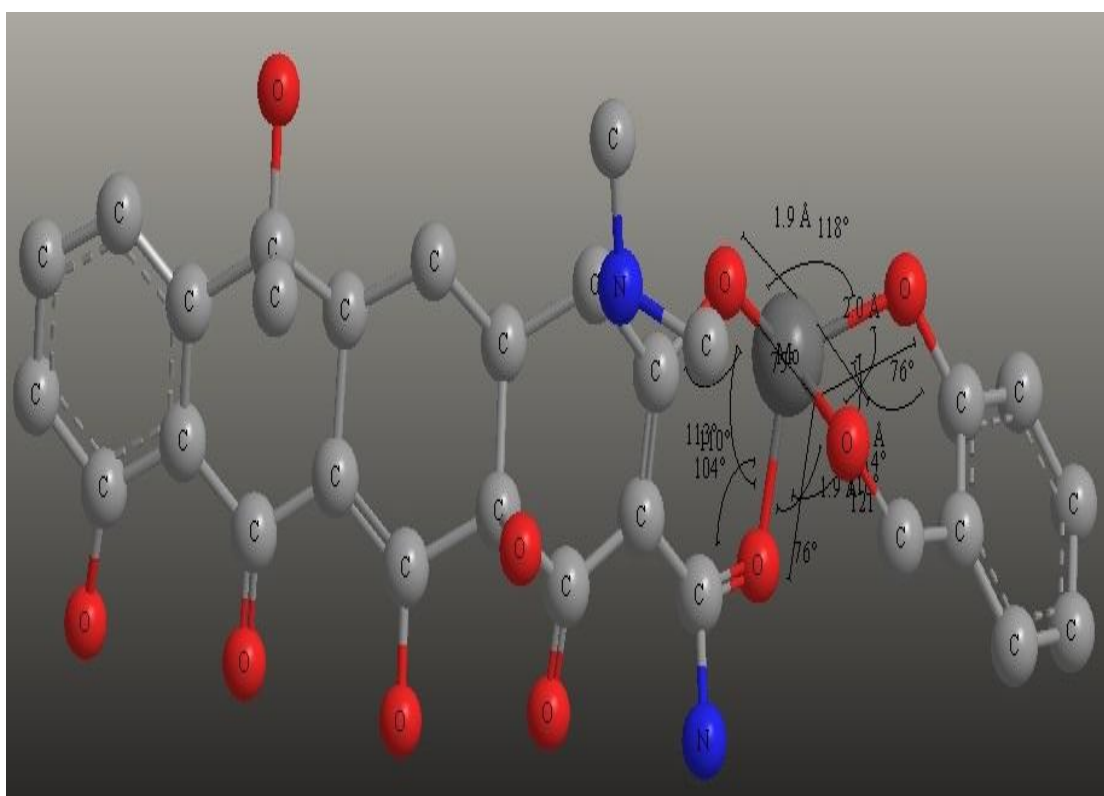


Figure 30: Optimized structure of Mo-TC/Sal metal complex

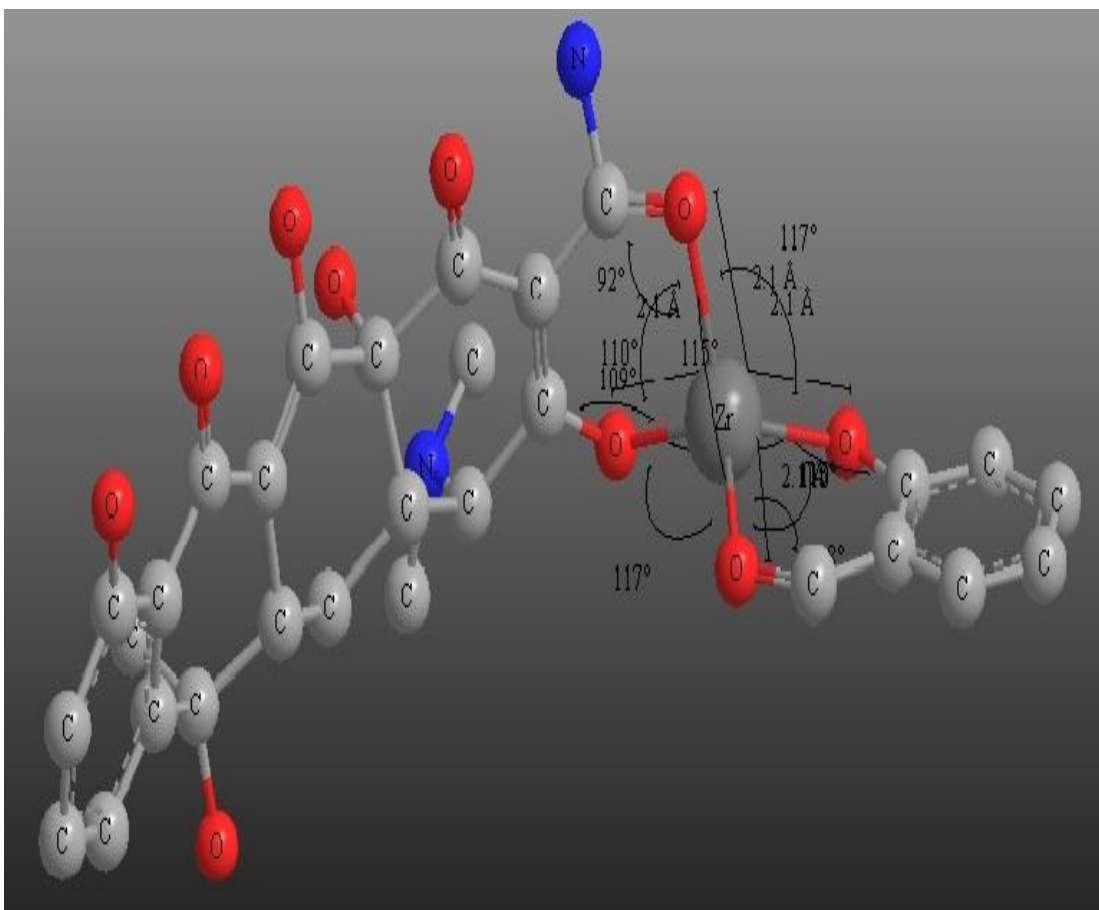


Figure 31: Optimized structure of Zr-TC/Sal metal complex

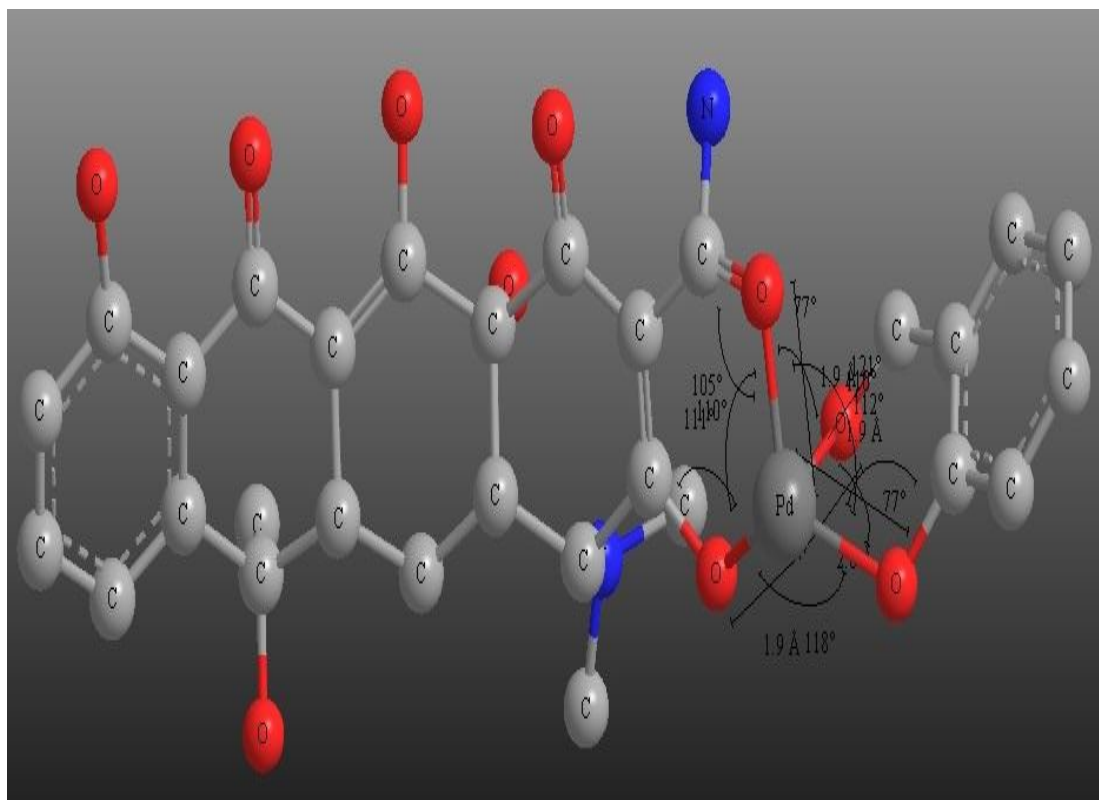


Figure 32: Optimized structure of Pd-TC/Sal metal complex

Table 17: Selected bond lengths, bond angles, and bond energies of the M-TC/Sal metal complexes [M=Cd(II), Mo(III), Zr(II), and Pd(II)]

Complexes	Atoms	Bond length (Å)	Optimized minimum energy (kcal/mol)	Atoms	Bond Angle (°)	Final geometry
Cd-TC/Sal	N(5)-Cd(44)	2.1617	916.7135	N(5)-Cd(44)-O(3)	115.92	Tetrahedral
	O(3)-Cd(44)	2.1326		N(5)-Cd(44)-O(6)	117.62	
	O(6)-Cd(44)	2.1202		N(5)-Cd(44)-O(4)	92.68	
	O(4)-Cd(44)	2.1250		O(3)-Cd(44)-O(6)	97.99	
				O(3)-Cd(44)-O(4)	116.43	
				O(6)-Cd(44)-O(4)	117.75	
				Cd(44)-O(6)-C(11)	111.90	
				Cd(44)-N(5)-C(9)	105.13	
				Cd(44)-O(4)-C(7)	113.34	
		Cd(44)-O(3)-C(12)	110.10			
Mo-TC/Sal	N(5)-Mo(44)	1.9718	928.8980	N(5)-Mo(44)-O(3)	73.08	Octahedral
	O(3)-Mo(44)	1.9855		N(5)-Mo(44)-O(6)	118.86	
	O(6)-Mo(44)	1.9306		N(5)-Mo(44)-O(4)	95.67	
	O(4)-Mo(44)	1.9338		O(3)-Mo(44)-O(6)	74.66	
				O(3)-Mo(44)-O(4)	75.67	
				O(6)-Mo(44)-O(4)	124.07	
				Mo(44)-O(6)-C(11)	114.33	
				Mo(44)-N(5)-C(9)	109.41	
				Mo(44)-O(4)-C(7)	115.63	
		Mo(44)-O(3)-C(12)	110.55			
Zr-TC/Sal	O(28)-Zr(41)	2.0989	1719.6070	O(28)-Zr(41)-O(37)	117.43	Tetrahedral
	O(25)-Zr(41)	2.0844		O(25)-Zr(41)-O(40)	116.54	
	O(40)-Zr(41)	2.0968		O(25)-Zr(41)-O(37)	119.57	
	O(37)-Zr(41)	2.0831		O(40)-Zr(41)-O(37)	97.53	
				Zr(41)-O(40)-C(36)	110.24	
				Zr(41)-O(37)-C(35)	113.12	
				Zr(41)-O(28)-C(26)	110.36	
		Zr(41)-O(25)-C(17)	108.76			
Pd-TC/Sal	O(28)-Pd(41)	1.9186	1729.6133	O(28)-Pd(41)-O(25)	105.41	Square planar
	O(25)-Pd(41)	1.9067		O(28)-Pd(41)-O(40)	77.24	
	O(40)-Pd(41)	1.9577		O(28)-Pd(41)-O(37)	120.99	
	O(37)-Pd(41)	1.9093		O(25)-Pd(41)-O(40)	76.02	
				O(40)-Pd(41)-O(37)	118.44	

O(40)-Pd(41)-O(37)	77.31
Pd(41)-O(40)-C(36)	110.32
Pd(41)-O(37)-C(35)	111.97
Pd(41)-O(28)-C(26)	110.27
Pd(41)-O(25)-C(17)	111.25

4.7.2 Molecular Modeling Study of the M-OTC/Sal Metal Complexes

The various data of atoms in the compounds are optimized through MM2 calculations are presented in **(Figs. 33-36)** and **Table 18**. After geometrical optimization, the tetrahedral and octahedral geometries are shown by the Cd-OTC/Sal and Mo-OTC/Sal metal complexes with an optimized minimum energy of 923.1740 and 899.3184 kcal/mol, respectively. Thus, provides stability to the complex. Similarly, the tetrahedral and square planar geometries are shown by the Zr(II)Otc/Sal and Pd(II)Otc/Sal metal complexes with an optimized minimum energy of 921.7712 and 915.1880 kcal/mol, respectively. With the help of MM2 calculations, the energy optimization was repeated several times to note down the value of optimized minimum energy. Hence, the difference values between M-N and M-O compared with those of ligands reflect the complexation of ligands with the metal ions (Siddappa *et al.*, 2014; Benyei & Sovago, 2003). The computational data showed better results for the proposed structure of the metal complex.

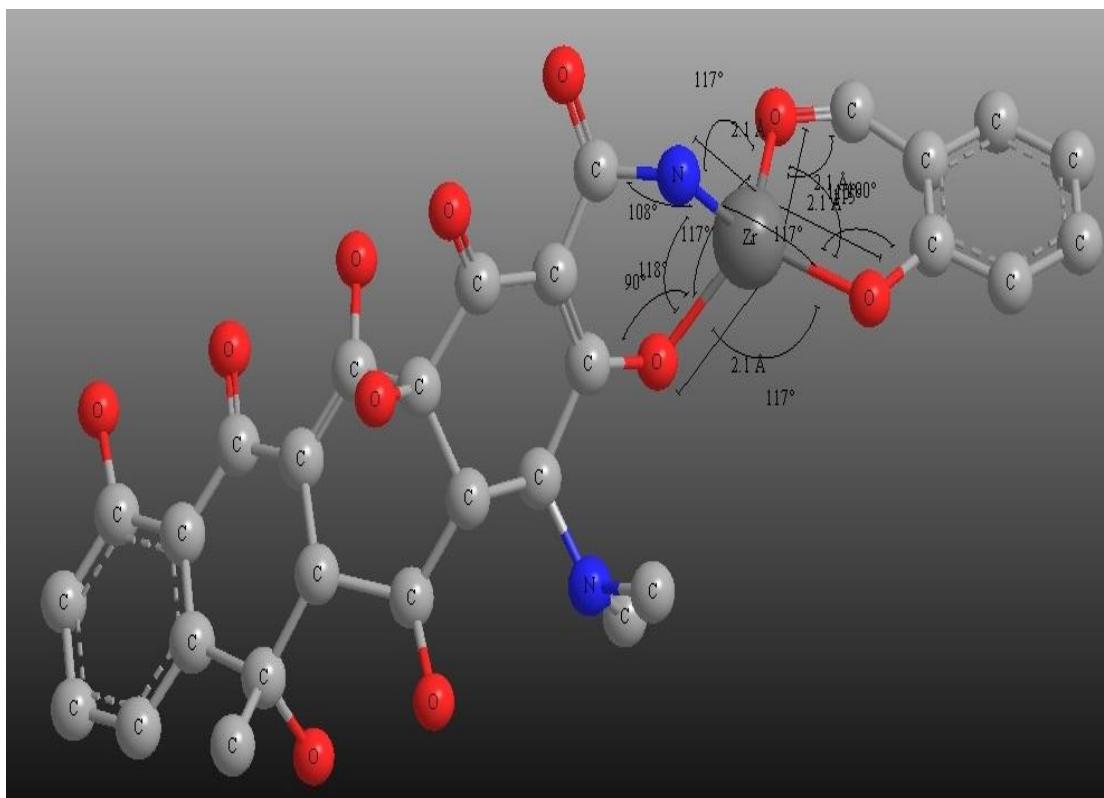


Figure 35: Optimized structure of Zr(II)Otc/Sal metal complex

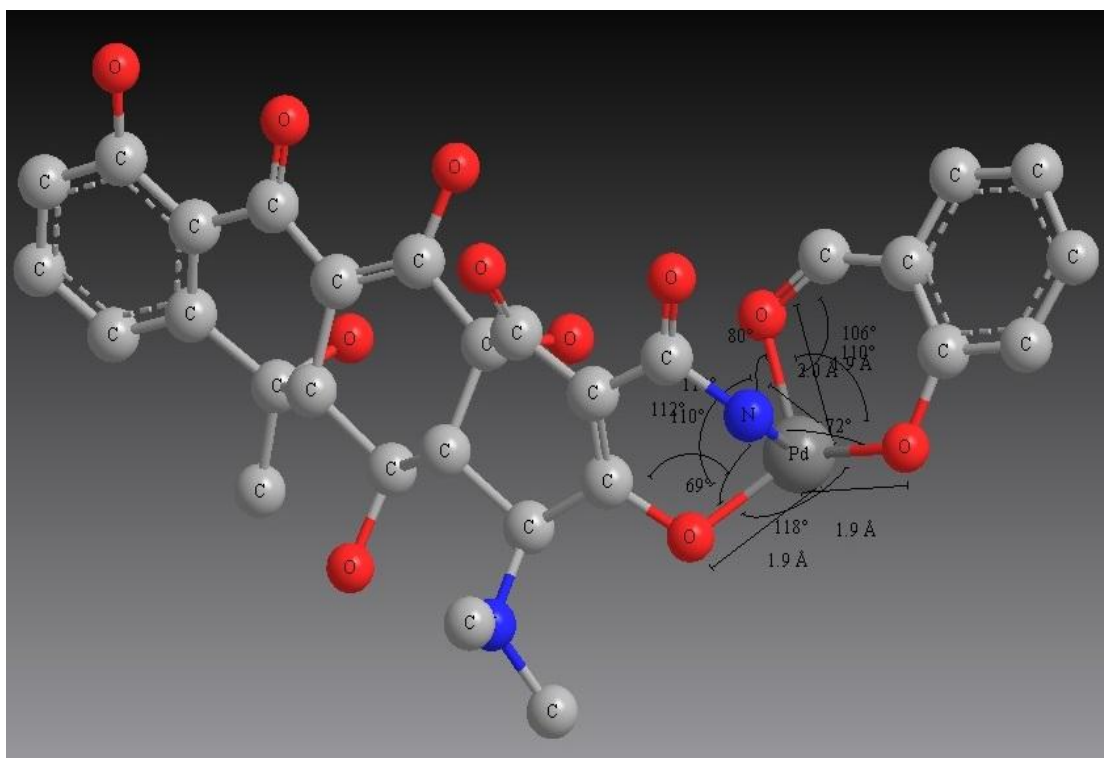


Figure 36: Optimized structure of Pd(II)Otc/Sal metal complex

Table 18: Selected bond lengths, bond angles, and bond energies of the M-OTC/Sal metal complexes [M=Cd(II), Mo(V), Zr(II), and Pd(II)]

Complexes	Atoms	Bond length (Å)	Optimized minimum energy (kcal/mol)	Atoms	Bond Angle (°)	Final geometry
Cd-OTC/Sal	N(5)-Cd(45)	2.162	923.1740	N(5)-Cd(45)-O(3)	116.04	Tetrahedral
	O(3)-Cd(45)	2.133		N(5)-Cd(45)-O(6)	117.62	
	O(6)-Cd(45)	2.120		N(5)-Cd(45)-O(4)	92.55	
	O(4)-Cd(45)	2.125		O(3)-Cd(45)-O(6)	97.74	
				O(3)-Cd(45)-O(4)	116.72	
				O(6)-Cd(45)-O(4)	117.77	
Mo-OTC/Sal	Mo(45)-Cl(47)	2.295	899.3184	Cl(47)-Mo(45)-Cl(46)	89.96	Octahedral
	Mo(45)-Cl(46)	2.295		Cl(47)-Mo(45)-N(5)	87.43	
	N(5)-Mo(45)	1.984		Cl(47)-Mo(45)-O(3)	96.97	
	O(3)-Mo(45)	1.963		Cl(47)-Mo(45)-O(6)	104.54	
	O(6)-Mo(45)	1.945		Cl(47)-Mo(45)-O(4)	170.29	
	O(4)-Mo(45)	1.947		Cl(46)-Mo(45)-N(5)	101.05	
				Cl(46)-Mo(45)-O(3)	173.30	
				Cl(46)-Mo(45)-O(6)	94.08	
				Cl(46)-Mo(45)-O(4)	85.86	
				N(5)-Mo(45)-O(3)	78.57	
				N(5)-Mo(45)-O(6)	160.76	
				N(5)-Mo(45)-O(4)	84.78	
				O(3)-Mo(45)-O(6)	85.03	
				O(3)-Mo(45)-O(4)	87.45	
		O(6)-Mo(45)-O(4)	84.53			
Zr(II)Otc/Sal	N(5)-Zr(45)	2.1251	921.7712	N(5)-Zr(45)-O(3)	116.72	Tetrahedral
	O(3)-Zr(45)	2.0954		N(5)-Zr(45)-O(6)	116.86	
	O(6)-Zr(45)	2.0822		N(5)-Zr(45)-O(4)	89.75	
	O(4)-Zr(45)	2.0885		O(3)-Zr(45)-O(6)	100.36	
				O(3)-Zr(45)-O(4)	116.89	
				O(6)-Zr(45)-O(4)	117.48	
				Zr(45)-O(6)-C(11)	114.57	
				Zr(45)-N(5)-C(9)	108.29	
				Zr(45)-O(4)-C(7)	118.06	
				Zr(45)-O(3)-C(12)	110.38	
Pd(II)Otc/Sal	O(3)-Pd(39)	1.9146	915.1880	O(3)-Pd(39)-O(5)	118.30	Square planar
	O(5)-Pd(39)	1.9093		O(3)-Pd(39)-N(4)	69.13	
	N(4)-Pd(39)	1.9824		O(3)-Pd(39)-O(2)	111.90	

O(2)-Pd(39)	1.9219	O(5)-Pd(39)-N(4)	71.92
		O(5)-Pd(39)-O(2)	106.02
		N(4)-Pd(39)-O(2)	79.99
		Pd(39)-O(5)-C(10)	113.27
		Pd(39)-N(4)-C(8)	117.68
		Pd(39)-O(3)-C(6)	110.34
		Pd(39)-O(2)-C(11)	110.35

4.8 Antibacterial Sensitivity Study

In recent decades, increased resistance of bacteria to antibiotics has been a global health problem. Therefore, metal-based organic coordination has a great interest in the field of antimicrobial activity (El-Shwiniy & Sadeek, 2015; Maurya *et al.*, 2011). Furthermore, the deactivating character of the ligand can be enhanced by coordinating the ligand with metal ions (Musa *et al.*, 2018; Harinath *et al.*, 2013). Complexes show high activation due to the interaction of metal ions on the surface of microbes. Here, the metal chelates have polar and non-polar properties, making them suitable for entry into the cells and tissues by transforming them into lipophilicity and hydrophilicity, which can reduce the solubility and permeability of cells. The reduced activity in the metal complex may be due to low lipid solubility, pharmacokinetics, and steric factors that play the main role in deciding the ability of antibacterial agents (Nair *et al.*, 2011; Geeta *et al.*, 2010). Therefore, an attempt was made to increase the antibacterial activity with a metal complex of the mixed ligand.

A general experimental analysis suggested that the antimicrobial activities detected a significant increase of organic ligands and metal complexes against all bacterial pathogens. Antimicrobial studies also proved that the solid metal complexes showed incredible importance towards antibacterials due to their biologically active nature. The mechanism of an increase in antibacterial activity may be due to the concept of Overton's and Tweedy's chelation theory. In coordination chemistry, the polarity of metal ions will decrease, due to the partial sharing of donor atoms between positively charged ions during complex formation within the chelate ring. Therefore, these processes enhance the lipophilic character of the central ion, resulting in penetration through the lipid layer of microorganisms and ultimately deactivating the cell action of microorganisms (El-Shwiniy & Zordok, 2018; Hazra *et al.*, 2017; El-Sherif *et al.*,

2012; Kalinowska *et al.*, 2014). A different type of physical parameter of the complex indicates the presence of metal ions and enhances their antimicrobial activity. Therefore, in the present study, antimicrobial tests were carried out at the Microbiology Laboratory of Mahendra Morang Adarsha Multiple Campus, Tribhuvan University, Biratnagar, Morang, Nepal.

4.8.1 Antibacterial Sensitivity Study of M-TC/Sal Metal Complexes

The antibacterial sensitivity of the prepared complexes was screened using the modified Kirby-Bauer paper disc diffusion method against four different types of human clinical pathogenic bacteria: *S. aureus* (gram-positive), *K. pneumonia*, *E. coli*, and *P. aeruginosa* (gram-negative). The test solutions were prepared by dissolving metal complexes in 30% DMSO at four different concentrations (25, 12.5, 6.25, and 3.125 $\mu\text{g}/\mu\text{L}$). For antibacterial testing, the first fresh culture of microorganisms was prepared with an MHA plate and blank disc. The regenerated and fresh bacterial culture was slowly swabbed into sterile media. Blank discs were loaded with the calculated amount of the test solution at different concentrations. Amikacin acts as a standard positive control, while a blank disc soaked with DMSO is used as a solvent control to measure its effectiveness. After performing all the above procedures, the loaded plates were placed inside an incubator at 37 °C for 36 h to measure the diameter of the zone of inhibition in mm (El-Tabl *et al.*, 2013; El-Ghamry *et al.*, 2012).

The antibacterial activity results of growth inhibitory data are presented in **Tables 19 and 20** and their illustrated representations are also stated in (**Figs. 37-44**). The study revealed increased antibacterial activity for moderate to better results. By the antibacterial testing, it was concluded that all complexes showed better antibacterial activity in high concentrations and considerable activity in low concentrations. The type of species of microorganisms helps with the intensity of the antibacterial action of ligands and their metal complexes. In addition, commercial antibiotics showed significantly higher antibacterial activity than the tested complexes (Stojković *et al.*, 2018). Here, the parent drug (tetracycline) showed a better inhibitory effect relative to the complexes. Antibacterial potency is based on the concept of Overton's and Tweedy's chelation principle. Chelation theory provides the stability and easy entry of

a complex compound into the cell of microorganisms, resulting in the breakdown of the cell wall of microorganisms, neutralizing the action of bacteria, and ultimately the death of the organism. *E. coli* of the Mo-TC/Sal complex was found to be much less active, whereas *S.aureus* of the Cd-TC/Sal complex showed better results. Similarly, *P. aeruginosa* of the Zr-TC/Sal and Pd-TC/Sal was found to be less active, whereas *E.coli* of the Pd-TC/Sal complex showed better results. Therefore, all pathogens were found to be susceptible to tetracycline.

Table 19: Antibacterial growth data of the Cd-TC/Sal and Mo-TC/Sal metal complexes

Pathogenic Bacteria	The diameter of the zone of inhibition (in mm)											
	<i>S. aureus</i>				<i>P. aeruginosa</i>				<i>E. coli</i>			
Concentrations ($\mu\text{g}/\mu\text{L}$)	25	12.5	6.25	3.125	25	12.5	6.25	3.125	25	12.5	6.25	3.125
Cd-TC/Sal	28	24	22	16	17	16	15	14	22	21	19	18
Mo-TC/Sal	20	18	16	14	12	11	10	9	11	10	9	8
Amk (30 mcg/disc)	27				21				23			
TC	31				31				31			
DMSO	0				0				0			

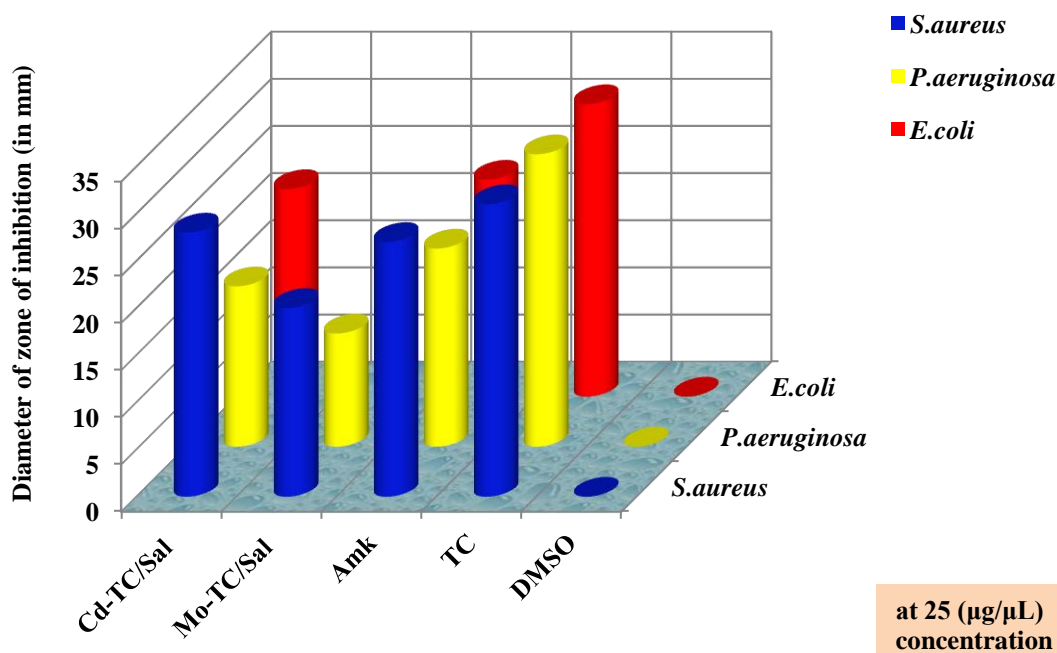


Figure 37: Bar graph of the antibacterial sensitivity of Cd-TC/Sal and Mo-TC/Sal metal complexes at 25 ($\mu\text{g}/\mu\text{L}$) concentration

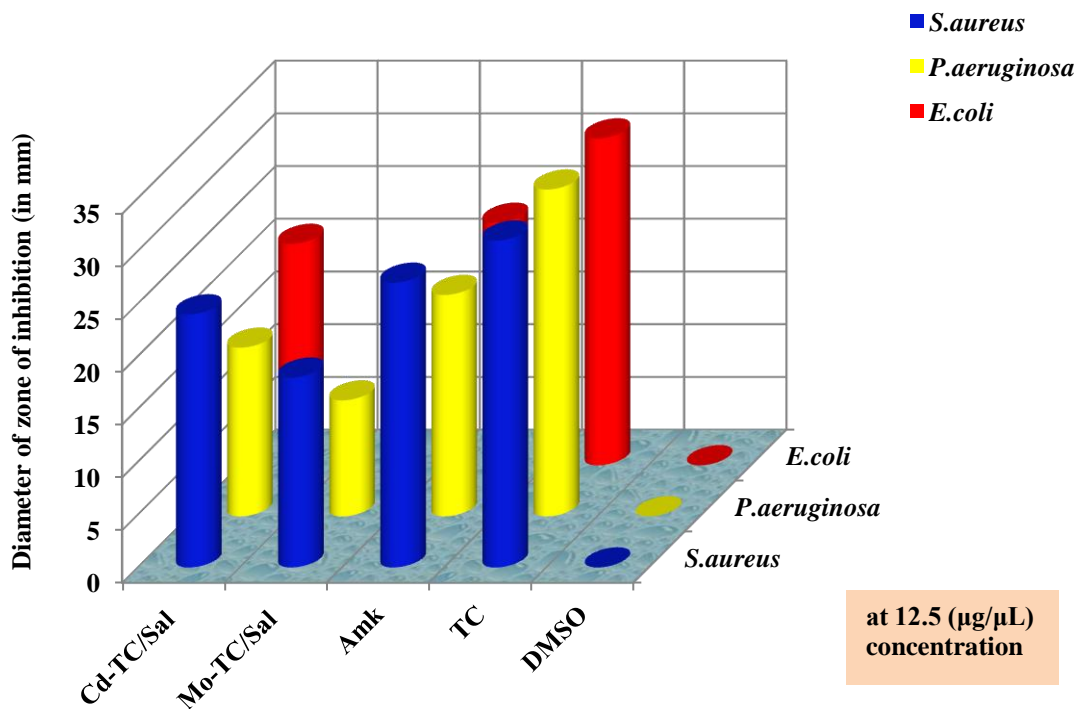


Figure 38: Bar graph of the antibacterial sensitivity of Cd-TC/Sal and Mo-TC/Sal metal complexes at 12.5 ($\mu\text{g}/\mu\text{L}$) concentration

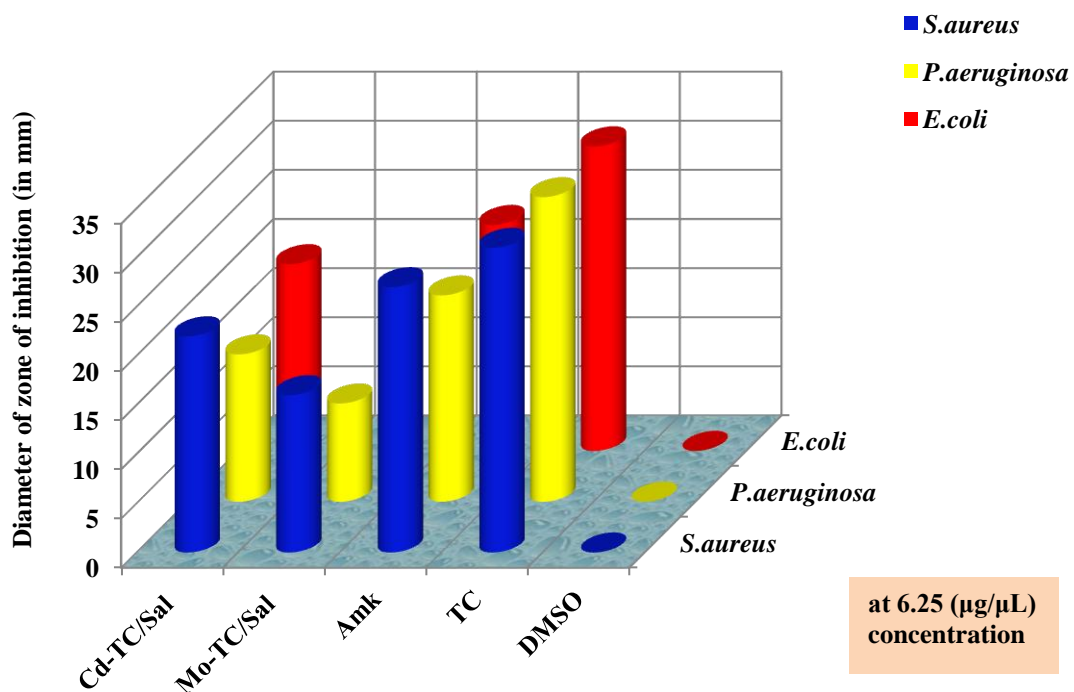


Figure 39: Bar graph of the antibacterial sensitivity of Cd-TC/Sal and Mo-TC/Sal metal complexes at 6.25 ($\mu\text{g}/\mu\text{L}$) concentration.

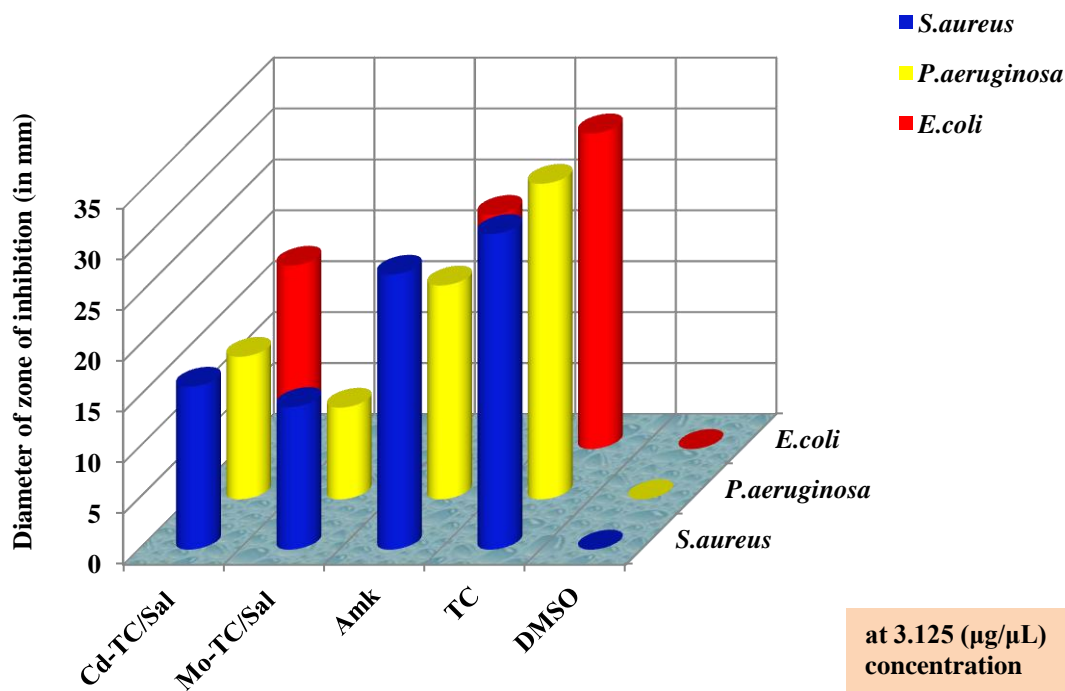


Figure 40: Bar graph of the antibacterial sensitivity of Cd-TC/Sal and Mo-TC/Sal metal complexes at 3.125 (µg/µL) concentration.

Table 20: Antibacterial growth data of the Zr-TC/Sal and Pd-TC/Sal metal complexes

Complexes	The diameter of the zone of inhibition (mm)											
	<i>S. aureus</i>				<i>P. aeruginosa</i>				<i>E. coli</i>			
Pathogenic bacteria	<i>S. aureus</i>				<i>P. aeruginosa</i>				<i>E. coli</i>			
Concentrations (µg/µL)	25	12.5	6.25	3.125	25	12.5	6.25	3.125	25	12.5	6.25	3.125
Zr-TC/Sal complex	12	11	10	9	13	12	10	9	13	12	10	8
Pd-TC/Sal complex	26	24	23	22	14	13	12	10	27	24	23	21
Amk (30mcg/disc)	18				25				28			
TC	31				31				31			
DMSO	0				0				0			

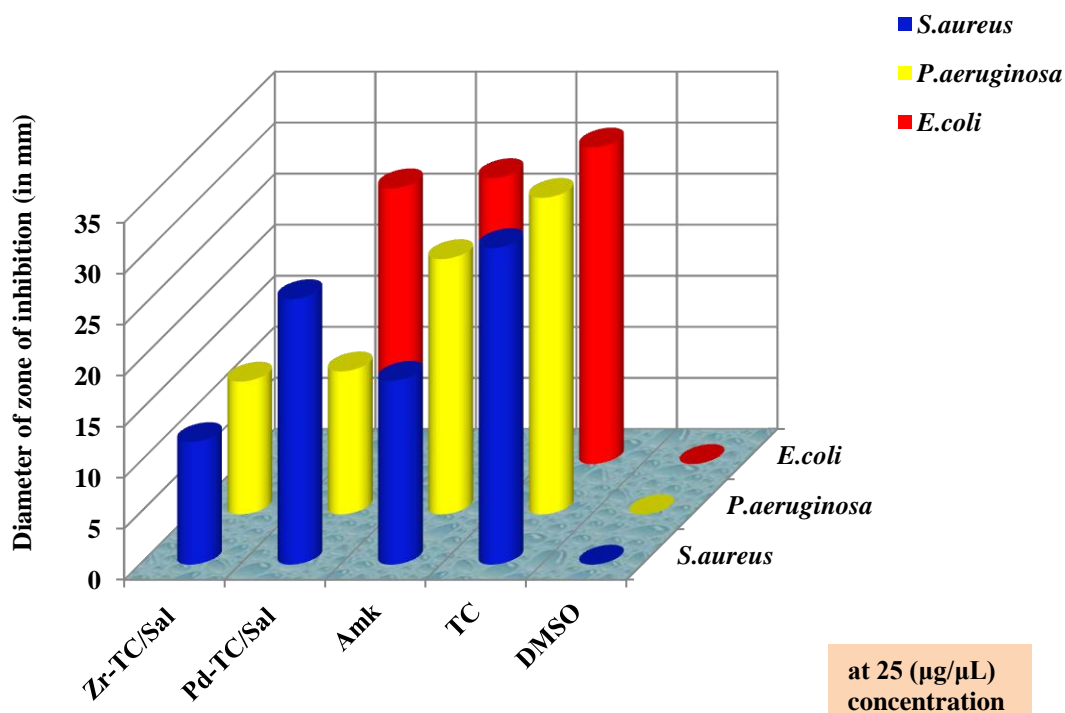


Figure 41: Bar graph of the antibacterial sensitivity of Zr-TC/Sal and Pd-TC/Sal metal complexes at 25 (µg/µL) concentration

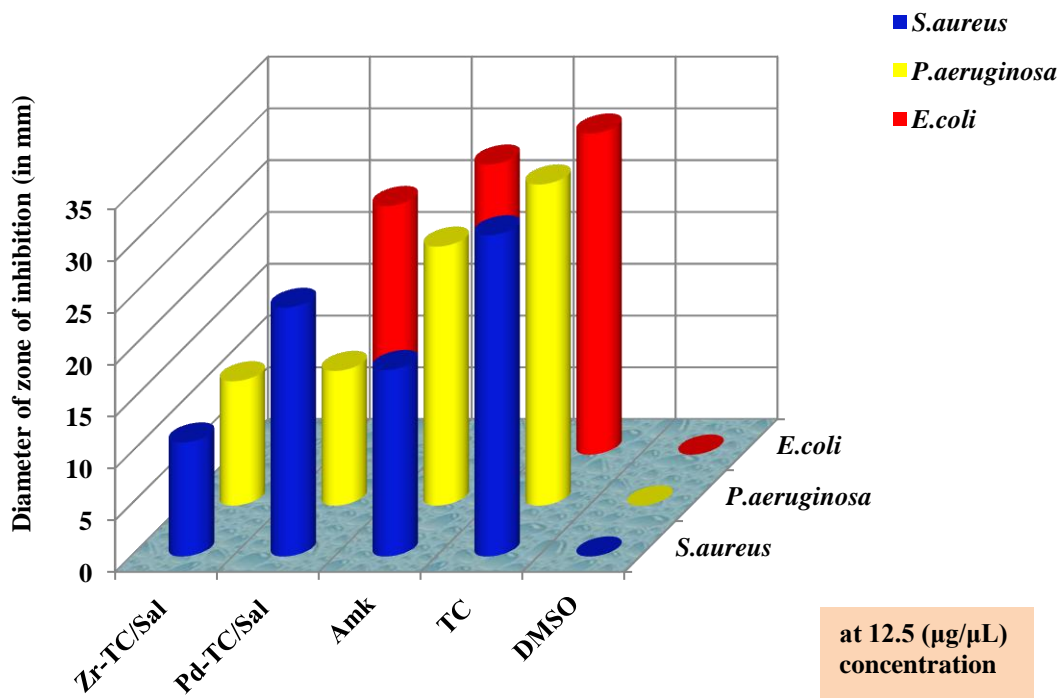


Figure 42: Bar graph of the antibacterial sensitivity of Zr-TC/Sal and Pd-TC/Sal metal complexes at 12.5 (µg/µL) concentration

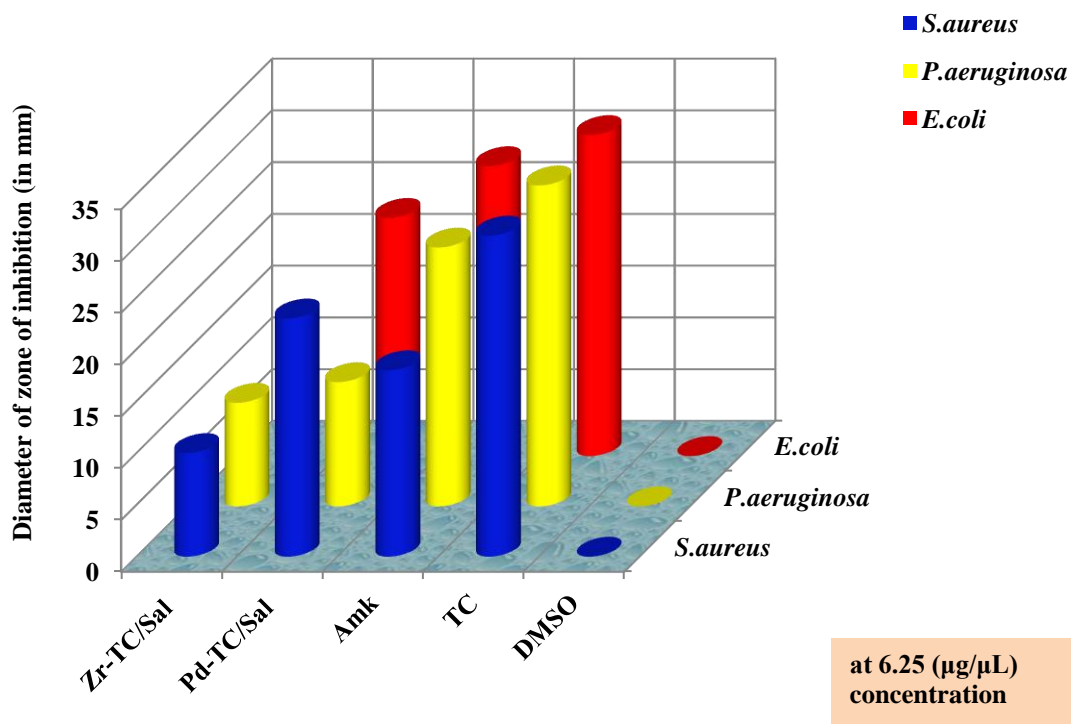


Figure 43: Bar graph of the antibacterial sensitivity of Zr-TC/Sal and Pd-TC/Sal metal complexes at 6.25 ($\mu\text{g}/\mu\text{L}$) concentration

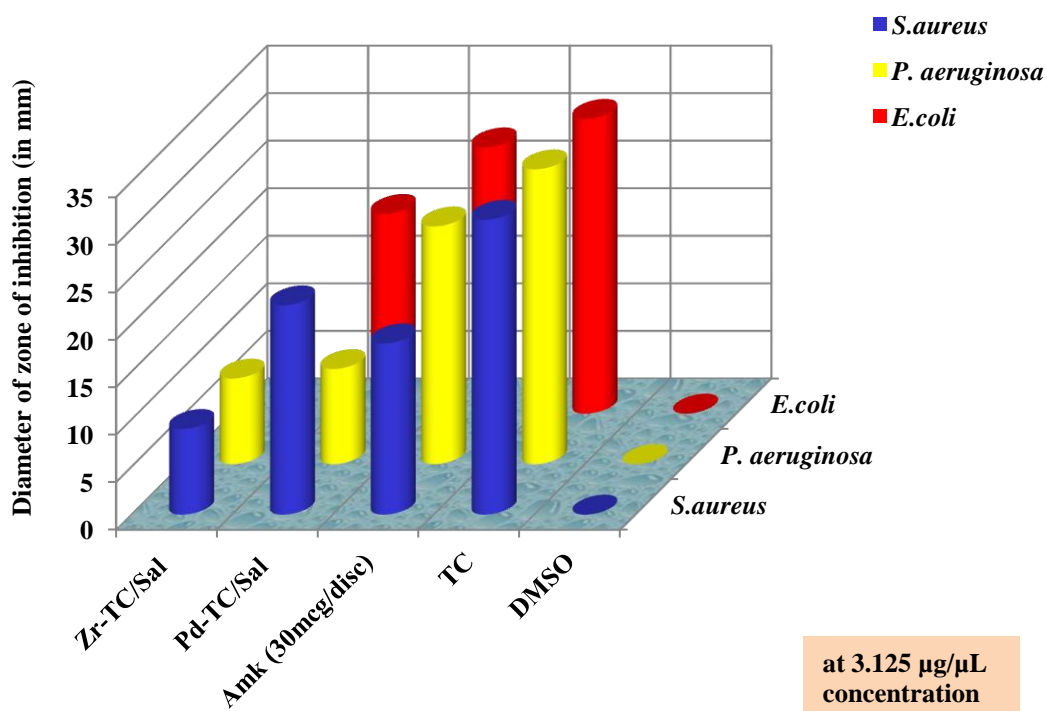


Figure 44: Bar graph of the antibacterial sensitivity of Zr-TC/Sal and Pd-TC/Sal metal complexes at 3.125 ($\mu\text{g}/\mu\text{L}$) concentration

4.8.2 Antibacterial Sensitivity of M-OTC/Sal Metal Complexes

Three human clinical pathogenic bacterial strains were selected for the antibacterial test in the current research study. The strains were *S. aureus* (gram-positive), *E. coli*, and *P. aeruginosa* (gram-negative). The test is performed using the Kirby-Bauer paper disc diffusion method. 30% DMSO solvent is used for the test solutions. Here, DMSO-soaked blank discs serve as solvent control while amikacin serves as a standard positive control to measure its effectiveness. The area of inhibition zone of the metal complex was compared with the control drug (amikacin) and the parent drug tetracycline (Mousavi *et al.*, 2020; Tabrizi *et al.*, 2015; Fiori-Duarte *et al.*, 2019). The measured data and results are presented in **Tables 21 and 22** and their pictorial representation is in **(Figs. 45-50)**. The obtained results showed a better antibacterial susceptibility test for the entire metal complex. The study proved the considerable antibacterial potency of the synthesized compound against all pathogenic bacteria. OTC showed a greater inhibitory effect on the metal complex. The strength of the antibacterial activity of complexes is based on the concept of Overton's and Tweedy's chelation theory. In coordination chemistry, polarity will decrease in complexity due to the partial sharing of donor atoms of positively charged metal ions during complex formation within the chelate ring. Therefore, these processes enhance the lipophilic character of the central ion, help microorganisms penetrate through the lipid layer, and ultimately deactivate the cell action (Kavitha & Reddy, 2016).

It is clear from the reported data that Cd-OTC/Sal and Mo-OTC/Sal metal complexes show better results at higher concentrations and decrease at lower concentrations. *E. coli* of Zr(II)Otc/Sal and Pd(II)Otc/Sal complexes were found to be less active, while *S.aureus* of Cd-OTC/Sal complex showed better results. Therefore, all pathogens were found to be susceptible to the prepared complexes of oxytetracycline.

Table 21: Antibacterial growth data of the Cd-OTC/Sal and Mo-OTC/Sal metal complexes

Complexes	Diameter of the zone of inhibition in mm								
	<i>S. aureus</i>			<i>P. mirabilis</i>			<i>E. coli</i>		
Pathogenic bacteria									
Concentrations ($\mu\text{g}/\mu\text{L}$)	50	25	12.5	50	25	12.5	50	25	12.5
Cd-OTC/Sal	30	28	26	26	24	21	24	23	20
Mo-OTC/Sal	18	16	15	24	23	21	23	19	18
Amikacin (30 mcg/ disc)	21			21			14		
OTC (ethanol)	37			33			28		
OTC (DMSO)	41			34			29		

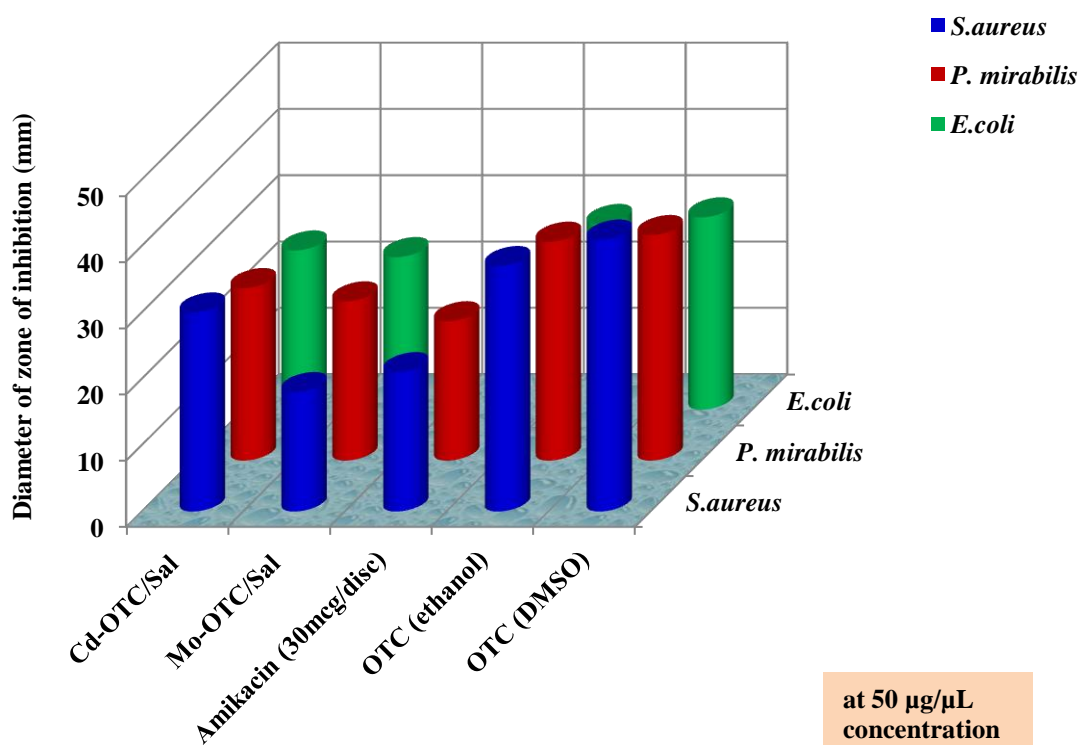


Figure 45: Bar graph of the antibacterial sensitivity of Cd-OTC/Sal and Mo-OTC/Sal metal complexes at 50 ($\mu\text{g}/\mu\text{L}$) concentration.

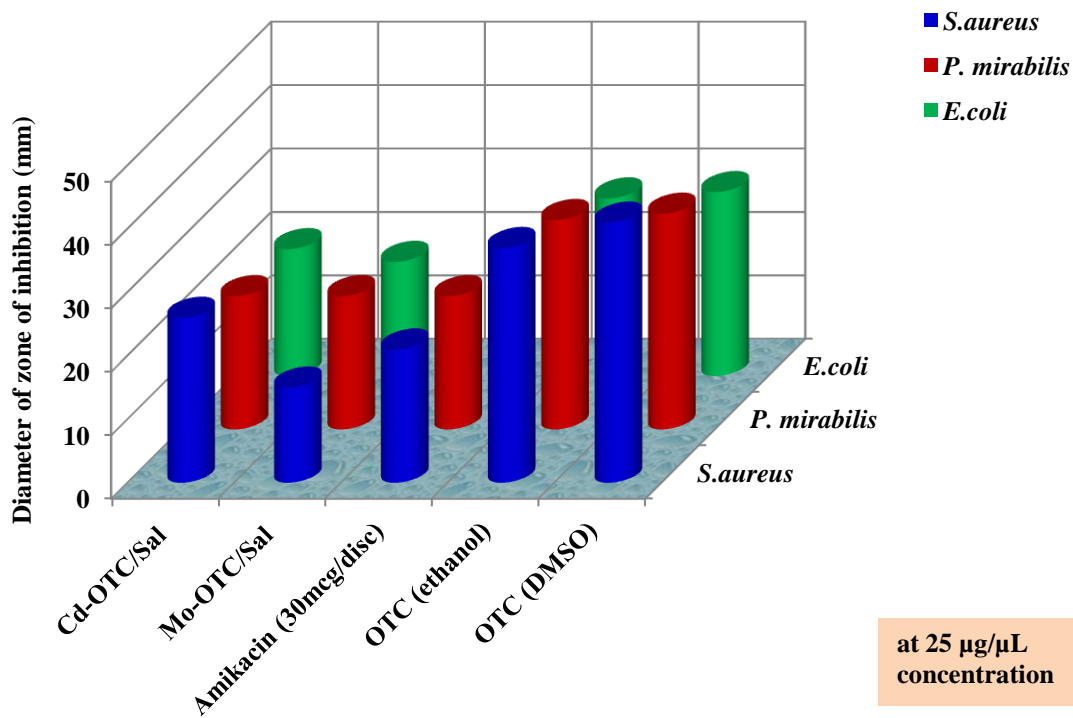


Figure 46: Bar graph of the antibacterial sensitivity of Cd-OTC/Sal and Mo-OTC/Sal metal complexes at 25 (µg/µL) concentration.

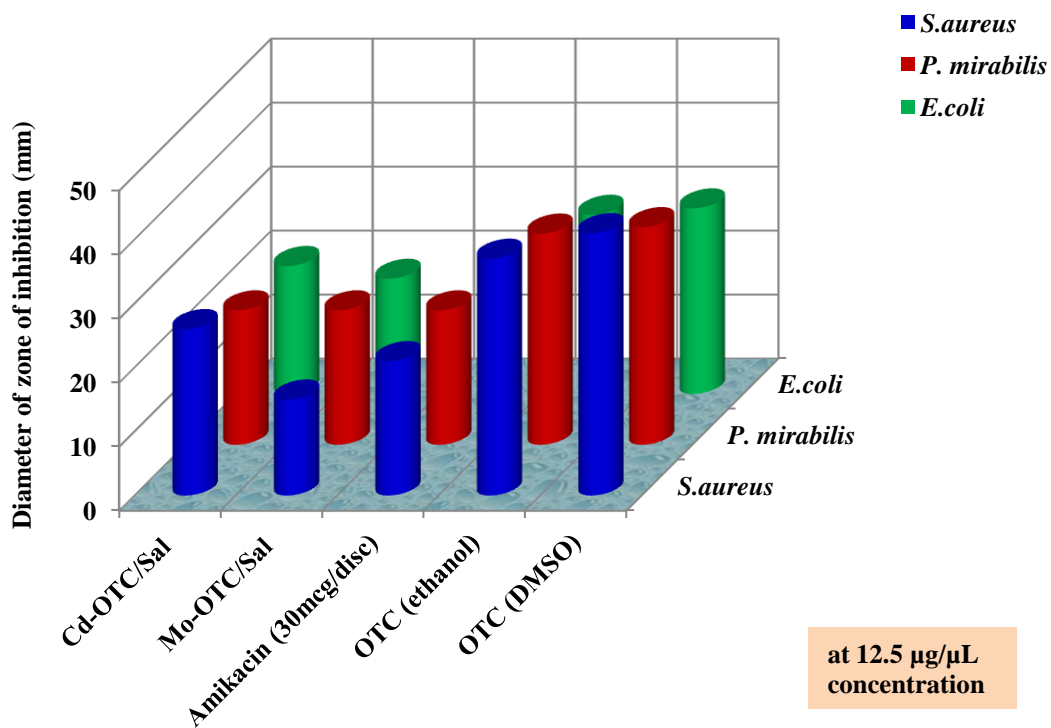


Figure 47: Bar graph of the antibacterial sensitivity of Cd-OTC/Sal and Mo-OTC/Sal metal complexes at 12.5 (µg/µL) concentration.

Table 22: Antibacterial growth data of the Zr(II)Otc/Sal and Pd(II)Otc/Sal metal complexes.

Complexes	The diameter of the zone of inhibition (mm)								
	<i>S. aureus</i>			<i>P. mirabilis</i>			<i>E. coli</i>		
Pathogenic Bacteria									
Concentrations ($\mu\text{g}/\mu\text{L}$)	50	25	12.5	50	25	12.5	50	25	12.5
Zr(II)Otc/Sal complex	23	21	20	14	12	10	12	11	10
Pd(II)Otc/Sal complex	18	17	12	18	13	12	10	9	8
Amk (30mcg/disc)		21			21			14	
OTC-Ethanol		37			33			28	
OTC-DMSO		41			34			29	
DMSO		0			0			0	

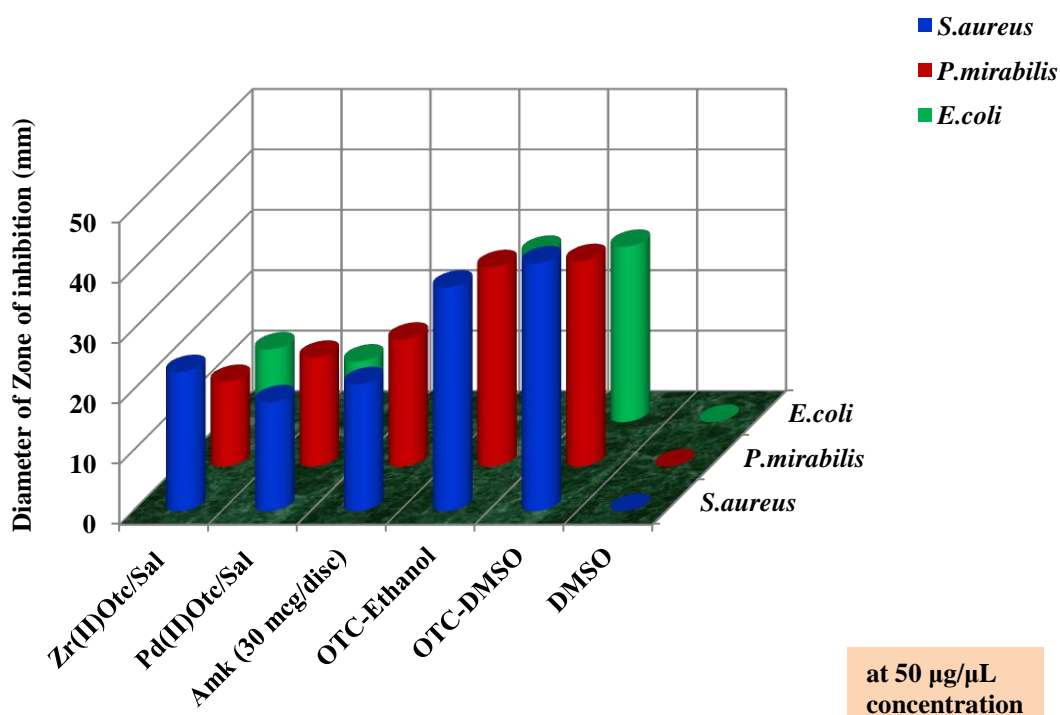


Figure 48: Bar graph of the antibacterial sensitivity of Zr(II)Otc/Sal and Pd(II)Otc/Sal metal complexes at 50 ($\mu\text{g}/\mu\text{L}$) concentration.

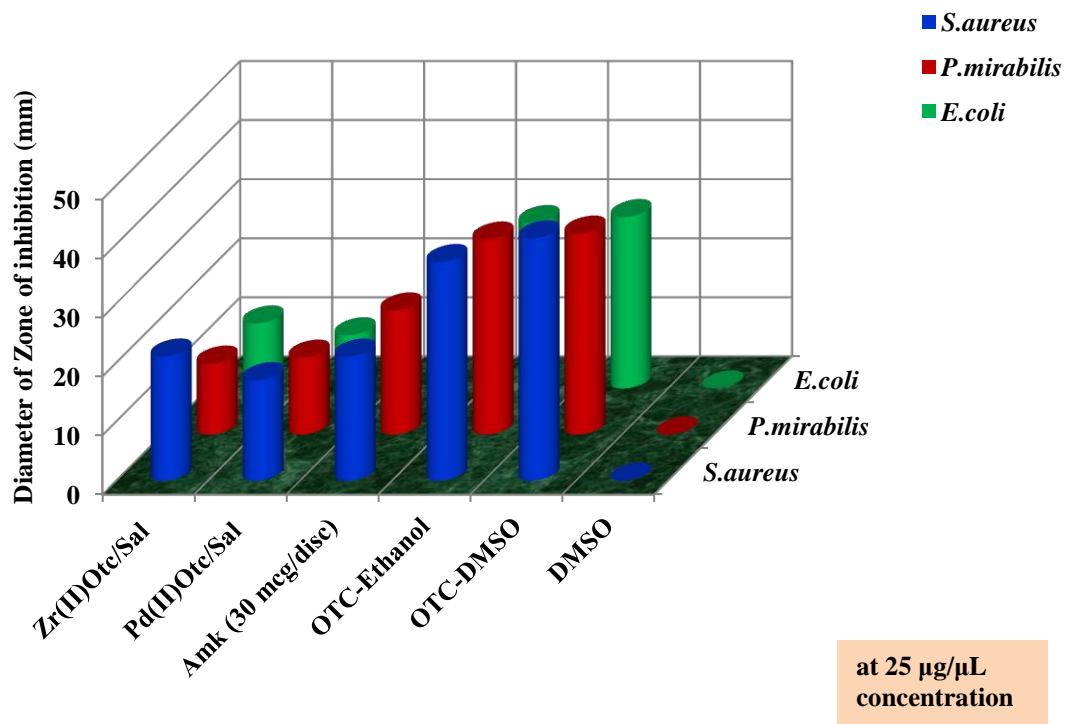


Figure 49: Bar graph of the antibacterial sensitivity of Zr(II)Otc/Sal and Pd(II)Otc/Sal metal complexes at 25 (µg/µL) concentration.

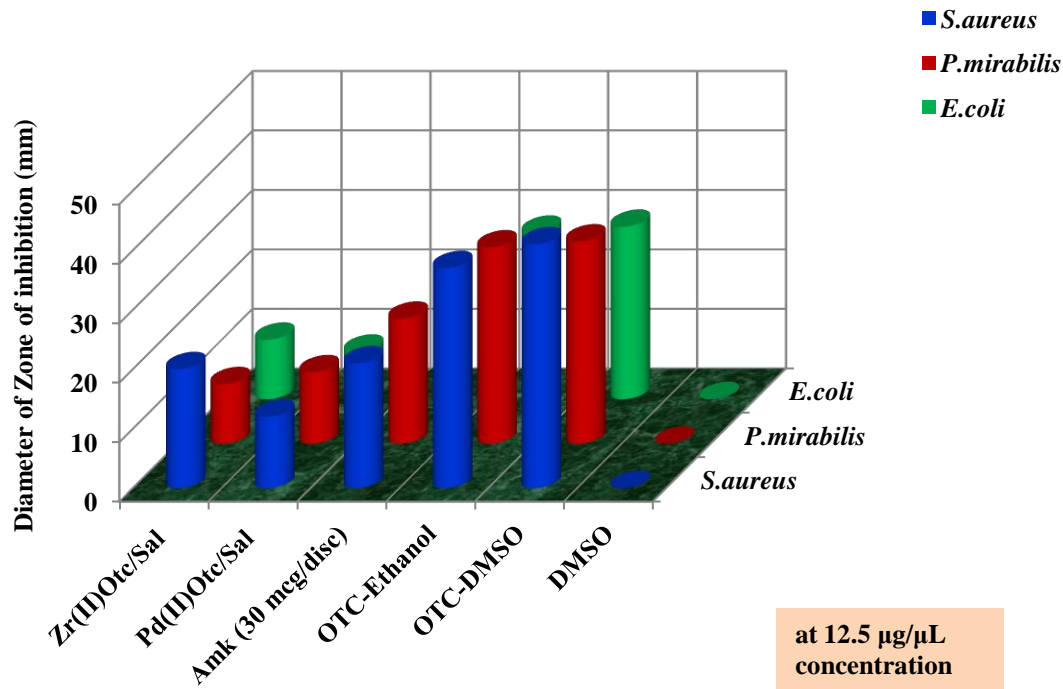


Figure 50: Bar graph of the antibacterial sensitivity of Zr(II)Otc/Sal and Pd(II)Otc/Sal metal complexes at 12.5 (µg/µL) concentration.

CHAPTER 5

CONCLUSION AND RECOMMENDATIONS

Metal complexes play an important role in the field of coordination chemistry. Simple synthetic routes and easy complexation with metal ions have attracted all researchers and scientists in the field of coordination chemistry. Currently, metal complexes of coordination compounds have attracted much attention due to their wide application in various fields such as antitumor, antibacterial, antimitotic, antifungal, antithyroid, antimetabolites, antipyretic, and antiviral. They are also used in analytical, biomedical, chemical, pollution control, industrial and material science, and photochemistry. In the present research study, metal complexes are synthesized from an equimolar mixture of primary ligand, secondary ligand, and metal salts by continuous stirring and refluxing the mixture. Various physicochemical and spectroscopic techniques analyzed the complexes. Antibacterial, as well as molecular modeling, is the highlight of this research.

5.1 Conclusion

Today, the modern world suffers from a shortage of antibiotics. Bacterial resistance occurs due to misuse and overdose of antibiotics. Therefore, there is an urgent need for metal-based-high grade drugs with higher biological activities than traditional medicines to treat the diseases of the present condition. In addition to biological interest, metal complexes have wide applications in various fields of chemistry. The present research aimed at the synthesis of eight metal complexes by refluxing an equimolar mixture of the primary ligand (TC or OTC), secondary ligand (Sal.) along with the metal salts [M=Cd(II), Zr(II), Mo(III/V), and Pd(II)]. The ligand contains donor atoms such as nitrogen or oxygen, which can readily coordinate with the metal salts and eventually form a metal complex, which is presented in the scheme of the proposed structure of the compound.

The prepared complexes were analyzed through various physicochemical measurements such as CHN, pH, conductivity, viscosity, density, surface tension,

melting point, color, and density measurement. The spectroscopic method includes FT-IR, $^1\text{H-NMR}$ and $^{13}\text{C-NMR}$, UV/Visible, and ESI-MS, which revealed the involvement of nitrogen or oxygen donor atoms with metal ions. Thermal and kinetic stability can calculate various parameters of activations: E^* , ΔS^* , ΔH^* , and ΔG^* from TGA/DTA techniques. The surface morphology of the complexes was obtained with a scanning electron microscope (SEM). The geometries of complexes can be identified from molecular modeling. The antibacterial potency was performed with the use of modified Kirby-Bauer paper disc diffusion techniques against two strains of pathogenic bacteria viz. gram-positive and gram-negative. The last two techniques are the main features of the research work.

The spectral data revealed the interaction of metal ions through O at C3 and N atom of C2 of ring A (TC) and O atom of salicylaldehyde during complex formation. The complexes were amorphous solid, colored, and insoluble in water but soluble in organic solvents such as DMSO and DMF. A change in color seen during the chemical procedures indicates deprotonation during complex formation. The FT-IR as well as $^1\text{H-NMR}$ spectral data supported this fact. Molar conductivity of metal complexes value indicated both electrolytic and non-electrolytic in nature. The electronic absorption spectral data supported the tetrahedral [Cd-TC/Sal, Zr-TC/Sal, Cd-OTC/Sal, Zr(II)Otc/Sal], octahedral [Mo-TC/Sal, Mo-OTC/Sal], and square planar [Pd-TC/Sal, Pd(II)Otc/Sal] geometries of the metal complexes. This has also been supported from the molecular modeling study. From the Redfern equation, the activation energy decreases while moving down to another decomposition step resulting higher stability.

In this current research, two strains of human clinical pathogenic bacteria were selected for their antibacterial study of all the synthesized metal complexes. Tetracycline showed a high inhibitory effect on the metal complex. The potency of the antibacterial activity of complexes is based on the concept of Overton's and Tweedy's chelation theory. In coordination chemistry, complexation will decrease the polarity due to the partial sharing of donor atoms of positively charged metal ions during complex formation within the chelate ring. Therefore, these processes enhance the lipophilic character of the central ion, helping microorganisms to penetrate through the lipid layer and eventually destroy the cell action and cause death to the

microorganisms. Hence, the synthesized metal complex will be new hope for the development of better antibiotics in the field of medical science.

5.2 Recommendations

Following are the plans for future studies on metal complexes:

- To perform antioxidant, anticancer, antifungal, antitoxicity, and *in vivo* antibacterial activities of the metal complexes.
- To check the minimum inhibitory concentration (MIC) and minimum bactericidal concentration (MBC) measurements of the synthesized metal complexes.
- To obtain a single crystal of metal complexes and to study their geometrical structure.
- To investigate the anticorrosion activity of metal complexes.
- To prepare the metal-based antibiotics in bulk for their commercial application.

CHAPTER 6

SUMMARY

The thesis entitled “Synthesis, Characterization, and Biological Investigations of Heteroleptic Complexes of Tetracyclines and Salicylaldehyde Mixed Ligands” has been documented into six chapters. Each chapter has been summarized herein to represent all mandatory facts related to the present research work.

Chapter 1 deals with the general introduction of metal complexes of mixed ligand and their chemistry with 4d-Transition metal. Biological and other applications of metal complexes are also highlighted in this chapter. In addition, brief about the structure and chemical information of tetracycline and oxytetracycline are also stated. In this chapter, the choices of Metallo-elements are clearly described. There are also main, general, and specific objectives within this chapter. The last part of this chapter highlights the scope of the current research work.

Chapter 2 explains the detailed literature review of the current research work, which is an important part of any research work. Here, the literature review explains a general overview of the research. This technique explains pharmaceutical and biomedical applications, catalytic applications, and applications in modern technology. The end of the chapter deals with surfactant and corrosion inhibition.

Chapter 3 explains the detailed materials or reagents used in the current research work. The physical parameters such as CHN, pH, viscosity, conductivity, surface tension, and density along with spectral characterization techniques like FT-IR, (^1H & ^{13}C)-NMR, UV/Vis., and ESI-MS are also described in this chapter. This chapter also deals with TGA/DTA, SEM, molecular modeling, and procedures for antibacterial testing of the metal complexes.

Chapter 4 explains the results and discussion of the current research work which is the important backbone and skeleton part of any thesis. FT-IR spectral studies have shown the complexation of donor atoms (nitrogen and oxygen) of tetracycline with

metal ions and salicylaldehyde during the complex formation. The coordination bonds of the metal ion with nitrogen or oxygen lie at the lowest wavenumber (cm^{-1}) range. The proposed structure and geometry were obtained from the findings of the UV/Vis spectra. TGA/DTA results showed that the complexes have high thermal and kinetic stabilities. Here, all tables and figures represent the analyzed data that are positioned at appropriate locations in this chapter. Antibacterial and molecular modelings are the highlights of this chapter.

Chapter 5 deals with the conclusion of the current research work. Planning for the future and recommendations of the current research work were clearly explained in this chapter.

Chapter 6 has summarizes all the chapters of the present thesis.

The present research aimed at the synthesis of eight metal complexes by refluxing an equimolar mixture of the primary ligand (TC or OTC), secondary ligand (Sal) along with the metal salts [M= Cd(II), Zr(II), Mo(III/V), and Pd(II)]. The prepared complexes were analyzed through various physicochemical measurements such as CHN, pH, conductivity, viscosity, density, surface tension, melting point, color. The spectroscopic method is also included to characterize the complexes prepared.

REFERENCES

- Abdelhamid, H. N., & Wu, H. F. (2018). Selective Biosensing of *Staphylococcus aureus* using Chitosan Quantum Dots. *Spectrochimica Acta-Part A: Molecular and Biomolecular Spectroscopy*, **188**: 50–56. DOI: 10.1016/j.saa.2017.06.047
- Abdel-Mottaleb, M. S. A., & Ismail, E. H. (2019). Transition Metal Complexes of Mixed Bioligands: Synthesis, Characterization, DFT Modeling, and Applications. *Journal of Chemistry*, **2019**: 1-18. DOI: 10.1155/2019/3241061
- Abdel-Rahman, L. H., Abu-Dief, A. M., Ismail, N. M., & Ismael, M. (2017). Synthesis, Characterization, and Biological Activity of New Mixed Ligand Transition Metal Complexes of Glutamine, Glutaric, and Glutamic Acid with Nitrogen Based Ligands. *Inorganic and Nano-Metal Chemistry*, **47**(3): 467–480. DOI: 10.1080/15533174.2015.1137057
- Abdul-ghani, A. J., & Khaleel, A. M. N. (2009). Synthesis and Characterization of New Schiff Bases Derived from N (1) -Substituted Isatin with Dithiooxamide and their Co(II), Ni(II), Cu(II), Pd(II), and Pt(IV) Complexes. *Bioinorganic Chemistry and Applications*, **2009**: 1-12. DOI: 10.1155/2009/413175
- Abebe, A., & Hailemariam, T. (2016). Synthesis and Assessment of Antibacterial Activities of Ruthenium(III) Mixed Ligand Complexes Containing 1,10-Phenanthroline and Guanide. *Bioinorganic Chemistry and Applications*: **2019**: 1–10. DOI: 10.1155/2016/3607924
- Abu-Dief, A. M., & Mohamed, I. M. A. (2015). A Review on Versatile Applications of Transition Metal Complexes Incorporating Schiff Bases. *Beni-Suef University Journal of Basic and Applied Sciences*, **4**: 119–133. DOI: 10.1016/j.bjbas.2015.05.004
- Adediji, J. F., Olayinka, E. T., Adebayo, M. A., & Babatunde, O. (2009). Antimalarial Mixed Ligand Metal Complexes: Synthesis, Physicochemical and Biological Activities. *International Journal of Physical Sciences*, **4**(9): 529–534.
- Ahmed, A., & Lal, R. A. (2013). Synthesis and Electrochemical Characterisation of Molybdenum(VI) Complexes of Disalicylaldehyde Malonoyl-Dihydrazone.

Journal of Molecular Structure, **1048**: 321–330. DOI: 10.1016/j.molstruc.2013.05.056

Ahmed, A., Chanu, O. B., Koch, A., & Lal, R. A. (2012). Synthesis, Spectroscopic and Electrochemical Characterisation of Binuclear Dioxomolybdenum Complexes Derived from Disalicylaldehyde Succinoyldihydrazone. *Journal of Molecular Structure*, **1029**: 161–168. DOI: 10.1016/j.molstruc.2012.06.053

Aiyelabola, T. O., Isabirye, D. A., Akinkunmi, E. O., Ogunkunle, O. A., & Ojo, I. A. O. (2016). Synthesis, Characterization, and Antimicrobial Activities of Coordination Compounds of Aspartic Acid. *Journal of Chemistry*. **2016**: 1-8: DOI: 10.1155/2016/7317015

Al-afyouni, M., Kayser, A., Hung-low, F., Tye, J. W., & Bradley, C. A. (2016). Synthesis and Reactivity of Molybdenum (0) Complexes Containing Sterically Expanded Arene Ligands. *Polyhedron*, **114**: 385-392. DOI: 10.1016/j.poly.2016.02.018

Alanis, A. J. (2005). Resistance to antibiotics: Are we in the Post-Antibiotic Era? *Archives of Medical Research*, **36**(6): 697–705. DOI: 10.1016/j.arcmed.2005.06.009

Al-Farhan, B. S., Basha, M. T., Abdel Rahman, L. H., El-Saghier, A. M. M., El-Ezz, D. A., Marzouk, A. A., Shehata, M. R., & Abdalla, E. M. (2021). Synthesis, DFT Calculations, Antiproliferative, Bactericidal Activity and Molecular Docking of Novel Mixed-Ligand Salen/ 8-hydroxyquinoline Metal Complexes. *Molecules*, **26**: 1-28. DOI: 10.3390/molecules26164725

Ali, H., Khan, E., & Ilahi, I. (2019). Environmental Chemistry and Ecotoxicology of Hazardous Heavy Metals: Environmental Persistence, Toxicity, and Bioaccumulation. *Journal of Chemistry*, **2019**: 1-14. DOI: 10.1155/2019/6730305

Alias, M., Kassum, H., & Shakir, C. (2013). Synthesis, Spectral, Thermal and Antibacterial Studies of Cd(II), Mn(II) and Fe(III) Complexes Containing Trithiocarbonate 1,3,4-thiadiazole Moiety. *Journal of King Saud University-Science*, **25**(2): 157–166. DOI: 10.1016/j.jksus.2012.11.002

- Alias, M., Kassum, H., & Shakir, C. (2014). Synthesis, Physical Characterization and Biological Evaluation of Schiff Base M(II) Complexes. *Journal of the Association of Arab Universities for Basic and Applied Sciences*, **15**(1): 28–34. DOI: 10.1016/j.jaubas.2013.03.001
- Al-Maythaly, B. A., Wazeer, M. I. M., Isab, A. A., Nael, M. T., & Ahmad, S. (2008). Complexation of Cd(SeCN)₂ with Imidazolidine-2-Thione and its Derivatives: Solid State, Solution NMR and Anti-Bacterial Studies. *Spectroscopy*, **22**(5): 361–370. DOI: 10.3233/SPE-2008-0359
- Al-Noaimi, M., Nafady, A., Warad, I., Alshwafy, R., Husein, A., Talib, W. H., & Hadda, T. Ben. (2014). Heterotrimetallic Ru(II)/Pd(II)/Ru(II) Complexes: Synthesis, Crystal structure, Spectral Characterization, DFT Calculation and Antimicrobial Study. *Spectrochimica Acta-Part A: Molecular and Biomolecular Spectroscopy*, **122**: 273–282. DOI: 10.1016/j.saa.2013.11.052
- Al-resayes, S. I. (2010). Kinetics Analysis for Non-Isothermal Decomposition γ -Irradiated Indium Acetate. *Arabian Journal of Chemistry*, **3**(3): 191–194. DOI: 10.1016/j.arabjc.2010.04.010
- Ashurov, J. M., Ibragimov, A. B., & Ibragimov, B. T. (2015). Mixed-Ligand Complexes of Zn(II), Cd(II) and Cu(II) with Triethanolamine and p-Nitrobenzoic Acid: Syntheses and Crystal Structures. *Polyhedron*, **102**: 441–446. DOI: 10.1016/j.poly.2015.05.044
- Aslan, H. G., Ozcan, S., & Karacan, N. (2011). Synthesis, Characterization and Antimicrobial Activity of Salicylaldehyde Benzenesulfonylhydrazone (Hsalbsmh) and its Nickel(II), Palladium(II), Platinum(II), Copper(II), Cobalt(II) Complexes. *Inorganic Chemistry Communications*, **14**(9): 1550–1553. DOI: 10.1016/j.inoche.2011.05.024
- Azevedo, P. A. A., Furlan, J. P. R., Gonçalves, G. B., Gomes, C. N., Goulart, R. da S., Stehling, E. G., & Pitondo-Silva, A. (2019). Molecular Characterisation of Multidrug-Resistant *Klebsiella pneumoniae* Belonging to CC258 Isolated from Outpatients with Urinary Tract Infection in Brazil. *Journal of Global Antimicrobial Resistance*, **18**: 74–79. DOI: 10.1016/j.jgar.2019.01.025
- Aziz, A. A. A., Salem, A. N. M., Sayed, M. A., & Aboaly, M. M. (2012). Synthesis, Structural Characterization, Thermal Studies, Catalytic Efficiency and

- Antimicrobial Activity of Some M (II) Complexes with ONO Tridentate Schiff Base. *Journal of Molecular Structure*, **1010**: 130–138. DOI: 10.1016/j.molstruc.2011.11.043
- Bai, Y., Shang, W. L., Dang, D. Bin, Sun, J. De, & Gao, H. (2009). Synthesis, Crystal Structure and Luminescent Properties of One Coordination Polymer of Cadmium(II) with Mixed Thiocyanate and Hexamethylenetetramine Ligands. *Spectrochimica Acta- Part A: Molecular and Biomolecular Spectroscopy*, **72**(2): 407–411. DOI: 10.1016/j.saa.2008.10.033
- Bajju, G. D., Devi, G., Katoch, S., Bhagat, M., Deepmala, Ashu, Kundan, S., & Anand, S. K. (2013). Synthesis, Spectroscopic, and Biological Studies on New Zirconium (IV) Porphyrins with Axial Ligand. *Bioinorganic Chemistry and Applications*, **2013**: 1-15. DOI: 10.1155/2013/903616
- Balakrishnan, S., Duraisamy, S., Kasi, M., Kandasamy, S., Sarkar, R., & Kumarasamy, A. (2019). Syntheses, Physicochemical Characterization, Antibacterial Studies on Potassium Morpholine Dithiocarbamate Nickel(II), Copper(II) Metal Complexes and their Ligands. *Heliyon*, **5**(5). DOI: 10.1016/j.heliyon.2019.e01687
- Barry, N. P. E., & Sadler, P. J. (2014). 100 Years of Metal Coordination Chemistry: From Alfred Werner to Anticancer Metallodrugs. *Pure and Applied Chemistry*, **86**(12): 1897–1910. DOI: 10.1515/pac-2014-0504
- Barve, A., Kumbhar, A., Bhat, M., Joshi, B., Butcher, R., Sonawane, U., & Joshi, R. (2009). Mixed-Ligand Copper(II) Maltolate Complexes: Synthesis, Characterization, DNA Binding and Cleavage, and Cytotoxicity. *Inorganic Chemistry*, **48**(19): 9120–9132. DOI: 10.1021/ic9004642
- Belghiti, M. E., Bouazama, S., Echihi, S., Mahsoun, A., Elmelouky, A., Dafali, A., Emran, K. M., Hammouti, B., & Tabyaoui, M. (2020). Understanding the Adsorption of Newly Benzylidene-Aniline Derivatives as a Corrosion Inhibitor for Carbon Steel in Hydrochloric Acid Solution: Experimental, DFT and Molecular Dynamic Simulation Studies. *Arabian Journal of Chemistry*, **13**(1): 1499–1519. DOI: 10.1016/j.arabjc.2017.12.003
- Benyei, A., & Sovago, I. (2003). Thermodynamic, Kinetic, and Structural Studies on the Mixed Ligand Complexes of Palladium (II) with Tridentate and

- Monodentate Ligands. *Journal of Inorganic Biochemistry*, **94**(3): 291–299. DOI: 10.1016/S0162-0134(03)00009-6
- Bernhoft, R. A. (2013). Cadmium Toxicity and Treatment. *The Scientific World Journal*, **2013**: 1-7. DOI: 10.1155/2013/394652
- Bie, F., Cao, H., Yan, P., Cui, H., Shi, Y., Ma, J., Liu, X., & Han, Y. (2020). A Cyanobiphenyl-based Ratiometric Fluorescent Sensor for Highly Selective and Sensitive Detection of Zn²⁺. *Inorganica Chimica Acta*, **508**: 119652. DOI: 10.1016/j.ica.2020.119652
- Bonaccorso, C., Marzo, T., & La Mendola, D. (2020). Biological Applications of Thiocarbohydrazones and Their Metal Complexes: A Perspective Review. *Pharmaceuticals*, **13**(1). DOI: 10.3390/ph13010004
- Bouki, C., Venieri, D., & Diamadopoulos, E. (2013). Detection and Fate of Antibiotic Resistant Bacteria in Wastewater Treatment Plants: A Review. *Ecotoxicology and Environmental Safety*, **91**: 1–9. DOI: 10.1016/j.ecoenv.2013.01.016
- Cao, J., Yang, Z., Xiong, W., Zhou, Y., Peng, Y., Li, X., Zou, C, Xu, R, & Zhang, Y. (2018). One-step Synthesis of Co-Doped Uio-66 Nanoparticle with Enhanced Removal Efficiency of Tetracycline: Simultaneous Adsorption and Photocatalysis. *Chemical Engineering Journal*, **353**: 126–137. DOI: 10.1016/j.cej.2018.07.060
- Cestari, S. E., Ludovico, M. S., Martins, F. H., Da Rocha, S. P. D., Elias, W. P., & Pelayo, J. S. (2013). Molecular Detection of HpmA and HlyA Hemolysin of Uropathogenic *Proteus mirabilis*. *Current Microbiology*, **67**(6): 703–707. DOI: 10.1007/s00284-013-0423-5
- Chandra, S., Tyagi, M., & Agrawal, S. (2011). Spectral and Antimicrobial Studies on Tetraaza Macrocyclic Complexes of Pd(II), Pt(II), Rh(III) and Ir(III) Metal Ions. *Journal of Saudi Chemical Society*, **15**(1): 49–54. DOI: 10.1016/j.jscs.2010.09.005
- Chandrathilaka, A. M. D. S., Ileperuma, O. A., & Hettiarachchi, C. V. (2013). Spectrophotometric and pH-metric Studies on Pb(II), Cd(II), Al(III) and Cu(II) Complexes of Paracetamol and Ascorbic Acid. *Journal of the National Science Foundation of Sri Lanka*, **41**(4): 337–344. DOI: 10.4038/jnsfsr.v41i4.6253

- Chaudhary, R. G., Ali, P., Gandhare, N. V., Tanna, J. A., & Juneja, H. D. (2019). Thermal Decomposition Kinetics of Some Transition Metal Coordination Polymers of Fumaroyl bis (paramethoxyphenylcarbamide) using DTG/DTA Techniques. *Arabian Journal of Chemistry*, **12**(7): 1070-1082. DOI: 10.1016/j.arabjc.2016.03.008
- Chen, Y., Shi, J., Du, Q., Zhang, H., & Cui, Y. (2019). Antibiotic Removal by Agricultural Waste Biochars with Different Forms of Iron Oxide. *RSC Advances*, **9**(25): 14143–14153. DOI: 10.1039/c9ra01271k
- Cheng, D. H., Yang, S. K., Zhao, Y., & Chen, J. (2013). Adsorption Behaviors of Oxytetracycline onto Sediment in the Weihe River, Shaanxi, China. *Journal of Chemistry*, **2013**: 1-10. DOI: 10.1155/2013/652930
- Cheng, F., Li, Z., Lan, S., Liu, W., Li, X., Zhou, Z., Song, Z., Wu, J., Zhang, M., & Shan, W. (2018). Characterization of *Klebsiella pneumoniae* Associated with Cattle Infections in Southwest China using Multi-Locus Sequence Typing (MLST), Antibiotic Resistance and Virulence-Associated Gene Profile Analysis. *Brazilian Journal of Microbiology*, **49**: 93–100. DOI: 10.1016/j.bjm.2018.06.004
- Coats, A. W., Redfern, J. P. (1963). Thermogravimetric Analysis. *Analyst*, **88**(1053): 906–924. DOI: 10.1039/AN9638800906
- Constable, E. C., & Gale, P. A. (2013). Celebrating the 100th Anniversary of the Nobel Prize in Chemistry Awarded to Alfred Werner. *Chemical Society Reviews*, **42**(4): 1427–1428. DOI: 10.1039/c2cs90118h
- Creutz, C., Ford, P. C., & Meyer, T. J. (2006). Henry Taube: Inorganic Chemist Extraordinaire. *Inorganic Chemistry*, **45**(18): 7059–7068. DOI: 10.1021/ic060669s
- Damena, T., Zeleke, D., Desalegn, T., Demissie, T. B., & Eswaramoorthy, R. (2022). Synthesis, Characterization, and Biological Activities of Novel Vanadium(IV) and Cobalt(II) Complexes. *ACS Omega*, **7**(5): 4389–4404. DOI: 10.1021/acsomega.1c06205
- Da Silva, J. D. S. F., Malo, D. L., Bataglion, G. A., Eberlin, M. N., Ronconi, C. M., Junior, S. A., & De Sá, G. F. (2015). Adsorption in a Fixed-bed Column and

- Stability of the Antibiotic Oxytetracycline Supported on Zn(II)-[2-methylimidazolate] Frameworks in Aqueous Media. *PLoS ONE*, **10**(6): 1–20. DOI: 10.1371/journal.pone.0128436
- Dar, O. A., Lone, S. A., Malik, M. A., Aqlan, F. M., Wani, M. Y., Hashmi, A. A., & Ahmad, A. (2019). Synthesis and Synergistic Studies of Isatin Based Mixed Ligand Complexes as Potential Antifungal Therapeutic Agents. *Heliyon*, **5**(7): DOI: 10.1016/j.heliyon.2019.e02055
- De La Mata, F. J., Giner, P., & Royo, P. (1999). Synthesis and Reactivity of New Silyl-Substituted Monocyclopentadienyl Molybdenum and Tungsten Complexes. *Journal of Organometallic Chemistry*, **572**(2): 155-161. DOI: 10.1016/S0022-328X(98)00962-0
- Deming, T. J. (2007). Synthetic Polypeptides for Biomedical Applications. *Progress in Polymer Science*, **32**(8–9): 858-875. DOI: 10.1016/j.progpolymsci.2007.05.010
- Desai, K. R., Pathan, A. A. & Bhasin, C. P. (2017). Synthesis, Characterization of Cadmium Sulphide Nanoparticles and its Application as Photocatalytic Degradation of Congo Red. Synthesis, Characterization of Cadmium Sulphide Nanoparticles and its Application as Photocatalytic Degradation of Congo Red. *International Journal of Nanomaterials and Chemistry*, **3**(2): 39–43. DOI: 10.18576/ijnc/030204
- Devi, J., & Batra, N. (2015). Synthesis, Characterization and Antimicrobial Activities of Mixed Ligand Transition Metal Complexes with Isatin Monohydrazone Schiff Base Ligands and Heterocyclic Nitrogen Base. *Spectrochimica Acta-Part A: Molecular and Biomolecular Spectroscopy*, **135**: 710–719. DOI: 10.1016/j.saa.2014.07.041
- Díaz, M., Diana, S., García, D., Prashar, S., & Gómez, S. (2019). Palladium Nanoparticles Supported on Silica, Alumina or Titania : Greener Alternatives for Suzuki–Miyaura and Other C–C Coupling Reactions. *Environmental Chemistry Letters*, 1–18. DOI: 10.1007/s10311-019-00899-5
- Dilip, C. S., Manikandan, K., Subhashini, D. R., & Thiruneelakandan, R. (2013). Synthesis, Spectroscopic Characterisation, and Biopotential and DNA Cleavage

- Applications of Mixed Ligand 4-N, N-Dimethylaminopyridine Metal Complexes. *Journal of Chemistry*, **2013**: 1-16. DOI: 10.1155/2013/195074
- Divsalar, N., Monadi, N., & Tajbaksh, M. (2016). Preparation and Characterization of a Molybdenum (VI) Schiff Base Complex as Magnetic Nanocatalyst for Synthesis of 2-amino- 4H-benzo [h] chromenes. *Journal of Nanostructures*, **6**(4): 312–321. DOI: 10.22052/jns.2016.34329
- Dupé, A., Judmaier, M. E., Belaj, F., Zangger, K., & Mösch-Zanetti, N. C. (2015). Activation of Molecular Oxygen by a Molybdenum Complex for Catalytic Oxidation. *Dalton Transactions*, **44**(47): 20514–20522. DOI: 10.1039/c5dt02931g
- Ebrahimi-Kahrizsangi, R., Abbasi, M. H. (2008). Evaluation of Reliability of Coats-Redfern Method for Kinetic Analysis of Non-Isothermal TGA. *Transactions of Nonferrous Metals Society of China*, **18**(1): 217-221. DOI: 10.1016/S1003-6326(08)60039-4
- El-ajaily, M. M., Abdullah, H. A., Al-janga, A., Saad, E. E., & Maihub, A. A. (2015). Zr(IV), La(III), and Ce(IV) Chelates with 2-[(4-[(Z)-1-(2-Hydroxyphenyl) Ethylidene]Aminobutyl)-Ethanimidoyl] phenol: Synthesis, Spectroscopic Characterization, and Antimicrobial Studies. *Advances in Chemistry*, **2015**:1–15. DOI: 10.1155/2015/987420
- El-Boraey, H. A., & El-gammal, O. A. (2018). Macrocyclic Cu(II) and Pd(II) Complexes with New 16-Membered Tetradentate [N₄] Ligand: Synthesis, Characterization, 3D Molecular Modeling and In Vitro Anticancer and Antimicrobial Activities. *Journal of Inclusion Phenomena and Macrocyclic Chemistry*, **90**: 123–134. DOI: 10.1007/s10847-017-0774-9
- El-Ghamry, A. H., Sakai, K., Masaoka, S., El-Baradie, K. Y., & Issa, R. M. (2012). Preparation, Characterization, Biological Activity and 3D Molecular Modeling of Mn(II), Co(II), Ni(II), Cu(II), Pd(II) and Ru(III) Complexes of Some Sulfadrag Schiff Bases. *Chinese Journal of Chemistry*, **30**(4): 881–890. DOI: 10.1002/cjoc.201280024
- El-Halim, H. F. A., Mohamed, G. G., El-Dessouky, M. M. I., & Mahmoud, W. H. (2011). Ligational Behaviour of Lomefloxacin Drug Towards Cr(III), Mn(II), Fe(III), Co(II), Ni(II), Cu(II), Zn(II), Th(IV) and UO₂(VI) Ions: Synthesis,

- Structural Characterization and Biological Activity Studies. *Spectrochimica Acta-Part A: Molecular and Biomolecular Spectroscopy*, **82**(1): 8–19. DOI: 10.1016/j.saa.2011.05.089
- El-Halim, H. F. A., Mohamed, G. G., & Khalil, E. A. M. (2017). Synthesis, Spectral, Thermal and Biological Studies of Mixed Ligand Complexes with Newly Prepared Schiff Base and 1,10-Phenanthroline Ligands. *Journal of Molecular Structure*, **1146**: 153–163. DOI: 10.1016/j.molstruc.2017.05.092
- El-Lateef, H. M. A., Abbasov, V. M., Aliyeva, L. I., & Khalaf, M. M. (2015). Novel Naphthenate Surfactants Based on Petroleum Acids and Nitrogenous Bases as Corrosion Inhibitors for C1018-Type Mild Steel in CO₂-Saturated Brine. *Egyptian Journal of Petroleum*, **24**(2): 175–182. DOI: 10.1016/j.ejpe.2015.05.010
- El-Saied, F. A., Shakhofa, M. M. E., Tabl, A. S. El, Abd-Elzaher, M. M., & Morsy, N. (2017). Coordination Versatility of N₂O₄ Polydentate Hydrazonic Ligand in Zn(II), Cu(II), Ni(II), Co(II), Mn(II) and Pd(II) Complexes and Antimicrobial Evaluation. *Beni-Suef University Journal of Basic and Applied Sciences*, **6**(4): 310–320. DOI: 10.1016/j.bjbas.2017.09.005
- El-Sherif, A. A., Shoukry, M. M., & Abd-Elgawad, M. M. A. (2012). Synthesis, Characterization, Biological Activity and Equilibrium Studies of Metal(II) Ion Complexes with Tridentate Hydrazone Ligand Derived from Hydralazine. *Spectrochimica Acta - Part A: Molecular and Biomolecular Spectroscopy*, **98**: 307–321. DOI: 10.1016/j.saa.2012.08.034
- El-shwiniy, W. H., & Zordok, W. A. (2018). Synthesis, Spectral, DFT Modeling, Cytotoxicity and Microbial Studies of Novel Zr(IV), Ce(IV) and U(VI) Piroxicam Complexes. *Spectrochimica Acta Part A: Molecular and Biomolecular Spectroscopy*, **199**: 290–300. DOI: 10.1016/j.saa.2018.03.074
- El-Shwiniy, W. H., Sadeek, S. A. (2015). Synthesis and Characterization of New 2-Cyano-2-(p-Tolyl-Hydrazono)-Thioacetamide Metal Complexes and a Study on their Antimicrobial Activities. *Spectrochimica Acta Part A: Molecular and Biomolecular Spectroscopy*, **137**: 535–546. DOI: 10.1016/j.saa.2014.08.124
- El-Shwiniy, W. H., Shehab, W. S., Mohamed, S. F., & Ibrahim, H. G. (2018). Synthesis and Cytotoxic Evaluation of Some Substituted Pyrazole Zirconium

- (IV) Complexes and their Biological Assay. *Applied Organometallic Chemistry*, **32**: 1–16. DOI: 10.1002/aoc.4503
- El-Sonbati, A. Z., Diab, M. A., Morgan, S. M., Abou-Dobara, M. I., & El-Ghettany, A. A. (2020). Synthesis, Characterization, Theoretical and Molecular Docking Studies of Mixed-Ligand Complexes of Cu(II), Ni(II), Co(II), Mn(II), Cr(III), UO₂(II) and Cd(II). *Journal of Molecular Structure*, **1200**: DOI: 10.1016/j.molstruc.2019.127065
- El-Sonbati, A. Z., Mahmoud, W. H., Mohamed, G. G., Diab, M. A., Morgan, S. M., & Abbas, S. Y. (2019). Synthesis, Characterization of Schiff Base Metal Complexes and their Biological Investigation. *Applied Organometallic Chemistry*, **33**(9): 1–16. DOI: 10.1002/aoc.5048
- El-Tabl, A. S., El-wahed, M. M. A., Mahmoud, A., & Mahmoud, S. (2013). Cytotoxic Behavior and Spectroscopic Characterization of Metal Complexes of Ethylacetoacetate bis (Thiosemicarbazone) Ligand. *Spectrochimica Acta Part A: Molecular and Biomolecular Spectroscopy*, **117**: 772–788. DOI: 10.1016/j.saa.2013.04.014
- Fang, C. T., Chen, Y. C., Chang, S. C., Sau, W. Y., & Luh, K. T. (2000). *Klebsiella pneumoniae* Meningitis: Timing of Antimicrobial Therapy and Prognosis. *An International Journal of Medicine*, **93**(1): 45–53. DOI: 10.1093/qjmed/93.1.45
- Feio, M. J., Sousa, I., Ferreira, M., Cunha-Silva, L., Saraiva, R. G., Queiros, C., Alexandre, J. G., Claro, V., Mendes, A., Ortiz, R., Lopes, S., Amaral, A. L., Lino, J., Fernandes, P., Silva, A. J., Moutinho, L., De Castro, B., Pereira, E., Perello, L., & Gameiro, P. (2014). Fluoroquinolone-Metal Complexes: A Route to Counteract Bacterial Resistance? *Journal of Inorganic Biochemistry*, **138**: 129–143. DOI: 10.1016/j.jinorgbio.2014.05.007
- Feng, L., Yin, C., Zhang, H., Li, Y., Song, X., Chen, Q., & Liu, H. (2018). Cationic Gemini Surfactants with a Bipyridyl Spacer as Corrosion Inhibitors for Carbon Steel. *ACS Omega*, **3**(12): 18990–18999. DOI: 10.1021/acsomega.8b03043
- Fiori-duarte, A. T., Bergamini, F. R. G., Enoque, R., Paiva, F. De, Manzano, C. M., Lustri, W. R., & Corbi, P. P. (2019). A New Palladium (II) Complex with Ibuprofen: Spectroscopic Characterization, DFT Studies, Antibacterial

Activities and Interaction with Biomolecules. *Journal of Molecular Structure*, **1186**: 144–154. DOI: 10.1016/j.molstruc.2019.03.020

- Fragoza-Mar, L., Olivares-Xometl, O., Domínguez-Aguilar, M. A., Flores, E. A., Arellanes-Lozada, P., & Jiménez-Cruz, F. (2012). Corrosion Inhibitor Activity of 1, 3-Diketone Malonates for Mild Steel in Aqueous Hydrochloric Acid Solution. *Corrosion Science*, **61**: 171–184. DOI: 10.1016/j.corsci.2012.04.031
- Gaber, M., El-ghamry, H., Atlam, F., & Fathalla, S. (2015). Synthesis, Spectral and Theoretical Studies of Ni(II), Pd(II) and Pt(II). *Spectrochimica Acta Part A: Molecular and Biomolecular Spectroscopy*, **137**: 919–929. DOI: 10.1016/j.saa.2014.09.015
- Gao, L., Wang, H., Zheng, B., & Huang, F. (2021). Combating Antibiotic Resistance: Current Strategies for the Discovery of Novel Antibacterial Materials Based on Macrocyclic Supramolecular Chemistry. *Giant*, **7**: 1-28. DOI: 10.1016/j.giant.2021.100066
- Gaur, R., & Jeevanandam, P. (2015). Effect of Anion on Morphology of Cds Nanoparticles Prepared via Thermal Decomposition of Different Cadmium Thiourea Complexes in a Solvent and Solid State. *New Journal of Chemistry*, **39**: 9442-9453. DOI: 10.1039/C5NJ01605C
- Geeta, B., Shravan kumar, K., Reddy, P. M., Ravikrishna, E., Sarangapani, M., Reddy, K. K., & Ravinder, V. (2010). Binuclear Cobalt (II), Nickel (II), Copper (II) and Palladium (II) Complexes of a New Schiff-Base as Ligand: Synthesis, Structural Characterization, and Antibacterial Activity. *Spectrochimica Acta Part A: Molecular and Biomolecular Spectroscopy*, **77**(4): 911–915. DOI: 10.1016/j.saa.2010.08.004
- Ghanghas, P., Choudhary, A., Kumar, D., & Poonia, K. (2021). Coordination Metal Complexes with Schiff Bases: Useful Pharmacophores with Comprehensive Biological Applications. *Inorganic Chemistry Communications*, **130**: 108710. DOI: 10.1016/j.inoche.2021.108710
- Giamarellou, H., & Kanellakopoulou, K. (2008). Current Therapies for *Pseudomonas aeruginosa*. *Critical Care Clinics*, **24**(2): 261–278. DOI: 10.1016/j.ccc.2007.12.004

- Gomes, T. A. T., Elias, W. P., Scaletsky, I. C. A., Guth, B. E. C., Falcao, J., Piazza, R. M. F., Ferreira, L. C., & Martinez, M. B. (2016). Diarrheagenic *Escherichia coli*. *Brazilian Journal of Microbiology*, **47**: 3–30. DOI: 10.1016/j.bjm.2016.10.015
- Guerra, W., De Andrade Azevedo, E., De Souza Monteiro, A. R., Bucciarelli-Rodriguez, M., Chartone-Souza, E., Nascimento, A. M. A., Fontes, A. P. S., Le Moyec, L., & Pereira-Maia, E. C. (2005). Synthesis, Characterization, and Antibacterial Activity of Three Palladium (II) Complexes of Tetracyclines. *Journal of Inorganic Biochemistry*, **99**(12): 2348–2354. DOI: 10.1016/j.jinorgbio.2005.09.001
- Guerra, W., Silva-Caldeira, P. P., Terenzi, H., & Pereira-Maia, E. C. (2016). Impact of Metal Coordination on the Antibiotic and Non-Antibiotic Activities of Tetracycline-Based Drugs. *Coordination Chemistry Reviews*, **327–328**: 188–199. DOI: 10.1016/j.ccr.2016.04.009
- Gupta, R., Luxami, V., & Paul, K. (2021). Insights of 8-hydroxyquinolines: A Novel Target in Medicinal Chemistry. *Bioorganic Chemistry*, **108**:104633. DOI: 10.1016/j.bioorg.2021.104633
- Hammouti, B., Dafali, A., Touzani, R., & Bouachrine, M. (2012). Inhibition of Copper Corrosion by Bipyrazole Compound in Aerated 3% NaCl. *Journal of Saudi Chemical Society*, **16**(4): 413–418. DOI: 10.1016/j.jscs.2011.02.009
- Harinath, Y., Kumar, D. H., Kumar, B. N., Apparao, C., & Seshaiyah, K. (2013). Synthesis, Spectral Characterization and Antioxidant Activity Studies of a Bidentate Schiff Base, 5-Methyl Thiophene-2-Carboxaldehyde-Carbohydrazone and its Cd(II), Cu(II), Ni(II) and Zn(II) Complexes. *Spectrochimica Acta Part A: Molecular and Biomolecular Spectroscopy*, **101**: 264–272. DOI: 10.1016/j.saa.2012.09.085
- Hazra, M., Dolai, T., Giri, S., Patra, A., & Dey, S. K. (2017). Synthesis of Biologically Active Cadmium (II) Complex with Tridentate N₂O Donor Schiff Base: DFT Study, Binding Mechanism of Serum Albumins (Bovine, Human) and Fluorescent Nanowires. *Journal of Saudi Chemical Society*, **21**: S445–S456. DOI: 10.1016/j.jscs.2014.10.007

- Hein, C. D., Liu, X. M., & Wang, D. (2008). Click Chemistry, A Powerful Tool for Pharmaceutical Sciences. *Pharmaceutical Research*, **25**(10): 2216–2230. DOI: 10.1007/s11095-008-9616-1
- Hernandez, W., Paz, J., Carrasco, F., Vaisberg, A., Spodine, E., Manzur, J. Beyer, L. (2013). Synthesis and Characterization of New Palladium(II) Thiosemicarbazone Complexes and Their Cytotoxic Activity against Various Human Tumor Cell Lines. *Bioinorganic Chemistry and Applications*, 2013: 1-12. DOI: 10.1155/2013/524701
- Huma, R., Mahmud, T., Awan, S. J., Ashraf, M., Khan, S. U., Rasheed, H., Hasany, S. M., & Yousaf, A. (2022). Thermal and Spectroscopic Studies of Some Metal Complexes with a New Enaminone Ligand 3-Chloro-4-((4-methoxyphenyl) amino) pent-3-en-2-one) and their Investigation as Anti-Urease and Cytotoxic Potential Drugs. *Arabian Journal of Chemistry*, **15**(3): 103640. DOI: 10.1016/j.arabjc.2021.103640
- Hu, S., Shima, T., Luo, Y., & Hou, Z. (2013). Tetranuclear Zirconium and Hafnium Polyhydride Complexes Composed of the “CpMH₂” Units. *Organometallics*, **32**(7): 2145–2151. DOI: 10.1021/om400012a
- Hu, T., Jia, Q., He, S., Shan, S., Su, H., Zhi, Y., & He, L. (2017). Novel Functionalized Metal-Organic Framework MIL-101 Adsorbent for Capturing Oxytetracycline. *Journal of Alloys and Compounds*, **727**: 114–122. DOI: 10.1016/j.jallcom.2017.08.116
- Hussein, M. A., Guan, T. S., Haque, R. A., Ahamed, M. B. K., & Abdul Majid, A. M. S. (2015). Mononuclear dioxomolybdenum (VI) Thiosemicarbazonato Complexes: Synthesis, Characterization, Structural Illustration, In Vitro DNA Binding, Cleavage, and Antitumor Properties. *Spectrochimica Acta Part A: Molecular and Biomolecular Spectroscopy*, **136**: 1335–1348. DOI: 10.1016/j.saa.2014.10.021
- Huynh, H. V., Han, Y., Jothibas, R., & Yang, J. A. (2009). ¹³C-NMR Spectroscopic Determination of Ligand Donor Strengths using N-Heterocyclic Carbene Complexes of Palladium (II). *Organometallics*, **28**(18): 5395–5404. DOI: 10.1021/om900667d

- Huynh, H. V., Van, D. Le, Hahn, F. E., & Hor, T. S. A. (2004). Synthesis and Structural Characterization of Mixed Carbene-carboxylate Complexes of Palladium (II). *Journal of Organometallic Chemistry*, **689**(10): 1766–1770. DOI: 10.1016/j.jorganchem.2004.02.033
- Jacobsen, S. M., & Shirtliff, M. E. (2011). *Proteus mirabilis* Biofilms and Catheter-Associated Urinary Tract Infections. *Virulence*, **2**(5): 460–465. DOI: 10.4161/viru.2.5.17783
- Kalinowska, M., Piekut, J., Bruss, A., Follet, C., Sienkiewicz-Gromiuk, J., Świsłocka, R., Rzaczyńska, Z., & Lewandowski, W. (2014). Spectroscopic (FT-IR, FT-Raman, ^1H , ^{13}C -NMR, UV/VIS), Thermogravimetric and Antimicrobial Studies of Ca(II), Mn(II), Cu(II), Zn(II) and Cd(II) Complexes of Ferulic Acid. *Spectrochimica Acta Part A: Molecular and Biomolecular Spectroscopy*, **122**: 631–638. DOI: 10.1016/j.saa.2013.11.089
- Kargar, H., Kaka-Naeini, A., Fallah-Mehrjardi, M., Behjatmanesh-Ardakani, R., Amiri Rudbari, H., & Munawar, K. S. (2021). Oxovanadium and Dioxomolybdenum Complexes: Synthesis, Crystal Structure, Spectroscopic Characterization and Applications as Homogeneous Catalysts in Sulfoxidation. *Journal of Coordination Chemistry*, **74**: 1563–1583. DOI: 10.1080/00958972.2021.1915488
- Kavitha, P., & Reddy, K. L. (2016). Pd (II) Complexes Bearing Chromone Based Schiff Bases: Synthesis, Characterisation and Biological Activity Studies. *Arabian Journal of Chemistry*, **9**: 640–648. DOI: 10.1016/j.arabjc.2013.06.018
- Khalil, M. M. H. & Al-Seif, F. A. (2008). Molybdenum and Tungsten Tricarbonyl Complexes of Isatin with Triphenylphosphine. *Research Letters in Inorganic Chemistry*, **2008**: 1-4. DOI: 10.1155/2008/746058
- Khalil, M. M. H., & Al-Seif, F. A. (2010). Group 6 Metal Carbonyl Complexes of 3'H-Spiro[indole-3,2'-[1,3]Benzothiazole-2(1H)]-one. *Journal of Saudi Chemical Society*, **14**(1): 33–39. DOI: 10.1016/j.jscs.2009.12.006
- Khan, H., Badshah, A., Said, M., Murtaza, G., Ahmad, J., Jean-claude, B. J., & Butler, I. S. (2013). Anticancer Metallopharmaceutical Agents Based on Mixed-Ligand Palladium(II) Complexes with Dithiocarbamates and Tertiary

Organophosphine Ligands. *Applied Organometallic Chemistry*, **27**(7): 387–395.
DOI: 10.1002/aoc.2991

- Khanderi, J., Davaasuren, B., & Rothenberger, A. (2016). Synthesis and Characterization of Cadmium(II), Lead(II), and Indium(III) Ketoacidoximate Complexes and their Conversion to Metal Oxides. *Chemistry Select*, **1**(9): 1897–1903. DOI: 10.1002/slct.201600513
- Khedr, A. M., Gaber, M., & Diab, H. A. (2012). Synthesis, Characterization, Molecular Modeling, and Thermal Analyses of Bioactive Co(II) and Cu(II) Complexes with Diacetylmonoxime and Different Amines. *Journal of Coordination Chemistry*, **65**(10): 1672–1684. DOI: 10.1080/00958972.2012.678338
- Khedr, A. M., Jadon, S., & Kumar, V. (2011). Synthesis, Spectral Analysis, and Molecular Modeling of Bioactive Sn(II)-Complexes with Oxadiazole Schiff Bases. *Journal of Coordination Chemistry*, **64**(8): 1351–1359. DOI: 10.1080/00958972.2011.569541
- Kose, D. A., ozturk, B., Şahin, O., & Buyukgungor, O. (2014). Mixed Ligand Complexes of Coumarilic Acid/Nicotinamide with Transition Metal Complexes: Synthesis and Structural Investigation. *Journal of Thermal Analysis and Calorimetry*, **115**(2): 1515–1524. DOI: 10.1007/s10973-013-3415-6
- Koyun, O., Gorduk, S., Arvas, M. B., & Sahin, Y. (2017). Direct, One-Step Synthesis of Molybdenum Blue using an Electrochemical Method, and Characterization Studies. *Synthetic Metals*, **233**: 111–118. DOI: 10.1016/j.synthmet.2017.09.009
- Kumar, A., Borthakur, R., Koch, A., Chanu, O. B., Choudhury, S., Lemtur, A., & Lal, R. A. (2011). Synthesis and Characterization of Heterobimetallic Molybdenum and Nickel Complexes Derived from Polyfunctional Disalicylaldehyde Oxaloyldihydrazone. *Journal of Molecular Structure*, **999**(1-3): 89–97. DOI: 10.1016/j.molstruc.2011.05.041
- Kumar, D., Chadda, S., Sharma, J., & Surain, P. (2013). Syntheses, Spectral Characterization, and Antimicrobial Studies on the Coordination Compounds of Metal Ions with Schiff Base Containing both Aliphatic and Aromatic Hydrazone Moieties. *Bioinorganic Chemistry and Applications*, **2003**: 1-10. DOI: 10.1155/2013/981764

- Kumari, L., Du, G. H., Li, W. Z., Vennila, R. S., Saxena, S. K., & Wang, D. Z. (2009). Synthesis, Microstructure and Optical Characterization of Zirconium Oxide Nanostructures. *Ceramics International*, **35**(6): 2401–2408. DOI: 10.1016/j.ceramint.2009.02.007
- Kuriakose, D., Aravindakshan, A. A., & Kurup, M. R. P. (2017). Synthesis, Spectroscopic, Crystal Structures and Photoluminescence Studies of Cadmium(II) Complexes Derived from di-2-Pyridyl Ketone Benzoylhydrazone: Crystal Structure of a Rare Eight Coordinate Cadmium(II) Complex. *Polyhedron*, **127**: 84–96. DOI: 10.1016/j.poly.2017.01.041
- Leal, J. F., Santos, E. B. H., & Esteves, V. I. (2018). Oxytetracycline in Intensive Aquaculture: Water Quality During and After its Administration, Environmental Fate, Toxicity and Bacterial Resistance. *Reviews in Aquaculture*, **11**(4): 1176–1194. DOI: 10.1111/raq.12286
- Liu, X., Vonk, D., Jiang, H., Kisslinger, K., Tong, X., Ge, M., Nazaretski, E., Ravel, B., Foster, K., Petrash, S., & Chen-Wiegart, Y. C. K. (2019). Environmentally Friendly Zr-based Conversion Nanocoatings for Corrosion Inhibition of Metal Surfaces Evaluated by Multimodal X-ray Analysis. *ACS Applied Nano Materials*, **2**(4): 1920–1929. DOI: 10.1021/acsanm.8b02309
- Mahapatra, B. B., Chaulia, S., Sarangi, A. K., Dehury, S., & Panda, J. (2015). Synthesis, Characterisation, Spectral, Thermal, XRD, Molecular Modelling and Potential Antibacterial Study of Metal Complexes Containing Octadentate Azodye Ligands. *Journal of Molecular Structure*, **1087**: 11–25. DOI: 10.1016/j.molstruc.2015.01.030
- Mahapatra, B. B., Mishra, R. R., & Sarangi, A. K. (2013). Synthesis, Characterisation, XRD, Molecular Modelling and Potential Antibacterial Studies of Co(II), Ni(II), Cu(II), Zn(II), Cd(II) and Hg(II) Complexes with Bidentate Azodye Ligand. *Journal of Saudi Chemical Society*, **2013**: 1-9. DOI: 10.1016/j.jscs.2013.07.002
- Mahmoud, M. A., Ammar, A. A., & Sallam, S. A. (2017). Synthesis, Characterization and Toxicity of Cu(II) Complexes with Metformin Schiff-Bases. *Journal of the Chinese Advanced Materials Society*, **5**(2): 79–102. DOI: 10.1080/22243682.2017.1296370

- Mahmoud, W. H., Mahmoud, N. F., Mohamed, G. G., El-sonbati, A. Z., & El-bindary, A. A. (2015). Synthesis, Spectroscopic, Thermogravimetric and Antimicrobial Studies of Mixed Ligands Complexes. *Journal of Molecular Structure*, **1095**: 15–25. DOI: 10.1016/j.molstruc.2015.04.004
- Mahmoud, W. H., Mohamed, G. G., & El-dessouky, M. M. I. (2013). Coordination Modes of Bidentate Lornoxicam Drug with Some Transition Metal Ions. Synthesis, Characterization and In Vitro Antimicrobial and Antitumor Cancer Activity Studies. *Spectrochimica Acta Part A: Molecular and Biomolecular Spectroscopy*, **122**: 598–608. DOI: 10.1016/j.saa.2013.11.069
- Majumder, I., Chakraborty, P., Álvarez, R., Gonzalez-Diaz, M., Peláez, R., Ellahioui, Y., Bauza, A., Frontera, A., Zangrando, E., Gómez-Ruiz, S., & Das, D. (2018). Bioactive Heterometallic Cu^{II} - Zn^{II} Complexes with Potential Biomedical Applications. *ACS Omega*, **3**(10): 13343–13353. DOI: 10.1021/acsomega.8b01260
- Mandal, M., List, M., Teasdale, I., Chakraborty, D., & Monkowius, U. (2017). Palladium Complexes Containing Imino Phenoxide Ligands: Synthesis, Luminescence, and their use as Catalysts for the Ring-Opening Polymerization of Rac-Lactide. *Monatshefte für Chemie Chemical Monthly*, 1–8. DOI: 10.1007/s00706-017-2119-1
- Markley, J. L., & Wencewicz, T. A. (2018). Tetracycline-Inactivating Enzymes. *Frontiers in Microbiology*, **9**: 1–22. DOI: 10.3389/fmicb.2018.01058
- Maurya, R. C., Bohre, P., Sahu, S., Martin, M. H., Sharma, A. K., & Vishwakarma, P. (2011). Oxoperoxomolybdenum (VI) Complexes of Catalytic and Biomedical Relevance: Synthesis, Characterization, Antibacterial Activity and 3D-Molecular Modeling of Some Oxoperoxomolybdenum (VI) Chelates in Mixed (O,O) Coordination Environment Involving. *Arabian Journal of Chemistry*, **9**: 1878–5352. DOI: 10.1016/j.arabjc.2011.02.027
- Medici, S., Peana, M., Nurchi, V. M., Lachowicz, J. I., Crisponi, G., & Zoroddu, M. A. (2015). Noble Metals in Medicine: Latest Advances. *Coordination Chemistry Reviews*, **284**: 329–350. DOI: 10.1016/j.ccr.2014.08.002

- Merian, E. (1990). Environmental Chemistry and Biological Effects of Cadmium Compounds. *Toxicological & Environmental Chemistry*, **26**(1–4): 27–44. DOI: 10.1080/02772249009357530
- Mewis, R. E., & Archibald, S. J. (2010). Biomedical Applications of Macrocyclic Ligand Complexes. *Coordination Chemistry Reviews*, **254**(15-16): 1686–1712. DOI: 10.1016/j.ccr.2010.02.025
- Mirica, L. M., & Khusnutdinova, J. R. (2013). Structure and Electronic Properties of Pd(III) Complexes. *Coordination Chemistry Reviews*, **257**(2): 299–314. DOI: 10.1016/j.ccr.2012.04.030
- Mohammadikish, M., Masteri-farahani, M., & Mahdavi, S. (2014). Immobilized Molybdenum–Thiosemicarbazide Schiff Base Complex on the Surface of Magnetite Nanoparticles as a New Nanocatalyst for the Epoxidation of Olefins. *Journal of Magnetism and Magnetic Materials*, **354**: 317–323. DOI: 10.1016/j.jmmm.2013.11.013
- Montazerzohori, M., Zahedi, S., Naghiha, A., & Zohour, M. M. (2014). Synthesis, Characterization and Thermal Behavior of Antibacterial and Antifungal Active Zinc Complexes of Bis (3(4-Dimethylaminophenyl)-Allylidene-1, 2-Diaminoethane). *Materials Science & Engineering: C*, **35**: 195–204. DOI: 10.1016/j.msec.2013.10.030
- Moradi-shoeili, Z., Boghaei, D. M., Amini, M., Bagherzadeh, M., & Notash, B. (2013). New Molybdenum (VI) Complex with ONS-Donor Thiosemicarbazone Ligand: Preparation, Structural Characterization, and Catalytic Applications in Olefin Epoxidation. *Inorganic Chemistry Communications*, **27**: 26–30. DOI: 10.1016/j.inoche.2012.10.016
- Mousavi, S. A., & Mojahedi, S. (2020). Some Novel Hexa-Coordinated Cadmium Schiff Base Complexes: X-Ray Structure, Hirshfeld Surface Analysis, Antimicrobial and Thermal Analysis. *Applied Organometallic Chemistry*, 1–13. DOI: 10.1002/aoc.5550
- Musa, T. M., Al-jibouri, M. N., & Al-bayati, R. I. H. (2018). Synthesis, Characterization and Antimicrobial Study of Nickel(II), Palladium(II), Platinum (II), Rhodium(III), Cadmium(II) and Zirconium(IV) Complexes with (E)-1-(Benzo[D]Thiazol-2-Yl)-4-(Hydroxy(2-Hydroxyphenyl)Methylene)-3-Methyl-

- 1H-Pyrazol-5(4H)-one. *Journal of Physics: Conference Series*, **1032**: 1–14. DOI: 10.1088/1742-6596/1032/1/012057
- Nag, P., & Sharma, D. (2019). Synthesis, Characterization and Anticandidal Activity of Dioxomolybdenum(VI) Complexes of the Type $[\text{MoO}_2\{\text{ON}=\text{C}(\text{CH}_3)\text{Ar}\}_2]$. *Heliyon*, **5**(5): 1–5. DOI: 10.1016/j.heliyon.2019.e01729
- Nagalakshmi, V., Sathya, M., Premkumar, M., Kaleeswaran, D., Venkatachalam, G., & Balasubramani, K. (2020). Palladium (II) Complexes Comprising Naphthylamine and Biphenylamine Based Schiff Base Ligands: Synthesis, Structure and Catalytic Activity in Suzuki Coupling Reactions. *Journal of Organometallic Chemistry*, **914**: 1–23. DOI: 10.1016/j.jorganchem.2020.121220
- Naglah, A. M., Al-Omar, M. A., Almehezia, A. A., AlKahtani, H. M., Bhat, M. A., Al-Shakliah, N. S., Belgacem, K., Majrashi, B. M., Refat, M. S., & Adam, A. M. A. (2021). Synthesis, Thermogravimetric, and Spectroscopic Characterizations of Three Palladium Metal(II) Ofloxacin Drug and Amino Acids Mixed Ligand Complexes as Advanced Antimicrobial Materials. *Journal of Molecular Structure*, **1225**: 1–10. DOI: 10.1016/j.molstruc.2020.129102
- Nair, M., Nair, L. H., & Thankamani, D. (2011). Synthesis and Characterization of Oxomolybdenum (V) and Dioxomolybdenum (VI) Complexes Derived from N-(2-Hydroxy-3-Methoxybenzylidene) Isonicotinohydrazide. *Journal of the Serbian Chemical Society*, **76**(2): 221–233. DOI: 10.2298/JSC100208009N
- Nakata, N., Nakamura, K., Nagaoka, S., & Ishii, A. (2019). Carbazolyl-Substituted [OSSO]-type Zirconium(IV) Complex as a Precatalyst for the Oligomerization and Polymerization of α -Olefins. *Catalysts*, **9**(528): 1–9. DOI: 10.3390/catal9060528
- Nandanwar, S. K., & Kim, H. J. (2019). Anticancer and Antibacterial Activity of Transition Metal Complexes. *Chemistry Select*, **4**(5): 1706–1721. DOI: 10.1002/slct.201803073
- Nassar, M. Y., Attia, A. S., Alfallous, K. A., & El-Shahat, M. F. (2013). Synthesis of Two Novel Dinuclear Molybdenum (0) Complexes of Quinoxaline-2, 3-Dione: New Precursors for Preparation of α - MoO_3 Nanoplates. *Inorganica Chimica Acta*, **405**: 362–367. DOI: 10.1016/j.ica.2013.06.030

- Nath, B. D., Takaishi, K., & Ema, T. (2020). Macrocyclic Multinuclear Metal Complexes Acting as Catalysts for Organic Synthesis. *Catalysis Science and Technology*, **10**(1): 12–34. DOI: 10.1039/c9cy01894h
- Niazi, J. H., Lee, S. J., Kim, Y. S., & Gu, M. B. (2008). ssDNA Aptamers that Selectively Bind Oxytetracycline. *Bioorganic and Medicinal Chemistry*, **16**(3): 1254–1261. DOI: 10.1016/j.bmc.2007.10.073
- Oien, S., Wragg, D., Reinsch, H., Svelle, S., Bordiga, S., Lamberti, C., & Lillerud, K. P. (2014). Detailed Structure Analysis of Atomic Positions and Defects in Zirconium Metal-Organic Frameworks. *Crystal Growth and Design*, **14**(11): 5370–5372. DOI: 10.1021/cg501386j
- Okasha, R. M., Al Shaikh, N. E., Aljohani, F. S., Naqvi, A., & Ismail, E. H. (2019). Design of Novel Oligomeric Mixed Ligand Complexes: Preparation, Biological Applications and the First Example of their Nanosized Scale. *International Journal of Molecular Sciences*, **20**(3): 1-21. DOI: 10.3390/ijms20030743
- Omar, M. M., Abd El-Halim, H. F., & Khalil, E. A. M. (2017). Synthesis, Characterization, Biological and Anticancer Studies of Mixed Ligand Complexes with Schiff Base and 2, 2'-Bipyridine. *Applied Organometallic Chemistry*, **31**(10): 1–11. DOI: 10.1002/aoc.3724
- Pal, T. K., Alam, M. A., Hossen, J., Paul, S., Ahmad, H., & Sheikh, M. C. (2018). Spectral and Biological Studies on New Mixed Ligand Complexes. *Journal of Scientific Research*, **10**(3): 291-302. DOI: 10.3329/jsr.v10i3.36379
- Pal, T. K., Alam, M. A., Paul, S., & Sheikh, M. C. (2019). Spectral, Magnetic, Thermal, Antioxidant and Biological Studies on New Mixed Ligand Complexes. *Journal of King Saud University-Science*, **31**(4): 445–451. DOI: 10.1016/j.jksus.2017.12.010
- Pan, L., Heddy, R., Li, J., Zheng, C., Huang, X. Y., Tang, X., & Kilpatrick, L. (2008). Synthesis and Structural Determination of a Hexanuclear Zirconium Glycine Compound Formed in Aqueous Solution. *Inorganic Chemistry*, **47**(13): 5537–5539. DOI: 10.1021/ic800292e
- Pang, Z., Raudonis, R., Glick, B. R., Lin, T. J., & Cheng, Z. (2019). Antibiotic Resistance in *Pseudomonas aeruginosa*: Mechanisms and Alternative

- Therapeutic Strategies. *Biotechnology Advances*, **37**(1): 177–192. DOI: 10.1016/j.biotechadv.2018.11.013
- Pasayat, S., Dash, S. P., Saswati, Majhi, P. K., Patil, Y. P., Nethaji, M., Dash, H. R., Das, S., & Dinda, R. (2012). Mixed-Ligand Aroylhydrazone Complexes of Molybdenum: Synthesis, Structure and Biological Activity. *Polyhedron*, **38**(1): 198–204. DOI: 10.1016/j.poly.2012.03.007
- Pavia D. L., Lampman G. M., Kriz. G. S. & Vyvyan J. R. (2013). Introduction-to-Spectroscopy, 5th edition, 1–680. ISBN-13: 978-1-285-46012-3
- Pladzyk, A., Baranowska, K., Gudat, D., Godlewska, S., Wiczerzak, M., Chojnacki, J., Bulman, M., Januszewicz, K., & Dołęga, A. (2011). Mixed-Ligand Complexes of Zinc(II), Cobalt(II) and Cadmium(II) with Sulfur, Nitrogen and Oxygen Ligands. Analysis of the Solid State Structure and Solution Behavior. Implications for Metal Ion Substitution in Alcohol Dehydrogenase. *Polyhedron*, **30**(6): 1191–1200. DOI: 10.1016/j.poly.2011.01.026
- Pontrelli, S., Chiu, T. Y., Lan, E. I., Chen, F. Y. H., Chang, P., & Liao, J. C. (2018). *Escherichia coli* as a Host for Metabolic Engineering. *Metabolic Engineering*, **50**: 16–46. DOI: 10.1016/j.ymben.2018.04.008
- Prabhu, S. M., & Meenakshi, S. (2015). Novel One-Pot Synthesis of Dicarboxylic Acids Mediated Alginate– Zirconium Biopolymeric Complex for Defluoridation of Water. *Carbohydrate Polymers*, **120**: 60–68. DOI: 10.1016/j.carbpol.2014.11.058
- Prakasam, B. A., Lahtinen, M., Peuronen, A., Muruganandham, M., Kolehmainen, E., Haapaniemi, E., & Sillanpaa, M. (2016). Synthesis, NMR Spectral and Structural Studies on Mixed Ligand Complexes of Pd(II) Dithiocarbamates: First Structural Report on Palladium(II) Dithiocarbamate with SCN-Ligand. *Journal of Molecular Structure*, **1108**: 195–202. DOI: 10.1016/j.molstruc.2015.11.076
- Pulicharla, R., Hegde, K., Brar, S. K., & Surampalli, R. Y. (2017). Tetracyclines Metal Complexation: Significance and Fate of Mutual Existence in the Environment. *Environmental Pollution*, **221**: 1–14. DOI: 10.1016/j.envpol.2016.12.017

- Pullen, S., & Clever, G. H. (2018). Mixed-Ligand Metal-Organic Frameworks and Heteroleptic Coordination Cages as Multifunctional Scaffolds- A Comparison. *Accounts of Chemical Research*, **51**: 3052–3064. DOI: 10.1021/acs.accounts.8b00415
- Ramadan, R. M., Abdel-rahman, L. H., Ismael, M., Youssef, T. A., & Ali, S. A. (2013). Synthesis and Spectroscopic Studies of Some Chromium and Molybdenum Derivatives of bis-(Acetylaceton) Ethylenediimine Ligand. *Journal of Molecular Structure*, **1049**: 7–12. DOI: 10.1016/j.molstruc.2013.06.024
- Ramotowska, S., Wysocka, M., Brzeski, J., Chylewska, A., & Makowski, M. (2020). A Comprehensive Approach to the Analysis of Antibiotic-Metal Complexes. *Trends in Analytical Chemistry*, **123**: 1-9. DOI: 10.1016/j.trac.2019.115771
- Rao, T. N., Hussain, I., Lee, J. E., Kumar, A., & Koo, B. H. (2019). Enhanced Thermal Properties of Zirconia Nanoparticles and Chitosan-Based Intumescent Flame Retardant Coatings. *Applied Sciences*, **9**(17): 1-15. DOI: 10.3390/app9173464
- Razmara, Z., Saheli, S., Eigner, V., & Dusek, M. (2019). Synthesis, Crystal Structure and Magnetic Properties of a New Tri-nuclear Iron (II, III) Complex, a Precursor for the Preparation of Superparamagnetic Fe₃O₄ Nanoparticles Applicable in the Removal of Cd²⁺. *Applied Organometallic Chemistry*, **33**(5): 1–13. DOI: 10.1002/aoc.4880
- Refat, M. S., Al-Maydama, H. M. A., Al-Azab, F. M., Amin, R. R., & Jamil, Y. M. S. (2014). Synthesis, Thermal and Spectroscopic Behaviors of Metal-Drug Complexes: La(III), Ce(III), Sm(III) and Y(III) Amoxicillin Trihydrate Antibiotic Drug Complexes. *Spectrochimica Acta-Part A: Molecular and Biomolecular Spectroscopy*, **128**: 427–446. DOI: 10.1016/j.saa.2014.02.160
- Rijt, S. H. V., & Sadler, P. J. (2009). Current Applications and Future Potential for Bioinorganic Chemistry in the Development of Anticancer Drugs. *Drug Discovery Today*, **14**(23-24): 1089–1097. DOI: 10.1016/j.drudis.2009.09.003
- Rolain, J. M., Abat, C., Jimeno, M. T., Fournier, P. E., & Raoult, D. (2016). Do we Need New Antibiotics? *Clinical Microbiology and Infection*, **22**(5):408–415. DOI: 10.1016/j.cmi.2016.03.012

- Rubino, S., Busa, R., Attanzio, A., Alduina, R., Di Stefano, V., Girasolo, M. A., Orecchio, S., & Tesoriere, L. (2017). Synthesis, Properties, Antitumor and Antibacterial Activity of New Pt(II) and Pd(II) Complexes with 2,2'-Dithiobis(benzothiazole) Ligand. *Bioorganic and Medicinal Chemistry*, **25**(8): 2378–2386. DOI: 10.1016/j.bmc.2017.02.067
- Saghatforoush, L. A., Aminkhani, A., Ershad, S., Karimnezhad, G., Ghammamy, S., & Kabiri, R. (2008). Preparation of Zinc (II) and Cadmium (II) Complexes of the Tetradentate Schiff Base Ligand 2-((E)-(2-(2-(pyridine-2-yl)ethylthio)ethylimino) methyl)-4- bromophenol (PytBrsalh). *Molecules*, **13**(4): 804–811. DOI: 10.3390/molecules13040804
- Santos, A. F., Brotto, D. F., Favarin, L. R. V., Cabeza, N. A., Andrade, G. R., Batistote, M., Cavalheiro, A. A., Neves, A., Rodrigues, D. C. M., & dos Anjos, A. (2014). Study of the Antimicrobial Activity of Metal Complexes and their Ligands Through Bioassays Applied to Plant Extracts. *Revista Brasileira de Farmacognosia*, **24**(3): 309–315. DOI: 10.1016/j.bjp.2014.07.008
- Selvam, N. C. S., Manikandan, A., Kennedy, L. J., & Vijaya, J. J. (2013). Comparative Investigation of Zirconium Oxide (ZrO₂) Nano and Microstructures for Structural, Optical and Photocatalytic Properties. *Journal of Colloid and Interface Science*, **389**(1): 91–98. DOI: 10.1016/j.jcis.2012.09.014
- Shaban, N. S., Abdou, K. A., & Hassan, N. E. Y. (2016). Impact of Toxic Heavy Metals and Pesticide Residues in Herbal Products. *Beni-Suef University Journal of Basic and Applied Sciences*, **5**(1): 102–106. DOI: 10.1016/j.bjbas.2015.10.001
- Shaikh, S., Fatima, J., Shakil, S., Rizvi, S. M. D., & Kamal, M. A. (2015). Antibiotic Resistance and Extended Spectrum Beta-Lactamases: Types, Epidemiology and Treatment. *Saudi Journal of Biological Sciences*, **22**(1): 90–101. DOI: 10.1016/j.sjbs.2014.08.002
- Shakdofa, M. M. E., Mousa, H. A., Elseidy, A. M. A., Labib, A. A., Ali, M. M., & Abd-El-All, A. S. (2017). Anti-Proliferative Activity of Newly Synthesized Cd (II), Cu(II), Zn(II), Ni(II), Co(II), Vo(II), and Mn(II) Complexes of 2-((4,9-dimethoxy-5-oxo-5H-furo[3,2-G]chromen-6-yl)methylene)hydrazine carbothio

- amide on three Human Cancer Cells. *Applied Organometallic Chemistry*, **32**(1): 1–12. DOI: 10.1002/aoc.3936
- Shaker, S. A., Khaledi, H., Cheah, S. C., & Ali, H. M. (2016). New Mn(II), Ni(II), Cd(II), Pb(II) Complexes with 2-Methylbenzimidazole and other Ligands. Synthesis, Spectroscopic Characterization, Crystal Structure, Magnetic Susceptibility and Biological Activity Studies. *Arabian Journal of Chemistry*, **9**: S1943–S1950. DOI: 10.1016/j.arabjc.2012.06.013
- Shakir, M., Hanif, S., Asif, M., Mohammad, O., & Al-resayes, S. I. (2015). Pharmacologically Significant Complexes of Mn(II), Co(II), Ni(II), Cu(II) and Zn(II) of Novel Schiff Base Ligand, (E)-N-(Furan-2-yl methylene) quinolin-8-amine: Synthesis, Spectral, XRD, SEM, Antimicrobial, Antioxidant and In Vitro Cytotoxic Studies. *Journal of Molecular Structure*, **1092**: 143–159. DOI: 10.1016/j.molstruc.2015.03.012
- Sharma, K., Singh, R. V., & Fahmi, N. (2011). Palladium(II) and Platinum(II) Derivatives of Benzothiazoline Ligands: Synthesis, Characterization, Antimicrobial and Antispermatic Activity. *Spectrochimica Acta-Part A: Molecular and Biomolecular Spectroscopy*, **78**(1): 80–87. DOI: 10.1016/j.saa.2010.08.076
- Sharma, N. K., Ameta, R. K., & Singh, M. (2016). From Synthesis to Biological Impact of Pd(II) Complexes: Synthesis, Characterization, and Antimicrobial and Scavenging Activity. *Biochemistry Research International*, 1-8. DOI: 10.1155/2016/4359375
- Sharma, R. K., & Sharma, C. (2011). Zirconium (IV)-Modified Silica Gel: Preparation, Characterization and Catalytic Activity in the Synthesis of Some Biologically Important Molecules. *Catalysis Communications*, **12**: 327–331. DOI: 10.1016/j.catcom.2010.10.011
- Shobana, S., Subramaniam, P., Mitu, L., Dharmaraja, J., & Arvind Narayan, S. (2015). Synthesis, Structural Elucidation, Biological, Antioxidant and Nuclease Activities of Some 5-Fluorouracil-amino acid Mixed Ligand Complexes. *Spectrochimica Acta-Part A: Molecular and Biomolecular Spectroscopy*, **134**: 333–344. DOI: 10.1016/j.saa.2014.06.093

- Shoukry, A. A., & Al-Mhayawi, S. R. (2013). Synthesis, Characterization, Biological Activity and Equilibrium Studies of Cadmium(II) with 2, 6-diaminopyridine and Various Bio-Relevant Ligands. *European Journal of Chemistry*, **4**(3): 260–267. DOI: 10.5155/eurjchem.4.3.260-267.800
- Siddappa, K., Mane, S. B., & Manikprabhu, D. (2014). Spectral Characterization and 3D Molecular Modeling Studies of Metal Complexes Involving the O, N-Donor Environment of Quinazoline-4 (3H)-one Schiff Base and Their Biological Studies. *The Scientific World Journal*, **2014**: 1-13. DOI: 10.1155/2014/817365
- Singh, A. K., & Nakate, U. T. (2014). Microwave Synthesis, Characterization, and Photoluminescence Properties of Nanocrystalline Zirconia. *The Scientific World Journal*, **2014**: 1–7. DOI: 10.1155/2014/349457
- Singh, H. L. (2011). Synthesis, Spectroscopic Characterization, and 3D Molecular Modeling of Lead(II) Complexes of Unsymmetrical Tetradentate Schiff-Base Ligands. *Research on Chemical Intermediates*, **37**(8): 1087–1101. DOI: 10.1007/s11164-011-0319-6
- Singh, H. L., & Singh, J. (2013). Synthesis of New Zirconium (IV) Complexes with Amino Acid Schiff Bases: Spectral, Molecular Modeling, and Fluorescence Studies. *International Journal of Inorganic Chemistry*, **2013**: 1-10. DOI: 10.1155/2013/847071
- Singh, M. K., Sutradhar, S., Paul, B., Adhikari, S., Laskar, F., Butcher, R. J., Acharya, S., & Das, A. (2017). A New Cadmium (II) Complex with Bridging Dithiolate Ligand: Synthesis, Crystal Structure and Antifungal Activity Study. *Journal of Molecular Structure*, **1139**: 395–399. DOI: 10.1016/j.molstruc.2017.03.073
- Sliznev, V. V., & Belova, N. V. (2016). Geometrical and Electronic Structure of the Molybdenum and Tungsten Halides MX_3 and MX_4 (M= Mo, W ; X= F, Cl): Jahn-Teller Effect and Spin-Orbit Coupling. *Journal of Molecular Structure*, **4**: 1–15. DOI: 10.1016/j.molstruc.2016.08.017
- Smith, M. B., & Slawin, A. M. Z. (2000). Synthesis and Characterization of E, O-Mixed Donor (E =P, S Or Se) Ligand Complexes of Palladium(II) and Platinum (II). *Inorganica Chimica Acta*, **299**(2): 172–179. DOI: 10.1016/S0020-1693(99)00493-4

- Smrecki, N., Popovi, Z., & Jazwinski, J. (2016). Preparation and NMR Spectroscopic Study of Palladium (II) Complexes with N-arylalkyliminodiacetamide Derivatives. *Journal of Molecular Structure*, **1122**: 192–197. DOI: 10.1016/j.molstruc.2016.05.084
- Sobhani, S., & Zarifi, F. (2015). Pd- Isatin Schiff Base Complex Immobilized on Γ - Fe_2O_3 as a Magnetically Recyclable Catalyst for the Heck and Suzuki Cross-Coupling Reactions. *Chinese Journal of Catalysis*, **36**(4): 555–563. DOI: 10.1016/S1872-2067(14)60291-6
- Soliman, A. A., Alajrawy, O. I., Attabi, F. A., Shaaban, M. R., & Linert, W. (2016). New Formamidine Ligands and their Mixed Ligand Palladium (II) Oxalate Complexes: Synthesis, Characterization, DFT Calculations and In Vitro Cytotoxicity. *Spectrochimica Acta-Part A: Molecular and Biomolecular Spectroscopy*, **152**: 358–369. DOI: 10.1016/j.saa.2015.07.076
- Soliman, A. A., Ali, S. A., Marei, A. H., & Nassar, D. H. (2012). Synthesis, Characterization and Biological Activities of Some New Chromium, Molybdenum and Tungsten Complexes with 2, 6-Diaminopyridine. *Spectrochimica Acta - Part A: Molecular and Biomolecular Spectroscopy*, **89**: 329–332. DOI: 10.1016/j.saa.2011.12.061
- Steinhuebel, D. P., Fuhrmann, P., & Lippard, S. J. (1998). Synthesis, Characterization, and Reactivity of Organometallic Zr(IV) Carboxylate Complexes. *Inorganica Chimica Acta*, **270**: 527–536. DOI: 10.1016/S0020-1693(97)06117-3
- Stojković, D. L., Jevtić, V. V., Vuković, N., Vukić, M., Čanović, P., Zarić, M. M., Mišić, M. M., Radovanović, D. M., Baskić, D., Trifunović S. R. (2018). Synthesis, Characterization, Antimicrobial and Antitumor Reactivity of New Palladium (II) Complexes with Methionine and Tryptophane Coumarine Derivatives. *Journal of Molecular Structure*, **1157**(5): 425–433. DOI: 10.1016/j.molstruc.2017.12.095
- Sun, J., Ye, B., Xia, G., & Wang, H. (2017). A Multi-Responsive Squaraine-Based “Turn On” Fluorescent Chemosensor for Highly Sensitive Detection of Al^{3+} , Zn^{2+} and Cd^{2+} in Aqueous Media and its Biological Application. *Sensors and Actuators, B: Chemical*, **249**: 386–394. DOI: 10.1016/j.snb.2017.03.134

- Sutradhar, M., Martins, L. M. D. R. S., Guedes da Silva, M. F. C., & Pombeiro, A. J. L. (2015). Oxidovanadium Complexes with Tridentate Aroylhydrazone as Catalyst Precursors for Solvent-Free Microwave-Assisted Oxidation of Alcohols. *Applied Catalysis A: General*, **493**: 50–57. DOI: 10.1016/j.apcata.2015.01.005
- Tabrizi, L., Chiniforoshan, H., & Tavakol, H. (2015). New Mixed Ligand Palladium (II) Complexes Based on the Antiepileptic Drug Sodium Valproate and Bioactive Nitrogen-Donor Ligands: Synthesis, Structural Characterization, Binding Interactions with DNA and BSA, in Vitro Cytotoxicity Studies and DFT Calculations. *Spectrochimica Acta Part A: Molecular and Biomolecular Spectroscopy*, **141**: 16–26. DOI: 10.1016/j.saa.2015.01.027
- Tabrizi, L., Mcardle, P., Ektefan, M., & Chiniforoshan, H. (2016). Synthesis, Crystal Structure, Spectroscopic and Biological Properties of Mixed Ligand Complexes of Cadmium(II), Cobalt(II) and Manganese(II) Valproate with 1,10-Phenanthroline and Imidazole. *Inorganica Chimica Acta*, **439**: 138–144. DOI: 10.1016/j.ica.2015.10.015
- Taher, M. A., Jarelnabbi, S. E., Bayoumy, B. E., El-Medani, S. M., & Ramadan, R. M. (2010). Synthesis and Spectroscopic Studies of Some New Molybdenum, Tungsten, and Ruthenium Carbonyl Derivatives of 2-hydroxymethylpyridine. *International Journal of Inorganic Chemistry*, **2010**: 1–6. DOI: 10.1155/2010/296215
- Thakur, S., Sharma, P. K., & Malviya, R. (2017). Influence of Concentration on Surface Tension & Viscosity of Tamarind (*Tamarindus indica*) Seed Gum. *Annals Molecular Genetic Medicine*, **1**(1): 008-012
- Tistaert, C., Dejaegher, B., & Heyden, Y. V. (2011). Chromatographic Separation Techniques and Data Handling Methods for Herbal Fingerprints: A Review. *Analytica Chimica Acta*, **690**(2): 148–161. DOI: 10.1016/j.aca.2011.02.023
- Tomachynski, L. A., Chernii, V. Y., & Volkov, S. V. (2001). Synthesis and Properties of Axially Substituted Zirconium(IV) and Hafnium(IV) Phthalocyanines with Organic Ligands. *Journal of Porphyrins and Phthalocyanines*, **5**(10): 731–734. DOI: 10.1002/jpp.384

- Tongaree, S., Flanagan, D. R., Poust, R. I. (1999). The Interaction Between Oxytetracycline and Divalent Metal Ions in Aqueous and Mixed Solvent Systems. *Pharmaceutical Development and Technology*, **4**(4): 581–591. DOI: 10.1081/PDT-100101397
- Tordin, E., List, M., Monkowius, U., Schindler, S., & Knör, G. (2013). Synthesis and Characterisation of Cobalt, Nickel and Copper Complexes with Tripodal 4N Ligands as Novel Catalysts for the Homogeneous Partial Oxidation of Alkanes. *Inorganica Chimica Acta*, **402**: 90–96. DOI: 10.1016/j.ica.2013.03.034
- Totta, X., Hatzidimitriou, A. G., Papadopoulos, A. N., & Psomas, G. (2017). Nickel(II)-Naproxen Mixed-Ligand Complexes: Synthesis, Structure, Antioxidant Activity and Interaction with Albumins and Calf-Thymus DNA. *New Journal of Chemistry*, **41**(11): 4478–4492. DOI: 10.1039/c7nj00257b
- Turel, I. (2015). Special issue: Practical Applications of Metal Complexes. *Molecules*, **20**(5): 7951–7956. DOI: 10.3390/molecules20057951
- Tyagi, M., & Chandra, S. (2014). Synthesis and Spectroscopic Studies of Biologically Active Tetraazamacrocyclic Complexes of Mn(II), Co(II), Ni(II), Pd (II) and Pt(II). *Journal of Saudi Chemical Society*, **18**(1): 53–58. DOI: 10.1016/j.jscs.2011.05.013
- Vuotto, C., Longo, F., Balice, M. P., Donelli, G., & Varaldo, P. E. (2014). Antibiotic Resistance Related to Biofilm Formation in *Klebsiella pneumoniae*. *Pathogens*, **3**(3): 743–758. DOI: 10.3390/pathogens3030743
- Wang, S., Chu, W., Wang, Y., Liu, S., Zhang, J., Li, S., Wei, H., Zhou, G., & Qin, X. (2013). Synthesis, Characterization and Cytotoxicity of Pt(II), Pd(II), Cu(II) and Zn(II) Complexes with 4'-Substituted Terpyridine. *Applied Organometallic Chemistry*, **27**(7): 373–379. DOI: 10.1002/aoc.2988
- Warad, I., Azam, M., Al-Resayes, S. I., Khan, M. S., Ahmad, P., Al-Nuri, M., Jodeh, S., Husein, A., Haddad, S. F., Hammouti, B., & Al-Noaimi, M. (2014). Structural Studies on Cd(II) Complexes Incorporating di-2-pyridyl Ligand and the X-Ray Crystal Structure of the Chloroform Solvated DPMNPH/Cd₂ Complex. *Inorganic Chemistry Communications*, **43**: 155–161. DOI: 10.1016/j.inoche.2014.02.036

- Xie, Z., Tang, J., Wu, X., Li, X., & Hua, R. (2019). Bioconcentration, Metabolism and the Effects of Tetracycline on Multiple Biomarkers in *Chironomus riparius* Larvae. *Science of the Total Environment*, **649**: 1590–1598. DOI: 10.1016/j.scitotenv.2018.08.371
- Xiong, W., Wang, M., Dai, J., Sun, Y., & Zeng, Z. (2018). Application of Manure Containing Tetracyclines Slowed Down the Dissipation of *Tet* Resistance Genes and Caused Changes in the Composition of Soil Bacteria. *Ecotoxicology and Environmental Safety*, **147**: 455–460. DOI: 10.1016/j.ecoenv.2017.08.061
- Xu, T., Zhang, N., Nichols, H. L., Shi, D., & Wen, X. (2007). Modification of Nanostructured Materials for Biomedical Applications. *Materials Science and Engineering C*, **27**(3): 579–594. DOI: 10.1016/j.msec.2006.05.029
- Yadav, M., Behera, D., Kumar, S., & Sinha, R. R. (2013). Experimental and Quantum Chemical Studies on the Corrosion Inhibition Performance of Benzimidazole Derivatives for Mild Steel in HCl. *Industrial and Engineering Chemistry Research*, **52**(19): 6318–6328. DOI: 10.1021/ie400099q
- Yegorova, A., Vityukova, E., Beltyukova, S., & Duerkop, A. (2006). Determination of Citrate in Tablets and of Oxytetracycline in Serum using Europium(III) Luminescence. *Microchemical Journal*, **83**(1): 1–6. DOI: 10.1016/j.microc.2005.12.005
- Yuan, L., Yan, M., Huang, Z., He, K., Zeng, G., Chen, A., Hu, L., Li, H., Peng, M., Huang, T., & Chen, G. (2019). Influences of pH and Metal Ions on the Interactions of Oxytetracycline onto Nano-hydroxyapatite and their Co-Adsorption Behavior in Aqueous Solution. *Journal of Colloid and Interface Science*, **54**: 101–113. DOI: 10.1016/j.jcis.2019.01.078
- Yurdakul, O., & Kose, D. A. (2014). Mixed Ligand Complexes of Acesulfame/ Nicotinamide with Earth Alkaline Metal Cations Mg^{II}, Ca^{II}, Ba^{II} and Sr^{II}: Synthesis and Characterization. *Hittite Journal of Science & Engineering*, **1**(1): 51–57. DOI: 10.17350/HJSE19030000008
- Zakeri, B., & Lu, T. K. (2013). Synthetic Biology of Antimicrobial Discovery. *ACS Synthetic Biology*, **2**(7): 358–372. DOI: 10.1021/sb300101g

- Zhang, P., & Sadler, P. J. (2017). Advances in the Design of Organometallic Anticancer Complexes. *Journal of Organometallic Chemistry*, **839**: 5–14. DOI: 10.1016/j.jorganchem.2017.03.038
- Zhang, Z., Lan, H., Liu, H., & Qu, J. (2015). Removal of Tetracycline Antibiotics from Aqueous Solution by Amino-Fe (III) functionalized SBA15. *Colloids and Surfaces A: Physicochemical and Engineering Aspects*, **471**: 133–138. DOI: 10.1016/j.colsurfa.2015.02.018
- Zhou, Z. H., Wang, H., Yu, P., Olmstead, M. M., & Cramer, S. P. (2013). Structure and Spectroscopy of a Bidentate bis-homocitrate dioxo-molybdenum (VI) Complex: Insights Relevant to the Structure and Properties of the FeMo-Cofactor in Nitrogenase. *Journal of Inorganic Biochemistry*, **118**: 100–106. DOI: 10.1016/j.jinorgbio.2012.10.001

APPENDIX

Table A1: List of instruments and glassware apparatus		
S.No.	Instruments and Glassware apparatus	Source
1	Heating Mantle	Local company
2	Digital Balance with 4 digits	Afcoset Electronic balance
3	Easydyne Tensiometer	KRUSS Company
4	Conductivity meter	TDS Meter TCM 15+ Digital
5	pH Meter	EUTECH Instrument
6	Magnetic stirrer	Labinco L-34
7	Micro Pipette	Merilette
8	Magnetic beads	Local
9	Beaker	Borosil
10	Pipette pump	polylab
11	Measuring cylinder	Borosil
12	50 and 100 ml R.B. Flask	Borosil
13	Glass adapters	Borosil
14	Condenser	Borosil
15	Desiccator	Borosil
16	vial	Tarsons (Local)
17	Petridish	Borosil
18	Dropper	Borosil
19	Funnel	Borosil

Table A2: List of chemicals and reagents		
S.No.	Chemicals and reagents	Source
1	Tetracycline	Sigma Aldrich
2	Oxytetracycline	TCI
3	Salicylaldehyde, CdCl ₂ .H ₂ O, ZrOCl ₂ .8H ₂ O	Loba Chemie Pvt.Ltd
4	PdCl ₂ , Tryptone soya broth, Nutrient Agar and MHA	Himedia co.
5	MoCl ₃ and MoCl ₅	Alfa Aesar and Sigma-Aldrich

6	Ethanol	Merk
7	Ammonium hydroxide	Qualigens
8	pH buffer capsule	Merk
9	Acetone	Merk
10	Amikacin	Himedia co.
11	Peptone water	Himedia co.

Table A3: Solubility data of metal complexes of mixed ligand

S.No.	Complexes	Water	Methanol	CHCl ₃	DMF	Ethanol	DMSO
1	Tetracycline	IS	IS	IS	S	S	S
2	Oxytetracycline	IS	IS	IS	S	S	S
3	Salicylaldehyde	IS	IS	IS	S	S	S
4	Cd-TC/Sal Complex	IS	IS	IS	S	IS	S
5	Zr-TC/Sal Complex	IS	IS	IS	S	IS	S
6	Mo-TC/Sal Complex	IS	IS	IS	S	IS	S
7	Pd-TC/Sal Complex	IS	IS	IS	S	IS	S
8	Cd-OTC/Sal Complex	IS	IS	IS	S	IS	S
9	Zr(II)Otc/Sal Complex	IS	IS	IS	S	IS	S
10	Mo-OTC/Sal Complex	IS	IS	IS	S	IS	S
11	Pd(II)Otc/Sal Complex	IS	IS	IS	S	IS	S

IS= Insoluble

S= Soluble



Figure A1: Sample picture of M-TC/Sal and M-OTC/Sal metal complexes.

LIST OF PUBLICATIONS AND SCIENTIFIC PAPER PRESENTATIONS

List of Research Publications

1. **Dev, R. K.**, Mishra, P., Chaudhary, N. K., & Bhattarai, A. (2020). Synthesis, Characterization, and Antibacterial Evaluation of Heteroleptic Oxytetracycline-Salicylaldehyde Complexes. *Journal of Chemistry*, 10. <https://doi.org/10.1155/2020/7961345>
2. **Dev, R. K.**, Sahu, Y. R., Chaudhary, N. K., & Bhattarai, A. (2023). "Preparation, Spectroscopic Analysis, and Biological Assessment of Heteroleptic Zr(II) and Pd(II) Complexes From Otc/Sal Mixed Ligands. *Journal of Nepal Chemical Society*, 43(2): 110-124. <https://doi.org/10.3126/jncs.v43i2.53356>
3. **Dev, R. K.**, Bhattarai, A., Chaudhary, N. K., & Mishra, P. (2020). Synthesis, Spectroscopic Characterization & Antibacterial Assessment of Cadmium & Molybdenum complexes of TCSal mixed ligand. *Int. J. Pharm. Sci. Rev. Res.*, 60 (1): 115-121.
4. **Dev, R. K.**, Mishra, P., Chaudhary, N. K., & Bhattarai, A. (2020). Synthesis, Spectroscopic Characterization and Antibacterial Assessment of Zr(II) and Pd(II) Complexes of Tetracycline-Salicylaldehyde mixed ligand. *Asian Journal of Chemistry*, 32(6): 1473–1481. <https://doi.org/10.14233/ajchem.2020.22623>.

Scientific Paper Presentation

1. Scientific paper presentation entitled "**Synthesis, spectroscopic characterization, biological studies and bio-coordination of 4d-transition metal complexes with tetracycline and salicylaldehyde**" international seminar on recent trends in chemistry (RTC-2019) Department of Chemistry P. D. Women's College Club Road, Jalpaiguri West Bengal-735101. In Association with Indian Chemical Society, 92, Acharya Prafulla Chandra Road Kolkata-700 009, India, January 3, 2019.

2. Scientific paper presentation entitled **“Bio-coordination and computational modeling of 4d-transition metal complexes with tetracycline and salicylaldehyde mixed ligand: synthesis, spectroscopic characterization and biological studies”** at the 23rd International conference of International academy of physical sciences (CONIAPS XXIII) organized by Nepal Academy of Science and Technology (NAST), Nepal, November 18, 2018.
3. Scientific paper presentation entitled **“Synthesis, Spectroscopic Characterization and Antibacterial Assessment of Zirconium and Palladium complexes of TcSal Mixed Ligand”**, Research and innovation for prosperity, International youth conference on science, Technology, and Innovation, Kathmandu, Nepal, October 21-23, 2019.

Workshop Attended

1. Participated in three days workshop on **“Small molecules analysis by NMR Spectroscopy & Mass Spectrometry”**, organized by Sophisticated Analytical Instrument Facility (SAIF) sponsored by DST (Govt. of India) CSIR-Central Drug Research Institute, Lucknow, India, December 13– 15, 2017.
2. Participated in three days workshop on **“Provincial workshop on advanced research methodology”**, organized by Research management cell J. S. Murarka multiple campus, Lahan (Siraha) in collaboration with Nepal chemical Society & Eastern chapter of NCS, Biratnagar, Nepal, March 15- 17, 2019.
3. Participated in three days workshop on **“Workshop on tools & Techniques in chemistry”**, organized by Nepal chemical society in Cooperation with central department of chemistry, Kirtipur, T.U., Nepal, April 2-4, 2019.
4. Participated in two days workshop on **“Workshop on research writing and publishing”**, organized by Nepal physical society Eastern chapter, Biratnagar and co-organized by M.M.A.M. Campus, T.U., Biratnagar & Hissan, Morang, Nepal, March 29-30, 2019.

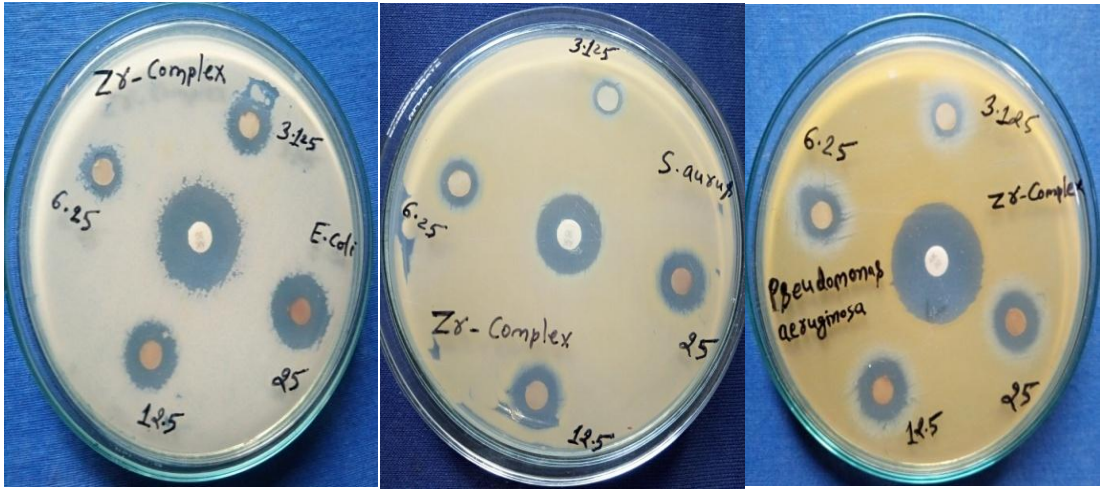
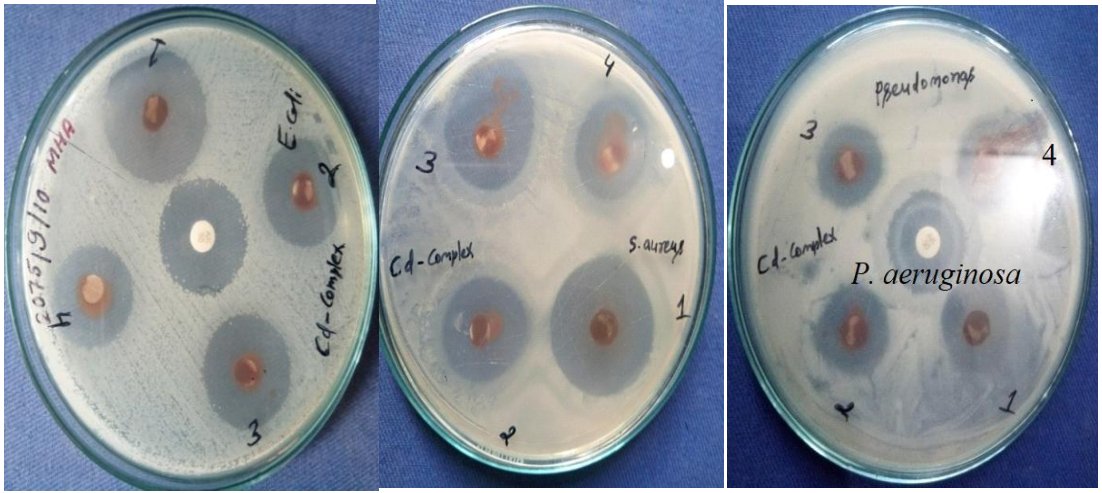
5. Participated in one day workshop on “**Carbon Dots (CDs): An amazing multi functional nano particles**”, organized by Department of chemistry, Mahendra Morang Adarsha Multiple Campus, Tribhuvan University and Nepal Chemical Society, Biratnagar, Province 1, Nepal, August 2, 2022.

Poster Presentation

1. Participated in poster presentation entitled “Preparation, spectroscopic, analysis and biological assessment of heteroleptic Zr(II) and Pd(II) complexes from Otc/Sal mixed ligands”, at **International Chemical Congress (ICC-2023): Chemistry for sustainable Development**” organized by Nepal Chemical Society in association with Central Department of Chemistry (CDC), Kirtipur, T. U., Nepal and School of Materials Science and Engineering, Liaocheng University, China on May 25-27, 2023.
2. Participated in poster presentation entitled “**Synthesis, Characterization, and Antibacterial Evaluation of Heteroleptic Oxytetracycline-Salicylaldehyde Complexes**”, on International Chemical Congress Chemistry for sustainable Development, organized by Nepal Chemical Society in cooperation with Department of Chemistry, Birendra Multiple Campus, Bharatpur (Sauraha Chitwan), T.U., Nepal, 8-10 March, 2018.
3. Participated in poster presentation on “**Synthesis, Spectroscopic Characterization and Antibacterial Assessment of Zirconium(II) and Palladium(II) Complexes of Tetracycline-Salicylaldehyde Mixed Ligand**”, in Provincial youth symposium on science & technology, Province 1, Biratnagar, Nepal, March 1-2, 2019.
4. Participated in poster presentation entitled “**Synthesis, characterization, and Antibacterial evaluation of heteroleptic oxytetracycline-salicylaldehyde complexes**”, Research and innovation for prosperity, International youth conference on science, Technology, and Innovation, Kathmandu, Nepal, October 21-23, 2019.

Participation in Seminar

- 1 Participated in the 7th International Symposium on “**Current Trends in Drug Discovery Research**” Organized by CSIR-Central Drug Research Institute, Sector 10, Jankipuram Extension, Sitapur Road, Lucknow-226031, Uttar Pradesh, India, February 20-23, 2019.
- 2 Participated in National Seminar on “**Provincial youth symposium on science & technology 2019**” held at Province 1, Biratnagar, Nepal, March 1-2, 2019.
- 3 Participated in the International Seminar on “**Frontiers in Chemistry 2018**” Organized by Department of Chemistry, University of North Bengal & CSIR North Bengal Local Chapter, Siliguri, India, August 27, 2018.



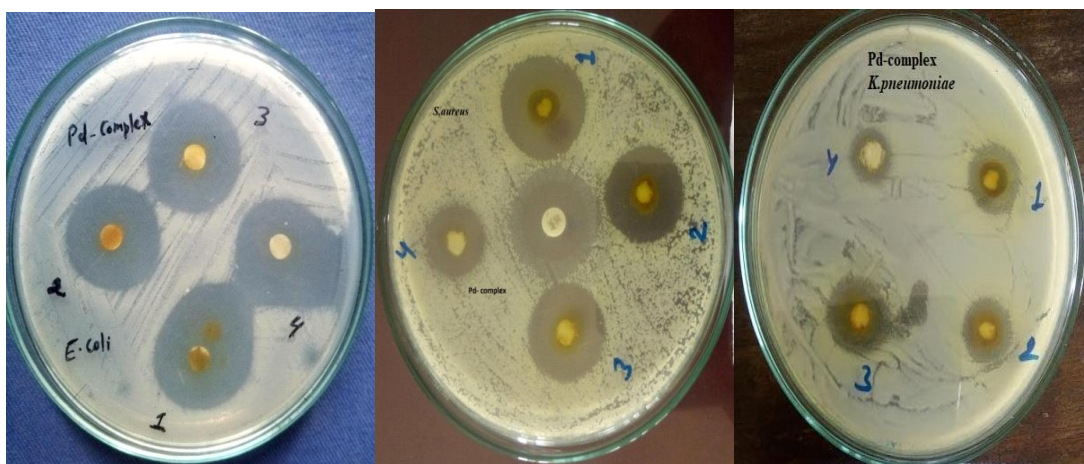
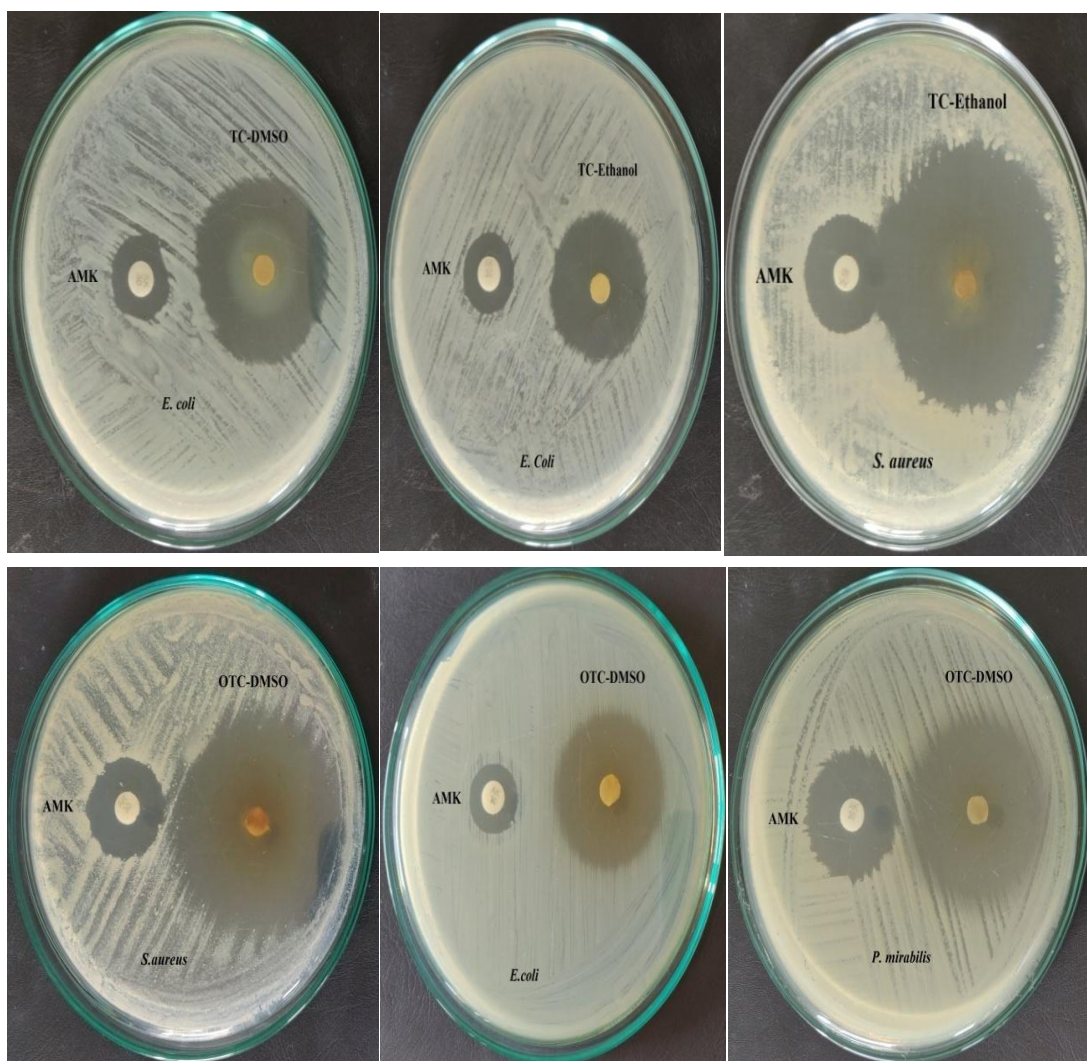
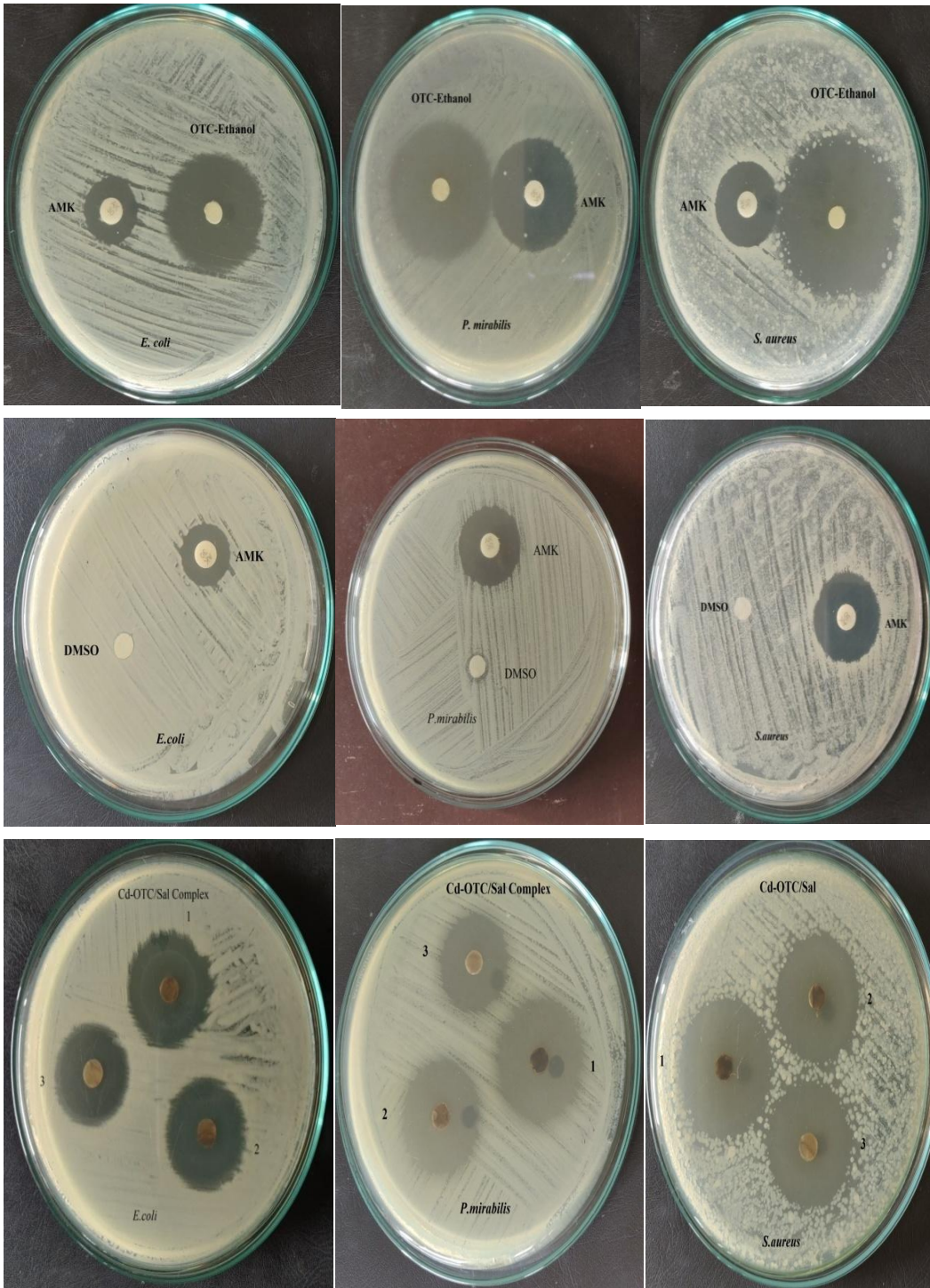


Figure A2: Antibacterial activity against pathogenic bacteria with M-TC/Sal metal complexes.





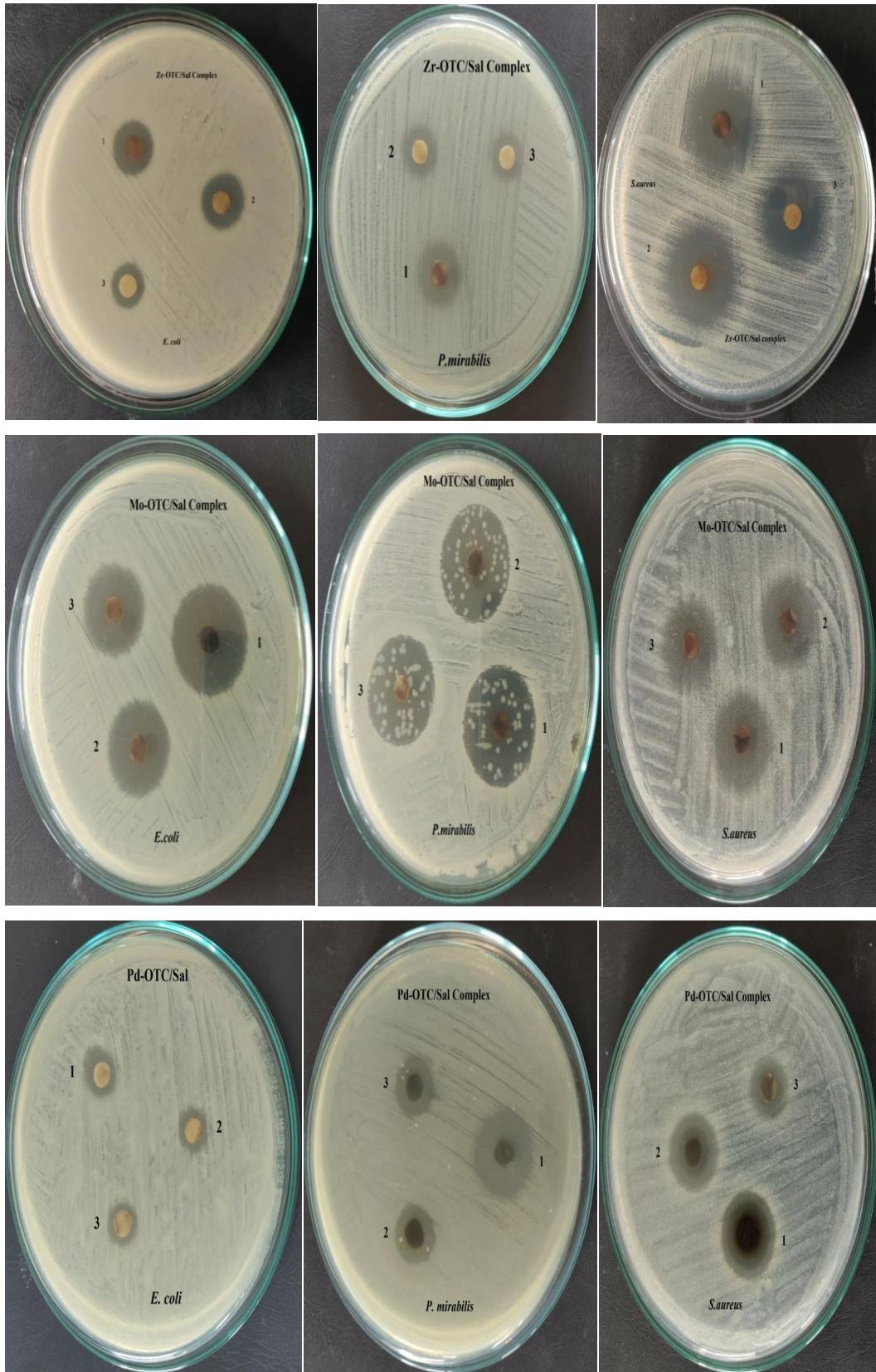


Figure A3: Antibacterial activity against pathogenic bacteria with M-OTC/Sal metal complexes. **Note:**
 - Concentration (50µg/µL) =1, (25µg/µL) =2, (12.5µg/µL) = 3

FT-IR spectral study of M-TC/Sal metal complexes

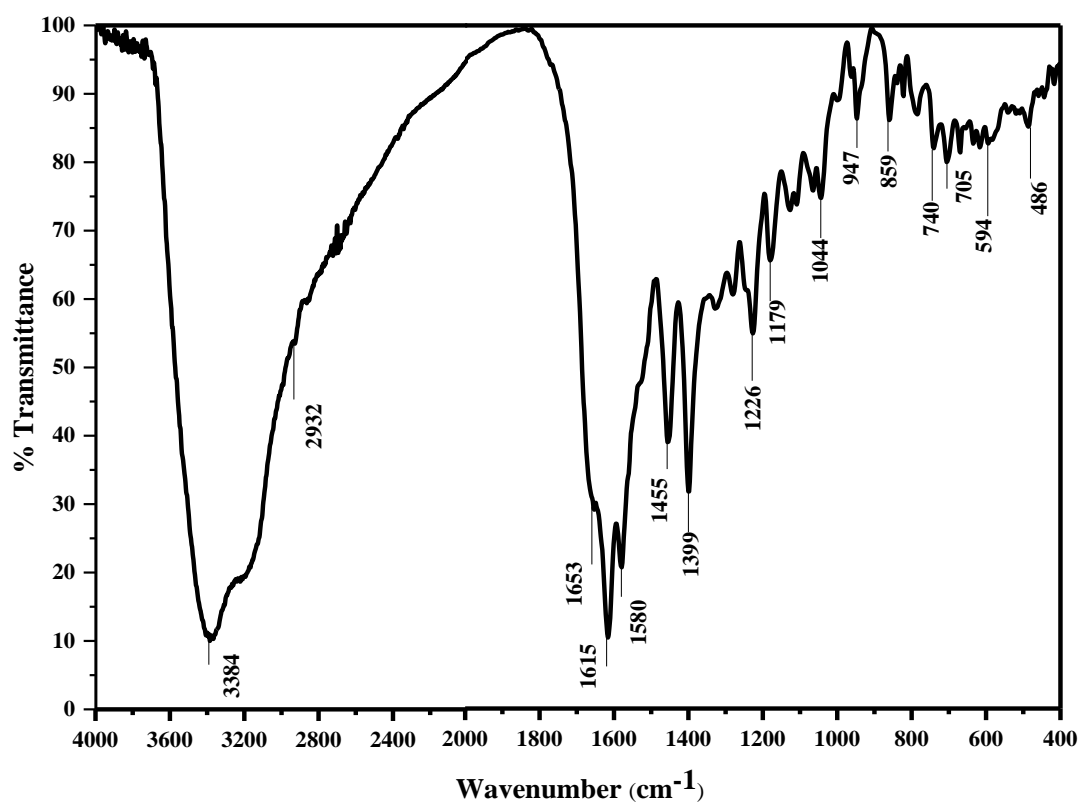


Figure A4: FT-IR spectrum of TC ligand

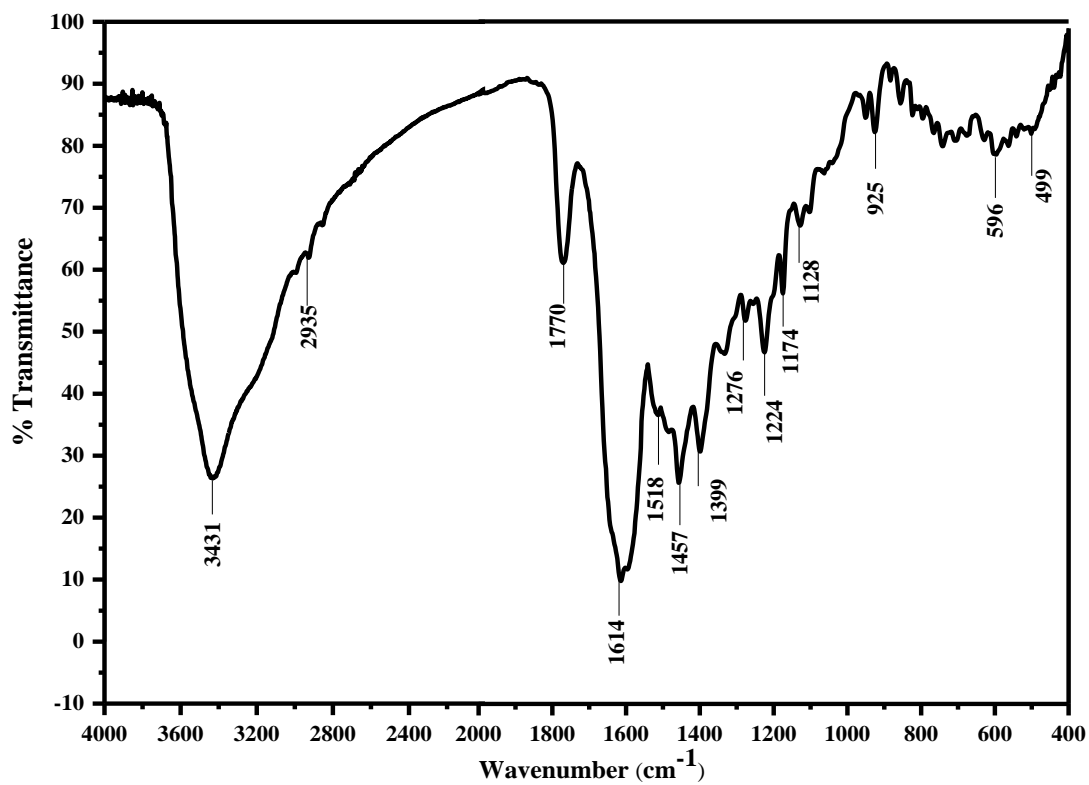


Figure A5: FT-IR Spectrum of Cd-TC/Sal metal complex

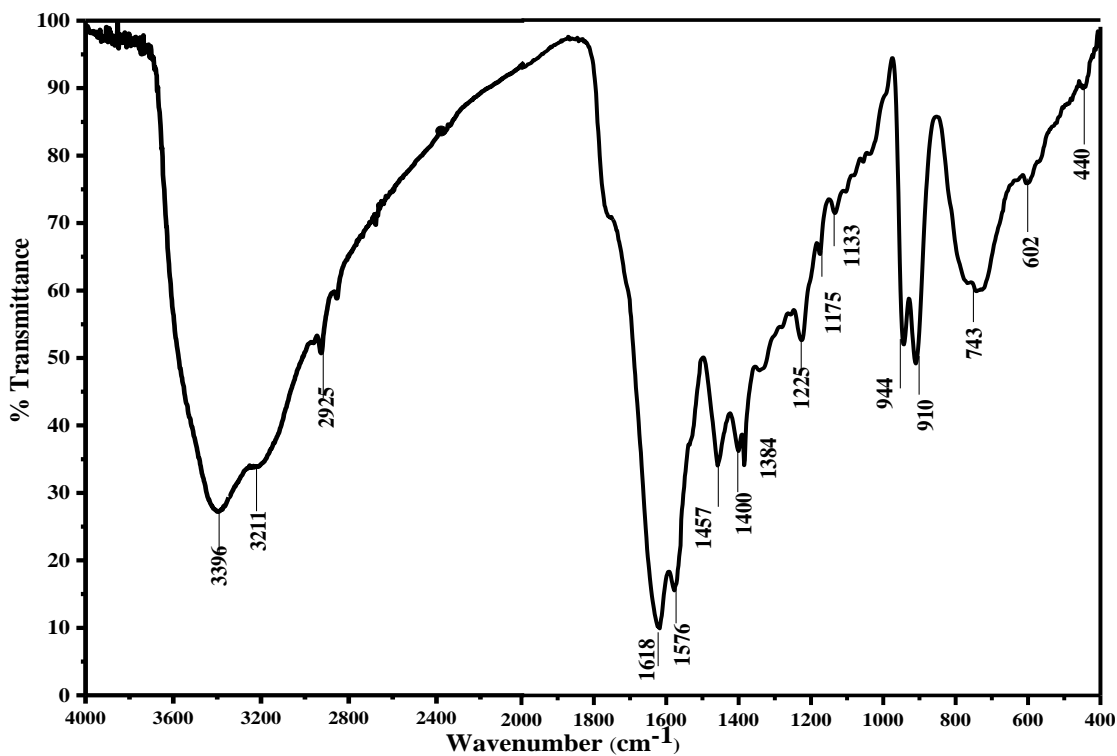


Figure A6: FT-IR Spectrum of Mo-TC/Sal metal complex

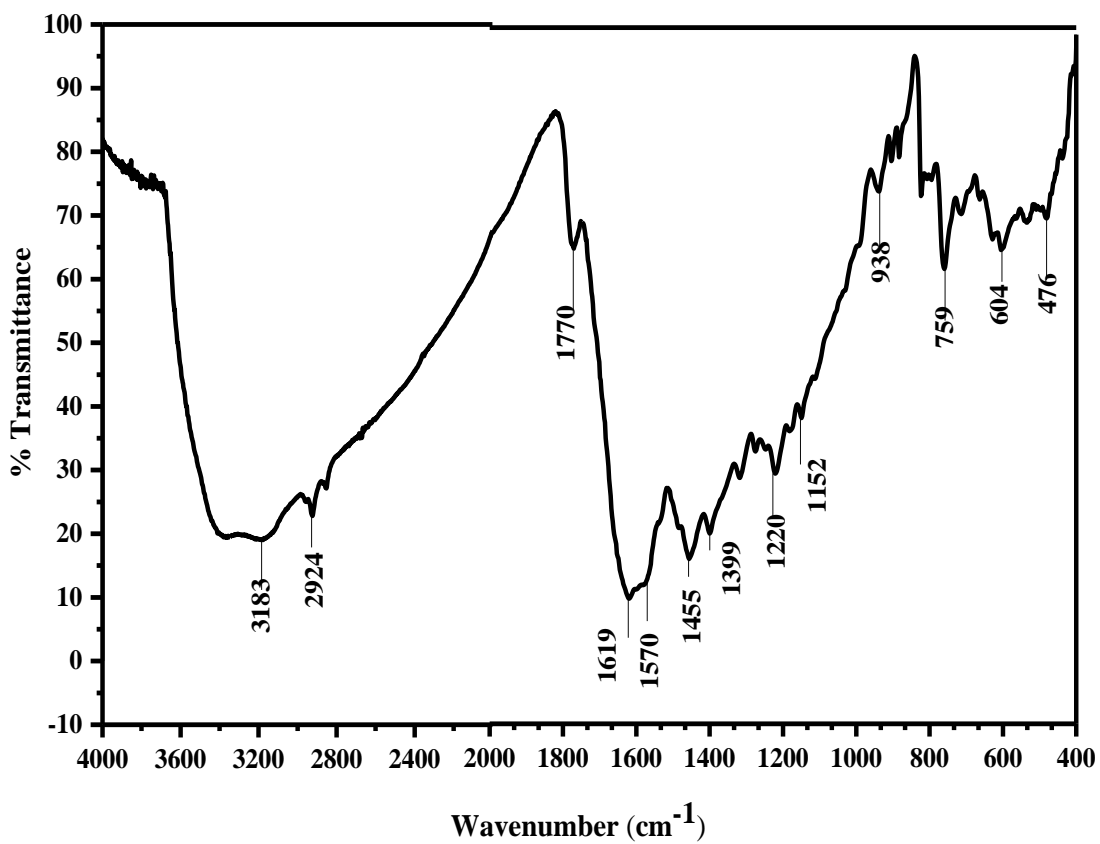


Figure A7: FT-IR Spectrum of Zr-TC/Sal metal complex

FT-IR spectral study of M-OTC/Sal metal complexes

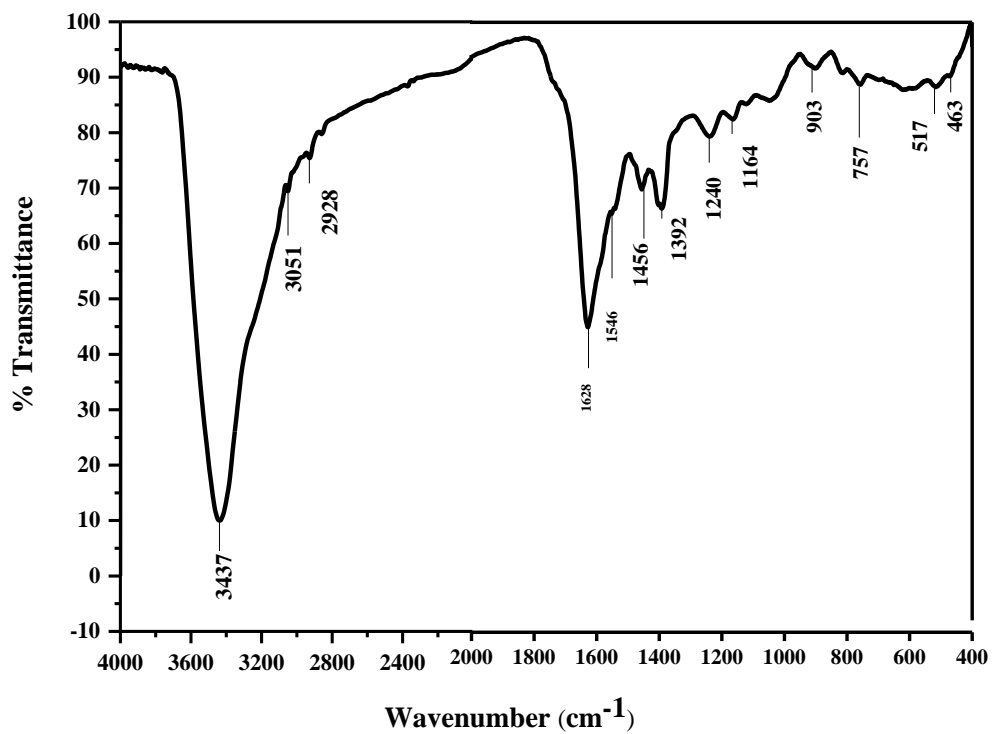


Figure A8: FT-IR Spectrum of Mo-OTC/Sal metal complex.

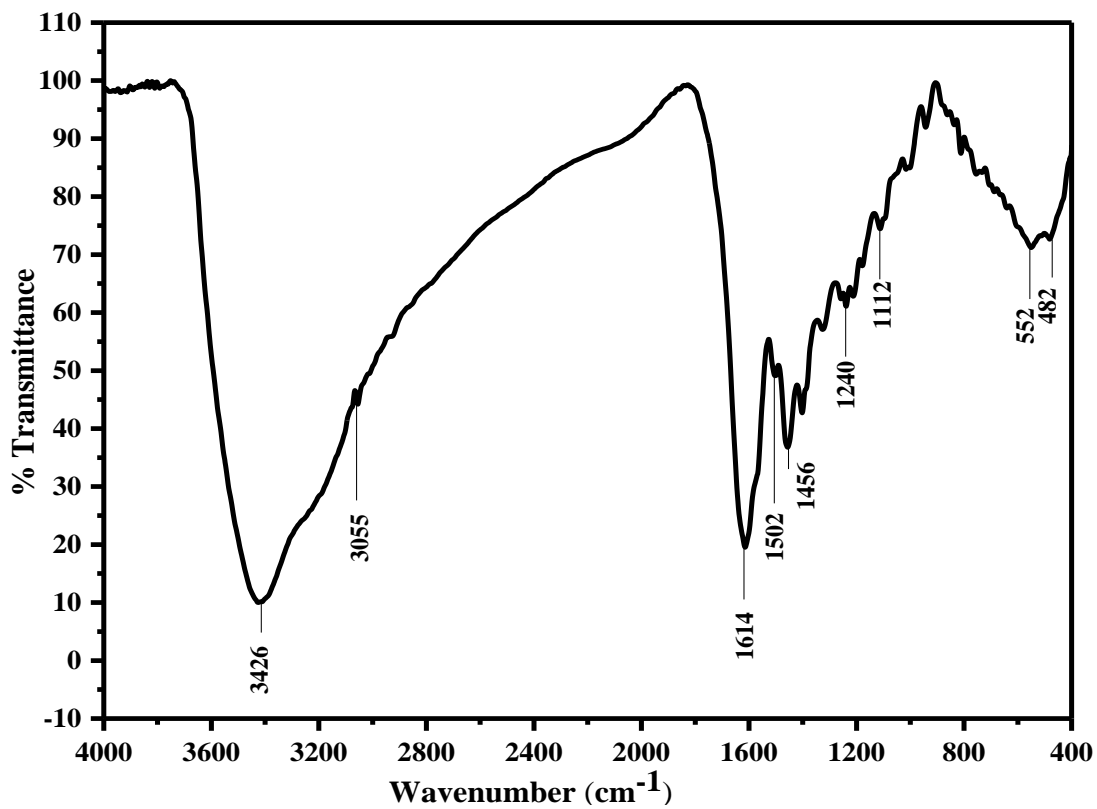


Figure A9: FT-IR Spectrum of Zr(II)Otc/Sal metal complex

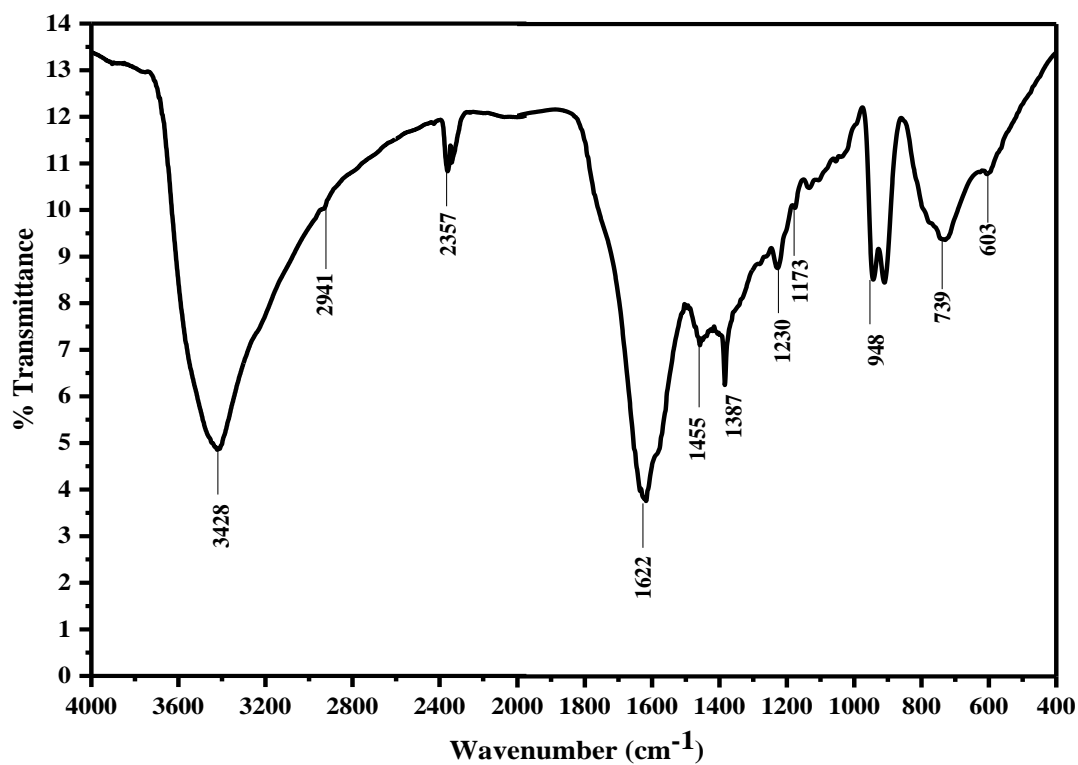


Figure A10: FT-IR Spectrum of Pd(II)Otc/Sal metal complex.

¹H-NMR spectral study of M-TC/Sal metal complexes

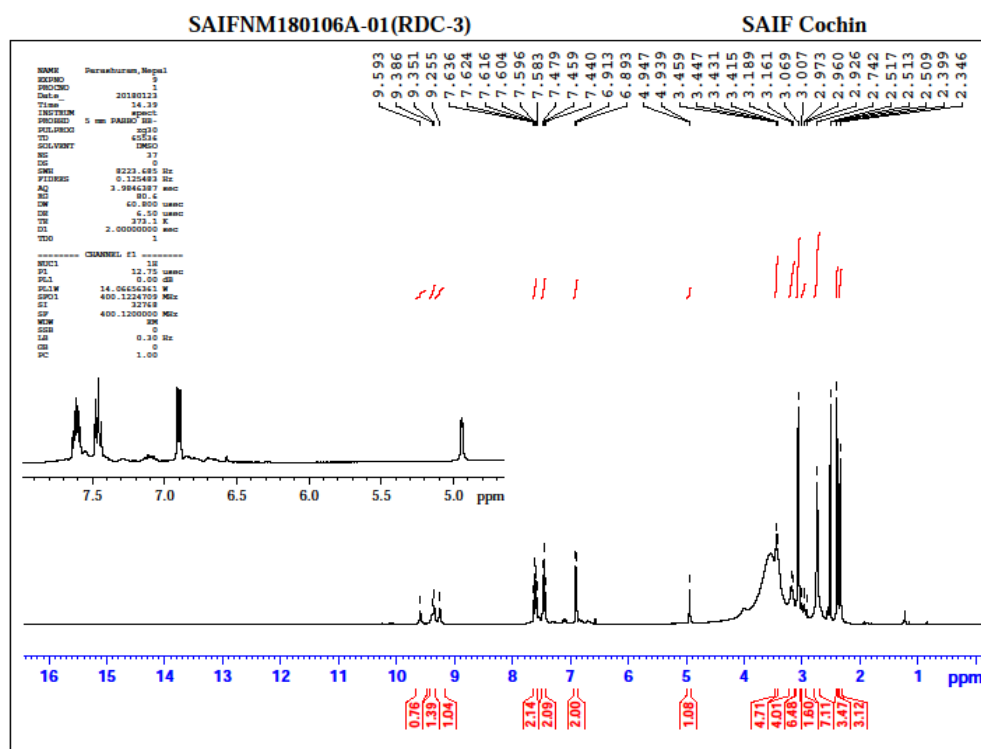


Figure A11: ¹H-NMR Spectrum of Mo-TC/Sal metal complex

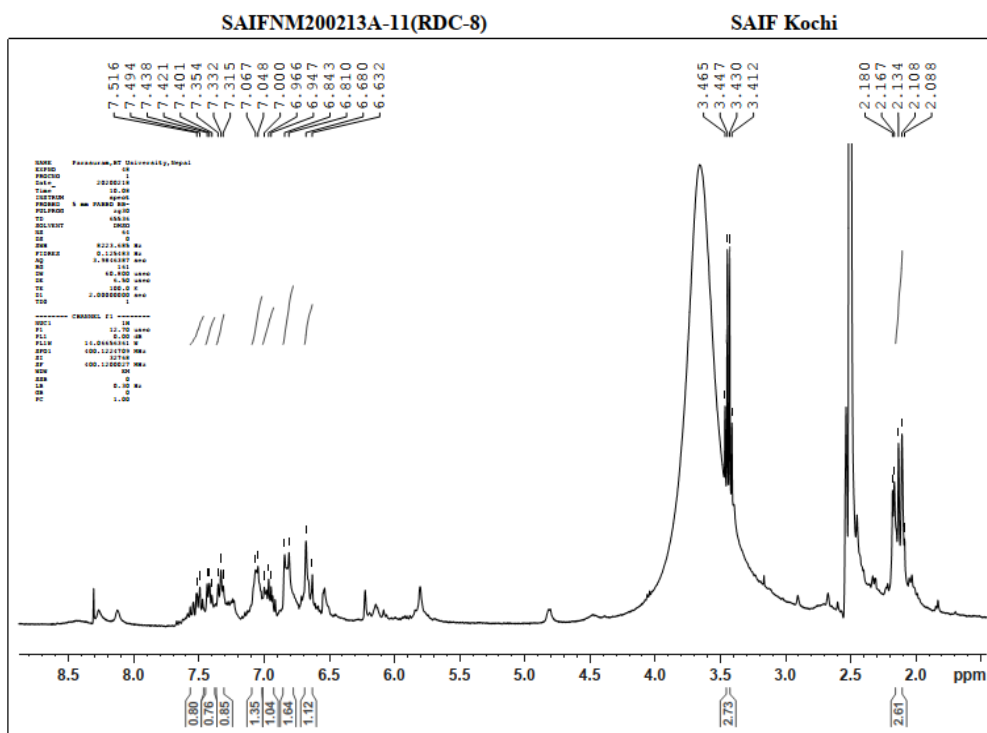


Figure A12: ¹H-NMR Spectrum of Pd(II)Otc/Sal metal complex

¹³C-NMR Spectral Study of M-TC/Sal Metal Complexes

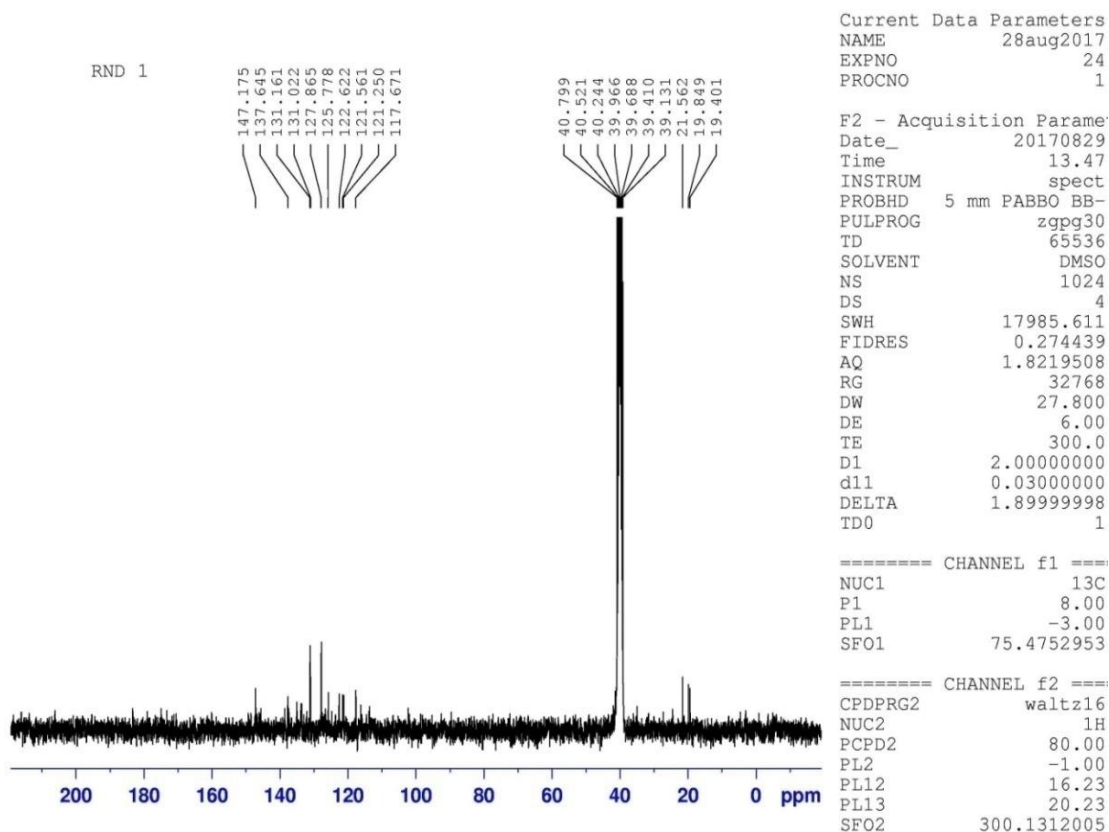


Figure A13: ¹³C-NMR spectrum of Cd-TC/Sal metal complex

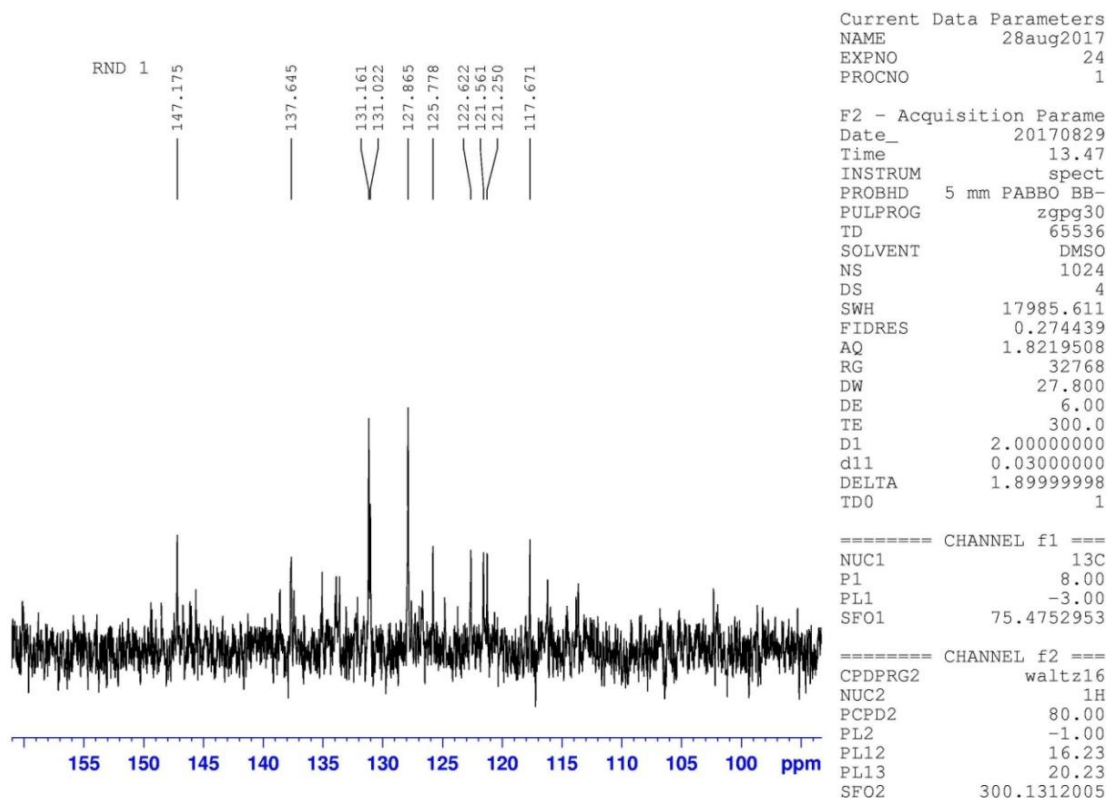


Figure A14: ¹³C-NMR spectrum of Cd-TC/Sal metal complex

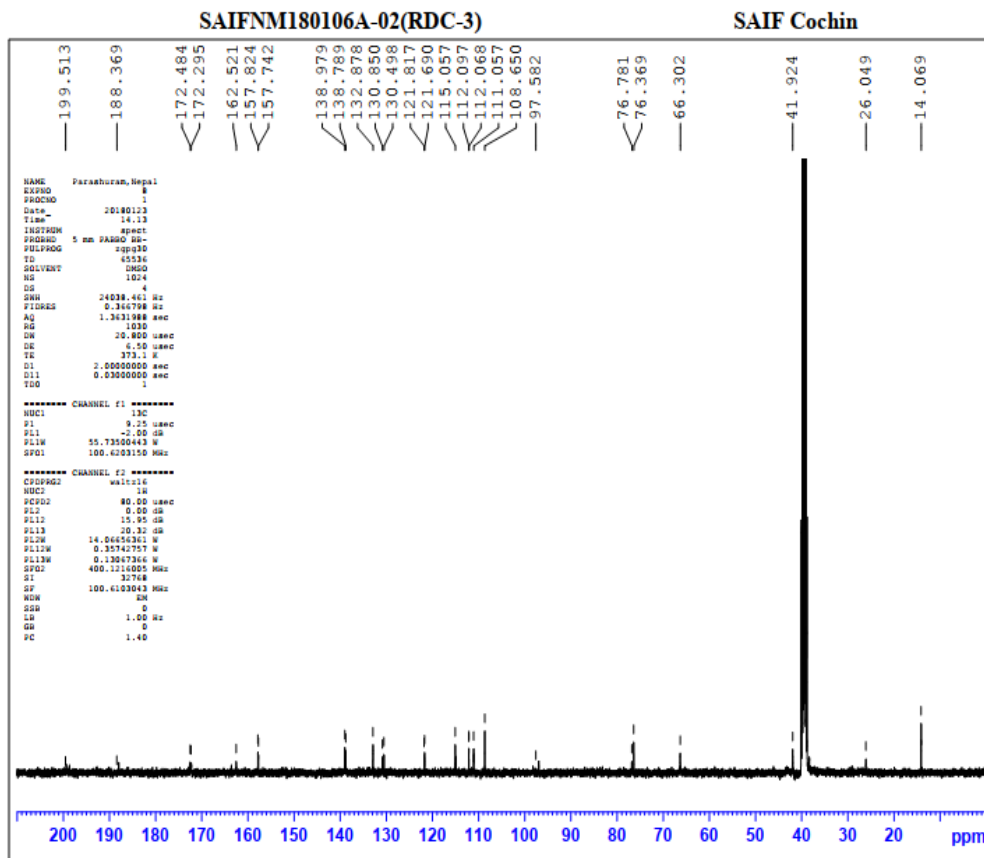


Figure A15: ^{13}C -NMR spectrum of Mo-TC/Sal metal complex

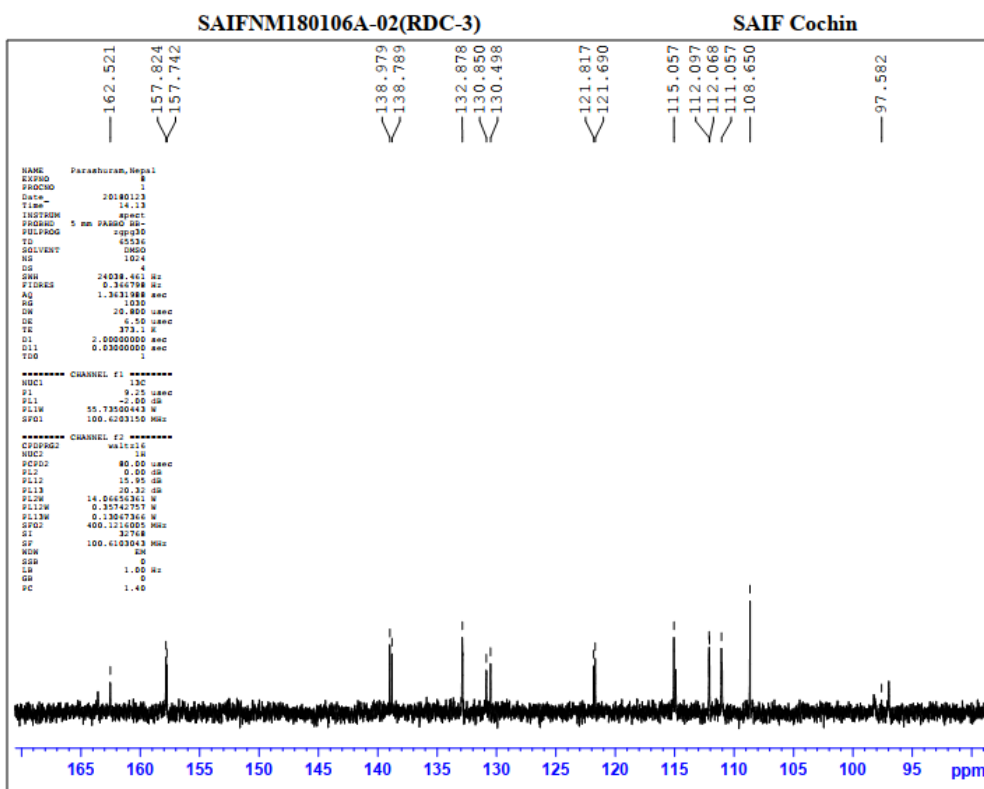


Figure A16: ^{13}C -NMR spectrum of Mo-TC/Sal metal complex

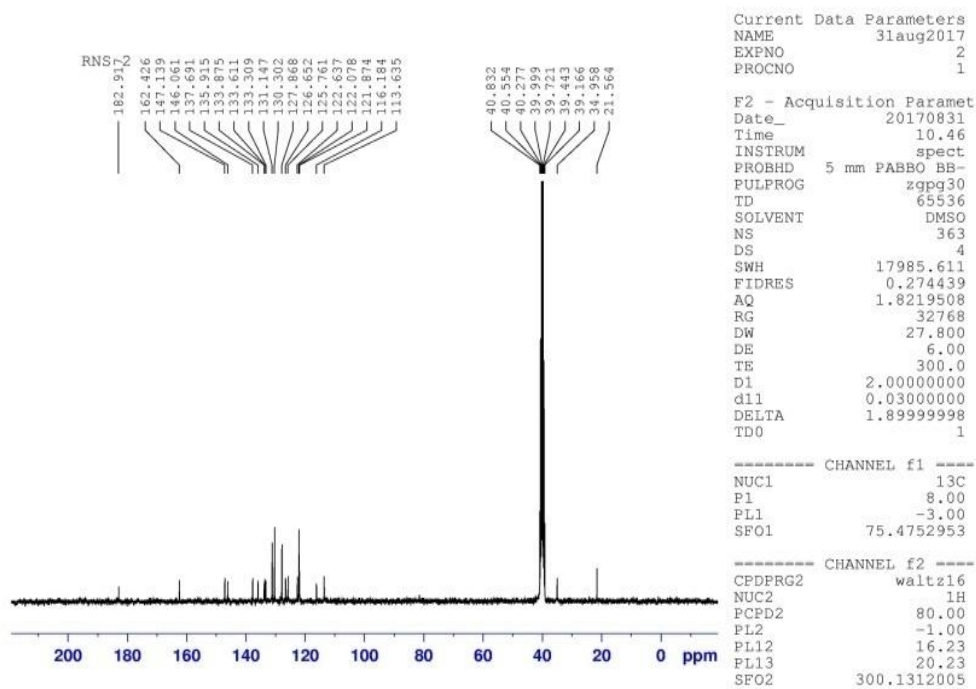


Figure A17: ^{13}C -NMR spectrum of Zr-TC/Sal metal complex

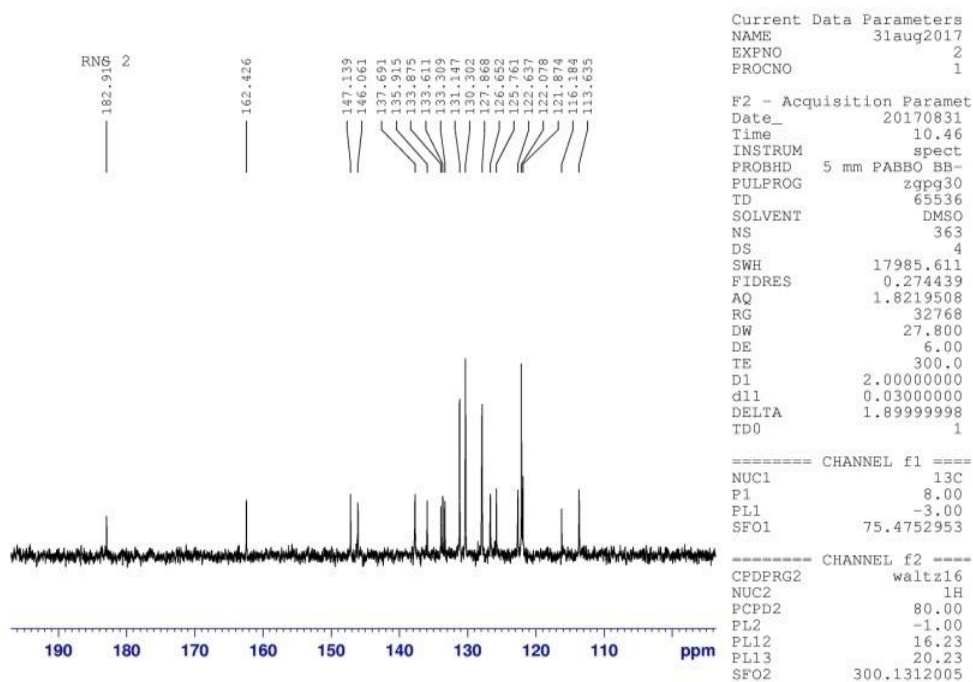


Figure A18: ^{13}C -NMR spectrum of Zr-TC/Sal metal complex

Research Article

Synthesis, Characterization, and Antibacterial Evaluation of Heteroleptic Oxytetracycline-Salicylaldehyde Complexes

Rohit Kumar Dev ¹, Parashuram Mishra ¹, Narendra Kumar Chaudhary ^{1,2},
and Ajaya Bhattarai ²

¹Bio-inorganic and Materials Chemistry Research Laboratory, Mahendra Morang Adarsh Multiple Campus, Tribhuvan University, Biratnagar, Nepal

²Department of Chemistry, Mahendra Morang Adarsh Multiple Campus, Tribhuvan University, Biratnagar, Nepal

Correspondence should be addressed to Ajaya Bhattarai; bkajaya@yahoo.com

Received 7 April 2020; Revised 9 June 2020; Accepted 3 July 2020; Published 30 July 2020

Academic Editor: Nenad Ignjatović

Copyright © 2020 Rohit Kumar Dev et al. This is an open access article distributed under the Creative Commons Attribution License, which permits unrestricted use, distribution, and reproduction in any medium, provided the original work is properly cited.

A new series of mixed ligand complexes of Cd(II) and Mo(V) were successfully synthesized by refluxing the mixture solution of oxytetracycline hydrochloride (OTC.HCl) with an aqueous and alcoholic solution of metal ($M = \text{Cd(II)}$ and Mo(V)) salts and an alcoholic solution of salicylaldehyde (Sal). The complexes were characterized by modern analytical and spectral methods such as elemental microanalysis, pH, conductivity, surface tension, viscosity, melting point, and spectral methods such as FT-IR, NMR, electronic absorption, SEM, and mass spectrometry. Conductivity measurements of the complexes revealed their electrolytic nature. The kinetic and thermal stabilities were investigated using thermogravimetric and differential thermal analysis techniques. Thermodynamic and kinetic parameters such as E^* , ΔH^* , ΔS^* , and ΔG^* were calculated from TG curves using the Coats–Redfern method. Geometry optimization of the proposed structure of the complexes was achieved by running MM2 calculations in a Gaussian-supported CS ChemOffice 3D Pro.12.0 version software. The final optimized geometrical energies for respective Cd-OTC/Sal and Mo-OTC/Sal complexes were found to be 923.1740 and 899.3184 kcal/mol. The electronic absorption spectral study revealed a tetrahedral geometry for the Cd-OTC/Sal complex and octahedral geometry for the Mo-OTC/Sal complex. The antibacterial sensitivity of the complexes was evaluated against three bacterial pathogens such as *S. aureus*, *E. coli*, and *P. mirabilis* using the modified Kirby–Bauer paper disc diffusion method. The antibacterial study revealed significant growth inhibitory action of the complexes.

1. Introduction

The current interest in the improvement of the functionality and applicability of metal complexes has become an important part of coordination chemistry research [1, 2]. Coordination compounds containing metals bound in the mesh of ligands have a variety of biological functions because many of them are used in the treatment of diseases in medical science [3]. Besides their biological functions, they are also used in chemical sciences as catalysts [4], reaction templates, and reaction activators [5]. The chief process for the fabrication of metal complexes is redox chemistry, where the metals provide a vacant orbital to the ligand for chelation. The ligand functions as an electron donor and

behaves as a Lewis base. The formation of the complex is therefore a simple Lewis acid-base reaction [6]. We have focused our research intended to address the antibacterial significance of the metal complexes of the oxytetracycline-salicylaldehyde mixed ligand. Recently, antibiotic discovery has become a critical issue in pharmaceutical science due to the increased risk of drug resistance [7, 8]. Medical science has established antibiotic therapy for the treatment of bacterial pathogens, and antibiotics are now considered one of the core drugs of modern medicine. Over the past few decades, these drugs have been losing their foundation in fighting bacteria. The bacterial strains are changing genomic characters by mutation process, and they are no longer affected by used antibiotics that once suppress their growth

and activity [9]. Several natural antibiotics have lost their activity, and we need to synthesize laboratory-based antibiotics to overcome the antibiotic resistance crisis. Therefore, it can be considered a better option to control disease outbreaks by metal-based drugs in an effective way [10, 11]. In this research study, the ligands used for heteroleptic complex formation are oxytetracycline and salicylaldehyde.

Oxytetracycline is a broad-spectrum antibiotic of the class tetracycline that performs antibiotic functions by inhibiting protein synthesis in bacteria. It was first isolated from the soil bacteria *Streptomyces rimosus* in 1948, patented in 1949, and came into commercial use in 1950 [12]. It stands parallel in properties to tetracycline, which is commonly used as a veterinary antibiotic. In humans, it is used to treat eye infection trachoma, genital infection, urethritis, chest infection, psittacosis, and pneumonia. As a veterinary medicine, oxytetracycline is used for the treatment of infections in animal husbandry and fish farming [13, 14], in agriculture as a pesticide, and as a dietary supplement for livestock [15]. In the past few decades, its use as an antibiotic has become less common due to increased antibacterial resistance among targeted pathogens. Structurally, oxytetracycline (Figure 1) has a naphthacene ring skeleton similar to tetracycline, with many chromophoric groups responsible for metal attachment in complex formation. It is a type II bacterial aromatic polyketide containing one aromatic ring. There is a structural difference between tetracycline and the presence of a substituent group -OH at the C5 of ring B [16]. This makes a vast difference in the physiological and biological profiles of the compounds. In a survey of its toxic profile, oxytetracycline can complex with Ca and Mg in vivo in the human body and cause severe physiological defects [17, 18]. Besides the in vivo physiological defects, it can also eliminate toxic heavy metals from the human body by complex formation processes. Almost 50–80% oxytetracycline undergoes excretion in its in vivo use in humans and animals because of its poorly absorbing nature. Therefore, the metal interaction chemistry of oxytetracycline can be considered an important part of research to standardize its physical and biological profiles.

For the continuation of our ongoing antibiotic research, this work focused on the synthesis of heteroleptic complexes using oxytetracycline and salicylaldehyde along with metal salts. The complexation behavior was investigated by physicochemical studies such as melting point, conductivity, pH, surface tension, viscosity, and density measurements. Their structural characterization was further investigated by spectroscopic studies such as electronic absorption, FT-IR, NMR, and ESI-MS. The surface morphology by SEM study and thermal stability by TGA/DTA study were performed to parameterize the complexes. The complexes were screened for their in vitro antibacterial susceptibility tests with three clinical pathogens to show their biological significance.

2. Experimental

2.1. Materials and Reagents. All chemicals and reagents which were used in the research were of analytical reagent grade (AR) with the highest purity. The chemicals were

purchased from various chemical agencies and included oxytetracycline hydrochloride (TCI), salicylaldehyde (Loba Chemie Pvt., Ltd.), $\text{CdCl}_2 \cdot \text{H}_2\text{O}$ (Loba Chemie Pvt., Ltd.), molybdenum (V) chloride (Sigma-Aldrich), and MHA (Himedia). Distilled ethanol was used for the synthesis. The glassware used in the research was a high-grade borosilicate type to provide overall performance and extreme precision. Double-distilled water was used to wash the equipment.

2.2. Instrumentation. The C, H, and N contents of the complexes were recorded using a Euro-E 3000 microanalyzer. Conductivity measurements were done at 25°C in DMSO solvent using an auto-ranging/TDS meter TCM 15+ digital conductivity meter. The VEEGO ASD-10013 programmable apparatus was used to record the melting point of the complex. At 25°C ± 0.1°C, the pH measurement was calculated using a digital pH meter AN ISO 9001: 2008 certified company instrument. Using the ring detachment technique, surface tension was measured using the help of Kruss K20S Easy Dyne Force Tensiometer. A PerkinElmer Spectrum II instrument was used to record the FT-IR spectra using KBr pellets in the wavenumber between 400 and 4000 cm^{-1} . At room temperature, NMR spectra were recorded from Bruker AvII-400 MHz spectrometer using the solvent DMSO- d_6 and TMS (tetramethylsilane) as the reference standard. UV/Vis spectral bands at 10^{-3} M concentration in DMSO were calculated using an instrument called Varian Cary 5000 in the range of 200 to 1000 nm. ESI-MS spectrometry technique is applied to record the mass spectra by using a water UPLC-TQD mass spectrometer. A PerkinElmer Diamond TG/DTA instrument was used to evaluate the thermal and kinetic properties of the complexes at room temperature to 1000°C under a nitrogen atmosphere with a linear heating rate of 10°C/min. A JEOL JSM-6390LV scanning electron microscope instrument was used to detect the surface morphology. The geometry optimization of the complexes was done with the help of 3D modeling via Chem3D Pro.12.0 software.

2.3. Synthesis of Complexes. The metal complexes Cd-OTC/Sal and Mo-OTC/Sal were prepared by heating the mixture solution of 20 ml oxytetracycline hydrochloride (0.9941 g, 2 mmol) in ethanol with 10 ml aqueous solution of $\text{CdCl}_2 \cdot \text{H}_2\text{O}$ (0.4029 g, 2 mmol) /10 ml alcoholic solution of MoCl_5 (0.5469 g, 2 mmol). To this solution, 0.2 ml of salicylaldehyde (2 mmol) was added and refluxed for 8 h. Ammonia solution was added dropwise to maintain a pH of 7. Under these conditions, precipitation of the complexes was formed and filtered, then washed with ethanol, and finally dried under vacuum desiccators over anhydrous CaCl_2 . The precipitate was then kept in an airtight vial for further use. The synthetic route for the metal complexes is shown in Scheme 1.

Cd-OTC/Sal: yield (75%). Color: gray, M.pt. >260°C, anal. $\text{C}_{29}\text{H}_{28}\text{CdN}_2\text{O}_{11}$ (692.95): calcd. C 50.26, H 4.07, N 4.04, O 25.40; Cd 16.22; found C 50.20, H 4.26, N 4.36, O 25.33, Cd 16.22. IR (KBr pellet, selected bands): $\bar{\nu}_{\text{max}}$ = 3432 (b, O-H/N-H str.), 1599 (s, C=O str.), 1501 (aromatic, C=C str.), 1452 (C-N), 1178 (C-O), 595 (M-O), 503 (M-N). UV/

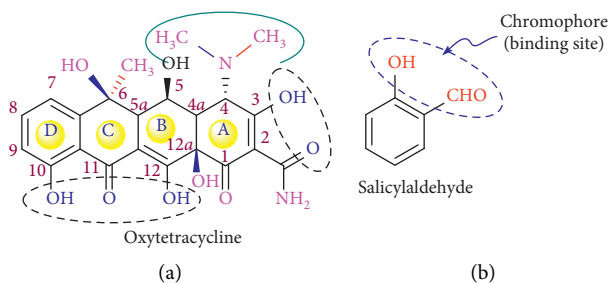
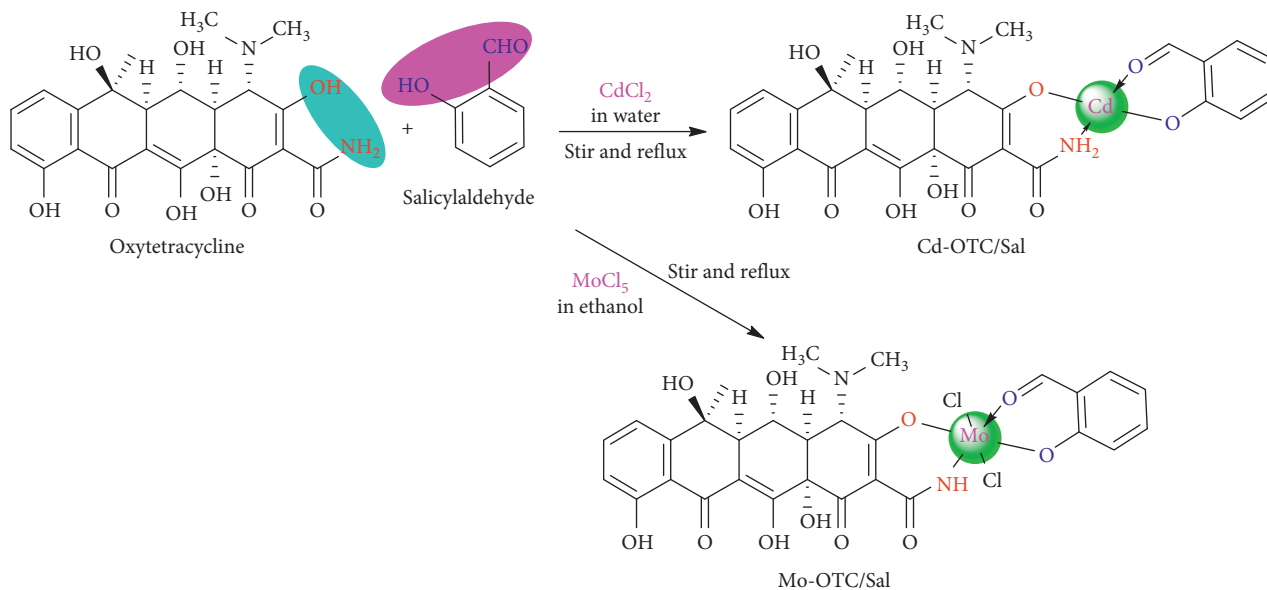


FIGURE 1: Structure of (a) oxytetracycline and (b) salicylaldehyde.



SCHEME 1: Synthetic route for Cd(II) and Mo(V) metal complexes.

Vis: $\lambda_{\max} = 267, 322, 375$ nm. ESI-MS, positive: $m/z = 693$ $[M + H]^+$. Conductivity: $\Lambda_M = 23.33$ ($\mu\text{S}/\text{cm}$), $\text{pH} = 7.42$, density = 0.954 (gm/ml), surface tension = 61.80 (mN/m), viscosity = 20.74 (cp).

Mo-OTC/Sal: yield (65%). Color: brown, M.pt. $>260^\circ\text{C}$, anal. $\text{C}_{29}\text{H}_{27}\text{Cl}_2\text{MoN}_2\text{O}_{11}$ (747.41): calcd. C 46.60, H 3.78, N 3.75, O 23.55, Cl 9.49, Mo 12.84; found C 46.59, H 3.77, N 3.74, O 23.54, Cl 9.48, Mo 12.83. IR (KBr pellet, selected bands): $\bar{\nu}_{\max} = 3437$ (b, O-H/N-H str.), 1628 (s, C=O str.), 1546 (aromatic, C=C str.), 1456 (C-N), 1164 (C-O), 517 (M-O), 463 (M-N). UV/Vis: $\lambda_{\max} = 264, 318$ nm. ESI-MS, positive: $m/z = 747.41$ $[M + H]^+$. Conductivity: $\Lambda_M = 243.40$ ($\mu\text{S}/\text{cm}$), $\text{pH} = 4.84$, density = 0.976 (gm/ml), surface tension = 60.50 (mN/m), viscosity = 21.03 (cp).

2.4. Antibacterial Assessment. The synthesized metal complexes were tested for their in vitro antimicrobial assessment which was done at the Microbiology Laboratory of MMAM Campus, Tribhuvan University, Biratnagar. The tests were performed by modified Kirby-Bauer paper disc diffusion on three pathogens: *S.aureus* (Gram-positive) and *E. coli* and *P mirabilis* (Gram-negative). The culture of bacteria was revived by inoculating the organism in freshly prepared nutrient agar and kept in an incubator at 37°C for a few hours for complete

growth. For the tests, test solutions were prepared by dissolving the synthesized complexes in 30% DMSO at three different concentrations (50, 25, and $12.5 \mu\text{g}/\mu\text{L}$) and blank paper discs of 5 mm diameter size with Whatman No. 1 filter paper cut by a punching machine and sterilized in an autoclave. The MHA media was prepared in an autoclave and solidified on Petri discs under UV laminar flow to decrease bacterial contamination. The fresh revived bacterial culture was spread on the solidified MHA media, and blank sterilized discs were also seeded and loaded with $10 \mu\text{L}$ test compounds under UV laminar flow to decrease their bacterial contamination. One blank disc soaked with DMSO acted as a solvent control while another amikacin ($30 \mu\text{g}/\text{disc}$) acted as a positive control to compare the effectiveness of the tested compounds. After performing all these tasks, the loaded Petri plates were placed in an incubator for up to 24 h at 37°C to note the diameter of the zone of inhibition measured by the help of the antibiogram zone measuring scale [19, 20].

3. Results and Discussion

3.1. Physical Characterization. In the present study, the structure of metal complexes was characterized by various physicochemical and spectroscopic techniques. At room temperature, the complexes are colored solid, moisture-free,

and air-stable and have greater melting points. All the complexes were soluble in DMSO and DMF, but insoluble in water. The complexes were stored in an airtight vial and kept in vacuum desiccators under anhydrous CaCl_2 . The change in the color of the ligand up to complex formation is the result of the complexation of the ligand with metal ions, which is further supported by pH, conductivity, surface tension, density, viscosity, and melting point. The TGA/DTA and electronic absorption denote better results of the calculated value and conclude a better relationship with the proposed structure.

3.2. Spectroscopic Characterization

3.2.1. FT-IR Spectral Study. Characteristic IR bands for the metal complexes and their assignments are presented in Figures 2 and S1. The FT-IR spectra of the Cd-OTC/Sal and Mo-OTC/Sal metal complexes showed characteristic bands at 3432 cm^{-1} and 3437 cm^{-1} , which may be assigned to the $\nu(\text{OH/NH})$ stretching vibration [21, 22]. Similarly, the $-\text{CH}_3$ stretching vibrations appeared at 2924 cm^{-1} and 2928 cm^{-1} region [23, 24]. The strong intensity bands at 1599 cm^{-1} and 1628 cm^{-1} are due to the carbonyl ($\text{C}=\text{O}$) group band, which partially overlaps the N-H band appearing as a small doublet [25, 26]. A band corresponding to the $\nu(\text{C-N})$ stretch appeared at 1452 cm^{-1} and 1456 cm^{-1} and was displaced by coordination with the metallic center. Such behavior of a band was also found in the literature [27]. At a lower frequency level, the metal complexes show bands at 595 cm^{-1} & 517 cm^{-1} and 503 cm^{-1} & 463 cm^{-1} , which may be due to the $\nu(\text{M-O})$ and $\nu(\text{M-N})$ coordination modes, respectively [28, 29].

3.2.2. $^1\text{H-NMR}$ Spectral Study. For further confirmation of the binding mode of metal ions in the complexes, the $^1\text{H-NMR}$ spectrum in DMSO-d_6 solvent was carried out at room temperature using TMS (tetramethylsilane) as a reference standard. The chemical shifts (δ) are measured in ppm units present in the downfield from TMS [30, 31]. The $^1\text{H-NMR}$ spectra of the metal complexes are presented in Figures S2 and S3, and the spectral data are presented in Table S1. The Cd-OTC/Sal showed spectral peaks at 6.889–7.355 ppm, attributed to aromatic protons. These aromatic protons are slightly moved up-field and support their coordination of ligands with metal ions [32]. The peaks in the region of 4.284–4.397 ppm suggest the peak for the -NH group [33]. A singlet peak at 1.670 ppm in the spectra of the metal complex was assigned to the methyl protons. Similarly, the peaks at 2.370–2.553 ppm are assigned to methylene protons [31]. The Mo-OTC/Sal complex shows a multiplet peak at 7.186–7.205 ppm, assignable to aromatic protons [34]. The peak at 1.047–1.082 ppm is due to a methyl group and a singlet peak at 2.551 ppm is assigned to methylene protons [35]. Each hydrogen of the aromatic ring observed one distinct peak at 4.414 ppm [36]. Hence, the values in the peaks show good agreement with the proposed structure of the metal complexes.

3.2.3. Mass Spectral Study. The ESI mass spectrometry is an instrumental technique for determining the molecular mass of compounds. It helps to determine the composition and purity of the compounds. The mass spectrum provides information about the stoichiometric compositions of the compounds. In our study, the mass spectral peaks at m/z 693 and 747.41 amu for the respective Cd-OTC/Sal and Mo-OTC/Sal complexes are assigned to the molecular ion peak $[\text{M}+\text{H}]^+$, and their corresponding base peaks are at $m/z = 461$ and $m/z = 616$, which signify the proposed molecular formula of the complex [37, 38]. Besides the molecular ion peak, there are additional peaks called fragment peaks formed by fragmentation of molecular ion peaks and lie in the region at m/z 690, 620, 543, 483, 385, and 300 in the Cd-OTC/Sal complex, and at m/z 743, 728, 723, 709, 674, 640, 537, 473, and 450, respectively, in the Mo-OTC/Sal complex. The ESI-MS spectra are presented in Figures 3 and S4.

3.2.4. Electronic Absorption Spectral Study. The important electronic absorption spectral bands for metal complexes were recorded in the 250–800 nm ranges of wavelength at room temperature in DMSO solvents taking the same solvents as the blank [30]. Electronic absorption spectroscopy is an analytical instrumental tool for determining the characterization and identification of binding modes for compounds. The metal complex of Cd-OTC/Sal shows peaks at 267, 322, and 375 may be due to $\pi \rightarrow \pi^*$, $n \rightarrow \pi^*$ transitions. The electronic configuration of the Cd(II) metal complex was d^{10} , which signifies the absence of any d-d electronic transition and the bands attributed to the CT (charge transition), compatible with tetrahedral geometry; hence, their absorption band spectra contain red and blue shifts with hyperchromic effect ions [21, 38]. In the same way, the metal complexes of Mo-OTC/Sal showed peaks at 264 and 318 nm, signifying the $\pi \rightarrow \pi^*$ and $n \rightarrow \pi^*$ transitions due to the $-\text{C}=\text{N}-$ and $-\text{C}=\text{O}-$ groups in the ligand. Band ~ 318 is denoted as the characteristic band of the ligand. Since the complex is diamagnetic and has an octahedral geometry, it is assigned as a ligand-metal charge transfer existing from the HOMO of phenolic oxygen to the LUMO of the molybdenum [39, 40]. All these bands are presented and assigned in Figure S5.

3.3. Thermal Study. TGA/DTA studies are used to determine the composition of materials and also to predict the thermal and kinetic stability of compounds. This analysis was done in the temperature range of 40°C to 860°C under a nitrogen atmosphere at a linear heating rate of $10^\circ\text{C}/\text{min}$. TGA/DTA is also an analytical instrumental technique that determines weight loss or gains due to various processes such as absorption, adsorption, sorption, or desorption of volatile components, decomposition, oxidation, and reduction reactions. The TGA curves help the scientist for profile structural information for new compounds having a coordination sphere. The initial decomposition steps in complexes are an endothermic process that denotes the loss of water molecules [41, 42].

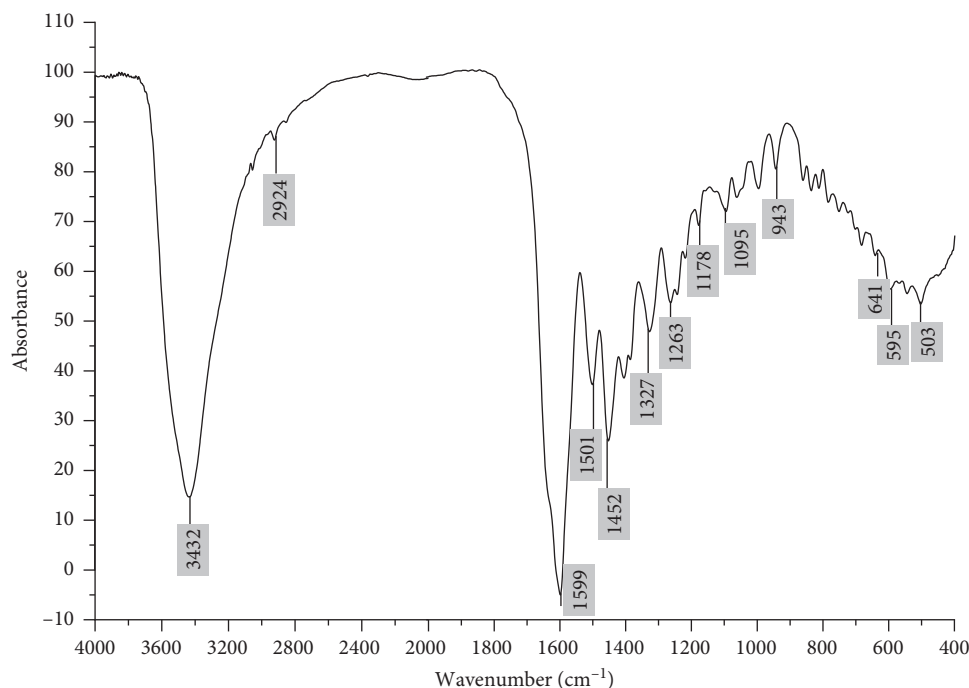


FIGURE 2: FT-IR spectrum of the Cd-OTC/Sal complex.

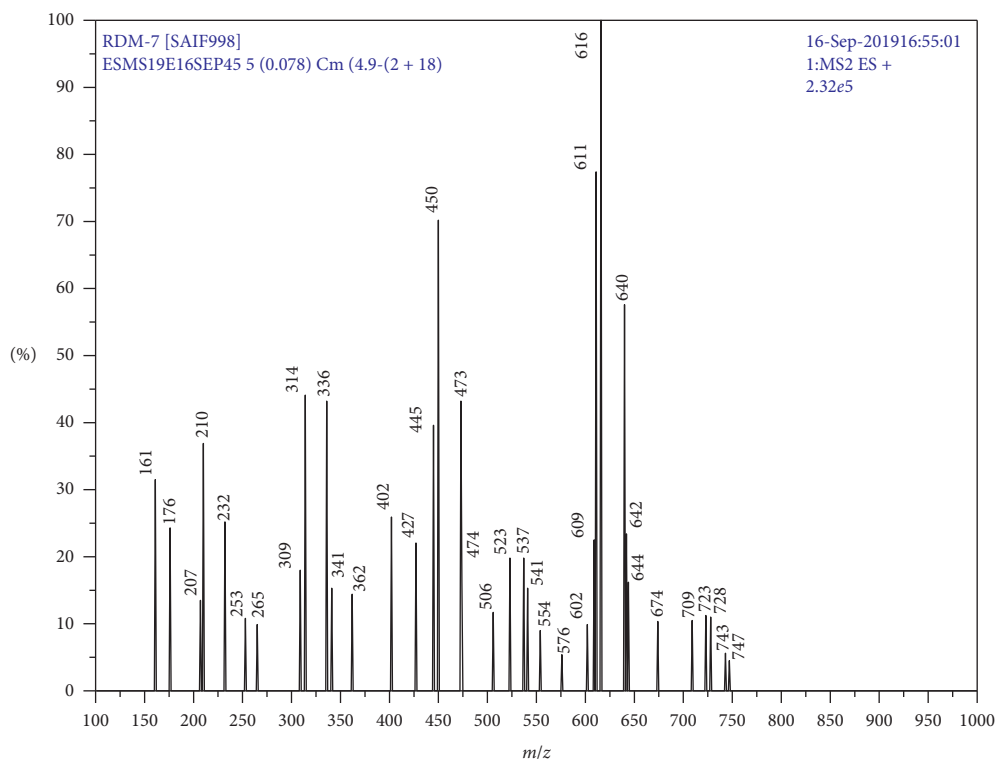


FIGURE 3: ESI-MS spectrum of the Mo-OTC/Sal complex.

The thermogram of the Cd-OTC/Sal metal complex showed decomposition at two steps between the temperature range of 362.05°C–680.76°C. The weight loss of 28.01% (–0.837 mg) occurred in the first decomposition step in the temperature range of 362.05°C–448.12°C. The second

decomposition takes place with a weight loss of 9.58% (–0.232 mg) within the temperature range of 611.13–680.76°C. The last step of decomposition explains the complete loss of the ligand from the complex, leaving behind metal oxide (CdO) as the end product. In the same way, the

thermogram of the Mo-OTC/Sal showed decomposition in three steps between the temperature range of 374.30°C–508.22°C. The weight loss of 13.022% (–0.742 mg) takes place in the first stage of decomposition at a temperature range of 374.30–397.33°C. The mass losses of 17.39% (–0.548 mg) and 6.08% (–0.657) occurred in the second and third decomposition steps within the temperature ranges of 407.21–417.17°C and 464.40–508.22°C. The final residue obtained during the decomposition stage is in the form of a metal oxide such as Mo₂O₅. The thermograms of the studied complexes are reported in Figures 4 and S6.

3.3.1. Kinetic Parameters. The thermodynamic and kinetic parameters of the complexes were obtained using the following Coats–Redfern relation:

$$\ln \left[-\frac{\ln(1-\alpha)}{T^2} \right] = \ln \left[\frac{AR}{\beta E^*} \right] - \frac{E^*}{RT} \quad (1)$$

where T represents the temperature observed on the DTG curve, A and E^* denote the Arrhenius pre-exponential factor and activation energy, which can be calculated from the graphical process. R denotes the universal gas constant and β is the linear heating rate. Using the equation $y = mx + c$, a linear plot on the left-hand side vs. $1/T$, whose slope ($-E^*/R$) gives the activation energy. Similarly, other kinetic parameters such as the entropy of activation (ΔS^*), enthalpy of activation (ΔH^*), and free energy of activation (ΔG^*) were calculated using the following equations:

$$\Delta S^* = R \ln \left[\frac{Ah}{K_B T} \right], \quad (2)$$

$$\Delta H^* = E^* - RT, \quad (3)$$

$$\Delta G^* = \Delta H^* - T\Delta S^*. \quad (4)$$

Here, various decomposition steps of the kinetic and thermodynamic parameters were calculated and are presented in Tables 1 and 2 [43]. All the complexes show greater values and reflect their high thermal stability because of their covalent bond character. In both complexes, all decomposition steps contain negative entropy of activation, which clearly shows a nonspontaneous dehydration reaction, and the positive values of ΔG^* of all decomposition stages for both complexes show nonspontaneous nature and ΔH^* is negative which indicates the exothermic process, and the correlation coefficient is shown in the graph indicating a better fit.

3.4. SEM Study. The coordination of metal with the ligand changes the metal complex surface morphology and was done by SEM (scanning electron microscopy) analysis. SEM is an important analytical instrumental technique for surface morphology. The micrograph shows the size, shape, ductility, strength, and arrangement of an object. The SEM micrograph of Cd-OTC/Sal metal complex (Figure 5(a)) exhibits microspheres-like morphology with aggregation of small nanoparticles, leading to the formation of a large

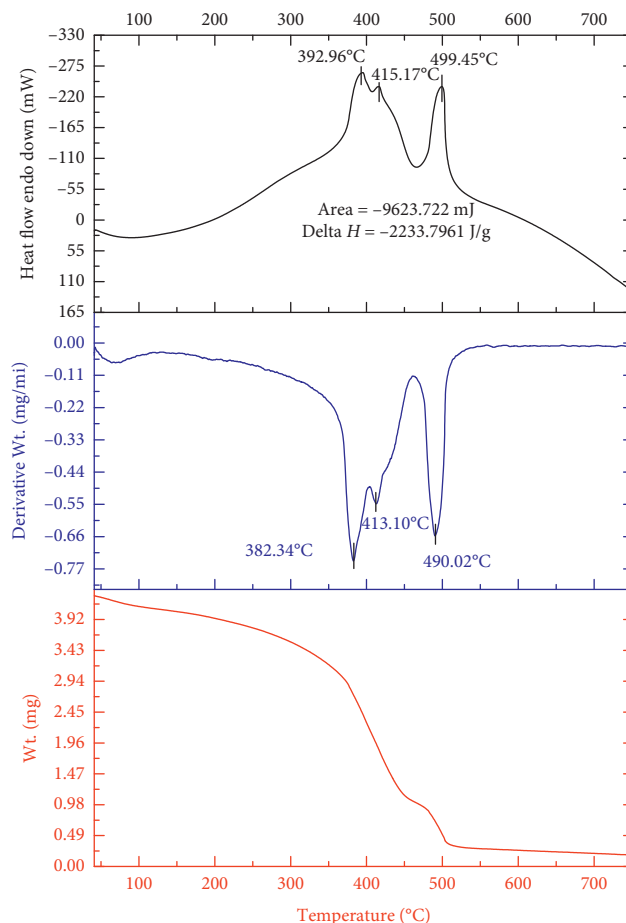


FIGURE 4: Thermogram of the Mo-OTC/Sal complex.

sphere. Similarly, Mo-OTC/Sal metal complex (Figure 5(b)) shows that the surface morphology is a spherical nano-material whose aggregation gives rise to an increase in the size of a large sphere [44–46], as presented in Figure 5.

3.5. Molecular Modeling Study. The synthesized complexes were geometrically analyzed and characterized by molecular simulation processed in CS ChemOffice 3D Pro.12.0 version software, which gives a better and more accurate assessment of the theoretical predictions and proposed structure of molecules. By using the MM2 program, the optimized structure of the complexes was predicted. Energy optimization was done repeatedly to obtain the minimum energy for the proposed geometry [47, 48]. The Cd-OTC/Sal and Mo-OTC/Sal metal complexes were reported to have tetrahedral and octahedral geometries with final geometrical energies of 923.1740 and 899.3184 kcal/mol, respectively. By performing the calculation, bonding parameters such as bond length and bond angle with their optimized 3D molecular structures were obtained and are presented in Table S2 and Figures 6 and 7. Through this discussion, the structure of the metal complexes was obtained. The potential energy is the sum of all different types of energy: $E = E_{\text{str}} + E_{\text{bend}} + E_{\text{tor}} + E_{\text{vdw}} + E_{\text{oop}} + E_{\text{ele}}$, where E 's signify the energy value for many interactions. Similarly, the

TABLE 1: Kinetic and thermodynamic parameters of the complexes.

Compounds	Step	r	A (s^{-1})	T_{max} (K)	E^* (kJ/mol)	ΔS^* (J/k-mol)	ΔH^* (kJ/mol)	ΔG^* (kJ/mol)
Cd-OTC/Sal	1	-0.99562	1468.354	661.32	341.955	-190.906	-5156.260	121095.353
	2	-0.99797	220.740	934.01	168.525	-209.533	-7596.834	188109.305
Mo-OTC/Sal	1	-0.98404	272.996	655.49	124.544	-204.823	-5325.200	128934.036
	2	-0.99555	124.558	686.25	53.708	-25.466	-5651.774	11824.561
	3	-0.99473	230.334	763.17	131.444	-207.500	-6213.551	152144.217

TABLE 2: Thermal decomposition data of the complexes.

Compounds	Steps	$\Delta_m\%$ found	TG range ($^{\circ}C$)			DTA		
			T_i	T_f	T_{DTG}	Mass loss	T_{dta}	Peak
Cd-OTC/Sal	1	28.01	362.05	448.12	258.18	-0.837	403.75	Exo
	2	9.58	611.13	680.76	371.70	-0.232		
Mo-OTC/Sal	1	13.022	374.30	397.33	382.34	-0.742	392.96	Exo
	2	17.39	407.21	417.17	413.10	-0.548	415.17	Exo
	3	6.08	464.40	508.22	490.02	-0.657	499.45	Exo

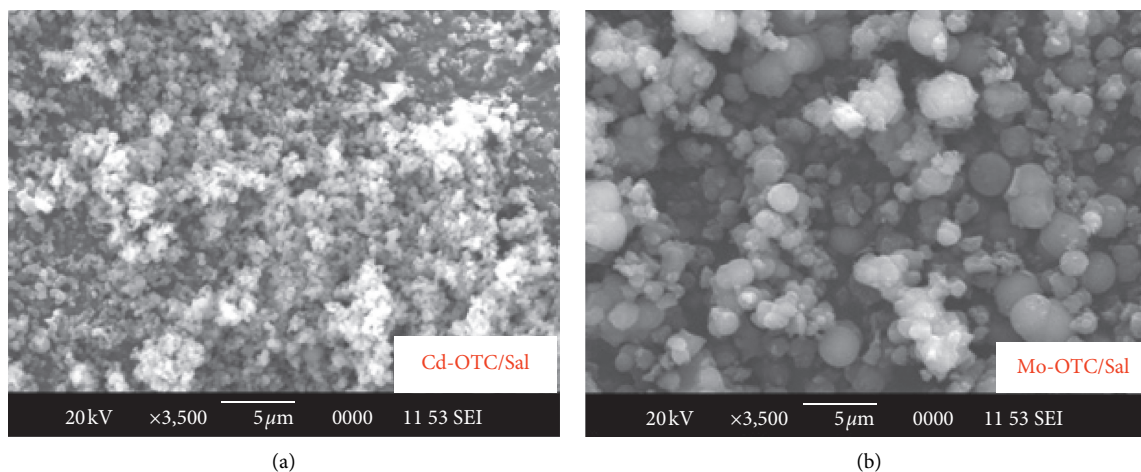


FIGURE 5: SEM micrograph of the complexes: (a) Cd-OTC/Sal and (b) Mo-OTC/Sal.

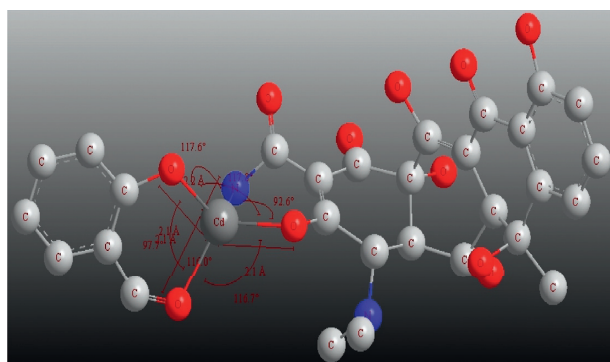


FIGURE 6: Optimized geometry of the Cd-OTC/Sal complex.

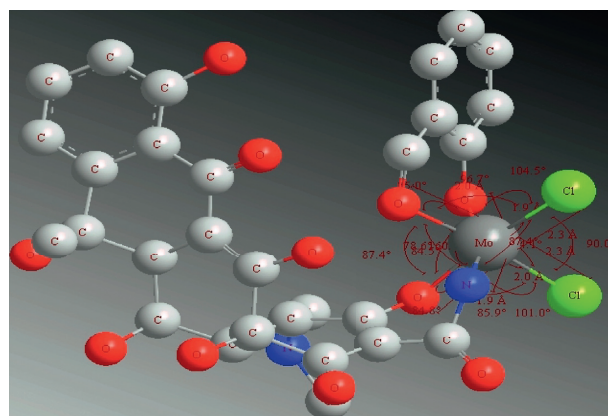


FIGURE 7: Optimized geometry of the Mo-OTC/Sal complex.

subscripts signify the bond stretching, angle bending, deformation angle, van der Waals interactions, out-of-plane bending, simple bending, and electronic interaction, respectively.

3.6. *Antibacterial Sensitivity Study.* Metal complexes (Cd-OTC/Sal and Mo-OTC/Sal) were screened for their antimicrobial evaluation using the modified Kirby-Bauer paper

TABLE 3: Antibacterial growth data of Cd-OTC/Sal and Mo-OTC/Sal metal complexes.

Compounds	The diameter of zone of inhibition in mm								
	<i>S. aureus</i>			<i>P. mirabilis</i>			<i>E. coli</i>		
Concentration ($\mu\text{g}/\mu\text{L}$)	50	25	12.5	50	25	12.5	50	25	12.5
Cd-OTC/Sal	30	28	26	26	24	21	24	23	20
Mo-OTC/Sal	18	16	15	24	23	21	23	19	18
Amikacin (30 $\mu\text{g}/\text{disc}$)	21			21			14		
OTC (ethanol)	37			33			28		
OTC (DMSO)	41			34			29		

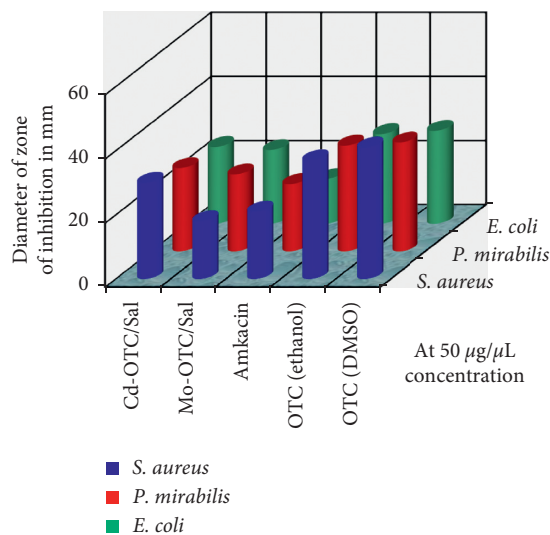


FIGURE 8: Bar graph showing antibacterial sensitivity at 50 $\mu\text{g}/\mu\text{L}$ concentration.

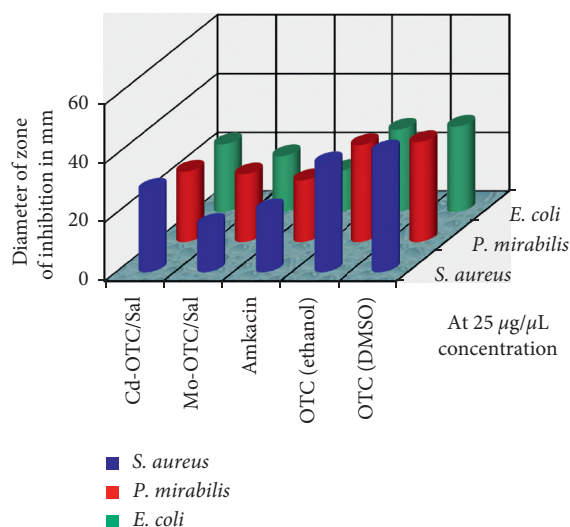


FIGURE 9: Bar graph showing antibacterial sensitivity at 25 $\mu\text{g}/\mu\text{L}$ concentration.

disc diffusion technique against *S. aureus*, *E. coli*, and *P. mirabilis* bacterial pathogens. Three different concentrations (50, 25, and 12.5 $\mu\text{g}/\mu\text{L}$) of the complexes were selected for the study. The growth inhibition data are presented in

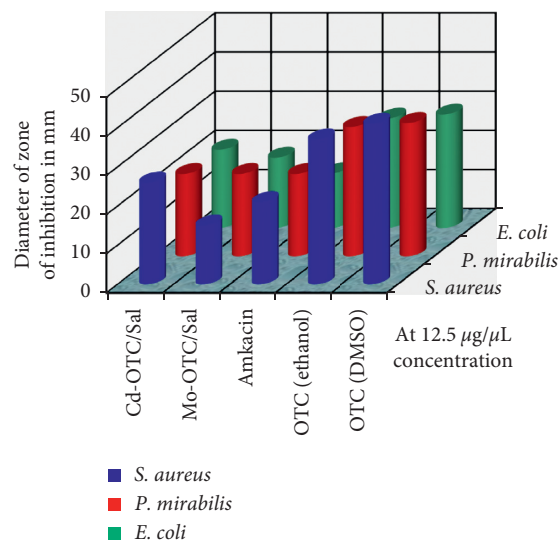


FIGURE 10: Bar graph showing antibacterial sensitivity at 12.5 $\mu\text{g}/\mu\text{L}$ concentration.

Table 3, and the pictorial representations are reported in Figures 8–10 and S7. The study revealed considerable antibacterial potency of the complexes with all bacterial pathogens. However, the parent drug oxytetracycline has shown a greater inhibitory effect relative to complexes. Moreover, the growth inhibitory effect is greater at higher concentrations of the complexes [49, 50]. Antibacterial potency of the complexes is based on the chelation theory. Chelation provides stability of the complex and also provides access for easy permeation of complex through the lipid layer of organisms. This helps in rupturing of the cell wall and deactivates bacterial action.

4. Conclusions

In summary, the Cd-OTC/Sal and Mo-OTC/Sal complexes were prepared successfully by coordination of metal ions with oxytetracycline and salicylaldehyde ligands. They were characterized using various spectral and physico-chemical techniques. The spectral analysis revealed coordination of metal ions through O at C3 and the amide N atom of C2 of ring A of oxytetracycline and O atoms of salicylaldehydes. The complexes were found as amorphous and colored solids that are insoluble in water but soluble in DMSO and DMF. The electronic absorption data concluded the tetrahedral and octahedral geometries of the Cd-OTC/Sal and Mo-OTC/Sal complexes. This was further supported by molecular modeling studies. Antibacterial studies revealed significant antibiotic action against *S. aureus*, *E. coli*, and *P. mirabilis* bacterial pathogens. The study showed a better antibiotic effect of Cd-OTC/Sal compared to Mo-OTC/Sal.

Data Availability

The authors share the data underlying the findings of the manuscript.

Conflicts of Interest

The authors declare that they have no conflicts of interest.

Acknowledgments

This research work was fully funded by Nepal Academy of Science and Technology (NAST), Khumaltar, Lalitpur, Nepal, by providing Ph.D. fellowship. Thus, the first author is highly thankful to this organization and the authors also acknowledge SAIF, IIT Bombay; CSIR-CDRI, Lucknow; STIC, Cochin, Kerala; NBU, Siliguri, India, for spectral study.

Supplementary Materials

Figure S1: FT-IR spectra of Mo-OTC/Sal metal complex. Figure S2: $^1\text{H-NMR}$ spectra of Cd-OTC/Sal metal complex. Figure S3: $^1\text{H-NMR}$ spectrum of Mo-OTC/Sal complex. Figure S4: ESI-MS spectrum of Cd-OTC/Sal complex. Figure S5: electronic absorption spectrum of complexes. Figure S6: thermogram of Cd-OTC/Sal complex. Figure S7: antibacterial activity showing growth inhibition zone around the loaded disc. Table S1: $^1\text{H-NMR}$ spectral data of complexes. Table S2: selected bond length, bond angle, and bond energy of complexes. (*Supplementary Materials*)

References

- [1] K. L. Haas and K. J. Franz, "Application of metal coordination chemistry to explore and manipulate cell biology," *Chemical Reviews*, vol. 109, no. 10, pp. 4921–4960, 2009.
- [2] A. Frei, J. Zuegg, A. G. Elliott et al., "Metal complexes as a promising source for new antibiotics," *Chemical Science*, vol. 11, no. 10, pp. 2627–2639, 2020.
- [3] T. Jurca, E. Marian, L. G. Vicaș, M. E. Mureșan, and L. Fritea, "Metal complexes of pharmaceutical substances," in *Spectroscopic Analyses—Developments and Applications*, Wiley, Hoboken, NJ, USA, 2017.
- [4] B. D. Nath, K. Takaishi, and T. Ema, "Macrocyclic multi-nuclear metal complexes acting as catalysts for organic synthesis," *Catalysis Science & Technology*, vol. 10, no. 1, pp. 12–34, 2020.
- [5] A. S. El-Tabl and S. M. Imam, "New copper (II) complexes produced by the template reaction of acetoacetic-2-pyridyl amide and amino-aliphatic alcohols," *Transition Metal Chemistry*, vol. 22, no. 3, pp. 259–262, 1997.
- [6] J. Bauer, H. Braunschweig, and R. D. Dewhurst, "Metal-only Lewis pairs with transition metal Lewis bases," *Chemical Reviews*, vol. 112, no. 8, pp. 4329–4346, 2012.
- [7] J. Qu, Y. Huang, and X. Lv, "Crisis of antimicrobial resistance in China: now and the future," *Frontiers in Microbiology*, vol. 10, 2019.
- [8] M. Gajdác and F. Albericio, "Antibiotic resistance: from the bench to patients," *Antibiotics*, vol. 8, no. 3, p. 129, Aug. 2019.
- [9] J. Lalucat, M. Mulet, M. Gomila, and E. García-Valdés, "Genomics in bacterial taxonomy: impact on the genus *Pseudomonas*," *Genes*, vol. 11, no. 2, p. 139, 2020.
- [10] C. S. Allardyce and P. J. Dyson, "Metal-based drugs that break the rules," *Dalton Transactions*, vol. 45, no. 8, pp. 3201–3209, 2016.
- [11] C. F. Markwalter, A. G. Kantor, C. P. Moore, K. A. Richardson, and D. W. Wright, "Inorganic complexes and metal-based nanomaterials for infectious disease diagnostics," *Chemical Reviews*, vol. 119, no. 2, pp. 1456–1518, 2018.
- [12] H. Petković, T. Lukežič, and J. Šušković, "Biosynthesis of oxytetracycline by *Streptomyces rimosus*: past, present and future directions in the development of tetracycline antibiotics," *Food Technology and Biotechnology*, vol. 55, no. 1, 2017.
- [13] C. Tafalla, B. Novoa, J. M. Alvarez, and A. Figueras, "In vivo and in vitro effect of oxytetracycline treatment on the immune response of turbot, *Scophthalmus maximus* (L.)," *Journal of Fish Diseases*, vol. 22, no. 4, pp. 271–276, Jan. 2002.
- [14] J. F. Leal, E. B. H. Santos, and V. I. Esteves, "Oxytetracycline in intensive aquaculture: water quality during and after its administration, environmental fate, toxicity and bacterial resistance," *Reviews in Aquaculture*, vol. 11, no. 4, pp. 1176–1194, 2018.
- [15] M. Cherlet, S. De Baere, and P. De Backer, "Quantitative analysis of oxytetracycline and its 4-epimer in calf tissues by high-performance liquid chromatography combined with positive electrospray ionization mass spectrometry," *The Analyst*, vol. 128, no. 7, p. 871, 2003.
- [16] S. Tongaree, D. R. Flanagan, and R. I. Poust, "The interaction between oxytetracycline and divalent metal ions in aqueous and mixed solvent systems," *Pharmaceutical Development and Technology*, vol. 4, no. 4, pp. 581–591, 1999.
- [17] S. Tongaree, A. M. Goldberg, D. R. Flanagan, and R. I. Poust, "The effects of pH and PEG 400-water cosolvents on oxytetracycline-magnesium complex formation and stability," *Pharmaceutical Development and Technology*, vol. 5, no. 2, pp. 189–199, 2000.
- [18] J. M. Wessels, W. E. Ford, W. Szymczak, and S. Schneider, "The complexation of tetracycline and anhydrotetracycline with Mg^{2+} and Ca^{2+} : a spectroscopic study," *The Journal of Physical Chemistry B*, vol. 102, no. 46, pp. 9323–9331, Nov. 1998.
- [19] A. Z. El-Sonbati, W. H. Mahmoud, G. G. Mohamed, M. A. Diab, S. M. Morgan, and S. Y. Abbas, "Synthesis, characterization of Schiff base metal complexes and their biological investigation," *Applied Organometallic Chemistry*, Article ID e5048, 2019.
- [20] S. A. Ali, A. A. Soliman, A. H. Marei, and D. H. Nassar, "Synthesis and characterization of new chromium, molybdenum and tungsten complexes of 2-[2-(methylaminoethyl)]pyridine," *Spectrochimica Acta Part A: Molecular and Biomolecular Spectroscopy*, vol. 94, pp. 164–168, 2012.
- [21] R. M. Ahmed, E. I. Yousif, and M. J. Al-Jeboori, "Co(II) and Cd(II) complexes derived from heterocyclic schiff-bases: synthesis, structural characterisation, and biological activity," *The Scientific World Journal*, vol. 2013, Article ID 754868, 6 pages, 2013.
- [22] A. Majumder, G. M. Rosair, A. Mallick, N. Chattopadhyay, and S. Mitra, "Synthesis, structures and fluorescence of nickel, zinc and cadmium complexes with the N,N,O-tridentate Schiff base N-2-pyridylmethylidene-2-hydroxy-phenylamine," *Polyhedron*, vol. 25, no. 8, pp. 1753–1762, 2006.
- [23] A. Golcu, M. Tumer, H. Demirelli, and R. A. Wheatley, "Cd(II) and Cu(II) complexes of polydentate Schiff base ligands: synthesis, characterization, properties and biological activity," *Inorganica Chimica Acta*, vol. 358, no. 6, pp. 1785–1797, Mar. 2005.
- [24] M. Kalinowska, J. Piekut, A. Bruss et al., "Spectroscopic (FT-IR, FT-Raman, ^1H , ^{13}C NMR, UV/VIS), thermogravimetric and antimicrobial studies of Ca(II), Mn(II), Cu(II), Zn(II) and Cd(II) complexes of ferulic acid," *Spectrochimica Acta Part A*:

- Molecular and Biomolecular Spectroscopy*, vol. 122, pp. 631–638, Mar. 2014.
- [25] J. dos Santos Ferreira da Silva, D. López Malo, G. Anceschi Bataglian et al., “Adsorption in a fixed-bed column and stability of the antibiotic oxytetracycline supported on Zn(II)-[2-Methylimidazole] frameworks in aqueous media,” *PLoS One*, vol. 10, no. 6, Article ID e0128436, 2015.
- [26] S. Gupta, A. K. Barik, S. Pal et al., “Oxomolybdenum(VI) and (IV) complexes of pyrazole derived ONO donor ligands—synthesis, crystal structure studies and spectroelectrochemical correlation,” *Polyhedron*, vol. 26, no. 1, pp. 133–141, 2007.
- [27] S. H. Tarulli, O. V. Quinzani, E. J. Baran, O. E. Piro, and E. E. Castellano, “Structural and spectroscopic characterization of two new Cd(II) complexes: bis(thiosaccharinato) bis(imidazole) cadmium(II) and tris(thiosaccharinato) aquacadmium(II),” *Journal of Molecular Structure*, vol. 656, no. 1–3, pp. 161–168, Aug. 2003.
- [28] G. More, D. Raut, K. Aruna, and S. Bootwala, “Synthesis, spectroscopic characterization and antimicrobial activity evaluation of new tridentate Schiff bases and their Co(II) complexes,” *Journal of Saudi Chemical Society*, vol. 21, no. 8, pp. 954–964, 2017.
- [29] S. Nzikayel, I. J. Akpan, and E. C. Adams, “Synthesis, FTIR and electronic spectra studies of metal (II) complexes of pyrazine-2-carboxylic acid derivative,” *Medicinal Chemistry*, vol. 7, no. 11, 2017.
- [30] M. M. Omar, H. F. Abd El-Halim, and E. A. M. Khalil, “Synthesis, characterization, and biological and anticancer studies of mixed ligand complexes with Schiff base and 2,2'-bipyridine,” *Applied Organometallic Chemistry*, vol. 31, no. 10, Article ID e3724, 2017.
- [31] D. Kumar, S. Chadda, J. Sharma, and P. Surain, “Syntheses, spectral characterization, and antimicrobial studies on the coordination compounds of metal ions with schiff base containing both aliphatic and aromatic hydrazide moieties,” *Bioinorganic Chemistry and Applications*, vol. 2013, Article ID 981764, 10 pages, 2013.
- [32] O. A. M. Ali, “Synthesis, spectroscopic, fluorescence properties and biological evaluation of novel Pd(II) and Cd(II) complexes of NOON tetradentate Schiff bases,” *Spectrochimica Acta Part A: Molecular and Biomolecular Spectroscopy*, vol. 121, pp. 188–195, Mar. 2014.
- [33] M. H. A. Al-Amery, “Synthesis, Characterization and antibacterial studies of mixed ligand complexes of 2-phenyl-2-(o-tolylamino) acetonitrile and 1,10-phenanthroline with some metal ions,” *Der Pharma Chemica*, vol. 9, pp. 59–69, 2017.
- [34] S. Pasayat, S. P. Dash, Saswati et al., “Mixed-ligand aroyl-hydrazone complexes of molybdenum: synthesis, structure and biological activity,” *Polyhedron*, vol. 38, no. 1, pp. 198–204, 2012.
- [35] M. Bagherzadeh, M. Amini, A. Ellern, and L. K. Woo, “Catalytic efficiency of a novel complex of oxoperoxo molybdenum (VI): synthesis, X-ray structure and alkane oxidation,” *Inorganic Chemistry Communications*, vol. 15, pp. 52–55, 2012.
- [36] A. M. Kamel, P. R. Brown, and B. Munson, “Electrospray ionization mass spectrometry of tetracycline, oxytetracycline, chlorotetracycline, minocycline, and methacycline,” *Analytical Chemistry*, vol. 71, no. 5, pp. 968–977, Mar. 1999.
- [37] R. Gomathi, A. Ramu, and A. Murugan, “Evaluation of DNA binding, cleavage, and cytotoxic activity of Cu(II), Co(II), and Ni(II) schiff base complexes of 1-phenylindoline-2,3-dione with isonicotinohydrazide,” *Bioinorganic Chemistry and Applications*, vol. 2014, Article ID 215392, 12 pages, 2014.
- [38] S. A. Shaker, “Preparation and spectral properties of mixed-ligand complexes of VO(IV), Ni(II), Zn(II), Pd(II), Cd(II) and Pb(II) with dimethylglyoxime and N-acetyl glycine,” *E-Journal of Chemistry*, vol. 7, no. 1, pp. S580–S586, 2010.
- [39] A. Ahmed and R. A. Lal, “Synthesis and electrochemical characterisation of molybdenum(VI) complexes of disalicylaldehyde malonoyl-dihydrazone,” *Journal of Molecular Structure*, vol. 1048, pp. 321–330, 2013.
- [40] M. M. H. Khalil and F. A. Al-Seif, “Molybdenum and tungsten tricarbonyl complexes of isatin with triphenylphosphine,” *Research Letters in Inorganic Chemistry*, vol. 2008, Article ID 746058, 4 pages, 2008.
- [41] M. Saif, M. M. Mashaly, M. F. Eid, and R. Fouad, “Synthesis, characterization and thermal studies of binary and/or mixed ligand complexes of Cd(II), Cu(II), Ni(II) and Co(III) based on 2-(Hydroxybenzylidene) thiosemicarbazone: DNA binding affinity of binary Cu(II) complex,” *Spectrochimica Acta Part A: Molecular and Biomolecular Spectroscopy*, vol. 92, pp. 347–356, 2012.
- [42] P. Cervini, B. Ambrozini, L. C. M. Machado, A. P. G. Ferreira, and É and ra Cavalheiro, “Thermal behavior and decomposition of oxytetracycline hydrochloride,” *Journal of Thermal Analysis and Calorimetry*, vol. 121, no. 1, pp. 347–352, 2015.
- [43] S. Ramotowska, M. Wysocka, J. Brzeski, A. Chylewska, and M. Makowski, “A comprehensive approach to the analysis of antibiotic-metal complexes,” *TrAC Trends in Analytical Chemistry*, vol. 123, p. 115771, 2020.
- [44] R. Gaur and P. Jeevanandam, “Effect of anions on the morphology of CdS nanoparticles prepared via thermal decomposition of different cadmium thiourea complexes in a solvent and in the solid state,” *New Journal of Chemistry*, vol. 39, no. 12, pp. 9442–9453, 2015.
- [45] X. Chen, J. Qi, P. Wang, C. Li, X. Chen, and C. Liang, “Polyvinyl alcohol protected Mo₂C/Mo₂N multicomponent electrocatalysts with controlled morphology for hydrogen evolution reaction in acid and alkaline medium,” *Electrochimica Acta*, vol. 273, pp. 239–247, 2018.
- [46] F. Chen, X. Zou, C. Chen et al., “Surfactant-free synthesis of homogeneous nano-grade cadmium sulfide grafted reduced graphene oxide composite as a high-activity photocatalyst in visible light,” *Ceramics International*, vol. 45, no. 11, pp. 14376–14383, 2019.
- [47] B. B. Mahapatra, R. R. Mishra, and A. K. Sarangi, “Synthesis, spectral, thermogravimetric, XRD, molecular modelling and potential antibacterial studies of dimeric complexes with bis bidentate ON-NO donor Azo dye ligands,” *Journal of Chemistry*, vol. 2013, Article ID 653540, 11 pages, 2013.
- [48] P. Mishra, “Biocoordination and computational modeling of novel ligands with Bi (V),” *International Journal of ChemTech Research*, vol. 1, no. 3, pp. 401–419, 2009.
- [49] S. A. Mousavi, M. Montazerzohori, R. Naghiha, A. Masoudiasl, S. Mojahedi, and T. Doert, “Some novel hexa-coordinated cadmium Schiff base complexes: X-ray structure, Hirshfeld surface analysis, antimicrobial and thermal analysis,” *Applied Organometallic Chemistry*, vol. 34, no. 4, Article ID e5048, 2020.
- [50] L. Tabrizi, P. McArdle, M. Ektefan, and H. Chiniforoshan, “Synthesis, crystal structure, spectroscopic and biological properties of mixed ligand complexes of cadmium(II), cobalt(II) and manganese(II) valproate with 1,10-phenanthroline and imidazole,” *Inorganica Chimica Acta*, vol. 439, pp. 138–144, 2016.

Preparation, Spectroscopic Analysis, and Biological Assessment of Heteroleptic Zr(II) and Pd(II) Complexes From Otc/Sal Mixed Ligands

Rohit Kumar Dev, Yuv RajSahu, Narendra Kumar Chaudhary, and Ajaya Bhattarai*

Department of Chemistry, Mahendra Morang Adarsh Multiple Campus, Tribhuvan University, Biratnagar, Nepal

*Corresponding author: bkajaya@yahoo.com

Submitted: 15 Oct 2022, 27 Dec 2022, accepted 07 Jan 2023

Abstract

The two new novel heteroleptic complexes of the type $[M(II)L_1.L_2]$ ($M = Zr(II) \& Pd(II)$, $L_1 =$ Oxytetracycline (Otc), and $L_2 =$ Salicylaldehyde (Sal)) have been synthesized and analyzed by physical measurements such as CHN, pH, and conductivity. The conductivity data revealed the electrolytic nature of Pd(II)Otc/Sal and the non-electrolytic nature of the Zr(II)Otc/Sal metal complex of mixed ligand. The structural characterizations of the metal complex were approved by spectroscopic analysis methods, such as FT-IR, 1H & ^{13}C -NMR, UV/Visible, and ESI-MS studies. Thermal analysis (TGA/DTA) determines the thermal and kinetic stabilities of the metal complexes using a popular Coats-Redfern equation through which the activation parameters can be calculated easily. SEM can determine the surface morphology of metal complexes. The selected bond lengths, bond angles, final optimized energy, and geometry of complexes were obtained by running an optimization task in the 3D molecular modeling software program via Chem 3D Pro. 12.0.2. The final geometrical energy was found to be 921.7712 for Zr(II)Otc/Sal and 914.6006 Kcal/mol for Pd(II)Otc/Sal complexes. Based on the above study, Zr(II)Otc/Sal complex has tetrahedral geometry and the Pd(II)Otc/Sal complex has square planar geometry. The complexes were tested *in vitro* for antibacterial susceptibility study against various strains of clinical pathogenic bacteria such as *Staphylococcus aureus* (Gram-positive), *Proteus mirabilis*, and *Escherichia coli* (Gram-negative). For the antibacterial study, the Kirby-Bauer paper disc diffusion technique is applied by using 50, 25, and 12.5 $\mu g/\mu L$ concentrations of the metal complex. All the synthesized complexes were found to have good antibacterial susceptibility against all tested pathogens.

Keywords: Antibacterial activity, Heteroleptic complex, Mixed ligand, Oxytetracycline, TGA/DTA.

Introduction

Diversity in the biochemical behavior of coordination compounds containing organic ligands with N, O, and S donor atoms has created a great impact on pharmacology because many such compounds are valuable in chemotherapeutics [1]. In the present day, the formation of a metal complex of mixed ligands between bioactive ligands (having binding sites) and 4d-transition metal (II) ions have gained much interest [2]. Coordination chemistry is an important

property of metal ions that use different ligands [3]. Here, metal ions can show an inductive effect through the coordination site of the reaction and serve as oxidation-reduction via electron transfer reaction [4]. The transition metal complexes of the mixed ligand are mediators of bio-reaction and the technological process of the living organism [5]. In addition to biological functions, metal complexes are widely used in analytical, oxygen carriers, and organic catalysis reactions [6]. Currently, antibiotics

are one of the biggest global health threats to the modern scientific world. The factors associated with antibiotic resistance are compounded by overuse of antibiotics, abuse of treatment, and lack of financial support for complete treatment [7, 8, 9].

Oxytetracycline (Otc) is a broad-spectrum antibiotic of the tetracycline family used to prepare metal complexes. The Otc can inhibit protein synthesis for fixation on the 30s ribosomal subunit and can apply to both veterinary and human medical treatment. Because of hydroxyl and amino groups, Otc has both an acidic and basic nature [10, 11, 12]. Otc is mostly applied on farms and poultry farming. Because of its soluble nature, the animal's body cannot absorb the Otc compound [13]. Nearly 10% - 40% is only absorbed by animals and the rest 60% - 90% is excreted out into the environment, causing negative effects on the environment and human beings. Currently, anaerobic digestion (AD) is mostly used as a cost-effective and environmentally friendly process to check manure or sludge. Because of the high concentration in manure, the effects of antibiotics on AD can be easily investigated [14, 15].

The next compound, salicylaldehyde (Sal) along with its derivatives, can strongly coordinate with complexes and gives a variety of geometries [16]. Besides, their derivatives and diamines can behave as a potential catalysts for introducing oxygen into an organic compound [17]. Among the transition metal, zirconium acts as a homogenous catalyst because of its biological and pharmaceutical nature [18]. Similarly, palladium is a versatile metal that acts as a homogeneous and heterogeneous catalyst with a wide range of C-C coupling, hydrocarbon oxidation reactions, and C-H functionalization reactions [19, 20]. Palladium is a suitable metal for metallodrugs because of its structural properties that are like those with platinum and can exhibit *in vitro* cytotoxicity and their ions in coordination can form square planar geometries [21]. Today, many studies have proved that Otc is an old-generation antibiotic because of its resistance to many pathogenic bacteria [22, 23]. Because of the chelating and biological nature of the

Zr(II) and Pd(II) complexes, it has been important to synthesize and characterize new derivatives of Otc.

In the current paper, we deal with the preparation of complexes by continuous heating and refluxing the equimolar mixture of the primary ligand (Otc), secondary ligand (sal), and 4d-transition metal salts [M=Zr(II) and Pd(II)]. This investigation was further extended to physicochemical and spectroscopic characterization: FT-IR, ^1H & ^{13}C -NMR, UV/Visible, ESI-MS, TGA/DTA, and SEM. The metal complexes were also done through molecular modeling and antibacterial susceptibility against various strains of bacteria.

Experimental Methods

Materials and reagents

The reagents and chemicals employed for the synthesis of metal complexes were of AR grade and were used without further purification. The used chemicals such as oxytetracycline hydrochloride (TCI), MHA, PdCl_2 (Himedia), $\text{ZrOCl}_2 \cdot 8\text{H}_2\text{O}$, and salicylaldehyde (Loba Chemie Pvt. Ltd) were collected from a supplier. Distilled ethanol and triple-distilled water were used during the synthesis process. High-grade borosilicate glassware was used during the research.

Physical measurements

The percentage of CHN was done by a micro analyzer, Euro-E 3000 for CHN analysis. pH was measured at $25\text{ }^\circ\text{C} \pm 0.1\text{ }^\circ\text{C}$ on Eutech Instrument, 2700 pH/Mv/ $^\circ\text{C}/^\circ\text{F}$ meter. The conductivity was measured by a digital conductivity meter called auto-ranging/TDSmeter TCM 15+ instrument. The instrument called VEEGO ASD-10013 programmable measures the melting point of the metal complex. In the range of $4000\text{-}400\text{ cm}^{-1}$, the FT-IR spectrum was recorded by Perkin Elmer Spectrum II instrument under KBr pellets. The ^1H and ^{13}C -NMR spectra were recorded on a Bruker AvII (400 MHz) instrument using DMSO- d_6 solvent at room temperature. Electronic absorption spectra were plotted in the range of 260-280 nm on a Varian Cary 5000 instrument in DMSO at 0.001M concentration. The ESI-MS spectra were recorded using an instrument called a water UPLC-TQD mass

spectrometer. At a room temperature of 756 °C, the kinetic and thermal stabilities of the complexes were calculated from Perkin Elmer Diamond TGA/DTA instrument with a linear heating rate of 10°C under a nitrogen atmosphere. The SEM instrument (JEOLJSM-6390 LV) helps to detect the surface morphology. Molecular modeling was done through the 3D modeling software program, Chem 3D Pro 12.0.2. Antibacterial activities were performed at the microbiological laboratory, Department of Microbiology, M. M. A.M. Campus, T.U., Biratnagar, Nepal.

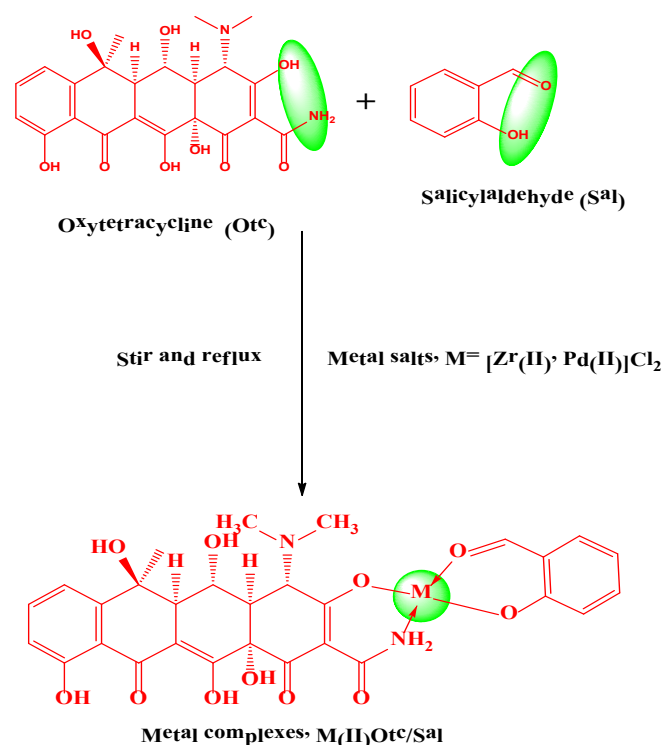
Synthesis of the metal complex of mixed ligands

The Zr(II)Otc/Sal and Pd(II)Otc/Sal metal complexes were prepared simply as mentioned below. To 10 ml of aq. solution of ZrOCl₂/ 10% HCl ethanolic solution and PdCl₂ (0.3565g, 2 mmol) was mixed with continuous stirring and heating 70% ethanolic solution (20ml) of Otc (0.9945g, 2mmol). To this following mixture, salicylaldehyde (0.2 ml, 2 mmol) was mixed in a drop-wise manner and stirred for an hour. The stirred solution was then refluxed for 8 h and ammonia solution was added to make a pH of 7, resulting in precipitates. The precipitate was filtered and then washed with ethanol. Thus, the obtained

dried precipitate was recrystallized and kept inside a vacuum desiccator over anhyd. CaCl₂. Finally, the dried complexes were stored in a vial for further use [24, 25]. The percentage yield was 50-60%. The synthetic route for M-Otc/Sal [M=Zr(II), Pd(II)] complexes are reported in **Scheme 1**.

Antibacterial susceptibility test

Zr(II)Otc/Sal and Pd(II)Otc/Sal complexes were screened for their anti bacterial susceptibility test with the help of human pathogenic bacteria such as *Staphylococcus aureus* (Gram-positive), *Escherichia coli*, and *Proteus mirabilis* (Gram-negative). The Kirby-Bauer paper disc diffusion method is applied for the study. For the test, 30% DMSO solvent of various concentrations such as 50, 25, and 12.5 µg/µL was selected for the test solution. The blank disc (5mm diameter) was prepared from filter paper (Whatman No. 1) using a punching machine. In a freshly prepared nutrient agar medium, the bacterial culture was revived and kept for a few hours in an incubator at 37 °C for the complete growth of the organism. MHA media, blank paper discs, and Petri plates were prepared and sterilized inside the autoclave. Under UV laminar flow, the media was solidified to prevent the contamination of bacteria. The solidified MHA plates were seeded with freshly revived bacteria and sterilized blank paper discs. 10 µL of test solutions (complex) was loaded into the disc under UV laminar flow. To compare the effectiveness of a metal complex, amikacin behaves as positive control while a blank disc soaked in DMSO as solvent control. While doing the above activities, the used plates are placed inside the incubator at 37 °C for 24 h. Finally, the antibiogram zone measuring scale measures the diameter of the inhibition zone (in mm) [26, 27].



Scheme 1: Synthetic route for the preparation of the metal complex.

RESULTS AND DISCUSSION

Properties of the complexes

The complexes explained in this current article were characterized by physicochemical and spectroscopic methods. The satisfactory result obtained from micro elemental analysis exhibited that the complexes are of a 1:1 molar ratio. Here, all the synthesized complexes are thermally stable and are not affected by air and

Table 1: Physical and microanalytical measurement data of Zr(II)Otc/Sal and Pd(II)Otc/Sal complexes

Complexes	Empirical formula	Mol. Weight	Color	m.p.	Calculated (found)%				
					C	H	N	O	M
Zr(II)Otc/Sal	C ₂₉ H ₂₈ ZrN ₂ O ₁₁	671.76	Black	>260	51.85 (51.80)	4.20 (4.26)	4.17 (4.15)	26.20 (26.24)	13.58 (13.55)
Pd(II)Otc/Sal	C ₂₉ H ₂₈ PdN ₂ O ₁₁	686.96	Black	>260	50.70 (50.67)	4.11 (4.08)	4.08 (4.17)	25.62 (25.84)	15.49 (15.24)

Table 2: The infrared spectral absorption data of Zr(II)Otc/Sal and Pd(II)Otc/Sal metal complex in cm⁻¹

Complexes	$\nu(\text{O-H/NH})$	$\nu(\text{CH})$ Methyl	$\nu(\text{C=O})$	$\nu(\text{C=C})$ Aromatic	$\nu(\text{C-N})$	$\nu(\text{C-O})$	$\nu(\text{M-O})$
Zr(II)Otc/Sal	3426	3055	1614	1502	1456	1240	552
Pd(II)Otc/Sal	3428	2941	1622	1455	1387	1230	603

moisture. The change in color during complex formation is because of the metallation of metal ions with ligands and different electronic transitions like π bonding or non-bonding or by the free electron. In the presence of auxochrome, the chromophore exhibits electronic absorption of the spectrum in the UV/Visible region and finally gives color to the complexes. The solubility behavior of metal complexes was investigated using various solvents such as water, ethanol, methanol, acetone, chloroform, DMF, and DMSO. All the complexes are miscible in DMF and DMSO solvents while immiscible in water.

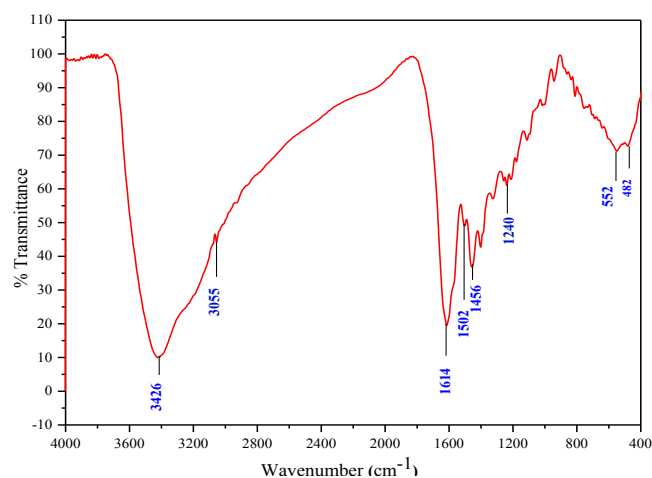
The higher value of conductivity shows a complexation behavior of metal ions. The obtained data showed that the synthesized metal complexes have electrolytic nature. The complex nature of the ligand during the formation of the metal complex is because of the deprotonation and change in pH. The physical and microanalytical measurement data Zr(II)Otc/Sal and Pd(II)Otc/Sal complexes were reported in Table 1.

Spectroscopic parameters

3.2.1 FT-IR spectroscopic study

Figure 1 and S1, show the FT-IR spectrum of the Zr(II)Otc/Sal and Pd(II)Otc/Sal complexes, and their characteristic absorption data were presented in Table 2. The intense peaks at 3426 cm⁻¹ and 3428 cm⁻¹, are assigned to $\nu(\text{OH/NH})$ stretching vibration [28, 29]. The C-H stretching and bending vibration lies in

the region of 3061 cm⁻¹ and 2941 cm⁻¹ respectively [30, 31]. Similarly, the strong absorption bands with stretching vibration of the carbonyl (C=O) group were seen at 1614 cm⁻¹ and 1622 cm⁻¹ regions in the spectrum [32, 33]. The aromatic $\nu(\text{C=C})$ absorption bands are at 1502 cm⁻¹ and 1455 cm⁻¹ respectively [34]. The complexes at (1456 and 1387) cm⁻¹ are due to a characteristic band $\nu(\text{C-N})$; this band denotes the carbon-nitrogen bond order intermediate between a single bond. Thus, metal shows the coordination of nitrogen with ions [35]. Similarly, the peak at 1240 cm⁻¹ and 1230 cm⁻¹ are due to $\nu(\text{C-O})$ [36, 37]. In addition, the peaks at 552 cm⁻¹ and 603 cm⁻¹, were assigned to the $\nu(\text{M-O})$ respectively, which is proved by the presence of the IR band of the low-frequency band of the coordination mode [38, 39].

**Figure 1.** The infrared spectrum of the Zr(II)Otc/Sal metal complex

¹H and ¹³C-NMR spectroscopic study

The ¹H-NMR gives information about the chemical shift value and proton environment of the complexes. The chemical shift data are reported in Table S1 and Figure S2 and S3. In the Zr(II)Otc/Sal metal complex, aromatic ring protons are assigned as multiplet between δ 7.023-7.279 ppm. These protons moved upfield slightly to confirm the coordination of metal ions with the ligands [40]. A single peak at δ 1.047-1.082 ppm, was assigned to the methyl proton. A high-intensity peak at δ 2.543 ppm is observed and is supposed to be of DMSO solvent and the peak at δ 3.399-3.406 ppm is assigned to be of -NCH₃. In the same way, in the Pd(II)Otc/Sal metal complex, aromatic ring protons are observed and are assigned as multiplet between δ 6.632-7.516 ppm [41]. These protons moved upfield slightly to confirm the coordination of metal ions with the ligands. A single peak at δ 1.040-1.075 ppm, is assigned to a methyl proton. A high-intensity peak observed at δ 2.500 ppm is supposed to be of DMSO solvent and the peak at δ 3.412-3.465 ppm is assigned to be of the -NCH₃ group [42]. Hence, all the values in the peak of the ¹H-NMR spectra showed a good relationship with the proposed structure of the complexes.

The ¹³C-NMR spectral study gives knowledge regarding the different carbon atoms, mode of bonding, and geometry of the complexes. The spectra were recorded in the DMSO-d₆ solvent and their pictorial representation was reported in Figure S4 and S5 and Table S2. In the ¹³C-NMR spectra of the Zr(II)Otc/Sal metal complex, the carbon resonance signals of methyl, DMSO, and CH group appeared at δ (18.366, 40, and 55.821-55.942) ppm respectively [43]. Similarly, in the Pd(II)Otc/Sal metal complex spectra, the signal observed at δ 137.147 ppm in the spectrum was assigned to the aromatic carbon signal, which remains the same in the literature. The upfield shift of the carbon signal, which appears at δ 34.257 ppm confirms the -CH₂ group. The signals that appeared at δ (40, 71.543, and 84.502) ppm in the spectra were assigned to be DMSO, -CH, and C=C groups respectively [44]. Thus, the (¹H and ¹³C)-NMR spectra, confirm all measured values of carbon atoms to their chemical shift value.

Mass spectroscopic studies

ESI-MS spectrum helps to explain the molecular weight and structure of ligand and metal complexes. The spectrum also displays the fragmentation pattern and the most fragile points in the compound. The ESI-mass spectrum of the metal complexes recorded important peaks and their intensities for molecular ions, as shown in Figure 2 and S6. Besides the most abundant peaks, there are many fewer abundant peaks seen in the spectrum that depends on the ligand. The mass spectrum of metal complexes showed a well-defined peak at *m/z*-671 and 687 amu signifies molecular-ion peak [M+H]⁺. assigned to the molecular formula of Zr(II)-Otc/Sal and Pd(II)-Otc/Sal metal complexes (C₂₉H₂₈ZrN₂O₁₁ and C₂₉H₂₈PdN₂O₁₁), which confirms that the stoichiometry ratio of the metal-to-ligand ratio is 1:1. The base peak lies at *m/z*-176 and *m/z*-365 amu respectively in Zr(II)-Otc/Sal and Pd(II)-Otc/Sal metal complexes. There is also another additional peak called fragment ion peak lies near *m/z* 665, 614, 608, 566, 538, 536, 502, 461, and 453 amu in the Zr(II)-Otc/Sal complex, while at *m/z* 659, 620, 600, 563, 510, 443, 426, and 410 amu respectively, for the Pd(II)-Otc/Sal metal complex [45, 46].

Electronic absorption spectra

The UV/Visible spectroscopy measures the geometry of the metal complex and the spectra determine the effect of splitting of d-orbital during complexation. At room temperature, the significant electronic spectral data of Zr(II)Otc/Sal and Pd(II)Otc/Sal complexes were measured in DMSO solvent from 200 to 630 nm using the same solvent as the blank. The spectral data and absorption bands were reported in Figure S7 and Table S3. The Zr(II)Otc/Sal metal complex showed the spectral bands at 379 nm, which corresponds to the ligand to metal-charge-transfer (Zr→L) or $\pi \rightarrow \pi^*$ transition [47, 48]. The Zr(II) metal complex has no d-d transition because of its d⁰ electronic configuration, and therefore, the complex has tetrahedral geometry and diamagnetic nature [49]. Similarly, the electronic spectrum of Pd(II) complexes showed four bands at 265, 271, 386, and 457 nm respectively. These are attributed due to the intraligand $\pi \rightarrow \pi$ as well as spin-allowed LMCT

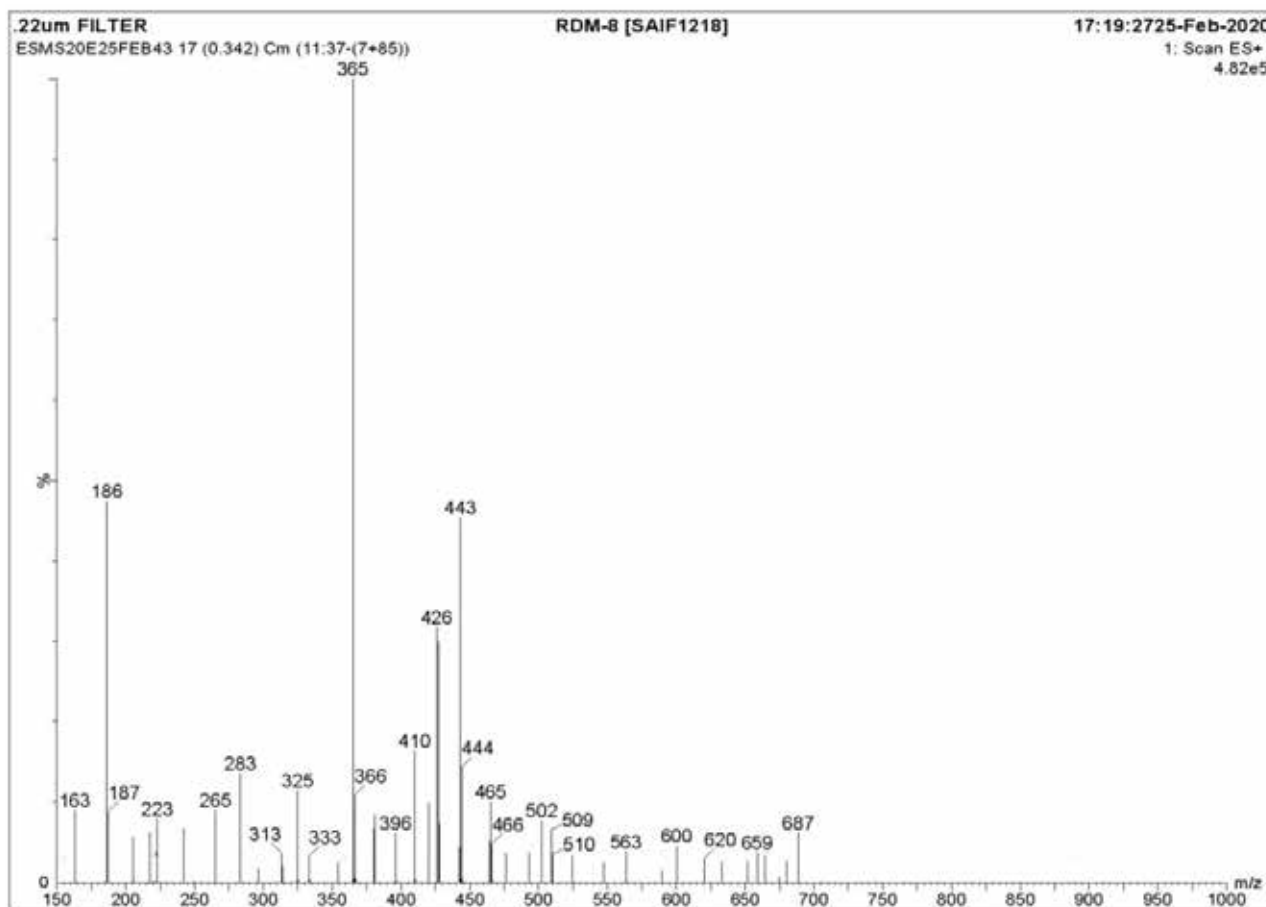


Figure 2. Mass spectrum of the Pd(II)Otc/Sal metal complex

d-d transition. The complex at 386 nm is attributed to the $1A_2g \rightarrow 1B_1g$. The above transitions showed that the complex has a diamagnetic nature, and this assignment refers that the complex has square planar coordination around the metal ions [50, 51, 52, 53].

TGA/DTA analysis

Thermal gravimetric analysis techniques help to determine the thermal behavior of the complexes. This technique also deals with decomposition steps, temperature range, % weight loss, and decomposition products. At room temperature (40.15°C – 755.5°C), the analysis was performed with a linear heating rate of $10^\circ\text{C}/\text{min}$ under a nitrogen atmosphere. The data of thermal decomposition was calculated and is presented in Table S4, which shows a better result than the data for the microanalytical. Consistent results were drawn from the current research work. In the thermogram of the Zr(II)Otc/Sal complex, the decomposition occurs at three different phases with a temperature range of 62.42°C – 750.58°C . The first decomposition step occurred at 62.42°C – 132.18°C ,

with a mass loss of 1.19% (-0.433 mg), which denotes the removal of hydrated water molecules. The second step appeared at 187.96°C – 291.00°C , with a mass loss of 1.51% (-0.350 mg). The final phase decomposition at 490.46°C – 750.58°C , representing a total mass loss of 7.56% (-0.929 mg) from the metal complex resulting in a stable residue as metal oxide (ZrO+C). Similarly, the thermogram of the Pd(II)Otc/Sal complex showed that the decomposition occurs in two different phases between a temperature range of 45.34°C – 252.87°C . The first decomposition step occurred at 45.34°C – 69.61°C , with a mass loss of 4.31% (-2.535 mg), which denotes the removal of hydrated water molecules. The second step appeared at 218.62°C – 252.87°C , with a mass loss of 8.69% (-2.751 mg) in the ligand from the metal complex, leaving behind a stable residue as metal oxide (PdO+C). The metal complexes showed their thermograms as presented in Figure 3 and S8.

Table 3. Thermodynamic and kinetic parameters of the Zr(II)Otc/Sal and Pd(II)Otc/Sal complexes

Complexes	r	A(s ⁻¹)	Tmax(K)	E*(kJ/mol)	ΔS*(j/kmol)	ΔH*(kJ/mol)	ΔG*(kJ/mol)
Zr(II)Otc/Sal	-0.99501	1727.835	365.86	1273.871	-184.630	-1766.642	65754.543
	-0.99424	890.887	513.75	968.248	-192.964	-3303.069	95831.9546
	-0.98972	386.589	868.33	641.508	-204.268	-6577.787	170794.268
Pd(II)Otc/Sal	-0.99622	2.99740	324.508	0.63236	-236.49	-2697.33	-74045.57
	-0.99043	0.77258	504.75	0.305955	-251.43	-4196.19	122714.24

Kinetic parameter study

The thermodynamic and kinetic parameters of metal complexes having different decomposition phases were calculated by using a very well-known equation called the Coats-Redfern equation. The parameters were graphically plotted with the help of the Coats-Redfern equation (1).

$$\ln \left[-\frac{\ln(1-\alpha)}{T^2} \right] = \ln \left[\frac{AR}{\beta E^*} \right] - \frac{E^*}{RT} \quad (1)$$

Here, T denotes the temperature of the DTG curve, β and R represent the linear heating rate, and the Universal gas constant. A and E* represent the Arrhenius pre-exponential factor and energy of activation. By applying a straight line equation, y = mx + c, a linear plot on the left-hand side vs 1/T, gives a slope (-E*/R) that determines the energy of activation. Finally, ΔS*, ΔH*, and ΔG* can be calculated by applying the successive relations 2-4.

$$\Delta S^* = R \ln \left[\frac{Ah}{K_B T} \right] \quad (2)$$

$$\Delta H^* = E^* - RT \quad (3)$$

$$\Delta G^* = \Delta H^* - T \Delta S^* \quad (4)$$

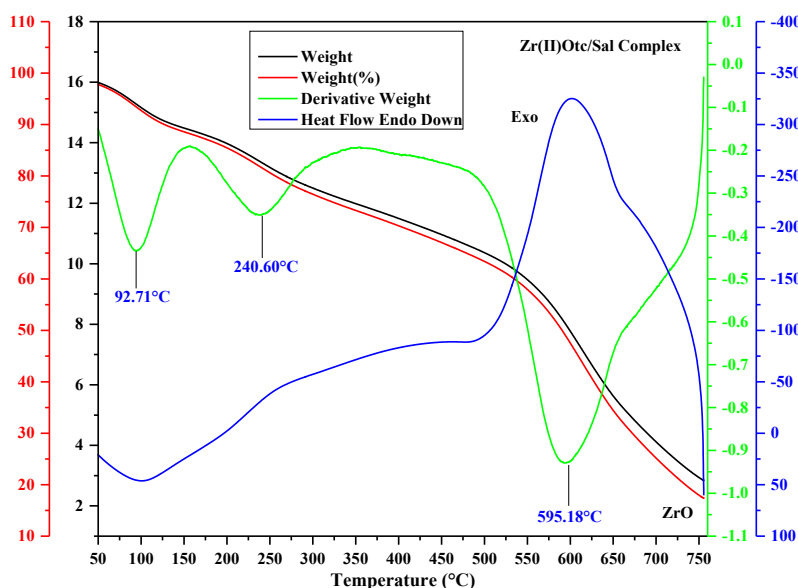
Here, kinetic and thermodynamic parameters of the different decomposition phases [54, 55, 56] are calculated and reported in Tables 3 and S4. The following remarks can be derived from the above results:

1. On moving to another decomposition step, the activation energy (E*) value decreases. Hence, the rate

becomes weak and shows higher stability of metal complexes.

2. In most of the decomposition steps, the entropy of activation having a negative value (-ΔS*) signifies the slowdown of the reaction condition having more ordered activated complexes and reflects spontaneous decomposition steps.
3. The negative value of enthalpy (-ΔH*) signifies the exothermic process of decomposition.
4. The positive value of Gibb's free energy of activation (-ΔG*) reflects its non-spontaneous nature.

Thus, the calculated data of the correlation coefficient (r) obtained with the help of the graphical plot signifies a better fit with the linear function.

**Figure 3.** Thermogram of Zr(II)Otc/Sal metal complex

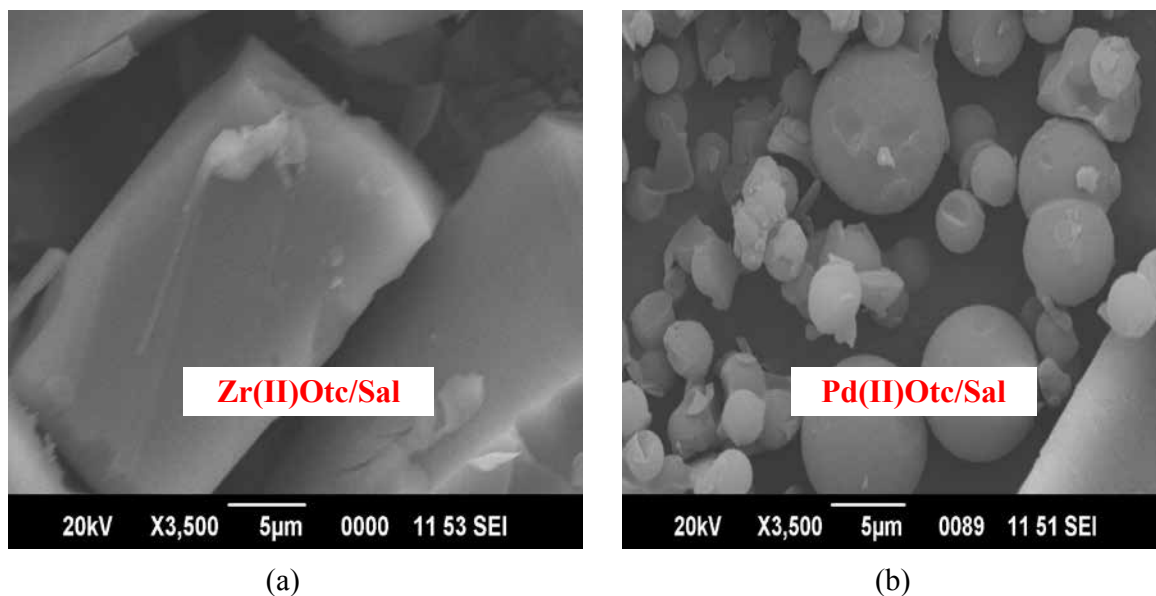


Figure 4. SEM micrograph of Zr(II)Otc/Sal and Pd(II)Otc/Sal metal complexes

SEM study of M(II)-Otc/Sal metal complexes

SEM (scanning electron microscopy) is an instrumental method that gives knowledge regarding the surface morphology comparison of metal complexes. The unique characteristics of the micrograph will indicate the shape, size, arrangement, ductility, and strength of the metal complexes. The micrograph of Zr(II)Otc/Sal complex (a) displays the surface particles are clear, smooth, and not aggregated, but besides the metal ion, the surface particles become rough and fully covered [57]. Similarly, Pd(II)Otc/Sal metal complex (b) revealed that the complex exhibits uniform and spherical morphology on its surface [58], and is presented in Figure 4.

Molecular Modeling

Molecular modeling investigates the clear and deep geometry of the proposed structure of the complex. Here, the modeling was performed through a 3D modeling software called the Chem 3D Pro12.0.2 program. After geometrical optimization, the complexes Zr(II)Otc/Sal and Pd(II)Otc/Sal have tetrahedral and square planar geometries with final geometrical energies of 921.7712 and 914.6006 (kcal/mol), resulting in stable stability. The optimized structures are shown in Fig.-S9 and S10. With the help of the MM2 program, energy minimization was repeated many times to note the minimum energy value. The difference in the values of M-N and M-O

in the complexes further shows the metallation of ligands with the metal ions [59]. The computational findings showed that the proposed structure and geometry of complexes are in better agreement with the literature. Table S5 represents the data of selected bond length, bond angle, final optimized energy, and geometry of the metal complexes.

Swiss ADME study

The web tool server (Swiss ADME) is used to calculate the parameters such as absorption, distribution, metabolism, and excretion as well as physicochemical properties [60, 61]. By this computation, the lipophilicity, pharmacokinetics, drug-likeness, and medicinal chemistry of the compound are depicted in Figure S12 and S13 [62]. Here, the drug-likeness is estimated as whether the molecule is considered an oral drug according to its availability. Pharmacokinetics properties such as BOB (Blood-brain barrier), GIA (gastrointestinal absorption), and penetration through P-gp substrate were studied and compared with oxytetracycline and salicylaldehyde as a controlled drug. When compared to the allowed value for polarity TPSA (Total polar surface area -217.15 Å), lipophilicity ($\log P_o/W < 1$), solubility ($\log S < 1$), size (MW- 671.76 g/mol), $\log K_p$ (skin permeation-10.27 Cm/S). These all values are reported in Table 6. The above metal complexes showed calculated values within these limits. Finally,

Table 4. The data of antibacterial growth inhibition zone of Zr(II)Otc/Sal and Pd(II)Otc/Sal metal complexes

Complexes	The diameter of the zone of inhibition in (mm)								
	<i>S. aureus</i>			<i>P. mirabilis</i>			<i>E. coli</i>		
Pathogenic Bacteria									
Concentrations ($\mu\text{g}/\mu\text{L}$)	50	25	12.5	50	25	12.5	50	25	12.5
Zr(II)Otc/Sal complex	23	21	20	14	12	10	12	11	10
Pd(II)Otc/Sal complex	18	17	12	18	13	12	10	9	8
Amk (30mcg/disc)	21			21			14		
OTC-Ethanol	37			33			28		
OTC-DMSO	41			34			29		
DMSO	0			0			0		

the complexes showed a low GIA (gastrointestinal absorption potential) and ability to cross the BBB (blood-brain barrier). These results eventually led to the conclusion that the prepared complexes may be a better candidate as an antibacterial drug soon [63]. The predicted description showed that the complexes have good lipophilicity and human intestinal absorption. In addition, it is easy to pass through the BBB, inhibiting various CYP metabolic enzymes to act as β -glycoprotein substrates, and ultimately has drug-like properties as adopted by such as Lipinski, Ghose, Egan, and Muegge. This rule does not violate the test [64].

Antibacterial Susceptibility Study

The *in vitro* antibacterial susceptibility activities of Zr(II)Otc/Sal and Pd(II)Otc/Sal metal complexes were done by measuring the zone of inhibition via the Kirby-Bauer paper disc diffusion technique [65, 66]. For the antibacterial test, two strains of bacteria were selected: *Staphylococcus aureus* (gram-positive), *Escherichia coli*, and *Proteus mirabilis* (gram-negative). In DMSO solvent, the three different concentrations (50, 25, 12.5 $\mu\text{g}/\mu\text{L}$) were prepared from the metal complex. These concentrations were selected for their antimicrobial activity. The data for the growth inhibition zone is presented in Table 4 along with bar graphs as shown in Figures 5, 6, 7, and S11. To differentiate the efficiency of the targeted complex, amikacin (30 mcg/disc) acts as the positive control while the blank disc soaked in DMSO is the

negative control. The observation of all the complexes showed better results at higher concentrations and considerable activity at a lower concentrations. Hence, the *in vitro* antibacterial activity showed that the complexes are bacteriostatic. The intensity of the antibacterial action of ligands and complexes depends upon the type of species of microorganisms. The tested complexes significantly showed lower antibacterial activity compared to commercial antibiotics [67, 68]. From the Table, Zr(II)Otc/Sal complex shows more reactive than Pd(II)Otc/Sal complex. Thus, the above complexes show better activity against the tested strains of bacteria.

The effect of metal ions on the surface of the cell membrane of an organism determines the high activity of the complex. Here, metal chelates contain both polar and non-polar groups that help for easy permeation into the cell and tissues of microorganisms, causing the decrease of the biochemical potential of the cell [69]. These antibacterial findings in our research work will be new hope for the development of more efficient metal-based therapeutic drugs in the future.

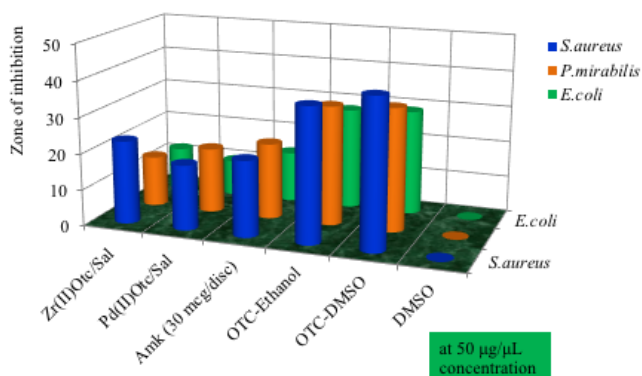


Figure 5. Bar graph for the antibacterial activity study of metal complexes at 50 µg/µL concentration.

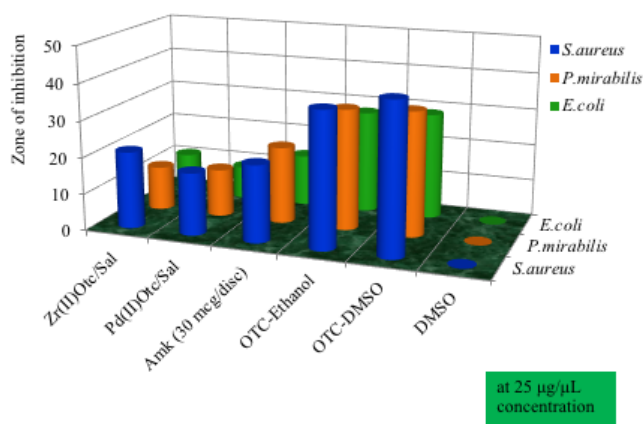


Figure 6. Bar graph for the antibacterial activity study of metal complexes at 25 µg/µL concentration.

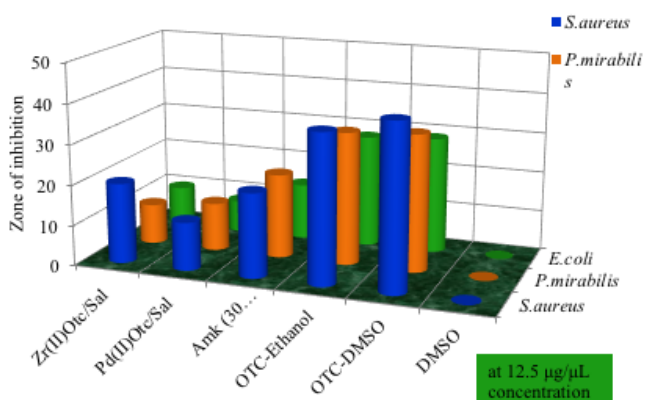


Figure 7. Bar graph for the antibacterial activity study of metal complexes at 12.5 µg/µL concentration.

CONCLUSION

The current article deals with the successful synthesis of two novel metal complexes (Zr(II)Otc/Sal and Pd(II)Otc/Sal) of the mixed lig and with the complexation of oxytetracycline, salicylaldehyde along with the metal ions. The formation of the synthesized complexes was monitored by physical and spectral methods. Metal complexes are colored, amorphous, soluble in organic solvents (DMSO and DMF), and insoluble in water. The FT-IR, UV/Vis., and NMR spectral data reveal the complexation of metal ions with amide N atom of C2 and O at C3 of oxytetracycline in ring A and O atom of salicylaldehyde. Electronic absorption data showed tetrahedral and square planar geometries for the Zr(II)Otc/Sal and Pd(II)Otc/Sal metal complexes. The selected bond lengths, bond angles, and optimized bond energies obtain from the 3D modeling software also suggest the above geometry. From the Coats-Redfern equation, the activation energy decreases on moving to another decomposition step, so the rate becomes weaker and the metal complexes show higher stability. The negative value of the activation energy indicates the slowness of the reaction condition and indicates the spontaneous decomposition steps. SEM images characterize the surface morphology of the metal complexes. The antibacterial evaluation showed significant antibiotic action against human clinical pathogens. The prepared complexes also showed antibacterial activity. Here, Zr(II)Otc/Sal metal complex revealed a better antibiotic effect than Pd(II)Otc/Sal. Therefore, these research works have created a golden opportunity for researchers and chemists to develop a more potent drug in the field of pharmaceutical science and also for the welfare of mankind.

Conflicts of Interest

There is no conflict of interest reported by the author.

Acknowledgments

One of the authors (Rohit Kumar Dev) is highly grateful to the NAST (Nepal Academy of Science and Technology), Khumaltar, Lalitpur, Nepal for funding the research work. The authors are also grateful to STIC Cochin, CSIR-CDRI, Lucknow, NBU Siliguri, and SAIF IIT Bombay, India for providing spectroscopic characterization facilities.

References

1. K. Sharma, R. V. Singh, and N. Fahmi, Palladium(II) and platinum(II) derivatives of benzothiazoline ligands: Synthesis, characterization, antimicrobial and antispermatic activity, *Spectrochimica Acta - Part A: Molecular and Biomolecular Spectroscopy*, 2011, 78(1), 80-87. (DOI: [10.1016/j.saa.2010.08.076](https://doi.org/10.1016/j.saa.2010.08.076))
2. S. Shobana, P. Subramaniam, L. Mitu, J. Dharmaraja, and S. A. Narayan, Synthesis, structural elucidation, biological, antioxidant and nuclease activities of some 5-Fluorouracil–amino acid mixed ligand complexes, *Spectrochimica Acta - Part A: Molecular and Biomolecular Spectroscopy*, 2015, 134, 333-344. (DOI: [10.1016/j.saa.2014.06.093](https://doi.org/10.1016/j.saa.2014.06.093))
3. A. Abebe, and T. Hailemariam, Synthesis and Assessment of Antibacterial Activities of Ruthenium(III) Mixed Ligand Complexes Containing 1,10-Phenanthroline and Guanide, *Bioinorganic Chemistry and Applications*, 2016, 1-9. (DOI: [10.1155/2016/3607924](https://doi.org/10.1155/2016/3607924))
4. H. Khan, N. Daraz, M. N. Khan, M. Said, N. Akhtar, A. Badshah, A. S. Khan, and M. Ali, Synthesis, Structural Characterization, and Evaluation of the Biological Properties of Heteroleptic Palladium(II) Complexes, *Bioinorganic Chemistry and Applications*, 2014, 1-7. (DOI: [10.1155/2014/916361](https://doi.org/10.1155/2014/916361))
5. A. K. Molodkin, N. Y. Esina, M. V. Tachaev, M. N. Kurasova, Mixed-Ligand Palladium(II) Complexes with Amino Acids, Cytosine, and Adenine, *Russian Journal of Inorganic Chemistry*, 2007, 52(10), 1567-1669. (DOI: [10.1134/S0036023607100166](https://doi.org/10.1134/S0036023607100166))
6. H. F. A. El-Halim, G. G. Mohamed, and E. A. M. Khalil, Synthesis, spectral, thermal and biological studies of mixed ligand complexes with newly prepared Schiff base and 1,10-phenanthroline ligands, *Journal of Molecular Structure*, 2017. (DOI: [10.1016/j.molstruc.2017.05.092](https://doi.org/10.1016/j.molstruc.2017.05.092))
7. A. J. Alanis, Resistance to Antibiotics: Are We in the Post-Antibiotic Era?, *Archives of Medical Research*, 2005, 36, 697-705. (DOI: [10.1016/j.arcmed.2005.06.009](https://doi.org/10.1016/j.arcmed.2005.06.009))
8. A. A. Salyers, A. Gupta, and Y. Wang, Human intestinal bacteria as reservoirs for antibiotic resistance genes, *TRENDS in Microbiology*, 2004, 12(9), 0-416. (DOI: [10.1016/j.tim.2004.07.004](https://doi.org/10.1016/j.tim.2004.07.004))
9. M. J. Feio, I. Sousa, M. Ferreira, L. Cunha-Silva, R. G. Saraiva, C. Queiros, J. G. Alexandre, V. Claro, A. Mendes, R. Ortiz, S. Lopes, A. L. Amaral, J. Lino, P. Fernandes, A. J. Silva, L. Moutinho, B. De Castro, E. Pereira, L. Perello, and P. Gameiro, Fluoroquinolone-metal complexes: a route to counteract bacterial resistance? *Journal of Inorganic Biochemistry*, 2014, 138, 129-143. (DOI: [10.1016/j.jinorgbio.2014.05.007](https://doi.org/10.1016/j.jinorgbio.2014.05.007))
10. P. Cervini, B. Ambrozini, L. Carlos, M. M. Ana, and P. Garcia, Thermal behavior and decomposition of oxytetracycline hydrochloride, *J Therm Anal Calorim*, 2015, 121(1), 347-352. (DOI: [10.1007/s10973-015-4447-x](https://doi.org/10.1007/s10973-015-4447-x))
11. V. L. Pham, D. Kim, and S. Ko, Oxidative degradation of the antibiotic oxytetracycline by Cu@Fe₃O₄ core-shell nanoparticles, *Science of the Total Environment*, 2018, 631-632, 608-618. (DOI: [10.1016/j.scitotenv.2018.03.067](https://doi.org/10.1016/j.scitotenv.2018.03.067))

12. S. Orellana, C. Soto, and M. I. Toral, UV–vis, IR and ¹H NMR spectroscopic studies and characterization of ionic-pair crystal violet–Oxytetracycline, *Spectrochimica Acta Part A: Molecular and Biomolecular Spectroscopy*, 2010, 75(1), 437-443. (DOI:[10.1016/j.saa.2009.11.002](https://doi.org/10.1016/j.saa.2009.11.002))
13. W. Qi, J. Long, C. Feng, Y. Feng, and D. Cheng, Fe³⁺ enhanced degradation of oxytetracycline in water by pseudomonas, *Water Research*, 2019, 160, 361. (DOI: [10.1016/j.watres.2019.05.058](https://doi.org/10.1016/j.watres.2019.05.058))
14. F. Yin, H. Dong, W. Zhang, Z. Zhu, and B. Shang, Antibiotic degradation and microbial community structures during acidification and methanogenesis of swine manure containing chlortetracycline or Oxytetracycline, *Bioresource Technology*, 2017, 250, 247. (DOI: [10.1016/j.biortech.2017.11.015](https://doi.org/10.1016/j.biortech.2017.11.015))
15. O. A. Arikan, L. J. Sikora, W. Mulbry, S. U. Khan, C. Rice, and G. D. Foster, The fate and effect of oxytetracycline during the anaerobic digestion of manure from therapeutically treated calves, *Process Biochemistry*, 2006, 41(7), 1637-1643. (DOI:[10.1016/j.procbio.2006.03.010](https://doi.org/10.1016/j.procbio.2006.03.010))
16. A. Zianna, G. D. Geromichalos, and A. G. Hatzidimitriou, Palladium(II) complexes with salicylaldehyde ligands: Synthesis, characterization, structure, in vitro and in silico study of the interaction with calf-thymus DNA and albumins, *Journal of Inorganic Biochemistry*, 2019, 194, 85. (DOI:[10.1016/j.jinorgbio.2019.02.013](https://doi.org/10.1016/j.jinorgbio.2019.02.013))
17. H. Kargar, V. Torabi, A. Akbari, and R. Behjatmanesh-ardakani, Pd(II) and Ni(II) complexes containing an asymmetric Schiff base ligand: Synthesis, x-ray crystal structure, spectroscopic investigations, and computational studies, *Journal of Molecular Structure*, 2020, 1205, 127642. (DOI:[10.1016/j.molstruc.2019.127642](https://doi.org/10.1016/j.molstruc.2019.127642))
18. R. K. Sharma, and C. Sharma, Zirconium(IV)-modified silica gel: Preparation, characterization and catalytic activity in the synthesis of some biologically important molecules, *CATCOM*, 2011, 12(5), 327-331. (DOI: [10.1016/j.catcom.2010.10.011](https://doi.org/10.1016/j.catcom.2010.10.011))
19. L. M. Mirica, and J. R. Khusnutdinova, Structure and electronic properties of Pd(III) complexes, *Coordination Chemistry Reviews*, 2013, 257(2), 299-314. (DOI: [10.1016/j.ccr.2012.04.030](https://doi.org/10.1016/j.ccr.2012.04.030))
20. V. Nagalakshmi, M. Sathya, M. Premkumar, D. Kaleeswaran, G. Venkatachalam, and K. Balasubramani, Palladium(II) Complexes comprising Naphthylamine and Biphenylamine based Schiff base Ligands: Synthesis, Structure and Catalytic activity in Suzuki coupling reactions, *Journal of Organometallic Chemistry*, 2020, 121220. (DOI: [10.1016/j.jorganchem.2020.121220](https://doi.org/10.1016/j.jorganchem.2020.121220))
21. S. Rubino, R. Busà, A. Attanzio, R. Alduina, V. Di. Stefano, M. A. Girasolo, S. Orecchio, and L. Tesoriere, Synthesis, properties, antitumor and antibacterial activity of new Pt(II) and Pd(II) complexes with 2,2'-dithiobis(benzothiazole) ligand, *Bioorganic & Medicinal Chemistry*, 2017, 25, 2378. (DOI: [10.1016/j.bmc.2017.02.067](https://doi.org/10.1016/j.bmc.2017.02.067))
22. C. D. Miranda, and R. Zemelman, Bacterial resistance to oxytetracycline in Chilean salmon farming, *Aquaculture*, 2002, 212(1-4), 31-47. (DOI: [10.1016/S0044-8486\(02\)00124-2](https://doi.org/10.1016/S0044-8486(02)00124-2))
23. O. B. Samuelsen, V. Torsvik, and A. Ervik, Long-range changes in oxytetracycline concentration and bacterial resistance towards oxytetracycline in a fish farm sediment after medication, *The Science of the Total Environment*, 1992, 114, 25-36. (DOI: [10.1016/0048-9697\(92\)90411-K](https://doi.org/10.1016/0048-9697(92)90411-K))
24. M. M. El-ajaily, H. A. Abdullah, A. Al-janga, E. E. Saad, and A. A. Maihub, Zr(IV), La(III), and Ce(IV) Chelates with 2-[(4-[(Z)-1-(2-Hydroxyphenyl)ethylidene]aminobutyl)-ethanimidoyl] phenol: Synthesis, Spectroscopic Characterization, and Antimicrobial Studies. *Advances in Chemistry*, 2015, 1–16. (DOI:[10.1155/2015/987420](https://doi.org/10.1155/2015/987420))
25. W. Guerra, E. de.A. Azevedo, A. R. de. S. Monteiro, M. Bucciarelli-Rodriguez, E. Chartone-Souza, A. M. A. Nascimento, A. P. S. Fontes, L. Le Moyec, and E. C. Pereira-Maia, Synthesis, characterization, and antibacterial activity of three Palladium (II) complexes of tetracyclines, *Journal of Inorganic Biochemistry*, 2005, 99, 2348–2354. (DOI: [10.1016/j.jinorgbio.2005.09.001](https://doi.org/10.1016/j.jinorgbio.2005.09.001))

26. A. T. Fiori-duarte, F. R. G. Bergamini, R. Enoque, F. De. Paiva, C. M. Manzano, W. R. Lustri, and P. P. Corbi, A new palladium(II) complex with ibuprofen: Spectroscopic characterization, DFT studies, antibacterial activities and interaction with biomolecules, *Journal of Molecular Structure*, 2019, 1186, 144. (DOI: [10.1016/j.molstruc.2019.03.020](https://doi.org/10.1016/j.molstruc.2019.03.020))
27. P. Kavitha, and K. L. Reddy, Pd(II) complexes bearing chromone based Schiff bases: Synthesis, characterization and biological activity studies, *ARABIAN JOURNAL OF CHEMISTRY*, 2016,9, 640. (DOI: [10.1016/j.arabjc.2013.06.018](https://doi.org/10.1016/j.arabjc.2013.06.018))
28. G. D. Bajju, G. Devi, S. Katoch, M. Bhagat, S. Kundan, and S. K. Anand, Synthesis, Spectroscopic, and Biological Studies on New Zirconium(IV) Porphyrins with Axial Ligand, *Bioinorganic Chemistry, and Applications*, 2013, 15. (DOI: [10.1155/2013/903616](https://doi.org/10.1155/2013/903616))
29. K. A. Abu-safieh, A.S. Abu-surrah, H. D. Tabbā, H. A. Almasri, R. M. Bawadi, F. M. Boudjelal, and L. H. Tahtamouni, Novel Palladium(II) and Platinum(II) Complexes with a Fluoropiperazinyl Based Ligand Exhibiting High Cytotoxicity and Anticancer Activity In Vitro, *Journal of Chemistry*, 2016,7. (DOI: [10.1155/2016/7508724](https://doi.org/10.1155/2016/7508724))
30. S. Chandra, M. Tyagi, and S. Agrawal, Spectral and antimicrobial studies on tetraaza macrocyclic complexes of Pd^{II}, Pt^{II}, Rh^{III}, and Ir^{III} metal ions, *Journal of Saudi Chemical Society*, 2011, 15(1), 49-54. (DOI: [10.1016/j.jscs.2010.09.005](https://doi.org/10.1016/j.jscs.2010.09.005))
31. Z. Tan, F. Tan, L. Zhao, and J. Li, The Synthesis, Characterization, and Application of Ciprofloxacin Complexes and Its Coordination with Copper, Manganese and Zirconium Ions, *Journal of Crystallization Process and Technology*, 2012, 2, 55-63. (DOI: [10.4236/jcpt.2012.22008](https://doi.org/10.4236/jcpt.2012.22008))
32. Z. Ghadamyari, A. Shiri, A. Khojastehnezhad, and S. M. Seyedi, Zirconium (IV) porphyrin graphene oxide: a new and efficient catalyst for the synthesis of 3, 4-dihydro pyrimidine- 2(1H)-ones, *Appl Organometal Chem.*, 2019,1. (DOI: [10.1002/aoc.5091](https://doi.org/10.1002/aoc.5091))
33. M. Gupta, S. Sihag, A. K. Varshney, and S. Varshney, Synthesis, Structural, and Antimicrobial Studies of Some New Coordination Compounds of Palladium(II) with Azomethines Derived from Amino Acids, *Journal of Chemistry*, 2013, 8. (DOI: [10.1155/2013/745101](https://doi.org/10.1155/2013/745101))
34. A. Chaudhary, and A. Singh, Synthesis, Characterization, and Evaluation of Antimicrobial and Antifertility Efficacy of Heterobimetallic Complexes of Copper (II), *Journal of Chemistry*, 2017, 9. (DOI: [10.1155/2017/5936465](https://doi.org/10.1155/2017/5936465))
35. S. I. Islam, S. B. Das, S. Chakrabarty, S. Hazra, A. Pandey, and A. Patra, Synthesis, Characterization, and Biological Activity of Nickel (II) and Palladium (II) Complex with Pyrrolidine Dithiocarbamate (PDTC), *Advances in Chemistry*, 2016, 6. (DOI: [10.1155/2016/4676524](https://doi.org/10.1155/2016/4676524))
36. D. Kumar, S. Chadda, J. Sharma, and P. Surain, Syntheses, Spectral Characterization, and Antimicrobial Studies on the Coordination Compounds of Metal Ions with Schiff Base Containing Both Aliphatic and Aromatic Hydrazide Moieties, *Bioinorganic Chemistry and Applications*, 2013, 10. (DOI: [10.1155/2013/981764](https://doi.org/10.1155/2013/981764))
37. F. A. El-Saied, M. M. E. Shakhdofo, A. S. El Tabl, M. M. Abd-Elzaher, and N. Morsy, Coordination versatility of N₂O₄ polydentate hydrazone ligand in Zn(II), Cu(II), Ni(II), Co(II), Mn(II) and Pd(II) complexes and antimicrobial evaluation, *Journal of Basic and Applied Sciences*, 2017, 6, 310. (DOI: [10.1016/j.bjbas.2017.09.005](https://doi.org/10.1016/j.bjbas.2017.09.005))
38. A. K. Singh, and U. T. Nakate, Microwave Synthesis, Characterization, and Photoluminescence Properties of Nanocrystalline Zirconia, *The scientific world journal*, 2014, 7. (DOI: [10.1155/2014/349457](https://doi.org/10.1155/2014/349457))
39. G. D. Bajju, G. Devi, S. Katoch, M. Bhagat, Deepmala, Ashu, S. Kundan, and S. K. Anand, Synthesis, spectroscopic, and biological studies on new Zirconium (IV) porphyrins with an axial ligand. *Bioinorganic Chemistry and Applications*, 2013, 15. (DOI: [10.1155/2013/903616](https://doi.org/10.1155/2013/903616))

40. N. Nakata, K. Nakamura, S. Nagaoka, and A. Ishii, Carbazolyl-Substituted [OSSO]-Type Zirconium(IV) Complex as a Precatalyst for the Oligomerization and Polymerization of α -Olefins, *Catalysts*, 2019, 9(6), 528. (DOI: [10.3390/catal9060528](https://doi.org/10.3390/catal9060528))
41. M. Mandal, M. List, I. Teasdale, D. Chakraborty, and U. Monkowius, Palladium complexes containing imino phenoxide ligands: synthesis, luminescence, and their use as catalysts for the ring-opening polymerization of rac-lactide, *Monatsh Chem*, 2017, 1. (DOI: [10.1007/s00706-017-2119-1](https://doi.org/10.1007/s00706-017-2119-1))
42. H. V. Huynh, D. Le. Van, F. E. Hahn, and T. S. A. Hor, Synthesis and structural characterization of mixed carbene-carboxylate complexes of palladium(II), *Journal of Organometallic Chemistry*, 2004, 689(10), 1766-1770. (DOI: [10.1016/j.jorganchem.2004.02.033](https://doi.org/10.1016/j.jorganchem.2004.02.033))
43. D. P. Steinhuebel, P. Fuhrmann, and S. J. Lippard, Synthesis, characterization, and reactivity of organometallic Zr(IV) carboxylate complexes, *Inorganica Chimica Acta*, 1998, 270, 527. (DOI: [10.1016/S0020-1693\(97\)06117-3](https://doi.org/10.1016/S0020-1693(97)06117-3))
44. N. Smrečki, J. Jaźwiński, and Z. Popović, Preparation and NMR spectroscopic study of palladium(II) complexes with N-arylalkyliminodiacetamide derivatives, *Journal of Molecular Structure*, 2016, 1122, 192. (DOI: [10.1016/j.molstruc.2016.05.084](https://doi.org/10.1016/j.molstruc.2016.05.084))
45. H. L. Singh, and J. Singh, Synthesis of New Zirconium(IV) Complexes with Amino Acid Schiff Bases: Spectral, Molecular Modeling, and Fluorescence Studies, *International Journal of Inorganic Chemistry*, 2013, 1-10. (DOI: [10.1155/2013/847071](https://doi.org/10.1155/2013/847071))
46. W. Hernandez, J. Paz, F. Carrasco, A. Vaisberg, E. Spodine, J. Manzur, and L. Beyer, *Bioinorganic Chemistry and Applications*, 2013, 12. (DOI: [10.1155/2013/524701](https://doi.org/10.1155/2013/524701))
47. W. H. El-Shwiniy, W. S. Shehab, S. F. Mohamed, and H. G. Ibrahim, *Applied Organometallic Chemistry*, 2018, 32, 1. (DOI: [10.1002/aoc.4503](https://doi.org/10.1002/aoc.4503))
48. K. I. Kallow, and A. Y. R. Al-Assaf, *E-Journal of Chemistry*, 2011, 8, 576.
49. I. M. I. Moustafa, and M. H. Abdellatif, *Mod Chem Appl*, 2017, 5. (DOI: [10.4172/2329-6798.1000202](https://doi.org/10.4172/2329-6798.1000202))
50. S. Tetteh, D. K. Doodoo, R. Appiah-pong, and I. Tuffour, *Journal of Inorganic Chemistry*, 2014, 7. (DOI: [10.1155/2014/586131](https://doi.org/10.1155/2014/586131))
51. P.A. Ajibade, and O. G. Idemudia, *Bioinorganic Chemistry and Applications*, 2013, 8. (DOI: [10.1155/2013/54954](https://doi.org/10.1155/2013/54954))
52. A. J. Abdul-Ghani, and A. M. N. Khaleel, *Bioinorganic Chemistry and Applications*, 2009, 12. (DOI: [10.1155/2009/413175](https://doi.org/10.1155/2009/413175))
53. S. A. Shaker, Synthesis and Study of Mixed Ligand-Metal Complexes of 1, 3, 7-Trimethylxanthine and 1, 3-Dimethyl-7H-purine-2, 6-dione with Some Other Ligands *E-Journal of Chemistry*, 2010, 8(1), 153-158
54. A. A. Abdel Aziz, A. N. M. Salem, M. A. Sayed, and M. M. Aboaly, Synthesis, structural characterization, thermal studies, catalytic efficiency and antimicrobial activity of some M(II) complexes with ONO tridentate Schiff base N-salicylidene-o-aminophenol (saphH₂), *Journal of Molecular Structure*, 2012, 1010, 130-138. (DOI: [10.1016/j.molstruc.2011.11.043](https://doi.org/10.1016/j.molstruc.2011.11.043))
55. M. Gaber, H. El-ghamry, F. Atlam, and S. Fathalla, Synthesis, spectral and theoretical studies of Ni(II), Pd(II) and Pt(II) complexes of 5-mercapto-1,2,4-triazole-3-imine-20-hydroxynaphthalene, *SPECTROCHIMICA ACTA PART A: MOLECULAR AND BIOMOLECULAR SPECTROSCOPY*, 2015, 137, 919-929. (DOI: [10.1016/j.saa.2014.09.015](https://doi.org/10.1016/j.saa.2014.09.015))
56. M. Montazerzohori, S. Zahedi, A. Naghiha, and M. M. Zohour, Synthesis, characterization and thermal behavior of antibacterial and antifungal active zinc complexes of bis (3(4-dimethylaminophenyl)-allylidene-1,2-diaminoethane), *Materials Science & Engineering*, 2014, 35, 195-204. (DOI: [10.1016/j.msec.2013.10.030](https://doi.org/10.1016/j.msec.2013.10.030))

57. S. M. Prabhu and S. Meenakshi, Novel one-pot synthesis of dicarboxylic acids mediated alginate zirconium biopolymeric complex for defluoridation of water, *Carbohydrate Polymers*, 2015, 120, 60-68. (DOI: [10.1016/j.carbpol.2014.11.058](https://doi.org/10.1016/j.carbpol.2014.11.058))
58. S. Sobhani, and F. Zarifi, Pd-isatin Schiff base complex immobilized on γ -Fe₂O₃ as a magnetically recyclable catalyst for the Heck and Suzuki cross-coupling reactions, *Chinese Journal of Catalysis*, 2015, 36(4), 555-563. (DOI: [10.1016/S1872-2067\(14\)60291-6](https://doi.org/10.1016/S1872-2067(14)60291-6))
59. A. Benyei, and I. Sovago, Thermodynamic, kinetic and structural studies on the mixed ligand complexes of palladium(II) with tridentate and monodentate ligands, *Journal of Inorganic Biochemistry*, 2003, 94(3), 291-299. (DOI: [10.1016/S0162-0134\(03\)00009-6](https://doi.org/10.1016/S0162-0134(03)00009-6))
60. L. H. Abdel-rahman, M. Shaker, S. Adam, N. Al-zaqri, M. R. Shehata, H. E. Ahmed, and S. K. Mohamed, Synthesis, characterization, biological and docking studies of ZrO (II), VO (II) and Zn (II) complexes of a halogenated tetra-dentate Schiff base. *Arabian Journal of Chemistry*, 2022, 15(5), 103737. (DOI: [10.1016/j.arabjc.2022.103737](https://doi.org/10.1016/j.arabjc.2022.103737))
61. D. A. Milenković, D. S. Dimić, E. H. Avdović, and Z. S. Marković, (2020). Several coumarin derivatives and their Pd(II) complexes as potential inhibitors of the main protease of SARS-CoV-2, an in silico approach†. *RSC Adv.*, 2020,10(58), 35099–35108. (DOI: [10.1039/d0ra07062a](https://doi.org/10.1039/d0ra07062a))
62. A. Zianna, G. D. Geromichalos, A. Pekou, G. Hatzidimitriou, E. Coutouli-argyropoulou, M. Lalia-Kantouri, A. A. Pantazaki, and G. Psomas, A palladium(II) complex with the Schiff base 4-chloro-2-(N-ethyliminomethyl)-phenol: Synthesis, structural characterization, and *in vitro* and *in silico* biological activity studies, *Journal of Inorganic Biochemistry*, 2019, 199(Ii), 110792. (DOI: [10.1016/j.jinorgbio.2019.110792](https://doi.org/10.1016/j.jinorgbio.2019.110792))
63. S. Guti, J. Espino, F. Luna-giles, A. B. Rodr, J. A. Pariente, and E. Viñuelas-zah, Synthesis, Characterization and Antiproliferative Evaluation of Pt (II) and Pd (II) Complexes with a Thiazine-Pyridine Derivative Ligand †. *Pharmaceuticals*, 2021, 14, 395. (DOI: [10.3390/ph14050395](https://doi.org/10.3390/ph14050395))
64. A. Kerflani, K. Si, A. Rabahi, A., Bouchoucha, and S. Zaater, *Inorganica Chimica Acta* Novel palladium (II) complexes with iminocoumarin ligands: Synthesis, characterisation, electrochemical behaviour, DFT calculations and biological activities, ADMET study and molecular docking. *Inorganica Chimica Acta*, 2021, 529, 120659. (DOI: [10.1016/j.ica.2021.120659](https://doi.org/10.1016/j.ica.2021.120659))
65. D. Kumar, and A. Kumar, Physicochemical, Spectral, and Biological Studies of Mn(II), Cu(II), Cd(II), Zr(OH)₂(IV), and UO₂(VI) Compounds with Ligand Containing Thiazolidin-4-one Moiety, *Journal of Chemistry*, 2014, 9. (DOI: [10.1155/2014/286136](https://doi.org/10.1155/2014/286136))
66. H. G. Aslan, S. Özcan, and N. Karacan, Synthesis, characterization and antimicrobial activity of salicylaldehyde benzene sulfonyl hydrazone (Hsalbsmh) and its Nickel(II), Palladium(II), Platinum(II), Copper(II), Cobalt(II) complexes, *INOCHÉ*, 2011, 14(9), 1550-1553. (DOI: [10.1016/j.inoche.2011.05.024](https://doi.org/10.1016/j.inoche.2011.05.024))
67. S. Andotra, S., Kumar, M. Kour, N. Kalgotra, and S. K. Pandey, Spectroscopic, thermal, quantum chemical calculations and in vitro biological studies of titanium/zirconium(IV) complexes of mono- and disubstituted aryldithiocarbonates, *Journal of Molecular Structure*, 2018, 1155, 215. (DOI: [10.1016/j.molstruc.2017.10.082](https://doi.org/10.1016/j.molstruc.2017.10.082))
68. D. L. Stojković, V. V. Jevtić, N. Vuković, M. Vukić, P. Čanović, M. M. Zarić, M. M., Mišić, D. M., Radovanović, D. Baskić, and S. R. Trifunović, Synthesis, characterization, antimicrobial and antitumor reactivity of new palladium(II) complexes with methionine and tryptophane coumarine derivatives, *Journal of Molecular Structure*, 2018, 1157, 425. (DOI: [10.1016/j.molstruc.2017.12.095](https://doi.org/10.1016/j.molstruc.2017.12.095))
69. W. H. El-shwiniy, and W. A. Zordok, Synthesis, spectral, DFT modeling, cytotoxicity and microbial studies of novel Zr(IV), Ce(IV) and U(VI) piroxicam complexes, *Spectrochimica Acta Part A: Molecular and Biomolecular Spectroscopy*, 2018, 199, 290. (DOI: [10.1016/j.saa.2018.03.074](https://doi.org/10.1016/j.saa.2018.03.074))

See discussions, stats, and author profiles for this publication at: <https://www.researchgate.net/publication/338801096>

Synthesis, Spectroscopic Characterization and Antibacterial Assessment of Cadmium and Molybdenum Complexes of TcSal Mixed Ligand

Article in *International Journal of Pharmaceutical Sciences Review and Research* · January 2020

CITATIONS

0

READS

284

4 authors, including:



Rohit Kumar Dev

Mahendra Morang Adarsh Multiple Campus, Biratnagar Tribhuvan university Nepal

5 PUBLICATIONS 4 CITATIONS

[SEE PROFILE](#)



Ajaya Bhattarai

Tribhuvan University

241 PUBLICATIONS 1,386 CITATIONS

[SEE PROFILE](#)



Narendra Kumar Chaudhary

Mahendra Morang Adarsh Multiple Campus, Biratnagar Tribhuvan university Nepal

49 PUBLICATIONS 246 CITATIONS

[SEE PROFILE](#)

Some of the authors of this publication are also working on these related projects:



TWAS Fellowship, Central University of Gujarat, Gandhinagar, India [View project](#)



Lab work collaboration [View project](#)

Research Article



Synthesis, Spectroscopic Characterization and Antibacterial Assessment of Cadmium and Molybdenum Complexes of *TcSal* Mixed Ligand

Rohit K. Dev, Ajaya Bhattarai, Narendra K. Chaudhary, Parashuram Mishra*
 Bio-inorganic and Materials Chemistry Research Laboratory, Department of Chemistry,
 M. M. A. M. Campus, Tribhuvan University, Biratnagar, Morang, Nepal.
 *Corresponding author's E-mail: prmmishra@rediffmail.com

Received: 08-11-2019; Revised: 21-12-2019; Accepted: 28-12-2019.

ABSTRACT

The metal complexes of Cadmium and Molybdenum (II) were synthesized by refluxing equimolar mixtures of Tetracycline (Tc) as primary ligand and Salicylaldehyde (Sal) as a secondary ligand with M (II) salts (M = Cd & Mo) in ethanol media. The metallation of two exclusive ligands with Cd & Mo was monitored by the observation of change in color, surface tension, and conductivity. The stoichiometric ratio of the synthesized complexes was carried out using the physicochemical approach like elemental microanalysis (CHN), melting point, surface tension, conductivity measurement. The spectroscopic methods like FT-IR, ^1H & ^{13}C -NMR spectroscopy, UV/Vis, Mass spectrometry techniques. The surface structure of the complex was carried out through scanning electron microscopy (SEM). The thermodynamic and kinetic studies were carried out via TGA/DTA curves through which ΔE^* , ΔH^* , ΔS^* & ΔG^* parameters of several decomposition stages were evaluated by Coats-Redfern equation. The consequences of elemental microanalysis signify that these metal complexes of the mixed ligand are determined to have a 1:1 metal-to-ligand molar ratio. Molecular modeling gives geometry of the complex which was accomplished through Cs-Chem Office software program. The antibacterial activity study was done by Kirby-Bauer Paper disc diffusion techniques with the help of using *S. aureus*, *E. coli*, & *P. aeruginosa* clinical bacterial pathogens. All synthesized metal complexes showed good consequences in opposition to the selected clinical pathogenic bacteria.

Keywords: Antibacterial activity, metal complexes, molecular modeling, tetracycline, thermal analysis.

INTRODUCTION

In the field of coordination chemistry, development is widely expansive in recent years due to the easy chelation of the ligand with the metallic ions and it further requires significant study for the generation of novel metal complexes. So, the research primarily based on metal complexes of the mixed ligand is of great interest for medicinal and analytical chemists¹. The modern-day antibiotics are underneath bacterial resistance due to their improper use in the therapy techniques and the world is going through a shortage of antibiotic drugs. This leads to accelerated mortality of the human population. So, there is the first need for antibiotic research to remedy the present trouble of drug resistance².

Metal complexes of Mixed ligand are of utmost significance in the discipline of coordination chemistry due to their varied applications in analytical, chemical and biomedical fields. Their functions in pollution, magneto and photochemistry, industrial and material science further decorate in the area of chemical research³. Tc is the 3rd generation broad-spectrum antibiotic which is used in the therapy of the various bacterial infections promoted using bacteria. The bacterial infection includes acne, cholera, brucellosis, plague, malaria, and syphilis, but due to cellular research in the bacterial pathogen, the current antibiotics are under bacterial resistance. This can also be triggered by way of anti-enzymatic actions on drug supplies⁴. Among transition metals, cadmium (d^{10}) forms a metal complex with coordination number ranging from

four to eight. Presently a cadmium (II) ion acts as the catalytic center for carbonic anhydrase. The d^{10} metal ions are used as photoluminescence materials which can enhance the nature of fluorescence⁵.

The combination of transition metal ions with antibiotics has focused our attention and forced us to interact their chemistry to established whether pharmacological properties of the ligand affects the complexation and also finds additional knowledge about the action of antibiotics⁶. There is fantastic endeavor in the discipline of coordination chemistry that cadmium is toxic metal and strong carcinogen in nature to the environment. So, the mobilization and immobilization of cadmium can be done with the help of some technical strategies such as in ligand exchange chromatography through complexation of the metal Center by way of chelating nitrogen donor ligands⁷. In the present work, we concentrated for the synthesis of Cd (II) & Mo (II) metal complexes of mixed ligand by taking tetracycline as primary ligand and salicylaldehyde as the secondary ligand. Besides of their spectroscopic characterizations, antibacterial susceptibility test was done by Kirby-Bauer Paper disc diffusion techniques using clinical pathogenic bacteria like *S.aureus*, *E. coli*, *P.aeruginosa*.

MATERIALS AND METHODS

The reagents, as well as solvents used in the laboratory work, were of analytical research-grade (AR). They were purified and dried under the standard procedure. The glassware used in the test was of high-grade and were used



for excessive precision overall performance experiment. The integral chemicals have been procured from various international chemical agencies such as Tetracycline (Sigma Aldrich), Salicylaldehyde, $\text{CdCl}_2 \cdot \text{H}_2\text{O}$, $\text{ZrOCl}_2 \cdot 8\text{H}_2\text{O}$ (LobaChemie Pvt. Ltd), PdCl_2 and MHA (Himedia), and MoCl_3 (Alfa Aesar). Triple distilled water was used in the whole experiment for washing of the equipment and also for a solvent. Distilled ethanol was used for the experimental work.

Instruments

The C, H and N content in the synthesized metal complexes of mixed ligand were determined with Euro-E 3000 microanalyzer. Electronic spectral data (UV/Visible) of the complexes prepared in DMSO solution had been monitored in the length range of 200-2000 nm on Varian, Cary 5000. The FT-IR spectra had been done from the region between $4000\text{-}400\text{ cm}^{-1}$ through Perkin Elmer **Spectrum II** by use of KBr pellets. $^1\text{H-NMR}$ was carried out in presence of DMSO-d_6 solvent on a **Bruker Avii- 400MHz** spectrometer and Me_4Si acts as an internal reference. The kinetic and thermal behavior (TGA/DTA) curves were calculated under the nitrogen atmosphere to room temperature up to $860\text{ }^\circ\text{C}$ at linear heating rate of $10\text{ }^\circ\text{C/min}$. The ESI-MS evaluation has been determined through water UPLC-TQD mass spectrometer within the vary of 0-1000 m/z. The melting point was recorded in VEEGO ASD-10013 programmable apparatus. Conductivity measurement was done at $25\text{ }^\circ\text{C}$ in DMSO using Conductivity/ TDS Meter TCM 15+ digital conductivity meter. The surface tension data were taken from KRUSS Easy Dyne Tensiometer by Wilhelmy plate with du Nouy ring method. The morphology of the synthesized metal complex surface was done with the help of JEOL model JSM-6390 LV through Scanning Electron Microscopy technique. The complexes molecular structures were performed by using the help of CsChem Draw Ultra-12.0 Pro software. The anti-bacterial study was done with the help of Kirby Bauer paper disc diffusion technique. The stock solutions were prepared by mixing the metal complexes in DMSO at different concentration.

In vitro antibacterial screening test of the ligand and synthesized complexes were done on two bacterial strains: gram-negative (*Escherichia coli* & *Pseudomonas aeruginosa*) and gram-positive (*Staphylococcus aureus*) clinical pathogens by using Kirby-Bauer paper disc diffusion technique. Test solutions of the complexes were prepared at three different concentrations (25, 12.5 and $6.25\text{ }\mu\text{g}/\mu\text{l}$) in 30% DMSO to measure their actual effectiveness. Initially, the fresh culture of organisms was prepared from broth and incubating them for 2 h at $37\text{ }^\circ\text{C}$ for proper and total growth. Paper disc with 5 mm diameter size (Whatman no.1) was sterilized and loaded with test solutions. The sterile MHA media for testing of antibacterial sensitivity was prepared according to the reported literature. The fresh and revived organism slowly swab inside the sterile media and complexes of different concentration were injected on the paper disc. Amikacin of 30 mcg/disc was applied as a standard antibiotic drug which acts as a positive control⁸. After finishing all these tasks, the loaded Petri plates were placed in an incubator about $37\text{ }^\circ\text{C}$ up to 36 hrs to observe the inhibition zone of bacterial growth.

Synthesis of Complex

The Tc (0.8890gm, 2 mmol) was dissolved in hot 20 ml (70% ethanol), introduced dropwise an aq. solution of M (II) salts ($\text{M} = \text{Cd} \text{ \& \ } \text{Mo}$) (2mmol) under stirring condition in a 50 ml R.B flask. The combination was refluxed for two hrs to homogenize it and to this well stirred ethanolic solution of Sal (0.2ml, 2mmol) was added to the reaction mixture. After refluxing for eight hrs, pH was adjusted at 7-8 by adding ammonia solution. The mixture was left overnight to room temperature until the precipitation occurs. The obtained precipitates were filtered off, wash with aqueous ethanol then recrystallized from ethanol which results in the formation of pure and pale orange amorphous form of Cadmium complex and dried in a desiccator over anhydrous CaCl_2 . The percentage yield of the metal complexes was of about 60-70 %.

The similar route has been employed for the preparation of the Molybdenum Complex (Mo-TcSal) of the mixed ligand (Figure 1).

Antibacterial sensitivity assay

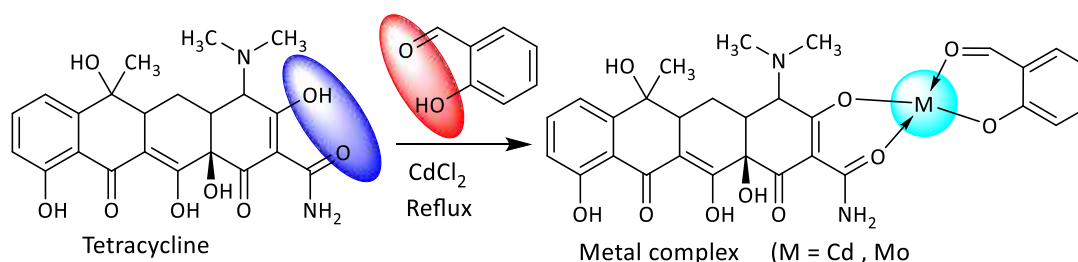


Figure 1: Proposed equation of reaction for the preparation of Cadmium complex of the mixed ligand.

Conductivity

The specific conductivity of ligand and the metal complexes of Cadmium and Molybdenum (II) decrease on decreasing the concentration (Table S1). On decreasing the

concentration, the conductivity also decreases because of the number of ions per unit volume carrying the current decreases on dilution^{9,10}. The greater conductivity was seen in the metal complexes in comparison to the ligand (Table S1) which also indicates the complex formation between

the ligands and the definite metal ions which could signify the greater tendency of formation of ions (complexion) in the metal complex¹¹. The specific conductivity of metal complex follows the charge density order since the specific conductivity increases with the metal complexation¹².

Surface Tension measurement

Surface tension is called as one of the crucial factors for measuring the wettability of a solution of a fluid which can spread over or stick to a solid surface¹³. The surface tension is a principle quantity which signifies the property of assembly and segregation dynamics of surface-active materials and plays an essential role in emulsion formation hence surface tension measures mechanism of kinetic diffusion¹⁴.

The surface tension of ligand and the metal complexes of Cadmium and Molybdenum (II) increase on decreasing the concentration (Table S1). Hence, this study shows that surface tension decreases as we increase the concentration of the solution. This occurs due to larger interaction between molecules of liquid than molecules present in air or in non-polar solvents¹⁵.

The surface tension of the metal complex often decreases as molecules become adsorbed¹⁶ in comparison with ligand

(Table S1). Because there is a greater probability of adsorbed molecules interacting as the surface coverage increases, the enthalpy of adsorption depends on the amount of surface coverage.

FT-IR spectroscopy

Characteristics frequencies of Infra-Red absorption band of metal complexes were introduced in Table 2 & Figures S1 & S2. These bands signify the nature of functional groups attached to the metal ions in the metal complexes. The complexes which show the bands within the range of 3431-3396 cm⁻¹ attributes to $\nu(\text{O-H})$ or $\nu(\text{N-H})$. The shoulder peaks lie at 2935 cm⁻¹ and 2925 cm⁻¹ corresponds to $\nu(\text{CH})$ Methyl. Similarly, peaks at 1600-1800 cm⁻¹ indicate the $\nu(\text{C=O})$. The peaks at 1515-1580 cm⁻¹ correspond to $\nu(\text{C=C})$ aromatic proton. The IR absorption frequency at 1457 cm⁻¹ signifies the $\nu(\text{C=N})$ Amide. The appearance of absorptions in the regions 1125-1140 cm⁻¹ denotes $\nu(\text{C-O})$. One of the essential characteristics absorption frequencies of metal complexes denoting their synthesis is the vibrational frequency of $\nu(\text{M-N})$ & $\nu(\text{M-O})$ bond which lies from the region between 440-500 cm⁻¹ and a medium intensity band at a region of 590-605 cm⁻¹.

Table 1: Elemental microanalysis, electronic absorption and physical measurement data

Complex	Empirical Formula	Mol. Wt.	Colour	M. Pt. (°C)	Calculated (found)%				Uv./Vis. Peak (nm)	Assignment
					C	H	N	O		
Cd-TcSal	C ₂₉ H ₂₈ CdN ₂ O ₁₀	676.95	Pale Orange	239.5	51.450 (51.102)	4.170 (5.706)	4.140 (4.256)	23.630 (14.251)	280 369 768	$\pi \rightarrow \pi^*$ $n \rightarrow \pi^*$ LMCT
Mo-TcSal	C ₂₉ H ₂₈ MoN ₂ O ₁₀	660.50	Pale Yellow	228.5	52.730 (42.789)	4.270 (4.635)	4.240 (4.686)	24.220 (17.003)	297 371 447	$\pi \rightarrow \pi^*$ $n \rightarrow \pi^*$ LMCT

Table 2: FT-IR spectral data of Cd & Mo- TcSal metal complexes

Complex	$\nu(\text{O-H})$ or $\nu(\text{N-H})$	$\nu(\text{CH})$ or Methyl	$\nu(\text{C=O})$	$\nu(\text{C=C})$ Aromatic	$\nu(\text{C=N})$ Amide	$\nu(\text{C-O})$	$\nu(\text{M-O})$	$\nu(\text{M-N})$
Cd-TcSal	3431	2935	1770	1518	1457	1128	596	499
Mo-TcSal	3396	2925	1618	1576	1457	1133	602	440

¹H & ¹³C-NMR spectral analysis

The ¹H-NMR spectrum of metal complexes was recorded in DMSO-d₆ solvent and offers about the precious facts about the structure, dynamic reaction state, proton environment and coordination sites of the metal complexes molecule. The ¹H-NMR spectra of metal complexes were shown in Figures S3-S4 & Table S2. The signals at (δ = 3.415 ppm) revealing to (CH₂) and singlet signal peak appeared at (δ = 2.5 ppm) is assigned to DMSO-d₆ solvent in the region between (δ = 2.509-2.517 ppm) and peaks in the location between (δ = 1.495-1.896 ppm) signify the peak for methyl proton. Similarly, the peaks in the region of (δ = 2.682-2.963 ppm) represent [N-(CH₃)₂]. The aromatic proton lies in the location of (δ = 6.904-7.539 ppm). Similarly, primary amide proton lies in the vicinity between (δ = 7.645 -7.660 ppm).

¹³C-NMR spectrums of metal complexes were done in DMSO-d₆ which display chemical shifts at (199.513) ppm indicate signal for phenyl ketone. Aromatic carbon confirmed a signal in the range between (111-131) ppm. The chemical shift for the carbon of the carbonyl group (-CO-) appears between (172.484-157.742) ppm. Also, the chemical shift at 40 ppm is due to DMSO-d₆. The measured value of all the carbon atoms with their chemical shifts is introduced in Figure S5-S8 & Table S3.

ESI-Mass spectral analysis

ESI- Mass spectrum of Cd (II) & Mo (II) metal complexes shows a peak at (M/Z=676.95) and (M/Z= 661) amu of the parents' ion which indicates proposed formula for the complexes. The value of molecular mass along with other



spectral data are necessary for the generation of the structure of the organic compounds. The rest peak of the mass spectrum is the fragment peaks. The successive decrease peak of the target compounds gives the series of the peak of various fragments. Their intensities provide stability of fragments ions. The mass spectrum of metal complexes is shown in Figures S9-S10.

Electronic Absorption Spectroscopy

UV/Visible spectrum of the metal complex (Cd-Tc/Sal) had been done on DMSO solution within a wavelength range between 250-800 nm. The electronic spectrum shows excessive-high intense absorption peaks at 280, 369 and 768 nm which signify ($\pi \rightarrow \pi^*$) & ($n \rightarrow \pi^*$) transitions. The spectral data was presented in Figure S11. Together with their electronic transition and suggested geometries. Electronic emission spectra of Cd (II) did not exhibit any d-d transition because its d^{10} orbital is filled but exhibit absorption bands due to metal-ligand charge transfer (MLCT) indicating the d^{10} system. Similarly Molybdenum complex shows absorption bands at 297, 371, 447 nm.

TGA/DTA Study

The thermogravimetric study provides useful information about the thermal and kinetic stability of the compounds which was carried by running the analysis in a nitrogen atmosphere at room temperature to 860 °C with a linear rate of heating at 10 °C/min. One important purpose of TGA records signifies that the associated molecules of water inside complexes help the elemental analysis. Correlation of thermal events with continuous heating of the chemicals is useful to withdraw information about kinetic parameters and the mass loss during the decomposition. The thermal records which include thermal decomposition, percentage mass loss, and thermodynamic and kinetic parameters of every decomposition steps have been derived and covered in Table 3 & 4. Results indicate good agreement with theoretical formula supported through micro- elemental analysis.

The thermogram of the cadmium complex has been shown that decomposition takes place in three steps within the temperature range of 246.89 - 634.32 °C. In the first decomposition stage, weight loss of 14.96% (3.1143 mg) in the temperature range 246.89-286.67 °C. The second and third stages occur with % weight loss of 11.7239% (11.7239 mg) and 1.9447% (1.9447 mg) within the temperature range of 341.54-398.11 °C and 580.03-634.32 °C. In every

case, decomposition starts by loss of coordinated or crystallized water molecules of the complexes only or other components of ligand moiety which confirms the composition of metal complexes. This suggests that cadmium complex is thermally stable. Similarly, the thermogram of Molybdenum complex was decomposed at three ranges in the temperature range of 197.38-805.15 °C. In the first decomposition stage, weight loss of 16.899% (1.6899 mg) take place within the temperature range of 197.38-260.48 °C. The second and third decomposition stages occur with % mass loss of 1.6459% (16.459mg) and 1.4743% (1.4743 mg) in the temperature range of 721.21-742.98 °C and 789.75-805.15 °C which are presented in Figure 2 & Figure S12. The residue formed was metal oxide such as CdO & MoO.

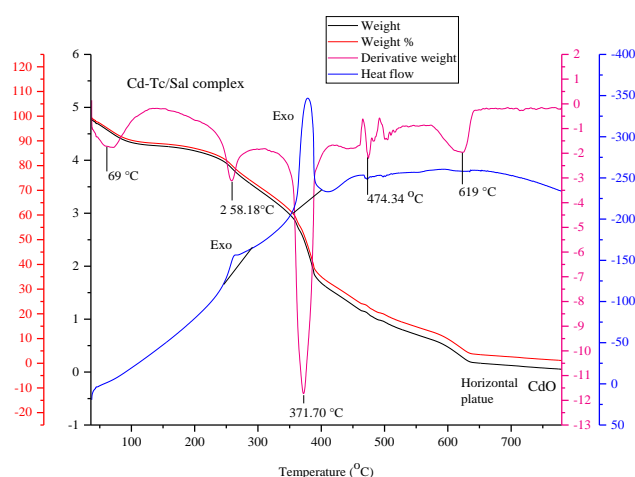


Figure 2: Thermogram of Cd-TcSal complex

Scanning Electron Microscopy Study

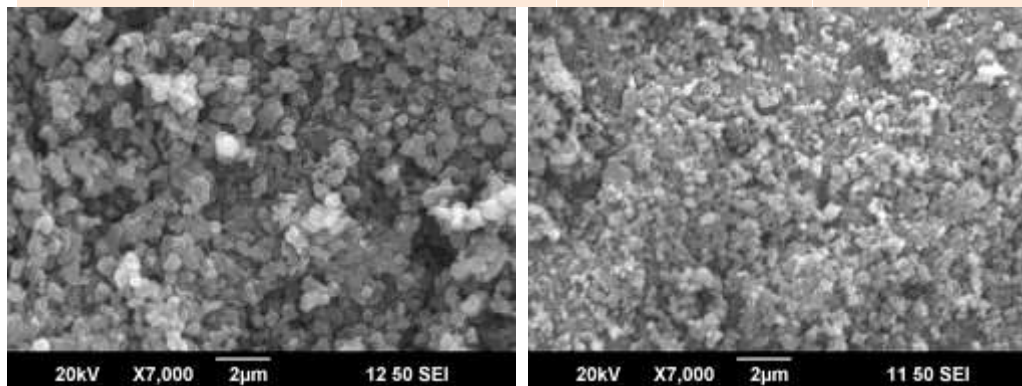
The microstructures, as well as morphological properties of metal complexes, were examined through SEM (Scanning electron microscopy). A high beam of energy of an electron of SEM produces a different variety of signals to the solid surface which results in the generation the image of shape, size, strength, ductility and the arrangement of atoms in an object. SEM is also an important tool in forensic science, metallurgy, gemology and in medicinal science¹⁷. The SEM micrographs of Cadmium and Molybdenum complex shown in Figure 3. From the SEM micrograph, it signifies the formation of successful nanosized particle. The cadmium complex shows that the particles are extremely agglomerated in nature due to induced crystal growth by itself¹⁸.

Table 3: Kinetics and thermodynamic parameter of Cadmium and Molybdenum metal complexes

Complexes	r	A(s ⁻¹)	Tmax (K)	E* (kJ/mol)	Δs* (j/kmol)	ΔH* (kJ/mol)	ΔG* (kJ/mol)
Cd-complex	-0.9955	2.05x10 ¹⁷	531.18	184.920	120.970	18.505	116.248
	-0.9986	4.01x10 ²¹	644.85	263.260	162.240	257.901	153.281
	-0.9988	1.72x10 ²⁴	892.81	421.170	209.930	413.751	226.324
Mo-complex	-0.9979	7.55x10 ⁹	496.22	102.526	-60.040	98.401	128.196
	-0.9992	7.16x10 ⁶¹	1007.15	1196.867	929.110	1188.494	252.745
	-0.9963	1.59x10 ¹⁰⁴	1070.54	2100.898	216.17	2091.997	186.058

Table 4: Thermal decomposition data of Cadmium and Molybdenum complexes

Complexes	TG range (°C)				DTA		
	Δm% (cal.)	Ti	Tf	T _{DTG}	Mass loss	T _{dta}	Peak
Cd-complex	14.96	246.89	286.67	258.18	-3.1143	246.89	Exo
	11.7239	341.54	398.11	371.70	-11.7239	-	Exo
	1.9447	580.03	634.32	619.81	-1.9447	634.11	
Mo-Complex	16.899	197.38	260.48	223.22	-1.6899	197.38	
	1.6459	721.21	742.98	734.15	-16.459	-	
	1.4743	789.75	805.15	797.54	-1.4743	805.15	

**Figure 3:** SEM micrograph of i) Cd-TcSal ii) Mo-TcSal

Similarly Molybdenum complex has the shape of nanoparticles which has almost spherical of some aggregation complex¹⁹. Careful examination of the single crystal honestly suggests the nanoscale measurement of the single crystal of the complexes.

Molecular Modeling Study

The proposed structure of metal complexes was carried out with 3D modeling Via the Cs Chem 3D program. Correct stereochemistry was once finished via manipulation and Change to gain low energy molecular geometry. Metal complexes, Potential energy will be the sum of all the energy of following types: $E = E_{str} + E_{ang} + E_{tor} + E_{vdw} + E_{oop} + E_{ele}$ where E's represents energy value for various interaction. The subscripts signify the bond stretching, angle bending, deformation angle, Van der Waals interactions, out of plane bending, simple bending, and electronic interaction respectively. The total steric energy for cadmium complex is 916.0934 Kcal/mol and has the geometry of Trig Planar and presented in Figure S13.

Antibacterial Sensitivity Study

The metal complexes were carried out the antibacterial sensitivity which was screened in vitro of their inhibitory

activity against some clinical pathogenic bacteria like *S. aureus*, *E. coli*, *P. aeruginosa* through the use of Kirby Bauer paper disc diffusion technique. For this test, the complex was prepared by dissolving in DMSO solvent. Zone of inhibition signifies mean of three readings which were presented in the Figures S14-15 & Table 5 that displays the effect of prepared complexes on different bacterial pathogens. From the antimicrobial study, all-metal complexes show activity towards tested pathogens while ligand does not show any effects. The complexes show the greater activity in comparison to ligand results in the complex formation where the ligand is bonded with the metal ions. Hence increase in the concentration of metal complexes increase the inhibition zone of bacterial growth²⁰. From the reported data, it is clear that Cadmium and Molybdenum metal complex shows better antibacterial activity at higher concentration and considerable activity at a lower concentration. The *E. coli* of Molybdenum complex found much less active. Similarly, *S. aureus* of Cadmium complex suggests better results. So all the pathogens had been found susceptible towards the synthesized derivatives of two Tetracycline (Figure S16).

Table 5: Antibacterial growth data of Cadmium and Molybdenum metal complexes.

Complexes	The diameter of zone of inhibition in (mm)								
	<i>S. aureus</i>			<i>P. aeruginosa</i>			<i>E. coli</i>		
Concentration (µg/µl)	25	12.5	6.25	25	12.5	6.25	25	12.5	6.25
Cd-Tc/Sal complex	28	24	22	17	16	15	22	21	19
Mo-Tc/Sal complex	20	18	16	12	11	10	11	10	9
Amk (30mcg/disc)		27			21			23	
Tc		31			31			31	
DMSO		0			0			0	

CONCLUSION

In this paper, the metal complex of Cd (II) & Mo (II) was successfully synthesized via by using Tetracycline as primary ligand and Salicylaldehyde as the secondary ligand. The synthesized complexes had been analyzed by way of micro-elemental analysis, FT-IR, (¹H & ¹³C)-NMR, UV/Vis, SEM, TGA /DTA. Molecular modeling suggests coordination behavior of metal ions with the ligand and as a result, received results are very much close to the experimental data. The color change has seen all through the chemical procedure truly indicates deprotonation for the duration of formation of the complex. The evidence for the purity of the complex was validated through the melting point. The anti-microbial tests had been carried under Kirby-Bauer paper disc diffusion technique by using clinical bacterial pathogens like *S.aureus*, *E. coli*, *P.aeruginosa* which suggests gorgeous antibacterial activity and comparable sensitivity test of ligand, as well as metal complexes truly, shows that they exhibit strong activity against *S.aureus*.

Acknowledgment: The first author is highly acknowledged to Nepal Academy of Science and Technology (NAST), Khumaltar, Lalitpur, Nepal for providing Ph.D. Fellowship.

REFERENCES

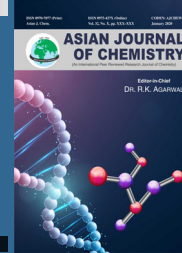
1. Abu Ali H, Fares H, Darawsheh M, Rappocciolo E, Akkawi M, Jaber S, Synthesis, characterization and biological activity of new mixed ligand complexes of Zn (II) naproxen with nitrogen-based ligands, *European Journal of Medicinal Chemistry*, 89, 2016, 67–76. <http://doi.org/10.1016/j.ejmech.2014.10.032>.
2. Kafi-Ahmadi L, Poursattar Marjani A , Pakdaman-Azari M, Synthesis, characterization and antibacterial properties of *N,N'*-Bis(4-dimethyl amino benzylidene) benzene-1,3-diamine as new schiff base ligand and its binuclear Zn(II), Cd(II) Complexes, *South African Journal of Chemistry*, 71, 2018,155-159. <http://dx.doi.org/10.17159/0379-4350/2018/v71a20>.
3. Akter J, Hanif Md A, Islam MS, Reza Md Y, Haque Md M, Zahid AASM, E-Zahan, Md K, Islam Md A, Banu L A, Mixed ligand complexes of Ni(ii) and Cd(ii) with Phthalic acid or Succinic acid and heterocyclic amines: Synthesis and characterization with the antimicrobial study, *European Journal of Medical and Pharmaceutical Research*, 5(4), 2018, 106-113.
4. Akila E, Usharani M, Vimala S, Rajavel R, Synthesis, spectroscopic characterization and biological evaluation studies of mixed ligand schiff base with metal (II) complexes derived from o-phenylenediamine, *Chemical Science Review and Letters*, 1(4), 2012, 181–194.
5. Kuriakose D, Aravindakshan A A, Kurup M R P, Synthesis, spectroscopic, crystal structures and photoluminescence studies of cadmium (II) complexes derived from di-2-pyridyl ketone benzoyl hydrazone : Crystal structure of a rare eight coordinatecadmium(II) complex, *Polyhedron*, 127, 2017, 84–96. <https://doi.org/10.1016/j.poly.2017.01.041>.
6. Anacona J R, Lopez M, Mixed-Ligand Nickel(II) complexes containing sulfathiazole and cephalosporin antibiotics: Synthesis, characterization, and antibacterial activity, *International Journal of Inorganic Chemistry*, 2012, 1–8. <http://doi.org/10.1155/2012/106187>.
7. Saghatforoush LA, Aminkhani A, Ershad S, Karimnezhad G, Ghammamy S, Kabiri R, Preparation of Zinc (II) and Cadmium (II) complexes of the tetradentate schiff base ligand 2-((E)-(2-(2-(pyridine-2-yl) ethyl thiol) ethyl imino)methyl)-4-bromophenol (PytBrsalH), *Molecules*, 13(4), 2008, 804-811.
8. Chaudhary N K, Guragain B, Synthesis, thermal characterization and invitro antibacterial assessment of Co (II) and Cd (II) complexes of schiff base derived from amoxicillin and thiophene-2- carbaldehyde, *Asian Journal of Chemistry*, 31(4), 2019, 951-959: <https://doi.org/10.14233/ajchem.2019.21882>.
9. Bhattarai A, Interaction behavior of polyion-counterion for sodium polystyrene sulfonate, *Data in brief*, 25, 2019, 104365.
10. Bhattarai A, Nandi P, Das B, The effects of concentration, relative permittivity and temperature on the transport properties of sodium polystyrene sulphonate in methanol-water mixed solvent media, *Journal of Polymer Research*, 13, 2006, 475-482.
11. Ogunniran K O, Ajanaku K O, James O O, Ajani O O, Nwinyi CO, Allensela MA, *Fe(III) and Co(II) complexes of mixed antibiotics: synthesis, characterization, antimicrobial potential and their effect on alkaline phosphatase activities of selected rat tissues*, *International Journal of Physical Sciences*, 3 (8), 2008, 177-182. <http://www.academicjournals.org/IJPS> ISSN 1992–1950 © 2008 Academic Journals.
12. Kavlak S, Kodolbas A O, Can H K, Guner A, Rzaev Z M O, Temperature dependence of electrical conductivity in acrylic acid) and Its transition metal complexes, *Advances in Polymer Technology*, 23(3), 2004, 222–229. <https://doi.org/10.1002/adv.20012>.
13. Giardino L, Andrade F B De, Beltrami R, Antimicrobial effect and surface tension of some chelating solutions with added surfactants, *Brazilian Dental Journal* 27, 2016, 584–588. <http://dx.doi.org/10.1590/0103-6440201600985>.
14. Rana S, Yu X, Patra D, Moyano D F, Miranda O R, Hussain I, Rotello V M, Control of surface tension at liquid – liquid interfaces using nanoparticles and nanoparticle – protein complexes, *Langmuir*, 28(4), 2012, 2023-2027. dx.doi.org/10.1021/la204017z.



15. Sunita T, Sharma P K, Malviya R, Influence of concentration on surface tension and viscosity of Tamarind (*Tamarindus indica*) seed gum, *Annals of Molecular and Genetic Medicine*, 1(1), 2017, 008-012, DOI:10.17352/amgm.000002.
16. Adamson A W, *Physical Chemistry of Surfaces*, John Wiley and Sons, Inc. Somerset, NJ, 1982.
17. Pal T, Alam M, Hossen J, Paul, S, Ahmad H, Sheikh M, Spectral and biological studies on new mixed ligand complexes, *Journal of Scientific Research* 10(3), 2018, 291–302.doi: <http://dx.doi.org/10.3329/jsr.v10i3.36379>.
18. Desai K R, Pathan A A, Bhasin C P, Synthesis, characterization of cadmium sulphide nanoparticles and its application as photocatalytic degradation of conged, *International Journal of Nanomaterial and Chemistry*, 3(2), 2017, 39–43.
19. Divsalar N, Monadi N, Tajbaksh M, Preparation and characterization of a molybdenum (VI) schiff base complex as magnetic nanocatalyst for synthesis of 2-Amino- 4H-benzo[h]chromenes, *Journal of Nanostructure*, 6(4), 2016, 312-321. DOI: 10.22052/jns.2016.34329.
20. El-tabl A S, El-wahed, M M A, MahmoudRez A M S, Cytotoxic behavior and spectroscopic characterization of metal complexes of ethyl acetoacetate bis(thiosemicarbazone) ligand, *Spectrochimica Acta Part A: Molecular and Biomolecular Spectroscopy*, 117(3), 2014, 772-788. <https://doi.org/10.1016/j.saa.2013.04.014>.

Source of Support: Nil, Conflict of Interest: None.





Synthesis, Spectroscopic Characterization and Antibacterial Assessment of Zirconium(II) and Palladium(II) Complexes of Tetracycline-Salicylaldehyde Mixed Ligand

R.K. DEV¹, A. BHATTARAI^{1*}, N.K. CHAUDHARY¹ and P. MISHRA¹

Bio-inorganic and Materials Chemistry Research Laboratory, Department of Chemistry, Tribhuvan University, M.M.A.M. Campus, Biratnagar, Nepal

*Corresponding author: E-mail: bkajaya@yahoo.com

Received: 4 January 2020;

Accepted: 15 March 2020;

Published online: 30 May 2020;

AJC-19900

Zirconium(II) and palladium(II) mixed ligand metal complexes were synthesized by using an equimolar mixture of tetracycline (Tc) as primary ligand and salicylaldehyde as secondary ligand. The metal complexes were characterized by physico-chemical and spectroscopic techniques like CHN analysis, surface tension, pH, conductivity and melting point measurements. The spectroscopic characterization technique includes IR, (¹H & ¹³C) NMR, UV/visible and Mass spectrometry methods. The SEM technique determines the surface morphology of the complexes. The thermal and kinetic stability of the complexes was obtained from TGA/DTA curves from which the parameters like E^* , ΔH^\ddagger , ΔS^\ddagger and ΔG^\ddagger have been calculated by using the Coats-Redfern equation. Molecular modeling gives a geometry of the complex which was obtained from Chem 3D Pro. 12.0 software program. The metal complexes of Zr-TcSal and Pd-TcSal have coordinated with tetrahedral and square planar geometry, respectively. The antibacterial susceptibility study of the synthesized metal complexes was done by Kirby-Bauer paper disc diffusion techniques on *S. aureus*, *E. coli* and *P. aeruginosa* clinical pathogens.

Keywords: Tetracycline, Metal complexes, Thermal analysis, Antibacterial activity.

INTRODUCTION

Since immemorial times, antibiotics have been used to cure the diseases of animals and human beings. Most of the antibiotics cannot be completely absorbed by the animals and humans due to their soluble nature. Nearly 90% prototype or metabolites of antibiotics are released out to the soil and water through manures or urine of patients, resulting in some degradation to the environment. Human utilization of animals' food and food products which have antibiotic residues causes chronic poisoning which results in mutation, cancer and embryotoxicity [1]. Metal complexes of mixed ligands have wide applications in the field of engineering, science and technology, hydrometallurgy, dyeing, analytical chemistry, textiles as well as in chemotherapy [2]. They are also used as antibacterial, antifungal, antitumor, antipyretic, antimetabolites, antithyroid, antiviral, anti-inflammatory and surface anesthesia activity [3]. The organometallic complexes of mixed ligand formed by the refluxation of the equimolar ratio of primary and secondary ligand along with their metal salts have been a

global interest for the researchers in the field of complexation. Transition metals of carbonyl derivatives are also used as intermediates in the synthesis of very useful organometallic complexes which has huge application in catalysis of reactions such as hydrogenation, epoxidation, carbonylation and hydroformylation [4]. In metal complexes, the ligand containing the O & N donor atom possesses great importance due to their binding nature with metal atoms. The existence of amine (-NH₂) and carboxyl (COO⁻) group in ligand also serves as a source of N/O donating groups which results in the formation of metal complexes of mixed ligands [5]. Biologically active compounds with metal interaction can be used as a specific goal to improve their activity and overcome their resistance [6]. Tetracyclines (TCs) are one of the most widely applied antibiotics in the field of coordination and medicinal chemistry. Today the cause of increasing antibiotic resistance of microorganisms and on plant development is due to misuse and overdose of antibiotics used by the human being [7]. Tetracycline contains the number of substitution patterns and significant structure deviation can change the antibacterial potency [8]. In this work,

we focused on the preparation of metal complexes of zirconium(II) and palladium(II) by using tetracycline as primary ligand and salicylaldehyde as the secondary ligand. Besides their physico-chemical microanalysis and spectroscopic characterizations, antimicrobial susceptibility test was done by Kirby-Bauer paper disc diffusion techniques using clinical pathogenic bacteria like *S. aureus*, *E. coli* and *P. aeruginosa*.

EXPERIMENTAL

The analytical research-grade (AR) chemicals and solvents were used for the experimental work and purified according to the standard process. Drugs such as tetracycline (Sigma-Aldrich), salicylaldehyde, $ZrOCl_2 \cdot 8H_2O$ (Loba Chemie Pvt. Ltd.), MHA and $PdCl_2$ (Himedia) were used during the research and triple distilled water and double-distilled ethanol were used for the experiment.

Elemental microanalysis (C, H, N) of the metal complexes was carried out in Euro-EA 3000 microanalyzer. The UV/visible spectra of the complexes in the DMSO solvent were recorded on Varian, Cary 5000 in the range of 800-260 nm. FT-IR spectral analysis was carried on Perkin Elmer Spectrum II as KBr pellets technique in the range of 4000-400 cm^{-1} . The 1H NMR was carried out in the presence of DMSO- d_6 solvents on Bruker AvII- 400 MHz Spectrometer and Me_4Si which acts as the internal reference. The kinetic and thermal analysis (TGA/DTA) was carried out under the nitrogen atmosphere at room temperature in the range of 40-750 $^{\circ}C$ at the linear heating rate of 10 $^{\circ}C$ min^{-1} . ESI-MS evaluation has been determined through a water UPLC-TQD mass spectrometer in the mass range of 0-1000 m/z . The melting point was recorded in VEEGO ASD-10013 programmable melting point apparatus. The surface morphology was done on the JEOL model JSM-6390 LV SEM technique. Molecular modeling of metal complexes was optimized through Chem 3D Pro 12.0 program. Conductance measurement was done in autoranging conductivity/TDS meter TCM 15+. The pH was recorded from Elico LI 613 pH meter. The antibacterial susceptibility test was carried out by Kirby Bauer's paper disc diffusion technique against clinical pathogens, which was done at the Microbiological Laboratory, Mahendra Morang Adarsh Multiple Campus, Biratnagar, Morang, Nepal.

Antibacterial sensitivity assay: Synthesized metal complexes of mixed ligand have been screened for their antibacterial susceptibility test by Kirby-Bauer paper disc diffusion method on two bacterial strains *i.e.* Gram-negative (*Escherichia coli* and *Pseudomonas aeruginosa*) and Gram-positive (*Staphylococcus aureus*). Test solutions of the metal complexes were prepared in 30% DMSO at four different concentrations (25, 12.5, 6.25 and 3.125 $\mu g/\mu L$) to measure their actual effectiveness. Firstly, the fresh culture of organisms was prepared in nutrient broth and incubating them for 2 h at 37 $^{\circ}C$ for their complete and total growth. Blank paper discs were prepared from filter paper (Whatman number1) of 5 mm diameter in size and were sterilized and loaded with test solutions. The sterile MHA (Muller Hinton Agar) media was prepared for antibacterial sensitivity according to their reported literature. The revived and fresh pathogens were slowly swabbed into the sterile media and complexes of different concentrations

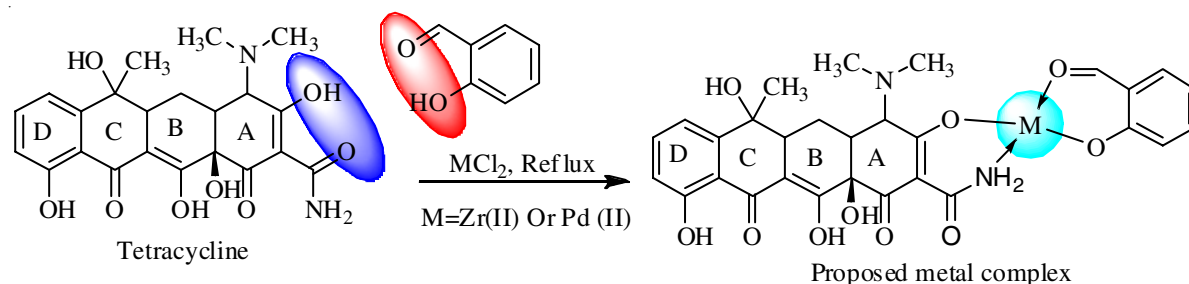
were added into the paper disc. The positive control standard antibiotic discs (Amikacin) of 30 mcg/disc were also applied during the tests. After completing all these activities, the loaded Petri plates were kept in an incubator for about 37 $^{\circ}C$ up to 36 h to observe the zone of inhibition for the bacterial growth [9]. The diameter of zone of inhibition (mm) was visualized through Hi Antibiotic Zone Scale-C.

Synthesis of zirconium complex (Zr-TC/Sal): A solution of primary ligand tetracycline (0.8892 g, 2 mmol) in 70% double distilled ethanol and a solution of $ZrOCl_2 \cdot 8H_2O$ (0.6446 g, 2 mmol) in water was stirred in a magnetic stirrer separately in 50 mL round bottom flask for 4 h and added to the tetracycline solution in dropwise condition. The reaction mixture was further stirred for a few hours more and further added with well-stirred secondary ligand salicylaldehyde (0.2 mL, 2 mmol) dissolved in ethanol. The reaction mixture was further stirred for a few hours and filtered. The filtered reaction mixture was refluxed for 8 h and pH was maintained at 7 by adding 2 N NH_4OH solution and left the beaker for 2 days without any disturbance. As a result, the precipitate was obtained and then filtered, washed with ethanol and water several times and dried. The dried precipitate was recrystallized from ethanol to obtain the black crystals of the zirconium complex (Scheme-I).

Synthesis of palladium complex (Pd-TC/Sal): A solution of primary ligand tetracycline (0.8897 g, 2 mmol) in 70% double distilled ethanol and a solution of $PdCl_2$ (0.0893 g, 0.5 mol) in aqueous ethanolic solution was stirred in a magnetic stirrer separately in 50 mL round bottom flask for 4 h. The reaction mixture was further stirred for a few hours more and further added with well-stirred secondary ligand salicylaldehyde (0.2 mL, 2 mmol) dissolved in ethanol. The reaction mixture was further stirred for a few hours and filtered. The filtered reaction mixture was refluxed for 8 h and pH was maintained at 6.7 by adding 2 N NH_4OH solution and left in the beaker for 2 days without any disturbance. As a result, the precipitate was obtained and then filtered, washed with ethanol and water several times and dried. The dried precipitate was recrystallized from ethanol to obtain the black crystals of palladium complex (Scheme-I).

RESULTS AND DISCUSSION

Physical characterization: Both metal complexes of zirconium(II) and palladium(II) were obtained as coloured solid by the reaction of primary ligand tetracycline (Tc) and secondary ligand (salicylaldehyde). The experimental data of elemental microanalysis and physico-chemical parameters such as melting point, colour change, electronic absorption of the metal complexes show good agreement with the calculated data and denotes the precise relationship to a molecular formula of the proposed complex (Table-1). The synthesized complexes are solid, higher melting points, generally stable around at room temperature and insoluble in water but soluble in common organic solvents like DMSO. The pH, density, viscosity, surface tension, conductivity of complexes obtained was 6.43 & 5.78, 1.048 & 1.076 (g/mL), 16.99 & 22.50 (cp), 56.30 & 57.50 (mN/m) and 14.70 & 17.80 ($\mu S/cm$) respectively for Zr-complex and Pd-complex and determines their non-electrolytic nature.



Scheme-I: Synthesis of zirconium(II) and palladium(II) metal complexes of TcSal mixed ligand [tetracycline (Tc) as primary ligand and salicylaldehyde (Sal) as secondary ligand]

TABLE-1
ELEMENTAL MICROANALYSIS, ELECTRONIC ABSORPTION AND PHYSICAL CALCULATION DATA

Complex	m.f.	m.w.	Colour	m.p. (°C)	Elemental analysis (%): Calcd. (found)				UV/vis peak (nm)	Assignment
					C	H	N	O		
Zr-TcSal	C ₂₉ H ₂₈ N ₂ O ₁₀ Zr	655.76	Black	175.9	53.12 (53.06)	4.30 (4.26)	4.27 (4.26)	24.40 (24.39)	268 342 446	$\pi \rightarrow \pi^*$ $n \rightarrow \pi^*$
Pd-TcSal	C ₂₉ H ₂₈ N ₂ O ₁₀ Pd	670.96	Black	265.5	51.91 (51.87)	4.21 (4.17)	4.18 (4.17)	23.85 (23.84)	263 307 343	$\pi \rightarrow \pi^*$ $n \rightarrow \pi^*$

FT-IR spectroscopy: The frequencies of FT-IR absorption spectra for zirconium and palladium complexes of mixed ligand was done from the range between 4000-400 cm⁻¹. The bands in the infrared spectrum signify the functional groups attached with the metal ions and also gives important information regarding the coordination sites which are involved during chelation. Broadbands within range of 3407-3183 cm⁻¹ were attributed to coalesce of $\nu(\text{OH}/\text{N-H})$ [10,11]. The bands between 1773-1653 cm⁻¹ indicate $\nu(\text{C=O})$. Similarly, the sharp IR bands in between 1635-1619 cm⁻¹ signify the $\nu(\text{C=N})$ which supports that the above complexes are azomethine derivatives [12]. The absorption peaks at 1580-1528 cm⁻¹ and 1404-1399 cm⁻¹ are due to $\nu_{\text{asym}}(\text{COO}^-)$ and $\nu_{\text{sym}}(\text{COO}^-)$. Similarly, the appearance of absorptions in the regions 1177-1126 cm⁻¹ denotes $\nu(\text{C-O})$. Here the coordination of azomethine nitrogen on a metal atom is confirmed by the presence of a new band at 604-602 cm⁻¹ and 476-470 cm⁻¹ are due to $\nu(\text{M-O})$ and $\nu(\text{M-N})$, respectively [13,14]. The FT-IR spectrum in combination with other spectral studies signifies the coordination of metal ions to the nitrogen atom of amide group (Table-2).

¹H & ¹³C NMR analysis: The ¹H NMR spectra of metal complexes was done in DMSO-*d*₆ solvent and gives the fruitful information of different proton environments as well as possible coordination sites to metal complexes. Their integral intensity of each signal was found to agree with the number of different types of protons present. The ¹H NMR spectrum of the Zr(II) complex, the peak signals at ($\delta = 2.478$ - 2.495 ppm) revealing to (CH₃) and singlet peak appeared at ($\delta = 2.491$ - 2.523 ppm) is assigned to DMSO-*d*₆. Similarly, the peaks in the region

of ($\delta = 2.5$ - 3.5 ppm) represent [N-(CH₃)₂]. The aromatic proton lies in the location of ($\delta = 6.950$ - 6.991 ppm) and primary amide proton lies in the vicinity between ($\delta = 10.214$ ppm). Similarly in the palladium(II) complex, the peak signals at ($\delta = 1.059$ - 1.226 ppm) signify (CH₃), ($\delta = 1.527$ - 1.544 ppm) as (CH₂NH) group and ($\delta = 3.51$ ppm) as -OH respectively [15,16].

In the ¹³C NMR spectra of zirconium metal complexes, the DMSO-*d*₆ solvent displays chemical shifts at 39.166-40.832 ppm and N(CH₃)₂ at 45.5 ppm. The aromatic ring carbon confirmed a signal in the range between 113.635-126.652 ppm while the carbonyl group (-CO-) appears in the region of 182.917 ppm. Similarly, palladium complex contains the chemical shift at the region of 40 ppm is due to DMSO-*d*₆ solvent and the aromatic carbon ring lies at 134.539-137.972 ppm [17].

ESI-Mass analysis: The metal complex of Zr(II) and Pd(II) displays the prominent peak of molecular ion (M⁺) at ($m/z = 656$) and ($m/z = 671$) amu of the parent ion and the base peak appears in $m/z = 445$ & $m/z = 171$ region indicates the proposed formula for the complexes. The molecular mass and other spectral data are essential for the generation of the structure of organic compounds. The rest peak in the mass spectrum is the fragment ion peaks. The successive decrease in the peak of the target compounds gives the peak of various fragments and intensities provide stability of fragments ions. The mass spectrum of metal complexes is shown in Fig. 1.

Electronic absorption: The electronic absorption spectroscopy tool is used for distinguishing the characterization for identifying the binding mode of complexes [18]. The spectra

TABLE-2
FT-IR SPECTRAL DATA OF Cd AND Mo-TcSal METAL COMPLEXES

Complex	$\nu(\text{O-H})$ or $\nu(\text{N-H})$	$\nu(\text{C=O})$	$\nu(\text{C=N})$	$\nu_{\text{asym}}(\text{COO}^-)$	$\nu_{\text{sym}}(\text{COO}^-)$	$\nu(\text{C-O})$	$\nu(\text{M-O})$	$\nu(\text{M-N})$
Tc Ligand	3384	1653	1615	1580	1399	1126	-	-
Zr-TcSal	3183	1770	1619	1570	1399	1152	604	476
Pd-TcSal	3407	1773	1635	1528	1402	1177	602	470

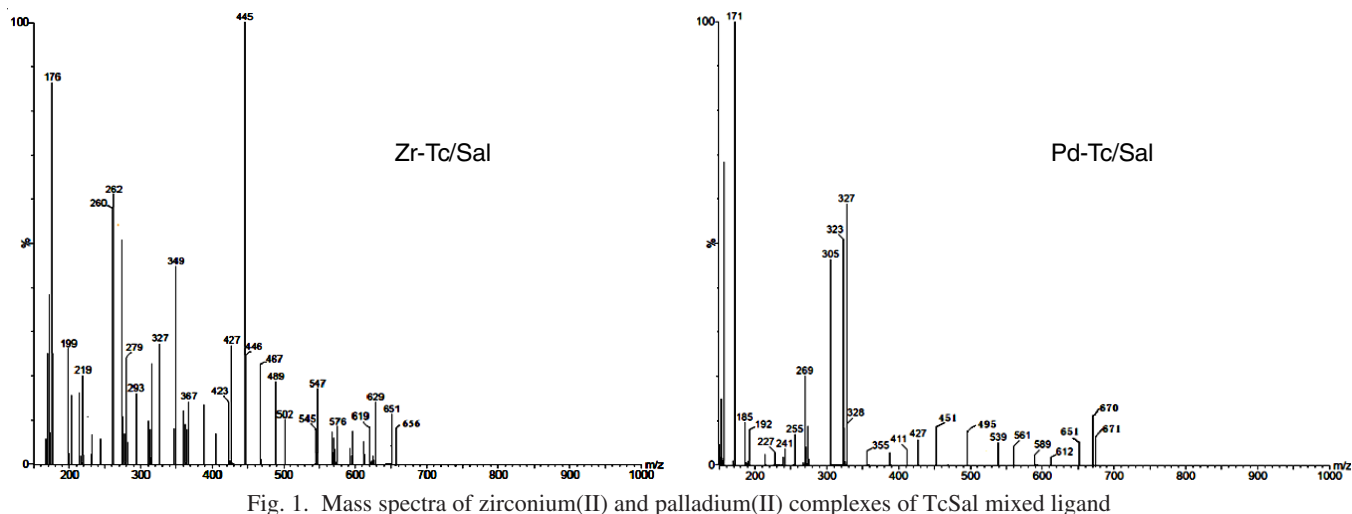


Fig. 1. Mass spectra of zirconium(II) and palladium(II) complexes of TcSal mixed ligand

were taken in a DMSO solvent within a range between 250–800 nm wavelength and are shown in Fig. 2. The electronic spectrum of Zr complex shows excessive-high intense absorption band at 268 and 342 nm, which signify ($\pi \rightarrow \pi^*$) transitions

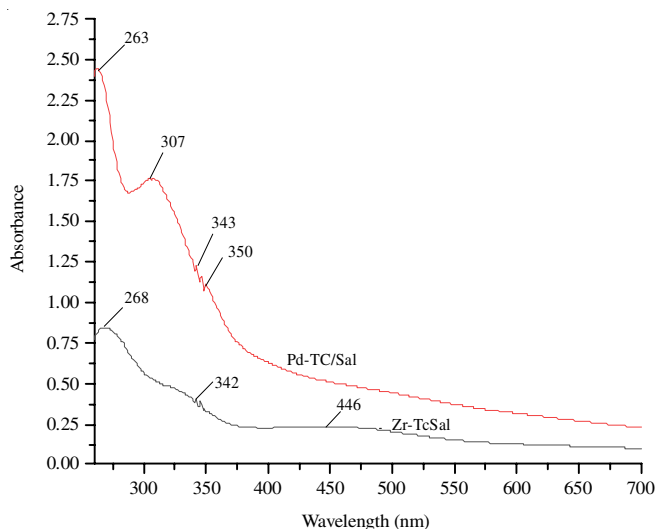


Fig. 2. Electronic absorption spectra of Zr and Pd-Tc/Sal metal complex of mixed ligand

of aromatic ring and remains unchanged in zirconium complex and next band at 446 nm signify ($n \rightarrow \pi^*$) transition of $>C=N$ chromophore and denotes bathochromic shift in zirconium complex arise because of coordination of zirconium metal ion with azomethine nitrogen. The following band moves slightly higher-energy due to polarization of electron interaction of zirconium with $>C=N$ chromophore. Hence due to their d^0 electronic configuration, there are no $d-d$ transitions in Zr(IV) complexes [13,14]. Zirconium complex has been assigned for tetrahedral geometry. Similarly, the electronic spectrum of the Pd-Tc/Sal complex possesses three absorption bands near 263, 307, 343 nm in the visible region. All bands of these types are assigned to have ($\pi \rightarrow \pi^*$) and ($n \rightarrow \pi^*$) transition which specifies the square planar geometry [19].

Thermal analysis: Thermogram of zirconium complex (Fig. 3) has been shown that decomposition takes place in three steps at the temperature between 50.7–755.48 °C. In the first decomposition stage, weight loss of 27.93% (–5.9503 mg) in the temperature range 50.7–108.05 °C. The second and third decomposition steps occurred with % weight loss of 40.60% (1.197 mg) and 83.89% (2.3386 mg) within the temperature range of 249.28–302.03 °C and 633.79–755.48 °C. In each case, decomposition starts with the loss of coordinated or crystallized

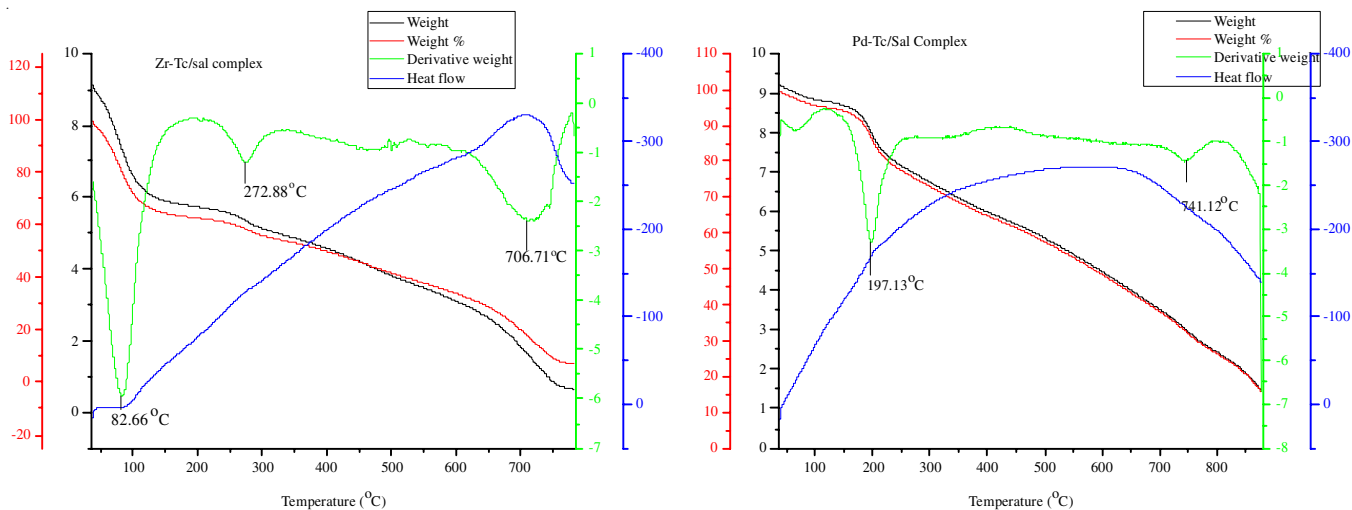


Fig. 3. Thermogram of zirconium and palladium complex

water molecules of the metal complexes only or other components of ligand moiety which confirms the composition of metal complexes. This suggests that zirconium complex is thermally stable. Similarly, thermogram of palladium complex (Fig. 3) was decomposed at two ranges in the temperature range of 164.01-769.19 °C. In the first decomposition stage, weight loss of 20.60% (-3.3048 mg) takes place within the temperature range of 164.01-247.37 °C. The second decomposition stages occur with a mass loss of 65.59% (-1.4339 mg) in the temperature range of 709.75-769.19 °C. The residue formed was metal oxide such as ZrO and PdO.

Kinetic parameters: The kinetic and thermodynamic parameters of the complexes were extracted by making calculation through Coats-Redfern equation. The thermal stability and kinetic parameters of different decomposition steps were calculated and plotted graphically by using the Coats-Redfern relation:

$$\ln\left(-\frac{\ln(1-\alpha)}{T^2}\right) = \ln\left(\frac{AR}{\beta E^*}\right) - \frac{E^*}{RT}$$

here α denotes decomposition fraction at temperature (K) and β signify linear heating rate (dT/dt). A and E^* represent the Arrhenius pre-exponential factor and activation energy. R denotes universal gas constant. Using the equation: $y = mx + c$, a linear plot of left-hand side versus $1/T$, whose slope E^*/R gives the activation energy. The other kinetic parameters such as entropy of activation (ΔS^*), enthalpy of activation (ΔH^*) and free energy of activation (ΔG^*) can be solved by using the relation as:

$$\Delta S^* = R \ln\left(\frac{Ah}{K_B T}\right)$$

$$\Delta H^* = E^* - RT$$

$$\Delta G^* = \Delta H^* - T\Delta S^*$$

The thermodynamic and kinetic activation parameters of various decomposition steps of metal complexes are calculated and presented in Table-3. The greater value seen in all the complexes in subsequent steps reflects high thermal stability caused by the covalent bond character. In the first decomposition steps, there is negative entropy of activation which indicates the non-spontaneous dehydration reaction process and positive value of ΔG^* of all complexes indicate the non-spontaneous nature of decomposition steps. The positive value of ΔH^* indicates the endothermic process and the correlation coefficient from the graph indicates a good fit [14,20].

SEM analysis: The SEM images of Zr-TcSal and Pd-TcSal complexes are shown in Fig. 4. Zirconium complex was found to be microcrystalline and nanograins in shape. Similarly, Pd(II) complex showed the agglomeration of hybrid nanomaterial [21,22].

Antibacterial sensitivity: Synthesized metal complexes of mixed ligand were carried out an antimicrobial sensitivity test by Kirby-Bauer paper disc diffusion method and screened *in vitro* of their inhibitory activity against some clinical pathogens with various concentrations (25, 12.5, 6.25 and 3.125 $\mu\text{g}/\mu\text{L}$). For this test, the calculated amount of metal complex was prepared in DMSO solvent. From the antimicrobial sensitivity study, all the metal complexes show better activity towards tested bacterial pathogens while ligand does not show any effects (Table-4). This result shows that metal complexes have greater activity in comparison to a ligand that indicates the formation of a metal complex where the ligand is bonded with the metal ions. Hence increase in the concentration of metal complexes increases the inhibition zone of bacterial growth [23]. From the presented data, it is clear that zirconium and palladium metal complex shows better results of antibacterial at higher concentrations and goes on decreasing at a lower

TABLE-3
KINETICS AND THERMODYNAMIC PARAMETERS OF ZIRCONIUM(II) AND PALLADIUM(II) METAL COMPLEXES

Complexes	Step	r	A (s ⁻¹)	T _{max} (K)	E* (kJ/mol)	ΔS* (J/kmol)	ΔH* (kJ/mol)	ΔG (kJ/mol)
Zr-complex	1	-0.9993	1.68 × 10 ⁸	355.66	60.311	-88.91	57.354	88.976
	2	-0.9981	2.64 × 10 ¹⁴	545.88	158.856	26.14	154.318	140.049
	3	-0.9993	7.14 × 10 ¹⁰	979.71	222.049	-47.02	213.903	259.970
Pd-complex	1	-0.9942	7.30 × 10 ⁶	470.13	70.608	-117.32	66.699	121.854
	2	-0.9990	2.71 × 10 ²³	1014.12	4498.82	193.5	4490.378	4294.096

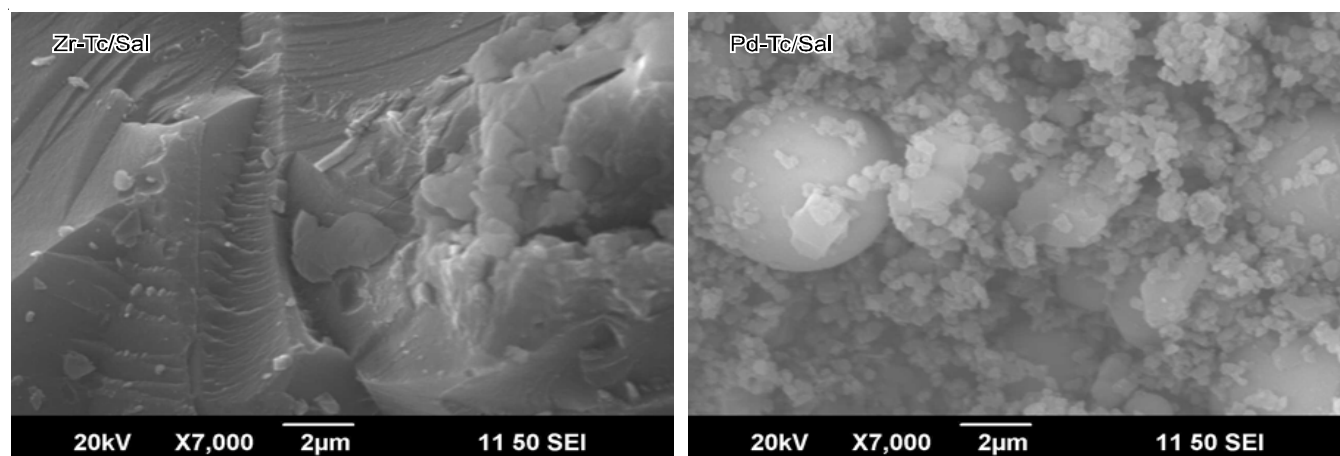


Fig. 4. SEM micrograph of zirconium and palladium complex

TABLE-4
ANTIBACTERIAL GROWTH DATA OF CADMIUM AND MOLYBDENUM METAL COMPLEXES

Complexes	Diameter of zone of inhibition (mm)											
	<i>S. aureus</i>				<i>P. aeruginosa</i>				<i>E. coli</i>			
Conc. ($\mu\text{g}/\mu\text{L}$)	25	12.5	6.25	3.125	25	12.5	6.25	3.125	25	12.5	6.25	3.125
Zr-Tc/Sal	12	11	10	9	13	12	10	9	13	12	10	8
Pd-Tc/Sal	26	24	23	22	14	13	12	10	27	24	23	21
Amk (30 mcg/disc)	18				25				28			
Tc	31				31				31			
DMSO	0				0				0			

concentration. *P. aeruginosa* of the zirconium and palladium complex found much less active. Similarly, *E. coli* of palladium complex suggests better results. So all the pathogens had been found susceptible to the synthesized derivatives of tetracycline.

Molecular modeling: The synthesized metal complexes can be structurally characterized based on special designed molecular modeling software by the 3D modeling *via* Chem 3D Pro-12.0 program. In the present study, the proposed structure of metal complexes was carried out. Correct stereochemistry was once finished *via* manipulation and Change to gain low energy molecular geometry. By the MM2 program present in the Cs chem. Office program, the optimized structure of metal complexes were done. The Zr-TcSal and Pd-TcSal have coordinated with tetrahedral and square planar geometry with steric energy of 1719.6070 and 1729.6133 Kcal/mol, respectively. The energy optimization was calculated many times so to obtain the minimum energy of molecular geometry. From the calculation, bond length, bond angles data as well as bonding parameters of Zr-TcSal and Pd-TcSal metal complexes were obtained and are presented in Tables 5 & 6 and their optimized 3D molecular structure is shown in Fig. 5. By the above experimental discussion, the structure of metal complexes of mixed ligand to be proposed. The potential energy will be the sum of all the energy of different types: $E = E_{\text{str}} + E_{\text{bend}} + E_{\text{tor}} + E_{\text{vdw}} + E_{\text{oop}} + E_{\text{ele}}$ where E 's denotes energy value for various interaction. The subscripts denote the bond stretching, angle bending, deformation angle, van der Waals interactions, out of plane bending, simple bending and electronic interaction, respectively.

Conclusion

In this present work, the metal complex of zirconium(II) and palladium(II) were successfully synthesized with the help

of tetracycline as primary ligand and salicylaldehyde as the secondary ligand. These complexes had been analyzed by their micro-elemental analysis, FT-IR, (^1H & C^{13}) NMR, UV/vis, SEM, TGA/DTA. Molecular modeling signifies the coordination behaviour of metal ions with the ligand and as a result, Zr complex was found to have tetrahedral geometry while Pd complex possesses square planar geometry. All the received results by the above parameters were very much closed to the experimental data. The colour change seen throughout the chemical procedure signifies deprotonation during the formation of the complex. The melting point also indicates the purity of metal complexes. The antimicrobial tests had been done by using Kirby-Bauer paper disc diffusion over metal complexes on three species namely, *Escherichia coli*, *Pseudomonas aeruginosa* (Gram-negative) and *Staphylococcus aureus* (Gram-positive) with various concentrations (25, 12.5, 6.25 and 3.125 $\mu\text{g}/\mu\text{L}$) which suggests gorgeous antibacterial activity and comparable sensitivity test of ligand, as well as metal complexes truly, shows that they exhibit strong activity against *E. coli*.

ACKNOWLEDGEMENTS

The authors are grateful to NAST (Nepal Academy of Science and Technology) for providing Ph.D. Fellowship and also thankful to STIC Cochin, Kerela, SAIF IIT Bombay, NBU Silligauri for their cooperation in carrying out the spectra of the compounds.

CONFLICT OF INTEREST

The authors declare that there is no conflict of interests regarding the publication of this article.

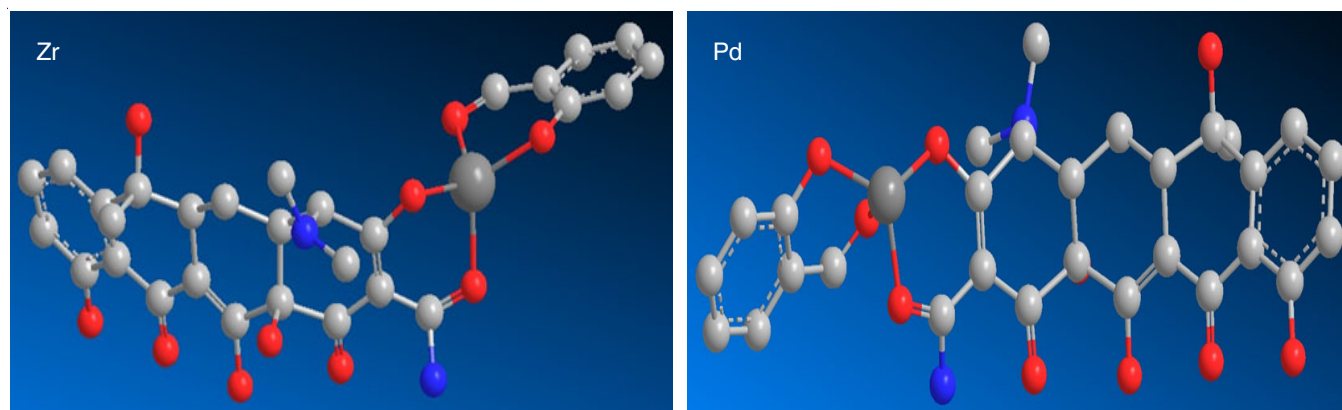


Fig. 5. Molecular modeling of zirconium and palladium complex

TABLE-5
BOND LENGTH AND BOND ANGLE OF Zr COMPLEX

Atom	Bond length (Å)		Atom	Bond angle (°)	
O(28)-Zr(41)	2.0989		C(33)-C(32)-C(31)	118.9784	
O(25)-Zr(41)	2.0844		C(32)-C(31)-C(30)	118.5948	
O(40)-Zr(41)	2.0968		C(35)-C(30)-C(31)	123.9296	
C(12)-O(42)	1.4195	1.4120	Zr(41)-O(28)-C(26)	110.3553	
O(37)-Zr(41)	2.0831		O(28)-C(26)-N(27)	111.0664	122.6000
C(36)-O(40)	1.2369	1.2080	O(28)-C(26)-C(16)	137.1615	123.0000
C(39)-N(22)	1.4593	1.4380	N(27)-C(26)-C(16)	109.9398	112.7400
N(22)-C(38)	1.4569	1.4380	Zr(41)-O(25)-C(17)	108.7610	
C(35)-O(37)	1.3776	1.3550	C(39)-N(22)-C(38)	108.5503	107.7000
C(34)-C(36)	1.3751	1.5170	C(39)-N(22)-C(18)	112.2253	107.7000
C(35)-C(30)	1.3514	1.4200	C(38)-N(22)-C(18)	115.6873	107.7000
C(34)-C(35)	1.3644	1.4200	N(22)-C(18)-C(13)	113.3836	108.8000
C(33)-C(34)	1.3532	1.4200	N(22)-C(18)-C(17)	113.5587	
C(32)-C(33)	1.3400	1.4200	C(13)-C(18)-C(17)	108.0743	109.5100
C(31)-C(32)	1.3362	1.4200	O(25)-C(17)-C(18)	109.6929	120.0000
C(30)-C(31)	1.3384	1.4200	O(25)-C(17)-C(16)	127.2787	124.3000
C(7)-O(29)	1.2134	1.2080	C(18)-C(17)-C(16)	123.0236	121.4000
C(26)-O(28)	1.2358	1.2080	C(26)-C(16)-C(17)	121.1101	117.6000
C(26)-N(27)	1.3661	1.3690	C(26)-C(16)-C(15)	119.0438	117.6000
C(16)-C(26)	1.3835	1.5170	C(17)-C(16)-C(15)	119.8314	117.6000
C(17)-O(25)	1.3763	1.3550	O(19)-C(15)-C(16)	121.6163	123.0000
C(10)-C(24)	1.5318	1.5140	O(19)-C(15)-C(12)	115.6718	122.5000
C(10)-O(23)	1.4124	1.4030	C(16)-C(15)-C(12)	122.7119	115.0000
C(18)-N(22)	1.4697	1.4380	C(9)-C(14)-C(13)	109.7934	109.5000
C(11)-O(21)	1.3637	1.3550	C(18)-C(13)-C(14)	114.9514	109.5100
C(3)-O(20)	1.3678	1.3550	C(18)-C(13)-C(12)	111.1424	109.5100
C(15)-O(19)	1.2138	1.2080	C(14)-C(13)-C(12)	109.9451	109.5100
C(18)-C(13)	1.5353	1.5230	O(42)-C(12)-C(15)	106.4210	109.5000
C(17)-C(18)	1.5263	1.4970	O(42)-C(12)-C(13)	112.1782	107.5000
C(16)-C(17)	1.3618	1.3370	O(42)-C(12)-C(11)	104.3920	109.5000
C(15)-C(16)	1.3754	1.5170	C(15)-C(12)-C(13)	106.4335	107.8000
C(12)-C(15)	1.5473	1.5090	C(15)-C(12)-C(11)	115.8653	109.4700
C(14)-C(9)	1.5336	1.5230	C(13)-C(12)-C(11)	111.5569	109.4700
C(13)-C(14)	1.5245	1.5230	O(21)-C(11)-C(12)	112.0453	120.0000
C(12)-C(13)	1.5209	1.5140	O(21)-C(11)-C(8)	123.2620	124.3000
C(11)-C(12)	1.5364	1.4970	C(12)-C(11)-C(8)	124.3437	121.4000
C(8)-C(11)	1.3566	1.3370	C(24)-C(10)-O(23)	107.7722	107.5000
C(10)-C(5)	1.5140	1.4970	C(24)-C(10)-C(5)	108.2598	109.4700
C(9)-C(10)	1.5230	1.5140	C(24)-C(10)-C(9)	115.0349	109.4700
C(8)-C(9)	1.5083	1.4970	O(23)-C(10)-C(5)	111.3993	109.5000
C(7)-C(8)	1.3730	1.5170	O(23)-C(10)-C(9)	107.1700	107.5000
C(4)-C(7)	1.3758	1.5170	C(5)-C(10)-C(9)	107.2569	109.4700
C(6)-C(1)	1.3354	1.4200	C(14)-C(9)-C(10)	111.7299	109.5100
C(5)-C(6)	1.3459	1.4200	C(14)-C(9)-C(8)	114.0193	109.5100
C(4)-C(5)	1.3547	1.4200	C(10)-C(9)-C(8)	109.7637	109.5100
C(3)-C(4)	1.3623	1.4200	C(11)-C(8)-C(9)	119.9329	121.4000
C(2)-C(3)	1.3460	1.4200	C(11)-C(8)-C(7)	121.9602	117.6000
C(1)-C(2)	1.3350	1.4200	C(9)-C(8)-C(7)	118.0044	120.0000
			O(29)-C(7)-C(8)	119.9074	123.0000
Atom	Bond angle (°)		O(29)-C(7)-C(4)	118.7473	123.0000
O(28)-Zr(41)-O(37)	117.4328		C(8)-C(7)-C(4)	121.3103	115.0000
O(25)-Zr(41)-O(40)	116.5393		C(1)-C(6)-C(5)	121.0918	
O(25)-Zr(41)-O(37)	119.5671		C(10)-C(5)-C(6)	117.8442	121.4000
O(40)-Zr(41)-O(37)	97.5287		C(10)-C(5)-C(4)	121.2058	121.4000
Zr(41)-O(40)-C(36)	110.2415		C(6)-C(5)-C(4)	120.7592	120.0000
Zr(41)-O(37)-C(35)	113.1231		C(7)-C(4)-C(5)	120.1926	117.6000
O(40)-C(36)-C(34)	138.2045		C(7)-C(4)-C(3)	121.4992	117.6000
O(37)-C(35)-C(30)	114.6912	124.3000	C(5)-C(4)-C(3)	118.2898	120.0000
O(37)-C(35)-C(34)	128.1872	124.3000	O(20)-C(3)-C(4)	126.3191	124.3000
C(30)-C(35)-C(34)	117.1135	120.0000	O(20)-C(3)-C(2)	114.4642	124.3000
C(36)-C(34)-C(35)	125.4398	117.6000	C(4)-C(3)-C(2)	119.1581	120.0000
C(36)-C(34)-C(33)	116.0640	117.6000	C(3)-C(2)-C(1)	122.5248	
C(35)-C(34)-C(33)	118.4962	120.0000	C(6)-C(1)-C(2)	118.1454	
C(34)-C(33)-C(32)	122.8864				

TABLE-6
BOND LENGTH AND BOND ANGLE OF Pd COMPLEX

Atom	Bond length (Å)		Atom	Bond angle (°)	
O(28)-Pd(41)	1.9186		C(34)-C(33)-C(32)	119.6599	
O(25)-Pd(41)	1.9067		C(33)-C(32)-C(31)	119.7177	
O(40)-Pd(41)	1.9577		C(32)-C(31)-C(30)	119.9319	
C(12)-O(42)	1.4198	1.4120	C(35)-C(30)-C(31)	121.3887	
O(37)-Pd(41)	1.9093		Pd(41)-O(28)-C(26)	110.2716	
C(36)-O(40)	1.2359	1.2080	O(28)-C(26)-N(27)	111.1774	122.6000
C(39)-N(22)	1.4590	1.4380	O(28)-C(26)-C(16)	136.4600	123.0000
N(22)-C(38)	1.4572	1.4380	N(27)-C(26)-C(16)	110.6701	112.7400
C(35)-O(37)	1.3647	1.3550	Pd(41)-O(25)-C(17)	111.2453	
C(34)-C(36)	1.3597	1.5170	C(39)-N(22)-C(38)	108.6976	107.7000
C(35)-C(30)	1.3464	1.4200	C(39)-N(22)-C(18)	112.1732	107.7000
C(34)-C(35)	1.3449	1.4200	C(38)-N(22)-C(18)	115.8804	107.7000
C(33)-C(34)	1.3444	1.4200	N(22)-C(18)-C(13)	113.2471	108.8000
C(32)-C(33)	1.3417	1.4200	N(22)-C(18)-C(17)	113.5017	
C(31)-C(32)	1.3411	1.4200	C(13)-C(18)-C(17)	107.9332	109.5100
C(30)-C(31)	1.3417	1.4200	O(25)-C(17)-C(18)	108.5516	120.0000
C(7)-O(29)	1.2134	1.2080	C(25)-C(17)-C(16)	128.4153	124.3000
C(26)-O(28)	1.2329	1.2080	C(18)-C(17)-C(16)	123.0186	121.4000
C(26)-N(27)	1.3653	1.3690	C(26)-C(16)-C(17)	121.8930	117.6000
C(16)-C(26)	1.3815	1.5170	C(26)-C(16)-C(15)	118.6487	117.6000
C(17)-O(25)	1.3732	1.3550	C(17)-C(16)-C(15)	119.4532	117.6000
C(10)-C(24)	1.5316	1.5140	O(19)-C(15)-C(16)	121.4936	123.0000
C(10)-O(23)	1.4124	1.4030	O(19)-C(15)-C(12)	115.2588	122.5000
C(18)-N(22)	1.4697	1.4380	C(16)-C(15)-C(12)	123.2467	115.0000
C(11)-O(21)	1.3634	1.3550	C(9)-C(14)-C(13)	109.4978	109.5000
C(3)-O(20)	1.3678	1.3550	C(18)-C(13)-C(14)	114.8769	109.5100
C(15)-O(19)	1.2138	1.2080	C(18)-C(13)-C(12)	111.1117	109.5100
C(18)-C(13)	1.5334	1.5230	C(14)-C(13)-C(12)	110.0174	109.5100
C(17)-C(18)	1.5241	1.4970	O(42)-C(12)-C(15)	106.5241	109.5000
C(16)-C(17)	1.3600	1.3370	O(42)-C(12)-C(13)	112.3297	107.5000
C(15)-C(16)	1.3761	1.5170	O(42)-C(12)-C(11)	104.3594	109.5000
C(12)-C(15)	1.5485	1.5090	C(15)-C(12)-C(13)	106.6587	107.8000
C(14)-C(9)	1.5334	1.5230	C(15)-C(12)-C(11)	116.0118	109.4700
C(13)-C(14)	1.5246	1.5230	C(13)-C(12)-C(11)	110.9949	109.4700
C(12)-C(13)	1.5207	1.5140	O(21)-C(11)-C(12)	112.2028	120.0000
C(11)-C(12)	1.5372	1.4970	O(21)-C(11)-C(8)	123.1081	124.3000
C(8)-C(11)	1.3568	1.3370	C(12)-C(11)-C(8)	124.3046	121.4000
C(10)-C(5)	1.5141	1.4970	C(24)-C(10)-O(23)	107.8185	107.5000
C(9)-C(10)	1.5226	1.5140	C(24)-C(10)-C(5)	108.3483	109.4700
C(8)-C(9)	1.5085	1.4970	C(24)-C(10)-C(9)	115.0343	109.4700
C(7)-C(8)	1.3730	1.5170	O(23)-C(10)-C(5)	111.3898	109.5000
C(4)-C(7)	1.3759	1.5170	O(23)-C(10)-C(9)	107.1622	107.5000
C(6)-C(1)	1.3354	1.4200	C(5)-C(10)-C(9)	107.1377	109.4700
C(5)-C(6)	1.3458	1.4200	C(14)-C(9)-C(10)	111.8702	109.5100
C(4)-C(5)	1.3548	1.4200	C(14)-C(9)-C(8)	114.0879	109.5100
C(3)-C(4)	1.3623	1.4200	C(10)-C(9)-C(8)	109.7362	109.5100
C(2)-C(3)	1.3460	1.4200	C(11)-C(8)-C(9)	120.0652	121.4000
C(1)-C(2)	1.3350	1.4200	C(11)-C(8)-C(7)	121.9652	117.6000
Atom	Bond angle (°)		C(9)-C(8)-C(7)	117.8666	120.0000
O(28)-Pd(41)-O(25)	105.4056		O(29)-C(7)-C(8)	119.8504	123.0000
O(28)-Pd(41)-O(40)	77.2374		O(29)-C(7)-C(4)	118.8096	123.0000
O(28)-Pd(41)-O(37)	120.9912		C(8)-C(7)-C(4)	121.3014	115.0000
O(25)-Pd(41)-O(40)	76.0215		C(1)-C(6)-C(5)	121.0809	
O(25)-Pd(41)-O(37)	118.4376		C(10)-C(5)-C(6)	117.8315	121.4000
O(40)-Pd(41)-O(37)	77.3124		C(10)-C(5)-C(4)	121.2188	121.4000
Pd(41)-O(40)-C(36)	110.3238		C(6)-C(5)-C(4)	120.7695	120.0000
Pd(41)-O(37)-C(35)	111.9655		C(7)-C(4)-C(5)	120.1932	117.6000
O(40)-C(36)-C(34)	128.9963		C(7)-C(4)-C(3)	121.4998	117.6000
O(37)-C(35)-C(30)	122.0481	124.3000	C(5)-C(4)-C(3)	118.2888	120.0000
O(37)-C(35)-C(34)	120.1909	124.3000	O(20)-C(3)-C(4)	126.3340	124.3000
C(30)-C(35)-C(34)	117.7490	120.0000	O(20)-C(3)-C(2)	114.4593	124.3000
C(36)-C(34)-C(35)	116.3097	117.6000	C(4)-C(3)-C(2)	119.1485	120.0000
C(36)-C(34)-C(33)	122.1389	117.6000	C(3)-C(2)-C(1)	122.5329	
C(35)-C(34)-C(33)	121.5510	120.0000	C(6)-C(1)-C(2)	118.1487	

REFERENCES

- P.H. Chang, W. Jiang, Z. Li, J. Jean and C.Y. Kuo, *Res. & Rev.: J. Pharm. Anal.*, **4**, 86 (2015).
- T.K. Pal, M.A. Alam and S.R. Paul, *J. Bangladesh Acad. Sci.*, **34**, 153 (1970);
<https://doi.org/10.3329/jbas.v34i2.6859>
- S. Shobana, P. Subramaniam, L. Mitu, J. Dharmaraja and S. Arvind Narayan, *Spectrochim. Acta A Mol. Biomol. Spectrosc.*, **134**, 333 (2015);
<https://doi.org/10.1016/j.saa.2014.06.093>
- A.A. Soliman, S.A. Ali, A.H. Marei and D.H. Nassar, *Spectrochim. Acta A Mol. Biomol. Spectrosc.*, **89**, 329 (2012);
<https://doi.org/10.1016/j.saa.2011.12.061>
- N. Qamar, H. Sultan, M. Khan, R. Azmat, R. Naz, A. Hameed and M. Lateef, *ChemSelect*, **4**, 3058 (2019);
<https://doi.org/10.1002/slct.201803882>
- H.F.A. El-Halim, G.G. Mohamed, M.M.I. El-Dessouky and W.H. Mahmoud, *Spectrochim. Acta A Mol. Biomol. Spectrosc.*, **82**, 8 (2011);
<https://doi.org/10.1016/j.saa.2011.05.089>
- Y. Zhao, Y. Tan, Y. Guo, X. Gu, X. Wang and Y. Zhang, *Environ. Pollut.*, **180**, 206 (2013);
<https://doi.org/10.1016/j.envpol.2013.05.043>
- J.A. Anderson, P.W. Groundwater, A. Todd and A.J. Worsley, *Pharm. J.*, **283**, 359 (2004).
- J.A. Obaleye, O.O. Abosede, A.S. Kumbhar and N. Olusola, *Can. Chem. Trans.*, **4**, 168 (2016);
<https://doi.org/10.13179/canchemtrans.2016.04.02.0257>
- M. M. El-Ajaily, H.A. Abdullah, A. Al-Janga, E.E. Saad and A.A. Maihub, *Adv. Chem.*, **2015**, 987420 (2015);
<https://doi.org/10.1155/2015/987420>
- W.H. El-Shwiniy, W.S. Shehab, S.F. Mohamed and H.G. Ibrahim, *Appl. Organomet. Chem.*, **32**, e4503 (2018);
<https://doi.org/10.1002/aoc.4503>
- K. Sharma, R.V. Singh and N. Fahmi, *Spectrochim. Acta A Mol. Biomol. Spectrosc.*, **78**, 80 (2011);
<https://doi.org/10.1016/j.saa.2010.08.076>
- H.L. Singh and J. Singh, *Int. J. Inorg. Chem.*, **2013**, 847071 (2013);
<https://doi.org/10.1155/2013/847071>
- I.M.I. Moustafa and M.H. Abdellatif, *Mod. Chem. Appl.*, **5**, 202 (2018);
<https://doi.org/10.4172/2329-6798.1000202>
- B.S. Prakash, C.I.S. Raj and R.G. Allen Gana, *J. Eng. Sci.*, **6**, 43 (2017).
- H. Khan, A. Badshah, M. Said, G. Murtaza, J. Ahmad, B.J. Jean-Claude, M. Todorova and I.S. Butler, *Appl. Organomet. Chem.*, **27**, 387 (2013);
<https://doi.org/10.1002/aoc.2991>
- N. Rathee and K.K. Verma, *J. Serb. Chem. Soc.*, **77**, 325 (2012);
<https://doi.org/10.2298/JSC101211200R>
- L. Tabrizi, H. Chiniforoshan and H. Tavakol, *Spectrochim. Acta A Mol. Biomol. Spectrosc.*, **141**, 16 (2015);
<https://doi.org/10.1016/j.saa.2015.01.027>
- H.G. Aslan, S. Özcan and N. Karacan, *Inorg. Chem. Commun.*, **14**, 1550 (2011);
<https://doi.org/10.1016/j.inoche.2011.05.024>
- N.K. Chaudhary and P. Mishra, *Bioinorg. Chem. Appl.*, **2017**, 6927675 (2017);
<https://doi.org/10.1155/2017/6927675>
- T.K. Pal, M.A. Alam, S. Paul and M.C. Sheikh, *J. King Saud Univ. Sci.*, **31**, 445 (2017);
<https://doi.org/10.1016/j.jksus.2017.12.010>
- M. Díaz-Sánchez, D. Díaz-García, S. Prashar and S. Gómez-Ruiz, *Environ. Chem. Lett.*, **17**, 1585 (2019);
<https://doi.org/10.1007/s10311-019-00899-5>
- H.A. EL-Ghamry, K. Sakai, S. Masaoka, K.Y. El-Baradie and R.M. Issa, *Chin. J. Chem.*, **30**, 881 (2012);
<https://doi.org/10.1002/cjoc.201280024>

International Seminar on
RECENT TRENDS IN CHEMISTRY
(RTC-2019)

JANUARY 03, 2019

- Organized by -

DEPARTMENT OF CHEMISTRY

P.D. WOMEN'S COLLEGE, JALPAIGURI
(Accredited with B++ by NAAC, second cycle)

- In association with -

INDIAN CHEMICAL SOCIETY, KOLKATA



CERTIFICATE

This is to certify that

Dr. /Mr./ Ms.*R. K. Dev*.....

has delivered Oral Presentation in the International Seminar on

"Recent Trends in Chemistry" held at the Department of Chemistry,

P.D. Women's College, Jalpaiguri on January 03, 2019.

W. Samanta
Organizing Secretary

V. Samanta
Convener

A. Chatterjee
Principal & President



23RD INTERNATIONAL CONFERENCE OF INTERNATIONAL ACADEMY OF PHYSICAL SCIENCES

(CONIAPS XXIII)



Advances in Physical Sciences to Achieve Sustainable Development Goals

On **November 18, 2018**

Organized by

NEPAL ACADEMY OF SCIENCE AND TECHNOLOGY, KATHMANDU, NEPAL

Certificate

This is to certify that Prof. /Dr./ Mr./Ms. **R. K. DEV**
Department of **Chemistry, MMAMC, TU Biratnagar, Nepal** has participated in the
23rd International Conference of International Academy of Physical Sciences on Advances in Physical Sciences to Achieve Sustainable Development Goals held at Nepal Academy of Science and Technology during November 16-18, 2018 and delivered Invited Lecture/Chaired a Session/ Presented a paper /Presented a paper in Young Scientist Award Category.

Title of the Invited Lecture/Paper **Bio-coordination and Computational Modelling of 4d-transition Metal Complexes with Tetra-cyclines and Schiffaldehyde Mixed Ligand: Synthesis, Spectroscopic Characterization and Biological Studies**

Prof. P. N. Paudyal
General Secretary
IAPS

Dr. Buddhi Ratna Khadge
Convener
CONIAPS XXIII

Ms. Ramila Raut
Organizing Secretary
CONIAPS XXIII



“Research and Innovation for Prosperity”

This certificate is awarded to

MR. R.K. DEV

in recognition of his/her valuable contribution

as the **ORAL PRESENTER** in

International Youth Conference on Science, Technology, and Innovation

21-23 Oct, 2019, Kathmandu, Nepal

Mr. Giriraj Mani Pokharel

Minister

Ministry of Education, Science and Technology

(MoEST)

Dr. Sunil Babu Shrestha

Vice Chancellor

Nepal Academy of Science and Technology

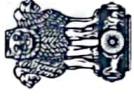
(NAST)

Mr. Madhab Prasad Dhungel

Executive Vice-Chairperson

National Youth Council

(NYC)



Department of Science and Technology (DST)

Sophisticated Analytical Instrument Facility (SAIF)

Sponsored by DST (Govt. of India)

CSIR-Central Drug Research Institute, Lucknow

Certificate of Participation

This is to certify that Mrs./Ms./Mr./Dr. *Rohit Kumar Dev*.....
from *M.M.A.M.C., T.U., Biratnagar*..... has attended the National Workshop
on "Small Molecule Analysis by NMR Spectroscopy & Mass Spectrometry" from 13th -15th December,
2017 at SAIF, CSIR-Central Drug Research Institute, Lucknow.

Dr. Sanjeev K. Shukla
Organizing Secretary

Dr. Sanjeev Kanojiya
Co-Organizing Secretary

Prof. Alok Dhawan
Director, CSIR-CDRI



Provincial Workshop on Advanced Research Methodology



Organized by

Research Management Cell

J.S. Murarka Multiple Campus, Lahan (Siraha)



(Province No. 2)

in collaboration with

Nepal Chemical Society & Eastern Chapter of NCS, Biratnagar



Certified that **Prof./Dr./Mr./Ms. Rohit Kumar Dex**.....

from **Ma. hindra Moxang, Biratnagar**....., participated as facilitator/participant in

3 days workshop held from 15th to 17th March, 2019 at J.S. Murarka Multiple Campus, Lahan (Siraha).

Chairperson
Mr. Tulsiram Pokharel
Campus Chief
J. S. M. M. C, Lahan

.....
Prof. Dr. Amar Pd. Yadav
President
Nepal Chemical Society

.....
Dr. Surya Kant Kalauni
General Secretary
Nepal Chemical Society

Chief Guest
Mrs. Sarita Giri
M. P.
Federal Parliament, Nepal



(नेपाल सरकारबाट स्वीकृत)

नेपाल केमिकल सोसाइटी Nepal Chemical Society

Regd. No. 8/042/043

Ref. No.:

Date:

Executive Council
2073-75 (2016-18)

President
Prof. Dr. Amar Prasad Yadav
Mobile: 9851124444
Email: amar2y@yahoo.com

Vice President
Dr. Bindra Shrestha
Mobile: 9841397290
Email: binraghu@yahoo.com

General Secretary
Dr. Surya Kant Kalauni
Mobile: 9841973753
Email: skkalauni@gmail.com

Secretary
Mr. Purna Prasad Dhakal
Mobile: 9841566860
Email: dhakalpurna1@gmail.com

Treasure
Mr. Ram Lochan Aryal
Mobile: 9851079735
Email: chemrlaryal@gmail.com

Members:
Dr. Randhir Kumar Jha
Mobile: 9851141069
Email: drrandhirjha123@gmail.com
Mr. Manoj Bista
Mobile: 9855059448
Email: bisttamanoj@gmail.com
Mr. Yub Raj Dangi
Mobile: 9857834054
Email: yubrajdangiai@gmail.com
Mr. Lekha Nath Khatiwada
Mobile: 9841817332
Email: lekhukhatiwada@gmail.com
Mr. Amit Dhungana
Mobile: 9841068883
Email: mtdhungana33@gmail.com

Chief Editor
Dr. Puspa Lal Homagai
Mobile: 9851182958
Email: homagaip1@gmail.com

Editors
Dr. Achyut Adhikari
Email: achyutraj05@gmail.com
Dr. Ajaya Bhattarai
Email: bkajaya@yahoo.com
Dr. Bhanu Bhakta Neupane
Email: newbhanu@gmail.com
Dr. Bishnu Bastakoti
Email: bishnubastakoti@hotmail.com
Mr. Dipak Kumar Gupta
Email: deepakguptas2012@yahoo.com
Dr. Hari Paudyal
Email: haripaudyal@gmail.com
Dr. Khaga Raj Sharma
Email: khagara_sharma33@yahoo.com
Mr. Nabin Karki
Email: nabin.guess@yahoo.com
Dr. Swagat Shrestha
Email: swagatstha@gmail.com

Workshop on Tools & Techniques in Chemistry

Organized by

Nepal Chemical Society in co-operation with Central
Department of Chemistry, TU, Kirtipur

Certificate

This is to certify that

Prof./Dr./Mr./Ms.....*Rohit Kumar Dev*.....
From.....*M.N.A.M. Campus, Bixatnagar*..... Participated as
resource person/participant in 3 days workshop held from
April 2-4, 2019 (Chaitra 19-21, 2075) at Central
Department of Chemistry, TU, Kirtipur.

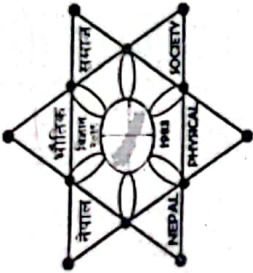
Prof. Dr. Amar Prasad Yadav
President
Nepal Chemical Society

Dr. Surya Kant Kalauni
General Secretary
Nepal Chemical Society

Prof. Dr. Ram Chandra Basnyat
Head
Central Dept. of Chemistry

Contact Point:

Central Department of Chemistry, Tribhuvan University, Kirtipur, Kathmandu, Nepal
P. O. Box: 6145, Kathmandu, Nepal, Mobile: +977-9840166321, Email: info@ncs.org.np, Website: www.ncs.org.np



This is to Certify that

MR. ROHIT KUMAR DEV

has Successfully Completed

Workshop on Research Writing and Publishing

March 29 – 30, 2019

Organized by

**Nepal Physical Society
Eastern Chapter, Biratnagar**

Co-organized by

Mahendra Morang Adarsh Multiple Campus, Tribhuvan University, Biratnagar

&

HISSAN, Morang



Mr. Kul Prasad Limbu
Facilitator



Dr. Shashit Kumar Yadav
Secretary / Facilitator
Nepal Physical Society
Eastern Chapter



Prof. Dr. Devendra Adhikari
President / Facilitator
Nepal Physical Society
Eastern Chapter



Prof. Dr. Shiva Kumar Rai
Facilitator





WORKSHOP ON

Carbon Dots (CDs): An amazing multi functional nano particle

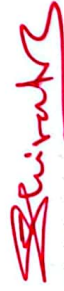
2 August, 2022

Certificate Of Participation

Awarded to

MR. Rohit Kumar Dev

For contributing as a participant in **Carbon Dots (CDs): An amazing multi functional nano particle** one-day workshop organized by Department of Chemistry, Mahendra Morang Adarsh Multiple Campus, Tribhuvan University and Nepal Chemical Society, Biratnagar, Province 1, Nepal.



Ghanshyam Shrivastav

Chairman

Department of Chemistry,
M.M.A.M.C., T.U.
Biratnagar-12



Prof. Dr. Ajaya Bhattarai

President

Nepal Chemical Society,
Province 1



Dr. Surendra Kumar Gautam

President

Nepal Chemical Society,
Kathmandu



Prof. Dr. Roger M. Leblanc

Fulbright Specialist

Department of Chemistry
University of Miami, FL, USA

International Chemical Congress (ICC-2023)

Chemistry for Sustainable Development

May 25-27, 2023 | Kathmandu, Nepal



Organized by
Nepal Chemical Society
in association with
Central Department of Chemistry
Tribhuvan University

Certificate of Participation

This is to certified that
Prof./Dr./Mr./Ms. ... **Rohit Kumar Dev**

.....
has participated and presented a poster in International
Chemical Congress (ICC-2023) held in Park Village Hotel,
Kathmandu, Nepal during May 25-27, 2023.

.....
Dr. Surendra K. Gautam
Conference Convener
(President NCS)

.....
Dr. Mahesh K. Joshi
Conference Secretary
(General Secretary NCS)

.....
Prof. Dr. Jagadeesh Bhattra
Conference Co-convener
(HoD, CDC, TU)

Date: May 27, 2023

International Chemical Congress

- Chemistry for Sustainable Development-

ICC-2018



Organized by

Nepal Chemical Society

In co-operation with

Department of Chemistry

Birendra M. Campus, Bharatpur, Tribhuvan University
Chitwan, Nepal

Certificate of Participation

This is to certify that

Ms. Rohit Kumar Dev

participated as Plenary/Keynote/Invited/Oral Lecture/Poster/Delegate in the

International Chemical Congress Chemistry for Sustainable Development

March 8-10, 2018, Sauraha, Chitwan, Nepal

Dr. Surya Kant Kalauni

General Secretary
Nepal Chemical Society

Govind Sapkota

Co-patron ICC-2018
Campus Chief, Birendra M. Campus

Prof. Dr. Amar Prasad Yadav

Convener ICC-2018
President Nepal Chemical Society

Chief Guest



Government of Nepal
Ministry of Youth and Sports
National Youth Council
Sanothimi, Bhaktapur

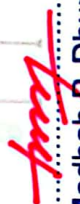


This certificate is awarded to

ROHIT KUMAR DEV

in recognition of your valuable contribution
as a **Poster Presenter** in *Provincial Youth Symposium on Science
& Technology 2019*
Province-1, Biratnagar, Nepal
March 1-2, 2019


Suresh Bhattarai
Co-ordinator
Organizing Committee


Madhab P. Dhungel
Executive Vice-Chairperson
National Youth Council


Hon. Sherdhan Rai
Chief Minister
Province-1, Nepal
Chief Guest



“Research and Innovation for Prosperity”

This certificate is awarded to

ROHIT KUMAR DEY

in recognition of his/her valuable contribution

as the **POSTER PRESENTER** in

International Youth Conference on Science, Technology, and Innovation

21-23 Oct, 2019, Kathmandu, Nepal

Mr. Giriraj Mani Pokharel

Minister

Ministry of Education, Science and Technology

(MoEST)

Dr. Sunil Babu Shrestha

Vice Chancellor

Nepal Academy of Science and Technology

(NAST)

Mr. Madhab Prasad Dhungel

Executive Vice-Chairperson

National Youth Council

(NYC)



7th International Symposium on

CURRENT TRENDS IN DRUG DISCOVERY RESEARCH

February 20-23, 2019

Certificate

The Organising Committee certifies and appreciates that
**Mr. Rohit Kumar Dev, Bio-inorganic and Materials Chemistry Research
Laboratory Mahendra Morang Adarsh Multiple Campus Biratnagar, Nepal,**
has participated in the Symposium held in CSIR-CDRI during February, 20-

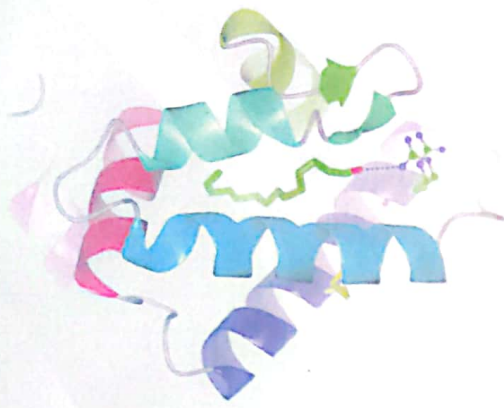
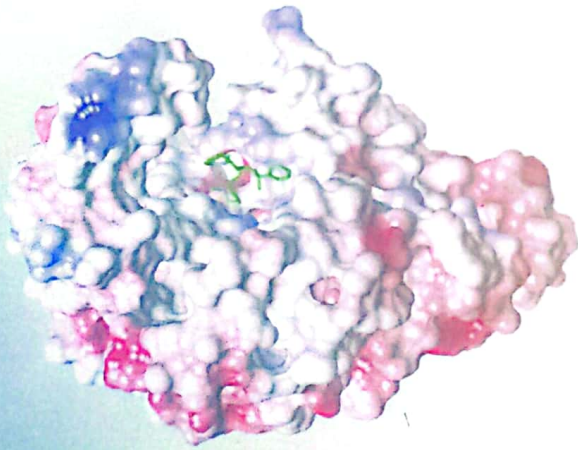
23, 2019

(Prof. Tapas K Kundu)
Chairperson

(Dr. Sanjay Batra)
Organizing Secretary



CSIR-Central Drug Research Institute
Sector 10, Jankipuram Extension, Sitapur Road, Lucknow-226031, UP, India





Government of Nepal
Ministry of Youth and Sports



NATIONAL YOUTH COUNCIL

Sanothimi, Bhaktapur



National Youth Council-Nepal
2016
Sanothimi, Bhaktapur

This certificate is awarded to

.....
Rohit Kumar Dev.....


*in recognition of your valuable contribution as a **PARTICIPANT**
in Provincial Youth Symposium on Science & Technology 2019.*

Province 1, Biratnagar, Nepal

March 1-2, 2019

.....
Khim Panthi
Co-ordinator
Organization Committee
& Member of National Youth Council

.....
Madhab P. Dhungel
Executive Vice-Chairperson
Nation Youth Council

.....

Hon. Shersham Koiri
Chief Minister
Province-1 Nepal
Chief Guest

International Seminar on "Frontiers in Chemistry 2018"



ENLIGHTENMENT TO PERFECTION

UNIVERSITY OF NORTH BENGAL

Accredited by NAAC with Grade A

Organized by

DEPARTMENT OF CHEMISTRY, UNIVERSITY OF NORTH BENGAL & CRSI North Bengal Local Chapter

CERTIFICATE

This is to certify that

Prof./Dr./Mr./Ms. *Rohit Kumar*.....*Dr.*.....
of.....*Tribhuvan University*.....*Nepal*.....

has delivered an invited lecture/ presented a poster/ participated in the

International Seminar on "Frontiers in Chemistry 2018"

held at the Department of Chemistry, University of North Bengal on August 27th, 2018.

A. K. Misra
Prof. (Dr.) A. Misra
Convenor
Department of Chemistry, N. B. U

S. S. Das
Dr. S. Das
Secretary, Organizing Committee
Department of Chemistry, N. B. U